



## Atypical Opioid Interactions – Development of Selective Mu-Delta Heterodimer Antagonists, Clinical Opioids at Non-Mu Pain Targets and Endogenous Biased Signaling

Item Type	text; Electronic Dissertation
Authors	Olson, Keith Mathew
Publisher	The University of Arizona.
Rights	Copyright © is held by the author. Digital access to this material is made possible by the University Libraries, University of Arizona. Further transmission, reproduction or presentation (such as public display or performance) of protected items is prohibited except with permission of the author.
Download date	22/05/2018 07:21:54
Link to Item	<a href="http://hdl.handle.net/10150/626669">http://hdl.handle.net/10150/626669</a>

ATYPICAL OPIOID INTERACTIONS – DEVELOPMENT OF SELECTIVE  
MU-DELTA HETERODIMER ANTAGONISTS, CLINICAL OPIOIDS AT  
NON-MU PAIN TARGETS AND ENDOGENOUS BIASED SIGNALING

by

Keith M. Olson

---

Copyright © Keith M. Olson 2017

A Dissertation Submitted to the Faculty of the

DEPARTMENT OF CHEMISTRY AND BIOCHEMISTRY

In Partial Fulfillment of the Requirements

For the Degree of

DOCTOR OF PHILOSOPHY

WITH A MAJOR IN BIOCHEMISTRY

In the Graduate College

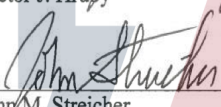
THE UNIVERSITY OF ARIZONA

2017

THE UNIVERSITY OF ARIZONA  
GRADUATE COLLEGE

As members of the Dissertation Committee, we certify that we have read the dissertation prepared by Keith M. Olson titled Atypical Opioid Interactions – Development of Selective Mu-Delta Heterodimer Antagonists, Clinical Opioid Activity at Non-Mu Targets and Endogenous Biased Signaling and recommend that it be accepted as fulfilling the dissertation requirement for the Degree of Doctor of Philosophy

  
\_\_\_\_\_  
Prof. Victor J. Hruby Date 6/2/17

  
\_\_\_\_\_  
Prof. John M. Streicher Date 6/2/17

  
\_\_\_\_\_  
Prof. Indraneel Ghosh Date 6/2/17

  
\_\_\_\_\_  
Prof. William Montfort Date 6/2/17

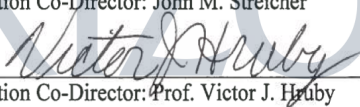
  
\_\_\_\_\_  
Prof. Frank Porreca Date 6/2/17

Final approval and acceptance of this dissertation is contingent upon the candidate's submission of the final copies of the dissertation to the Graduate College.



I hereby certify that I have read this dissertation prepared under my direction and recommend that it be accepted as fulfilling the dissertation requirement.

  
\_\_\_\_\_  
Dissertation Co-Director: John M. Streicher Date 6/2/17

  
\_\_\_\_\_  
Dissertation Co-Director: Prof. Victor J. Hruby Date: 6/2/17

## STATEMENT BY AUTHOR

This dissertation has been submitted in partial fulfillment of requirements for an advanced degree at the University of Arizona and is deposited in the University Library to be made available to borrowers under rules of the Library.

Brief quotations from this dissertation are allowable without special permission, provided that accurate acknowledgment of source is made. Requests for permission for extended quotation from or reproduction of this manuscript in whole or in part may be granted by the head of the major department or the Dean of the Graduate College when in his or her judgment the proposed use of the material is in the interests of scholarship. In all other instances, however, permission must be obtained from the author.

SIGNED: Keith M. Olson

## ACKNOWLEDGMENTS

First I would like to express my sincere gratitude to my advisors Dr. Victor J. Hruby and Dr. John M. Streicher for their immense professional and personal support. I greatly admire their knowledge, work ethic and compassion. Dr. Hruby's chemical perspective and Dr. Streicher's pharmacological expertise were fundamental for completing an interdisciplinary Ph. D. However, their professional guidance is dwarfed by their personal impact on my life.

Thank you Dr. Streicher for taking me into his lab over the past 18 months as his first graduate student. His instrumental support enabled me to go further in each project than previously believed. Second, I would like to thank Dr. Frank Porreca and Dr. Hruby. During my first year in graduate school I had several health problems. Each insisted "You won't be able to do good science until you are in good health". I am forever indebted; their support enabled me to get healthy and then focus on accomplishing science. Thanks to my additional committee members, Dr. William Montfort and Dr. Indraneel Gosh for all their valuable input and constructive skepticism. Thank you to my fellow graduate students; Dr. Stephanie Jensen, Dr. Ryan Eismen, Dr. Cyf Ramos, Dr. Michael Williams, Rob Baage and Justin Lavigne for your co-miseration over the last six years.

Most of all I'd like to thank my mom and dad. My dad passed away a few months before I moving across the country and beginning graduate school. While he will never be replaced, I am proud John and Victor provided great role models during this stage in my life. Words cannot describe how much I miss you dad and love you both. Thank you for everything.

## DEDICATION

Dedicated to my loving parents, Gary L. Olson and Christine M. Olson

**TABLE OF CONTENTS**

LIST OF TABLES.....	11
LIST OF FIGURES.....	13
LIST OF SCHEMES.....	15
ABSTRACT .....	16
ABRREVIATIONS.....	18
CHAPTER 1: INTRODUCTION.....	21
1.1 Chronic Pain, Treatment Limitations and Opioids.....	21
1.2 Clinical Opioid Analgesics and Opioid Signaling.....	24
1.3 Atypical Non-Opioid and Opioid Targets for Chronic Pain Treatment.....	26
1.3.1 MOR and DOR Synergy, Heterodimerization and Disease .....	26
1.3.2 Atypical Targets for Pain Treatment .....	31
1.3.3 Biased Agonists.....	35
1.4 Aims .....	38
1.4.1 Design, Synthesis and Evaluation of Mu-Delta Heterodimer Selective Antagonists.....	38
1.4.2 Evaluation of Clinical Analgesics at Atypical Targets for Pain.....	39
1.4.3 Biased Signaling of Endogenous Opioid Peptides at Mu, Delta and Kappa Opioid Receptors .....	40

## TABLE OF CONTENTS-Continued

### CHAPTER 2: DESIGN, SYNTHESIS AND EVALUATION OF MU-DELTA HETERODIMER SELECTIVE ANTAGONISTS

2.1 PART I: INTRODUCTION .....	43
2.1.1 GPCR Heterodimerization .....	43
2.1.2 Mu-Delta Opioid (MDOR) Heterodimers as Distinct Signaling Units	44
2.1.3 Mu and Delta Co-Localization and Physical Interactions.....	46
2.1.4 MOR, DOR and MDOR Distinct Pharmacological Properties and MDOR Disruption.....	47
2.1.5 Background of MDOR Selective Ligands .....	48
2.1.6 Bivalent Ligand Rationale and Design .....	51
2.2 PART II: MATERIALS AND METHODS .....	60
2.2.1 Reagents for Synthesis.....	60
2.2.2 Solid-Phase Peptide Synthesis.....	60
2.2.3 Peptide Purification and Analysis.....	65
2.2.4 Cell Culture .....	65
2.2.5 [ <sup>35</sup> S]-GTPγS Coupling Antagonist Assay .....	66
2.2.6 [ <sup>3</sup> H]-Diprenorphine Competition Binding Assay .....	66
2.2.7 [ <sup>35</sup> S]-GTPγS Mixed Membrane D24M Antagonist Activity.....	68
2.2.8 Tail-flick Antinociception.....	68
2.3 PART III: RESULTS .....	69
2.3.1 Synthesis and Characterization of MDOR Antagonists.....	69
2.3.2 Evaluation of MDOR Cell Line .....	73

### TABLE OF CONTENTS-Continued

2.3.3 Candidate Compounds [ <sup>35</sup> S]-GTPγS Antagonists Activity .....	76
2.3.4 Candidate Compounds [ <sup>3</sup> H]-Diprenorphine Binding .....	78
2.3.5 Mixed Membrane Control – [ <sup>35</sup> S]-GTPγS Antagonist Assay .....	81
2.3.6 Preliminary <i>In Vivo</i> Assessment of D24M .....	82
2.4 PART IV: DISCUSSION AND FUTURE PERSPECTIVES .....	83
2.4.1 Bivalent Ligand Length Dependence vs. Activity Discussion .....	83
2.4.2 Influence of Bivalent Ligand Spacer Properties on Activity .....	84
2.4.3 D24M <i>In Vivo</i> Preliminary Discussion .....	85
2.4.4 MDOR Agonist and Irreversible Antagonist Discussion .....	87
2.4.5 Future Directions and Experiments.....	88
2.4.6 Conclusions .....	93
 CHAPTER 3: BINDING AND FUNCTIONAL EVALUATION OF CLINICAL ANALGESICS AT OPIOID AND ATYPICAL PAIN TARGETS	
3.0 PART I: INTRODUCTION .....	95
3.1 Clinical Opioids – <i>In Vitro</i> and <i>In Vivo</i> Efficacy and Tolerance .....	95
3.1.1 Opioid Efficacy and Potency Between Assays.....	95
3.1.2 Differences in Opioid Tolerance.....	98
3.1.2 Rationale.....	99
3.2 PART II: MATERIALS AND METHODS .....	102
3.2.1 Stable Cell Line Creation.....	102
3.2.2 Membrane Preparations.....	103
3.2.3 Competition Radioligand Binding Assay.....	104

### TABLE OF CONTENTS-Continued

3.2.4 [ <sup>35</sup> S]-GTPγS Coupling Agonist Assays .....	104
3.2.5 Monoamine Transporter Functional Assays.....	105
3.3 PART III: RESULTS .....	106
3.3.1 Cell Line Evaluation.....	106
3.3.2 <i>In Vitro</i> Competition Binding and Functional Activity .....	116
3.3.3 Kappa Opioid Receptor Antagonist Activity .....	118
3.4 PART IV: DISCUSSION AND FUTURE PERSPECTIVES.....	119
3.4.1 Potency, Affinity and Efficacy Discussion.....	119
3.4.2 Differences in Clinical and <i>In Vitro</i> Efficacy .....	120
3.4.3 Clinical Opioid Affinity and Activity at Atypical Targets .....	125
3.4.4 Conclusions .....	129
CHAPTER 4: EVALUATION OF SIGNAL TRANSDUCTION BIAS OF ENDOGENOUS OPIOID PEPTIDES	
4.1 PART I: INTRODUCTION .....	132
4.1.1 Neuropeptides and Signal Modulation.....	132
4.1.2 Opioids and Biased Signaling.....	133
4.1.3 Rationale.....	135
4.2 PART II: MATERIALS AND METHODS .....	137
4.2.1 Reagents for Fmoc Solid Phase Peptide Synthesis (SPPS) .....	137
4.2.3 Peptide Purification and Characterization.....	138
4.2.4 [ <sup>35</sup> S]-GTPγS Agonist.....	138

### TABLE OF CONTENTS-Continued

4.2.5 $\beta$ -arrestin2 Recruitment Assay .....	138
4.2.6 Forskolin-stimulated cAMP Inhibition .....	138
4.2.7 Adenylyl Cyclase (AC) Super Activation.....	139
4.2 PART III: RESULTS .....	140
4.3.1 Biased Signaling of Endogenous Opioid Peptides at MOR, DOR and KOR .....	140
4.3.2 Dynorphin A(1-17) and Dynorphin B(1-13) Induced Internalization at DOR.....	142
4.3.3 Dynorphin A(1-17) and Dynorphin B(1-13) cAMP Inhibition and AC Super Activation.....	143
4.3.4 Dynorphin A(1-17) and Dynorphin B(1-13) Induced Receptor Regulation at DOR.....	143
PART VI: DISCUSSION AND FUTURE PERSPECTIVES .....	148
4.4.1 Bias Factor ( $\beta$ ) of [ $^{35}$ S]-GTP $\gamma$ S Coupling, $\beta$ arrestin2 recruitment and cAMP Inhibition.....	149
4.4.2 Dynorphin A (1-17) and Dynorphin B (1-13) Regulation of DOR.....	150
4.4.3 Future Directions and the Unique Challenges of Endogenous Biased Signaling .....	152
APPENDIX A: Supplementary Data .....	169
References .....	156

## LIST OF TABLES

### CHAPTER 1: INTRODUCTION

Table 1.1. Relative Efficacy ( $\tau$ ) of Various Clinical Opioids for <i>In vivo</i> Antinociception and <i>In Vitro</i> [ <sup>35</sup> S]-GTP $\gamma$ S Coupling .....	35
---	----

### CHAPTER 2: DESIGN, SYNTHESIS AND EVALUATION OF MU-DELTA HETERODIMER SELECTIVE ANTAGONISTS

Table 2.1 Chemical Properties of Bivalent Ligand Spacers .....	57
Table 2.2 Physical Constants and Characterization of Compounds .....	69
Table 2.3 MDOR [ <sup>3</sup> H]-Diprenorphine Saturation Binding.....	73
Table 2.4 CYM51010 MOR, DOR and MDOR [ <sup>35</sup> S]-GTP $\gamma$ S Coupling in MOR, DOR and MDOR Cell Lines.....	74
Table 2.5 Functional [ <sup>35</sup> S]-GTP $\gamma$ S Antagonist Activity and [ <sup>3</sup> H]-Diprenorphine Competition Binding of Potential MDOR Selective Antagonists .....	76

### CHAPTER 3: BINDING AND FUNCTIONAL EVALUATION OF CLINICAL ANALGESICS AT OPIOID AND ATYPICAL PAIN TARGETS

Table 3.1. Relative Efficacy ( $\tau$ ) of Various Clinical Opioids for <i>In Vivo</i> Antinociception and <i>In Vitro</i> [ <sup>35</sup> S]-GTP $\gamma$ S Coupling. ....	97
Table 3.2 Competition Binding and Functional Assay Buffer Composition and Conditions.....	103
Table 3.3 Saturation Binding of Transfected (SERT, NET, DAT and $\sigma$ 1r) and Commercial (CB1 and NOP) Cell Lines .....	109
Table 3.4 Competition Binding of Clinical Analgesics at MOR and 8 Atypical Pain Targets .....	112
Table 3.5 [ <sup>35</sup> S]-GTP $\gamma$ S Coupling of Clinical Analgesics at MOR, DOR, KOR, NOP and CB1 GPCRs .....	114
Table 3.6 Monoamine Transporter Inhibition Functional Assay for Clinical Analgesics at DAT, SERT and NET.....	117

**LIST OF TABLES-continued**

Table 3.7 MOR:Atypical Target Selectivity for Competition Binding (Top) and Functional Assessment (Bottom).....	122
Table 3.8 Clinical Antinociception and <i>In Vitro</i> MOR [ <sup>35</sup> S]-GTPγS Potency Comparison of Selected Clinical Analgesics.....	123

**CHAPTER 4: EVALUATION OF SIGNAL TRANSDUCTION BIAS OF ENDOGENOUS OPIOID PEPTIDES**

Table 4.1 Physical Constants and Characterization.....	137
Table 4.2 Preliminary Screen of Endogenous Opioid Activity at MOR, DOR and KOR.....	140
Table 4.3 Bias Factors (b) for Dynorphin A (1-17), Dynorphin B (1-13) and Leu-Enkephalin at DOR in [ <sup>35</sup> S]-GTPγS, βarrestin2 and cAMP Signaling.....	143
Table 4.4 Sequence of Endogenous Dynorphin and Leu-Enkephalin Peptides.....	151

## LIST OF FIGURES

### CHAPTER 1 – INTRODUCTION

Figure 1.1: Stepwise Clinical Treatments for Chronic Neuropathic Pain. ....	21
Figure 1.2: Opioid Receptor Signaling Pathways.....	24
Figure 1.3 Atypical Targets for Analgesics with Reduced Side Effects.....	31
Figure 1.4 Project Aims to Investigate Opioid Signaling Mechanisms.....	37

### CHAPTER 2: DESIGN, SYNTHESIS AND EVALUATION OF MU-DELTA HETERODIMER SELECTIVE ANTAGONISTS

Figure 2.1. MOR, DOR and MDOR Pharmacological Properties.....	44
Figure 2.2 Bivalent Ligand Design Strategy.....	51
Figure 2.3 Thermodynamic Enhancement for Targeting Heteromers with Bivalent Ligands.....	52
Figure 2.4 Lead Compound Structures .....	56
Figure 2.5 Myc-DOR Flag-MOR CHO Characterization.....	72
Figure 2.6 MDOR [ <sup>35</sup> S]-GTPγS Potency of MOR, DOR and MDOR Agonists vs. βFNA .....	74
Figure 2.7 MDOR Antagonists Target the MDOR <i>In Vitro</i> .....	77
Figure 2.8 MDOR Antagonists Summary for [ <sup>3</sup> H]-Diprenorphine Competition .....	79
Figure 2.9 D24M [ <sup>35</sup> S]-GTPγS Antagonist Potency in MOR+DOR Mixed Membrane .....	80
Figure 2.10 D24M Antagonist vs. CYM51010 Antinociception.....	82
Figure 2.11 MDOR Antagonists IC <sub>50HIGH</sub> vs. Spacer Properties .....	84
Figure 2.12 D24M Lead Compound Structure and Targeted Residues for Structural Modifications .....	92

## LIST OF FIGURES-continued

### CHAPTER 3: BINDING AND FUNCTIONAL EVALUATION OF CLINICAL ANALGESICS AT OPIOID AND ATYPICAL PAIN TARGETS

Figure 3.1 Clinical Opioids Established Activity for Selected Atypical Targets .....	99
Figure 3.2 Clinical Opioids Established Activity for Selected Atypical Targets and Compound Structures.....	100
Figure 3.3 SERT, DAT, NET and $\sigma$ 1R Immunocytochemistry .....	106
Figure 3.4 Monoamine Transporter Optimization for [ $^3$ H]-Mazindol Binding Under Various Conditions .....	107
Figure 3.5 $\sigma$ 1R S:N, pH and Binding Kinetics.....	110
Figure 3.6 Competition Binding of Clinical Analgesics at Nine Different Pain Targets.....	113
Figure 3.7 Functional Activity of Clinical Opioids .....	114
Figure 3.8 KOR [ $^{35}$ S]-GTP $\gamma$ S Antagonist Activity vs. 100 nM U50,488.....	118
Figure 3.9 Clinical Opioids Selectivity for MOR:Atypical Targets.....	120

### CHAPTER 4: EVALUATION OF SIGNAL TRANSDUCTION BIAS OF ENDOGENOUS OPIOID PEPTIDES

Figure 4.1 Opioid Biased Signaling.....	133
Figure 4.2 Endogenous Opioid $\beta$ arrestin2 Recruitment and [ $^{35}$ S]-GTP $\gamma$ S Coupling at DOR .....	142
Figure 4.3. Forskolin-stimulated AC Super Activation .....	144
Figure 4.4: Dynorphin A and B Induced DOR Internalization.....	145
Figure 4.5 Cartoon Representation of Dynorphin A (1-17) and Dynorphin B (1-13) Biases.....	148

**LIST OF SCHEMES****CHAPTER 2: DESIGN, SYNTHESIS AND EVALUATION OF MU-DELTA  
HETERODIMER SELECTIVE ANTAGONISTS**

Scheme 2.1. Bivalent Ligands Synthetic Scheme.....	61
Scheme 2.2. Synthesis of Bivalent Ligands via Fragment Condensation.....	62
Scheme 2.3. Example Synthetic Scheme for Linear Peptide Sequences .....	63
Scheme 2.4. CTAP Synthetic Scheme.....	64

## ABSTRACT

Most clinical opioids produce analgesia through the Mu Opioid Receptor (MOR) providing the only effective treatment for chronic pain patients. These studies explore three pre-clinical strategies to improve MOR analgesia and minimize side effects: 1) compounds that target G-protein Coupled Receptors (GPCRs) heterodimers, such as heterodimerization between the Delta Opioid Receptor (DOR) and MOR (MDOR); 2) multi-functional compounds that target multiple receptor systems for synergistic effects, such as a MOR agonist and a the serotonin reuptake transporter (SERT) inhibitor; or 3) biased agonists that preferentially activate one signaling pathway associated with analgesia over another associated with side effects at the same receptor.

First, several indirect lines of evidence indicate the MOR-DOR heterodimer (MDOR) can regulate MOR opioid tolerance and withdrawal. However, studying MDOR remains difficult because no selective MDOR antagonists are available. To address this need, we created a novel series of bivalent MDOR antagonists by connecting a low affinity MOR antagonist (H-Tyr-Pro-Phe-D1Nal-NH<sub>2</sub>) to a moderate affinity DOR (H-Tyr-Tic-OH) antagonist with variable length polyamide spacers (15-41 atoms). *In vitro* radioligand binding and [<sup>35</sup>S]-GTPγS coupling assays in MOR, DOR, and MDOR expressing cell lines show bivalent ligands produce a clear length dependence in MDOR but not MOR or DOR cell lines. The lead compound – D24M with a 24-atom spacer – displayed high potency (IC<sub>50MDOR</sub> = 0.84 nM) with 91-fold selectivity for MDOR:DOR and 1,000-fold MDOR:MOR selectivity.

Second, clinicians have long appreciated subtle but distinct differences in analgesia and side effects of MOR opioids. A variety of non-MOR targets including

DOR, Kappa Opioid Receptor (KOR), the Cannabinoid Receptor-1 (CB1), the Sigma-1 Receptor ( $\sigma$ 1R), the Dopamine- (DAT), Serotonin- (SERT) and Norepinephrine- Reuptake Transporters (NET) induce analgesia and/or modulate MOR mediated side effects. To determine if different opioid profiles arise from non-MOR interactions, we evaluated the binding and function of nine clinical analgesics at the nine aforementioned targets revealing several clinical opioids contain previously unidentified affinity's or activity's. Hydrocodone displayed low affinity at the MOR ( $K_I = 1800$  nM) and only  $\sim 2$  fold less affinity at the  $\sigma$ 1R ( $K_I = 4000$  nM). Second buprenorphine promoted monoamine influx at DAT, SERT and NET with  $EC_{50} > 1,000$  nM. These novel interactions suggest the nuanced differences of clinical opioids may arise from previously unappreciated off-target effects. Future studies will assess whether these *in vitro* results predict hydrocodone and buprenorphine activity *in vivo*.

Finally, the unique function of the numerous endogenous opioid peptides at a given receptor remains unclear. *How* endogenous ligands interact with ORs produces obvious drug design consequences. These studies show two endogenous Dynorphin analogues – Dynorphin A and Dynorphin B – differentially regulate two ubiquitous signaling modules –  $\beta$ arrestin2 and  $G\alpha_{i/o}$ – at the DOR. Dynorphin A and Dynorphin B swap potency rank orders for  $\beta$ -arrestin2 recruitment and [ $^{35}$ S]-GTP $\gamma$ S signaling, indicating two distinct signaling platforms are formed. Dynorphin A but not Dynorphin B treatment simulated AC super activation, while Dynorphin B internalized DOR better than Dynorphin A. These *in vitro* assays suggest endogenous Dynorphin analogues differentially regulate signals at the DOR *in vitro*. Future work includes further characterizing signaling differences *in vitro* and testing these changes *in vivo*.

### Abbreviations

[ <sup>3</sup> H]-DTG	[ <sup>3</sup> H]-1,3 di-ortho-tolylguanidine
5-HT	Serotonin
5'-NTII	5'-Naltrindole Isothiocyanate
α <sub>2c</sub> -AR	α <sub>2c</sub> -Adrenergic Receptor
AC	Adenylyl Cyclase
ADHD	Attention-Deficit/Hyperactivity Disorder
AT1R	Angiotensin 1 Receptor
β-FNA	Beta-funaltrexamine
Bcp	4'-[N-((4'-phenyl) phenethyl) carboxamido] Phenylalanine
Boc	Tert-butyloxycarbonyl
BOP	Benzotriazol-1-yloxy) tris(dimethylamino)
BRET	Bioluminescence Resonance Energy Transfer
BSA	Bovine Serum Albumin
cAMP	3',5'-cyclic Adenosine Monophosphate
CB1	Cannabinoid 1 Receptor
CBD	Cannabidiol
CHO	Chinese Hamster Ovary cells
Co-IP	Co-immunoprecipitation
CODA-RET	Complemented Donor-Acceptor Resonance Energy Transfer
CPP	Conditioned Place Preference
CTAP	D-Phe-c(Cys-Tyr-D-Trp-Arg-Thr-Pen)-Thr-NH <sub>2</sub>
DA	Dopamine
DAMGO	[D-Ala <sup>2</sup> , N-MePhe <sup>4</sup> , Gly-ol]-enkephalin
DBU	1,8-Diazabicyclo[5.4.0]undec-7-ene
DCM	Dichloromethane
DIC	N,N'-Diisopropylcarbodiimide
DIPEA	N,N-Diisopropylethylamine
DMAP	4-Dimethylaminopyridine
DMEM	Dulbecco's Modified Eagle Medium
DMF	Dimethylformamide
DMT	2,6-dimethyl-Tyrosine
DOR	Delta Opioid Receptor
DPDPE	[2-d-penicillamine,5-d-penicillamine]enkephalin
DTAH	H-DMT-Tic-Ala-OH
DTT	Dithiothreitol
ERK 1/2	Extracellular Signal-Regulated Kinase
F12K	Kaighn's Modification of Ham's F-12 Medium
Fmoc	Fluorenylmethyloxycarbonyl
FRET	Fluorescence Resonance Energy Transfer

GIRKs	G-protein coupled inwardly rectifying K <sup>+</sup> channels
GPCR	G Protein Coupled Receptor
GRKs	G protein-coupled Receptor Kinases
GTPγS	guanosine 5'-O-[gamma-thio]triphosphate
HATU	1-[Bis(dimethylamino)methylene]-1 <i>H</i> -1,2,3-triazolo[4,5- <i>b</i> ]pyridinium 3-oxid hexafluorophosphate
HFIP	Hexafluoroisopropanol
HOAt	1-Hydroxy-7-Azabenzotriazole
HOBt	Hydroxybenzotriazole
HPLC	High Performance Liquid Chromatography
HRMS	High-Res Mass Spectrometry
IBMX	isobutylmethylxanthine
IBS-d	Irritable Bowel Syndrome disorder
ICC	Immunocytochemistry
ICV	Intracerebroventricular
IT	Intrathecal
JNK	c-Jun N-terminal Kinase
KO	Knock-Out animals
KOR	Kappa Opioid Receptor
LRMS	Low-Res Mass Spectrometry
MDAN-21	Naltrindole+oxymorphone with 21 atom spacer
MDOR	Mu-Delta Opioid Receptor Heterodimer
Mdp	(2 <i>S</i> )-2-methyl-3-(2',6'-dimethyl-4'-hydroxyphenyl)-propionic acid
MOR	Mu Opioid Receptor
MS-MS	Tandem Mass Spectrometry
MTT	4-Methyltrityl
NE	Norepinephrine
NMP	N-Methyl-2-pyrrolidone
NOP	Nociceptin Opioid-like Receptor
NSAIDs	Non-Steroidal Anti-Inflammatory drugs
PAG	Periaqueductal Grey
PKA	Protein Kinase A
PKC	Protein Kinase C
PPM	Parts Per Million
PTX	Pertussis-toxin
PyBOP	Benzotriazol-1-yl-oxytrypyrrolidinophosphonium Hexafluorophosphate
PyBROP	Bromo-tris-pyrrolidino phosphoniumhexafluorophosphate
σ1R	Sigma 1 Receptor
SAR	Structure Activity Relationship
SPPS	Solid Phase Peptide Synthesis
tBu	tert-butyl
TCA	Tri-cyclic Anti-depressant

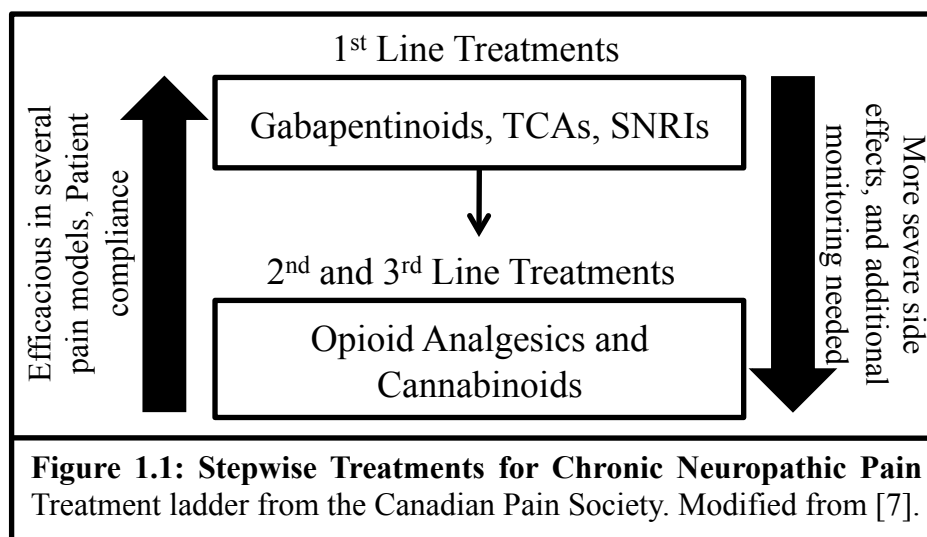
TFA	Trifluoroacetic acid
THC	Delta-9-Tetrahydrocannabinol
TM	Transmembrane
WT	Wild-type

## CHAPTER 1 – INTRODUCTION

### 1.1 Chronic Pain, Treatment Limitations and Opioids

Chronic pain, pain persisting longer than 3 months, affects 100 million Americans, costing the United States ~\$500 billion annually [1]. The prevalence of chronic pain is higher than that of heart disease, cancer, and diabetes combined [2-5], and can strongly diminish patient quality of life [6]. First-line clinical treatments include anticonvulsants and antidepressants, such as gabapentinoids, noradrenaline reuptake inhibitors (SNRIs) and tricyclic antidepressants (TCAs). These show moderate efficacy in randomized controlled trials against multiple pain models, and in general are well tolerated. If a patient does not respond to first line treatments, second-line treatments are tried which include opioids such as morphine or fentanyl, followed by third-line treatments including cannabinoids and stronger opioids (Figure 1.1) [7]. Unfortunately, TCAs and gabapentinoids are effective in only 42-76% of patients, depending on the study, leaving opioids as the primary treatment for many chronic pain patients [8].

While opioids effectively treat acute or post-surgical pain, numerous side effects –



including dependence, tolerance, constipation, nausea, addiction and respiratory depression – limit their long-term use for chronic pain. This limitation is emphasized by patient compliance, which falls to 44% after 7-24 months [8-11]. Furthermore, prescription opioids contribute to the U.S. opioid epidemic. From 1999-2010 opioid related deaths quadrupled [12]; and the percentage of drug related deaths attributed to clinical opioids doubled jumping from 30% to 60% [13]. The opioid crisis and the paucity of effective chronic pain treatments illustrate the need to identify and understand novel atypical pain treatments.

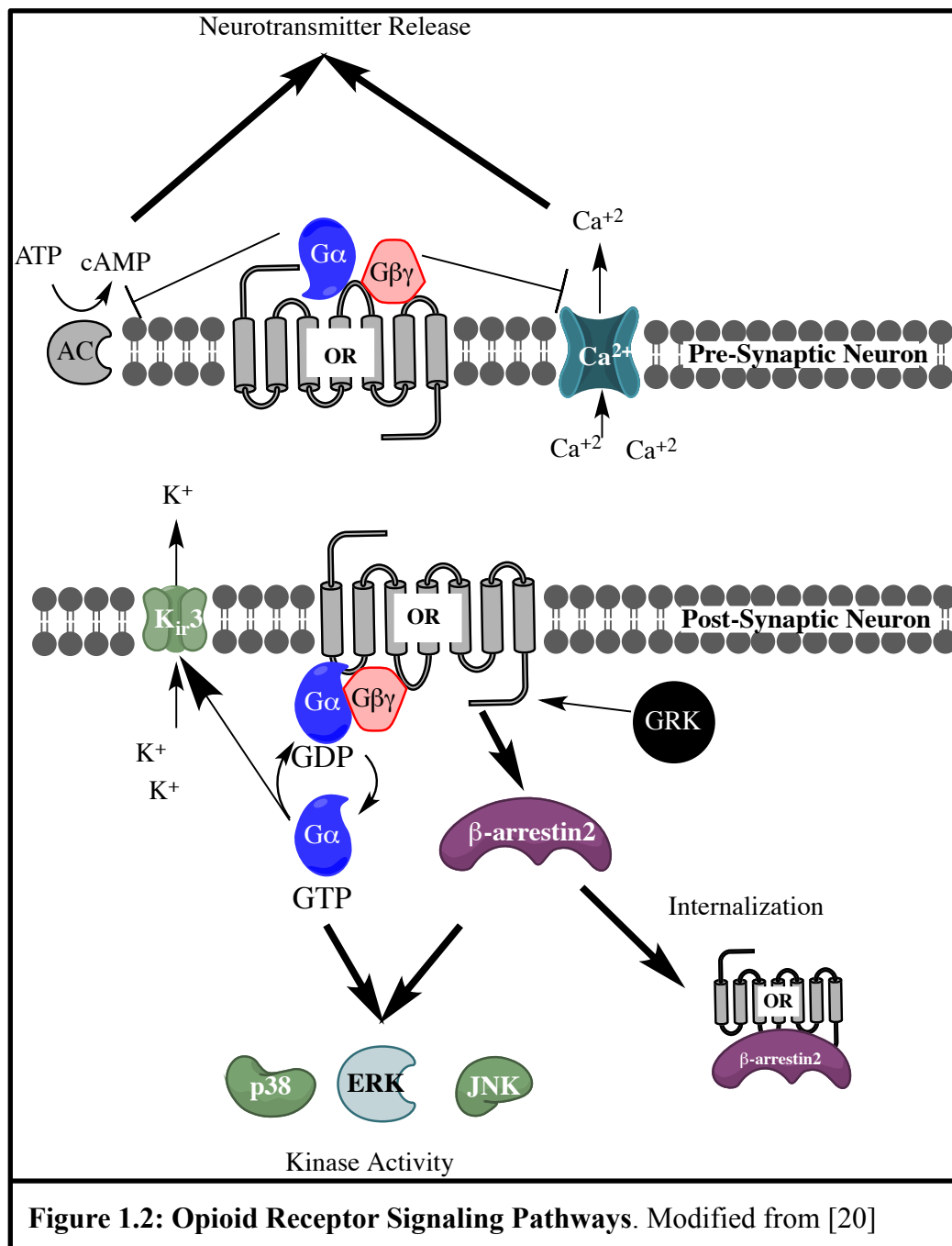
An *atypical target* – as defined in this paper – is a protein that facilitates (or modulates) analgesia and side effects in synergy with or in the absence of Mu Opioid Receptor (MOR) activation. While MOR produces most clinical opioid analgesia and side effects – such as addiction, withdrawal, constipation, etc. – non-MOR targets can modulate the therapeutic profile of MOR agonists (see section 1.3). Treatments acting via novel mechanisms at the MOR or at additional targets involved in pain processing can produce synergistic interactions to enhance analgesia and reduce side effects. For example, co-treatment with cannabinoids and an opioid improves opioid analgesia [14] in chronic pain patients. Multifunctional opioid compounds such as tapentadol – which acts as a MOR agonist and SSNRI – produce greater analgesia than hydromorphone with less adverse gastrointestinal effects than opioids such as fentanyl, hydromorphone or morphine [15].

In order to improve opioid therapeutic profiles, research has focused on several novel pre-clinical strategies including: 1) compounds which target G-protein Coupled Receptor (GPCR) heterodimers, frequently involving the MOR and a second GPCR

protomer; 2) multi-functional compounds, such as ligands that interact with the MOR and delta opioid receptors (DOR) [16], neurokinin-1 receptors (NK-1) [17], or bradykinin receptors (BKs)[18]; or 3) biased compounds which preferentially activate one OR pathway over another. However, the molecular mechanisms that drive these improved therapeutic profiles and different therapeutic profiles (See Section 1.3.2D) of clinical MOR agonists require further investigation.

## 1.2 Opioid receptor signaling

ORs are GPCRs consisting of seven trans-membrane helical proteins; GPCRs make up the largest family of membrane receptors. The opioid GPCR family consists of



four genetic subtypes, MOR, DOR, kappa- (KOR), and nociceptin (NOP)- opioid receptors and are activated by endogenous ligands including the Dynorphin, Enkephalin, Endomorphin and Nociceptin neuropeptides [19]. Upon binding, opioid agonists induce a conformational change in the receptor causing the inhibitory  $G\alpha_{i/o}$  to exchange GDP for GTP (Figure 1.2)[20]. Then the heterotrimeric G-protein disassociates into  $G\alpha_{i/o}$  and  $G\beta\gamma$  subunits, which inhibit cAMP accumulation, deactivate  $Ca^{2+}$  channels or activate G protein gated inwardly rectifying potassium (GIRK) channels. Next, G protein-coupled receptor kinases 2/3 (GRKs) phosphorylate intracellular OR residues, which desensitize the receptor and promote the recruitment of  $\beta$ arrestin2.  $\beta$ arrestin2 is a multifunctional scaffold molecule implicated in opioid mediated tolerance, constipation, dysphoria and nausea, and has a crucial role in receptor internalization.  $\beta$ arrestin2,  $G\alpha_{i/o}$  and  $G\beta\gamma$  act as primary effectors and subsequently modulate numerous kinases including extracellular signal-regulated kinases (ERK 1/2), c-Jun N-terminal kinases (JNKs), protein kinase A (PKA) and protein kinase C (PKC), as well as ion channels (Figure 1.2)[20].

Ultimately, opioids produce analgesia by activating inhibitory molecular pathways, leading to hyperpolarization and reducing the ability of neurons to depolarize and produce action potentials. Opioids hyperpolarize the post-synaptic membrane potential below the normal resting membrane potential of -70 mV, making neurons in pain pathways less likely to transmit pain signals [21]. Pre-synaptic inhibition of  $Ca^{2+}$  channels prevents release of excitatory neurotransmitters, such as Substance P and glutamate. This channel activity – opening GIRKs and inhibiting  $Ca^{2+}$  channels – is required for neuronal inhibition, while in general kinases or  $\beta$ arrestins appear to modulate

receptor and cellular responses to the drug via desensitization, transcriptional changes, receptor internalization, and similar regulatory processes.

### 1.3 Atypical Opioid and Non-Opioid Analgesic Targets

Clinical opioids typically mediate analgesia and their side effects through the MOR [22]. However, the on-going opioid [23] and chronic pain [24] epidemics emphasize the need for opioid and non-opioid analgesics with improved therapeutic profiles – drugs with reduced side effects such as tolerance, respiratory depression, withdrawal and addiction. Chronic opioid treatment results in regulatory changes to the opioidergic and pain systems to compensate for chronic MOR stimulation. In order to minimize these compensatory mechanisms, a variety of *atypical* molecular targets have been added to minimize MOR mediated side effects or enhance analgesia. Novel preclinical lead compounds typically fall into one of the following three categories: *biased signaling* drugs – preferentially activating one pathway over another at a single receptor; *multi-functional* drugs – targeting multiple components of the system independently within the same ligand; and *heteromer selective* drugs.

#### 1.3.1 Multi-functional Analgesic Compounds

Multi-functional compounds – that target the MOR and an additional molecular target – can show synergistic effects over MOR agonists alone. This secondary molecular target may include opioid receptors, the cyclooxygenase (COX) enzymes, cannabinoid receptors, the gabapentinoid molecular target(s), and the monoamine transporters. These targets can be modulated to manipulate the pain response by inhibiting the COX

nociceptive stimulus (NSAIDs), nociceptive spinal signal transduction (TCAs, opioids, gabapentinoids and cannabinoids), or supraspinal processing (TCAs, gabapentinoids opioids, and cannabinoids). One example is tapentadol or tramadol, which target the MOR and the norepinephrine and serotonin reuptake transporters [25]. Various drugs targeting combinations of the aforementioned pain related targets show promising pre-clinical results toward developing effective analgesics with reduced side effects such as withdrawal, tolerance or constipation. This section provides a brief overview of clinical and pre-clinical atypical pain targets and their interactions/synergies with classical MOR opioids.

### *1.3.2 MOR and DOR Synergy, Heterodimerization, and Disease*

One preclinical finding that showed improved MOR agonist profiles was multi-functional compounds targeting the MOR and DOR. While interactions between DOR and MOR clearly contribute to opioid mediated side effects (see below), it remains unclear whether these interactions occur at the molecular level (direct interaction between MOR and DOR), at the cellular level (signaling cross-talk), or at the level of neural circuitry. DOR receptor occupancy – by either agonists or antagonists – can potentiate analgesia and/or reduce MOR mediated tolerance. DOR selective antagonists and DOR KO mice reduce morphine mediated tolerance and dependence [26-29]. However, DOR selective agonists (DPDPE) increase morphine antinociceptive potency and efficacy [30]. These complex interactions between MOR and DOR cannot be explained by a simple positive or negative modulatory effect.

Several series of bifunctional MOR agonist, DOR antagonist compounds retain the above therapeutic profiles [31-36]. These compounds displayed potent antinociception with reduced tolerance, dependence and reward – via conditioned place preference (CPP) in rodent models – while MOR and DOR agonists combined in a single pharmacophore (e.g. MMP-2200 and biphalin) produced antinociception with reduced tolerance, dependence and self administration [37-40]. Collectively, these and related studies indicate a single molecular entity with overlapping MOR agonist and DOR agonist/antagonist pharmacophores may prove useful as therapeutics. The paradoxical nature of DOR agonists and antagonists producing similar (but not identical) improved therapeutic profiles highlights the need to better understand the underlying mechanisms. Whether these synergies arise from molecular interactions (heteromers), cellular crosstalk (downstream signaling), or systems level modulation (neurocircuitry) between MOR and DOR (or other systems) remains to be determined.

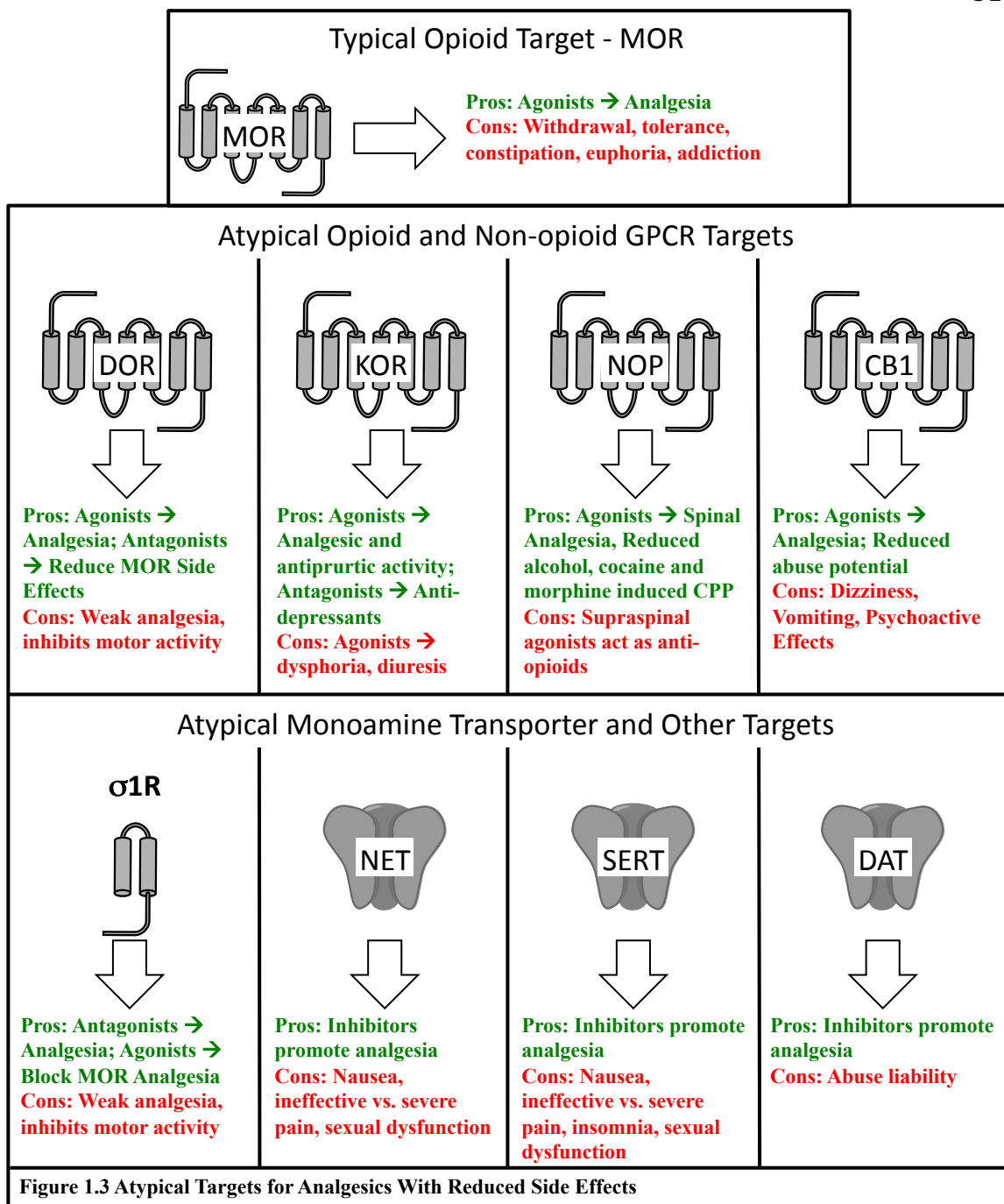
The molecular interaction of MOR and DOR heterodimerization (MDOR) has gained traction in the last decade. *In vitro* cell systems studied using Fluorescence Resonance Energy Transfer (FRET), Bioluminescence Resonance Energy Transfer (BRET), co-Immunoprecipitation, and various other pharmacological methods (see reviews [41, 42]) demonstrate co-proximity and physical interaction between the MOR and DOR, consistent with MDOR heterodimerization. Evidence continues to emerge that the MDOR produces a unique signaling unit with distinct pharmacological profiles *in vitro* (See 2.0.3 for more details). The unique binding and functional properties of MDOR indicate it may provide a suitable drug discovery target.

However, understanding the potential therapeutic and physiological consequences of MDOR remains difficult because no highly selective MDOR ligands exist. Frequently, studies probe MDOR by using various combinations of established MOR and DOR ligands and knockout animals. For example the DOR agonist TAN-67 decreases ethanol consumption in WT but not MOR KO mice in ethanol reward [43]. Similar *in vitro* studies with MOR, DOR and MOR+DOR co-expressing cells suggested this could be heteromer mediated. KO animal studies may produce confounding variables by altering OR expression or trafficking properties; consequently, KO studies require careful interpretation and further validation. Specifically, differentiating between heteromer-mediated and cross-talk is not really possible in these knockout studies. Further, as the authors noted, these type of studies are limited by potential changes of DOR expression in response to ethanol consumption[43]. In a similar vein, co-treatment with methadone (MOR selective agonist) and Naltriben (DOR selective antagonist) stabilizes MOR and DOR membrane expression levels. Co-expression on the membrane produced a shift in analgesic potency; this shift was not observed in methadone only treated animals when MDOR endocytosis occurred [44]. Co-treatment studies produce numerous pharmacodynamic and pharmacokinetic factors that may or may not involve the MDOR. Nonetheless, these studies indicate the MDOR may contribute to tolerant states.

Biochemical approaches to study MDOR take advantage of the putative interfaces between MOR and DOR to disrupt the heteromer. Treatment with a C-terminal tail sequence of DOR can disrupt MDOR formation and reduce antidepressant-like and anxiolytic-like activities induced by the DOR agonist UFP-512 [45]. Similarly, DOR

agonist mediated endocytosis of MOR and DOR in co-expressing cell lines was partially attenuated by treatment with the disruptor peptide sequence encoding MOR transmembrane region 1 (MOR<sup>TM1</sup>). *In vivo* these disruptor sequences reduced antinociceptive tolerance to morphine and enhanced morphine analgesia [46]. The necessity to use MOR or DOR selective agonists after MDOR disruption is a major limitation of these studies because differentiating between MOR and MDOR (or DOR and MDOR) mediated analgesia is very difficult.

However, disruption, co-treatment and knockout techniques may alter OR function by promoting co-degradation or altering with OR receptor levels. Thus more direct probes are needed to understand MDOR function. The lack of selective probes likely contributes to conflicts between different reports. For example, while disruptor sequences may reduce tolerance, MDOR preferring agonists such as CYM51010 show less tolerance than morphine [47]. Similarly MDAN-21 – a bivalent compound with a MOR agonist and DOR antagonist pharmacophore – reduces tolerance and withdrawal in mouse models [48] (see section 2.0.3). However, CYM51010's low selectivity limits its use and MDAN-21's dual agonist and antagonist properties produces uncertain pharmacological properties at MDOR. Thus discovery of MDOR selective ligands (agonists and antagonists) with clearly identified molecular pharmacology is required to test the above therapeutic and regulatory role of MDOR.



### 1.3.2 Atypical Targets for Pain Treatment

MDOR is one of many atypical targets implicated in pain research. These atypical target interactions can arise at the molecular, cellular or circuitry level, as discussed above. The following section reviews co-treatment studies, the development of

multivalent ligands, and related studies identifying atypical targets with desirable properties (Figure 1.3). Multivalent targets such as BK, NK-1 or cholecystokinin (CCK) are beyond the scope of this section and have been reviewed elsewhere [16, 17, 49].

### 1.3.2A Monoamine transporters

Dopamine (DA), norepinephrine (NE), and serotonin (5-HT) are amino acid derivatives, which activate inhibitory GPCRs, the D<sub>2</sub>, 5-HT<sub>1,5</sub>, and  $\alpha_2$ , respectively [50, 51]. To terminate neurotransmitter signaling after release into the synaptic cleft, 5-HT, NE and DA are transported back into the pre-synaptic cell by SERT, NET and respectively. Reuptake inhibitors increase neurotransmitter synaptic concentrations, reuptake transporters have been identified as therapeutic targets for pain, *attention-deficit/hyperactivity disorder* (ADHD) and affective disorders such as depression [52, 53]. 5-HT and NE antinociception [54] is mediated via  $\alpha_2$ -adrenergic or 5-HT receptors [55, 56], and these effects are reversed by their respective antagonists [51, 54, 57]. Monoamine transporter and MOR interactions are observed with the TCA amitriptyline (a SERT and NET inhibitor), which attenuates morphine tolerance while preserving its antinociceptive effect during co-treatment [58]. Several new clinical opioids – tapentadol and tramadol – take advantage of these effects, by utilizing multi-functional activities acting as SERT and NET reuptake inhibitors and MOR agonists. These compounds produce efficacious analgesia with reduced drug abuse liability [25]. The relatively low potency of tapentadol and tramadol at MOR, SERT and NET indicates that synergy between the monoamine transporters and MOR efficiently amplifies MOR analgesia while minimizing side effects such as abuse potential.

### *1.3.2B Atypical GPCR Targets – KOR, NOP and CBI*

Several additional opioid or opioid-like GPCRs induce analgesia and can modulate MOR activities – namely DOR (discussed in Section 1.3.1), the kappa opioid receptor (KOR) and the nociceptin opioid receptor (NOP). KOR agonists produce analgesia, antipruritic activity and abolish MOR-agonist mediated reward [59]. However, KOR drug development is most notably limited by dysphoric side effects [60] (See overview [61]). Recent studies indicate biased KOR agonists can tease apart the dysphoric and analgesic components in pre-clinical models [62] (see section 1.3.3 for biased signaling overview). Furthermore, KOR antagonists block stress-induced reinstatement of several drugs (such as cocaine and ethanol) while blocking MOR and cannabinoid withdrawal symptoms [63].

Similarly, the Nociception opioid receptor (NOP) – a non-opioid member of the opioid receptor family [64] – modulates reward by reducing CPP to cocaine [65], alcohol[66] and morphine[67] (see review [68]). While spinal NOP agonists mediate antinociception in a similar manner to classical opioids – through reducing cAMP, closing voltage gated Ca<sup>+</sup> channels and opening GIRKs - supraspinal NOP agonists act as anti-opioids blocking MOR mediated actions and producing hyperalgesia [66]. Taken together, atypical ORs including DOR, KOR and NOP can modulate MOR mediated effects or induce similar effects on their own. These opioid and opioid-like receptors can modulate addictive liabilities while producing some analgesia.

A non-opioid family GPCR that modulates analgesia and reward that has gained much recent attention is the cannabinoid-1 receptor (CB1). Cannabinoids including delta-

9-tetrahydrocannabinol (THC) and cannabidiol (CBD) have been used for thousands of years. Clinical evidence supports cannabinoid efficacy for treating chronic pain, cancer pain, headache, epilepsy and depression in some patient populations while significantly reducing abuse potential relative to opioids [69-71].

### *1.3.2C Sigma1 Receptors*

The sigma1 receptor ( $\sigma$ 1R) is an intracellular chaperone protein that was initially mistaken as an opioid receptor due to some opioid ligand cross-reactivity [72]. Activation of the  $\sigma$ 1R as chaperone helps assist in the proper folding and trafficking of proteins synthesized in a cell.  $\sigma$ 1R agonists are generally considered to increase intracellular  $\text{Ca}^{2+}$  and modulate  $\text{IP}_3$ , NMDA, GABA and potassium channels (see review [73]).  $\sigma$ 1R agonists produce pro-nociceptive effects, while  $\sigma$ 1R antagonists produce antinociception and can enhance morphine-mediated analgesia [74, 75]. In summary, MOR-mediated effects can be modulated by numerous atypical targets including KOR, DOR, CB1, NOP, NET, SERT, DAT and  $\sigma$ 1R (Figure 1.3) producing important differences in behavioral and physiological outcomes.

### *1.3.2D Clinical opioid therapeutic profiles incompletely explained by MOR activity*

Classically, clinical opioids act through MOR. However, clinicians have long appreciated subtle but important differences between opioids – particularly that different patients frequently show varied analgesic and side effects to the same opioid [76]. Opioid rotations, which change a patient's opioid every few months to minimize the development of tolerance and other side effects – suggest some opioids may also interact

with atypical or non-MOR targets [77]. Interestingly, the efficacy ( $\tau$ ) of *in vitro* GTP $\gamma$ S coupling and *in vivo* antinociception show different rank orders for the same opioids (Table 1.1) [78-82]. For example, *in vitro* morphine's  $\tau = 2.8-3.9$  which is less potent than oxycodone  $\tau = 5.1 (0.2)$ . However, in antinociceptive assays oxycodone's  $\tau = 19-21$  and significantly lower than morphine's  $\tau = 38-41$  (Table 1.1); a similar disparity occurs with fentanyl and etorphine. Furthermore, while methadone and morphine have similar antinociceptive  $\tau$ 's, morphine's  $\tau$  is significantly less than methadone *in vitro*. Based on these subtle differences between *in vivo* antinociceptive and *in vitro* signaling efficacy, we assessed clinical opioids for affinity and activity at for nine clinical analgesics.

### 1.3.3 Biased signaling

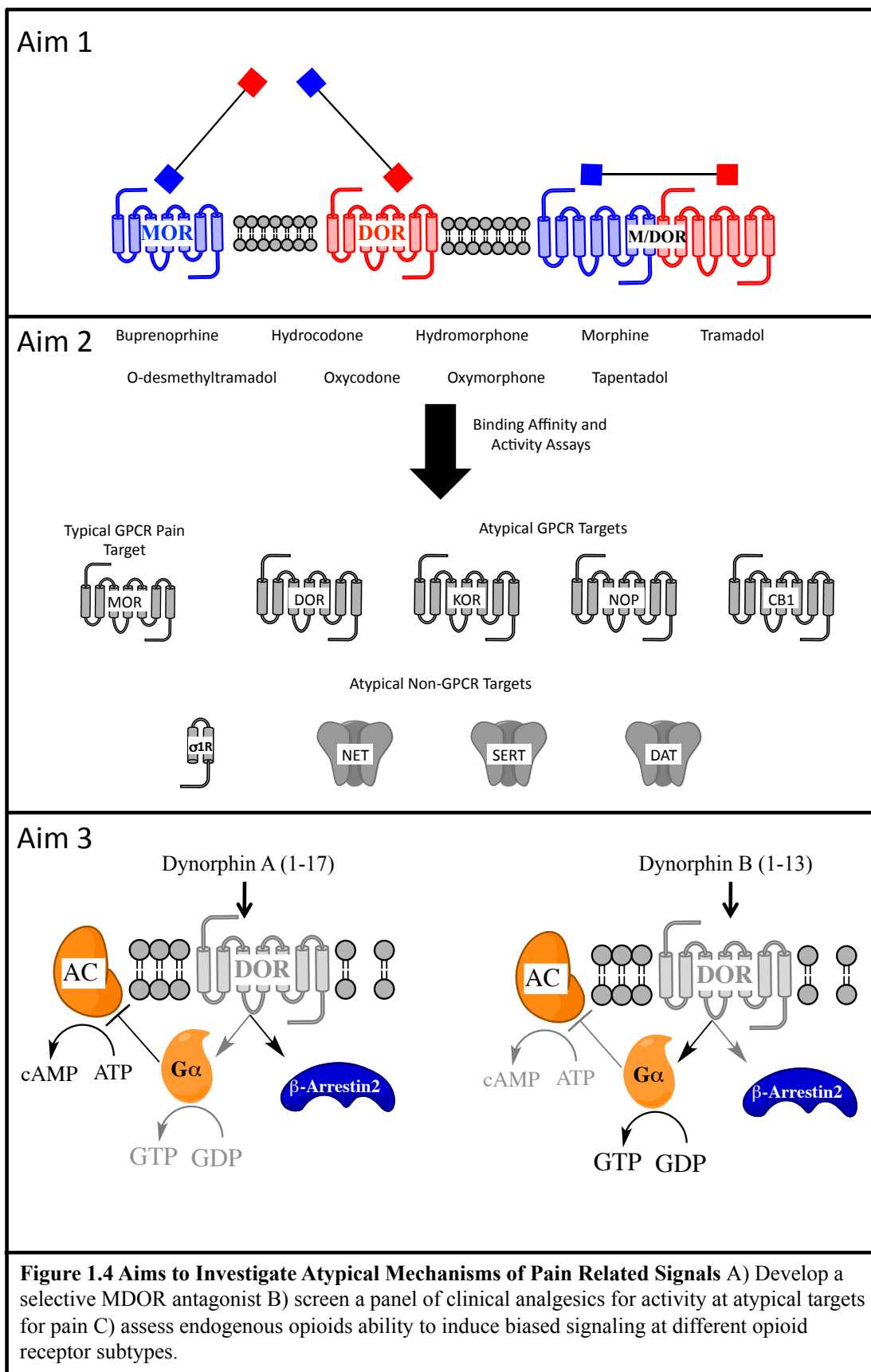
Classically, agonists bind to their cognate receptor and induce all downstream pathways – more-or-less to the same extent, with most differences attributable to differences in coupling efficacy or different receptor populations [83]. However, different signaling cascades at MOR may induce distinct aspects of the drug response – such as  $G\alpha_{i/o}$  mediating analgesia and  $\beta$ arrestin2 mediating side effects such as tolerance and withdrawal. These mechanisms were hypothesized based on  $\beta$ arrestin2 KO mice showing

Ligand	<i>in vivo</i> Antinociception		<i>in vitro</i> [ <sup>35</sup> S]GTP $\gamma$ S	
	$\tau$	Cite	$\tau$ (SEM)	Cite
Fentanyl	54-62 <sup>a</sup>	79	12.3 (0.6)	78
Etorphine	48-57 <sup>a</sup>	80	17.5-24.9 <sup>a</sup>	80
Methadone	35-44 <sup>a</sup>	81	18.2 (0.9)	78
Morphine	38-41 <sup>a</sup>	80	2.8-3.9 <sup>a</sup>	80
Oxycodone	19-21 <sup>a</sup>	80	5.1 (0.2)	78

**Table 1.1. Relative efficacy ( $\tau$ ) of Various Clinical Opioids for *In vivo* Antinociception and *In Vitro* [<sup>35</sup>S]-GTP $\gamma$ S Coupling <sup>a</sup>95% Confidence Intervals**

enhanced analgesia in response to morphine [84] and reduced respiratory depression, constipation, dependence and tolerance in  $\beta$ arrestin2 KO mice [85, 86].

Subsequent drug discovery efforts identified several **biased ligands** [87, 88], which prefer  $G\alpha$  stimulation to  $\beta$ arrestin2 recruitment [84], which would be hypothesized to produce potent analgesia and reduced side effects. Several labs have identified  $G\alpha$  biased ligands that show minimal  $\beta$ arrestin2 recruitment, including herkinorin [89, 90], TRV130 [91] and PZM21 [92]. *In vivo* treatment with these drugs produces some of the predicted side effect profiles from  $\beta$ arrestin2 KO mice. PZM21 did not induce conditioned place preference (CPP) in mice, while PZM21 and TRV130 reduced respiratory suppression and constipation in mice [91, 93, 94]. In clinical trials, TRV130 showed enhanced analgesia and reduced nausea in small group Phase I clinical trials [95, 96] but no difference in Phase II clinical trials. Nonetheless, preclinical and cellular models indicate that biased ligands can produce distinct physiological responses, which could produce analgesics with an improved therapeutic index.



## 1.4 Aims

The emerging relevance of *atypical* targets capable of contributing to or improving analgesics – heteromer selective ligands, multi-functional ligands or biased agonists - led us to pursue these three mechanisms to better understand the biology of opioid-mediated signaling. First, we designed and synthesized a first-in class selective MDOR heterodimer antagonist as a tool to better evaluate the role of MDOR *in vivo* (Figure 1.4 – Aim 1). Second we investigated nine clinical opioids for binding affinity and functional activity at MOR and 8 other atypical targets involved in the modulation of pain or MOR mediated side effects (see section 1.3.2) (Figure 1.4 – Aim 2). Third, we assessed whether a panel of endogenous opioids displayed functionally selective signaling between  $G\alpha_{i_o}$  signaling and  $\beta$ arrestin2 recruitment, and whether these differences corresponded to distinct receptor regulatory processes (Figure 1.4 – Aim 3).

**1.4.1 Aim 1: Design, synthesize and evaluate the *in vitro* and *in vivo* selectivity of an MDOR antagonist.** *Challenge and Background:* Opioid receptors have been shown to physically and functionally interact with each other, and studies have shown that the MOR and DOR heterodimerize to form a distinct molecular unit (MDOR) with distinct binding, signaling, and behavioral characteristics vs. MOR or DOR homomers alone [97]. However, the current methodologies to interrogate the role of MDOR are limited to *in vitro* models, an antibody [98], or a few mono- or bivalent agonists [47, 48, 99]. No selective antagonists for MDOR have been developed. Thus, while compelling evidence demonstrates that MDOR can form *in vitro* and *in vivo* [46, 100], current tools are inadequate to determine how MDOR affects processes such as pain, dependence, and

reward – and if MDOR antagonists could, in principle, serve as effective therapeutics.

*Goal:* To address this need, we synthesized a series of selective MDOR peptidic antagonists by linking MOR (H-Tyr-Pro-Phe-D1Nal-NH<sub>2</sub>) and DOR (H-Tyr-Tic-OH) antagonist pharmacophores with varying length spacers. Such bivalent ligands are expected to induce MDOR selectivity over MOR or DOR because of the well-established avidity phenomena – in which physically linking pharmacophores for two independent sites causes a synergistic affinity increase relative to either active site alone [101, 102].

*Methodology and Results:* Candidate compounds were assessed *in vitro* using [<sup>3</sup>H]-Diprenorphine competition binding and [<sup>35</sup>S]-GTP $\gamma$ S coupling in MOR, DOR, and MDOR expressing cell lines. *In vitro* screening of MDOR antagonism and affinity showed a clear length dependence in MDOR but not MOR or DOR cell lines, strongly supporting MDOR selectivity of the bivalent compounds. We identified a lead compound – D24M with a 24-atom spacer – which displayed high potency (IC<sub>50</sub>MDOR = 0.84 nM) with 91-fold selectivity for MDOR:DOR and >1:1,000 MDOR:MOR selectivity. Preliminary tail-flick anti-nociceptive assays indicated that D24M blocks CYM51010 mediated antinociception – a compound previously reported to mediate antinociception through MDOR. This first-in-class MDOR antagonist will enable future studies to directly probe how MDOR influences opioid behaviors such as antinociception, withdrawal and tolerance.

**1.4.2 Aim 2: Evaluate 9 clinical analgesics for activity and affinity at 8 atypical targets involved in pain.** *Challenge and Background:* A variety of non-MOR targets including monoamine transporters, DOR, CB1 and  $\sigma$ 1R can induce analgesia and/or

modulate MOR mediated effects – such as tolerance and withdrawal. Clinically, physicians have long appreciated subtle but distinct differences in analgesia and side effects of MOR opioid targets [76]. Thus we evaluated the binding and function of nine clinical analgesics at nine different molecular targets involved in pain.

*Methodology and Results:* Nine clinical analgesics – buprenorphine, hydrocodone, hydromorphone, morphine, O-desmethyltramadol, oxycodone, oxymorphone, tapentadol, and tramadol – were assessed for *in vitro* competition binding and [<sup>35</sup>S]-GTPγS activity at five GPCRs, – MOR, DOR, KOR, NOP, CB1; binding and modulation of transporter function was assessed at three neurotransmitter transporters – SERT, NET, and DAT; and for competition binding at the intracellular transmembrane protein σ1R. Interestingly, high concentrations of buprenorphine activated DAT, SERT and NET transport and acted as an inverse agonist at CB1; hydrocodone displayed nearly equal affinity at σ1R and CB1 agonist activity to MOR.

### **1.4.3 Aim 3: Evaluate an array of endogenous opioid peptides at the MOR, DOR and KOR opioid receptors for functionally selective signaling and regulation via Gα and βarrestin2 mediated pathways.**

*Challenge and background:* Classically, opioid-mediated effects occur via three OR subtypes – DOR, MOR and KOR. While endogenous opioid peptides were initially thought to selectively activate one receptor, subsequent studies demonstrate most endogenous peptides display limited receptor subtype selectivity. Independently, investigations studying opioid mechanisms and drug development independently revealed most endogenous neuropeptides bind to and activate most opioid subtypes, and several exogenous ligands can preferentially activate certain

signaling pathways over others at the same receptor – a phenomenon defined as biased signaling. However whether or not endogenous opioid peptides display biased signaling is largely unanswered in the literature, particularly at the DOR.

*Methodology and Results:* To address this question, we assessed a variety of endogenous opioids – including Endomorphin-1, Endomorphin-2, Met-enkephalin, Leu-Enkephalin,  $\beta$ endorphin(1-31),  $\alpha$ endorphin, DynorphinA(1-17) and DynorphinB(1-13) for  $G\alpha$  signaling and  $\beta$ arrestin2 recruitment at MOR, DOR and KOR to test for functional selectivity. Three-fold pathway differences in potency with the dynorphins at DOR were further assessed for downstream receptor mediated consequences to test if modest functional selectivity at the receptor potentiated larger downstream effects.

**CHAPTER 2:****DESIGN, SYNTHESIS AND BIOLOGICAL EVALUATION OF MDOR  
HETERODIMER SELECTIVE ANTAGONISTS**

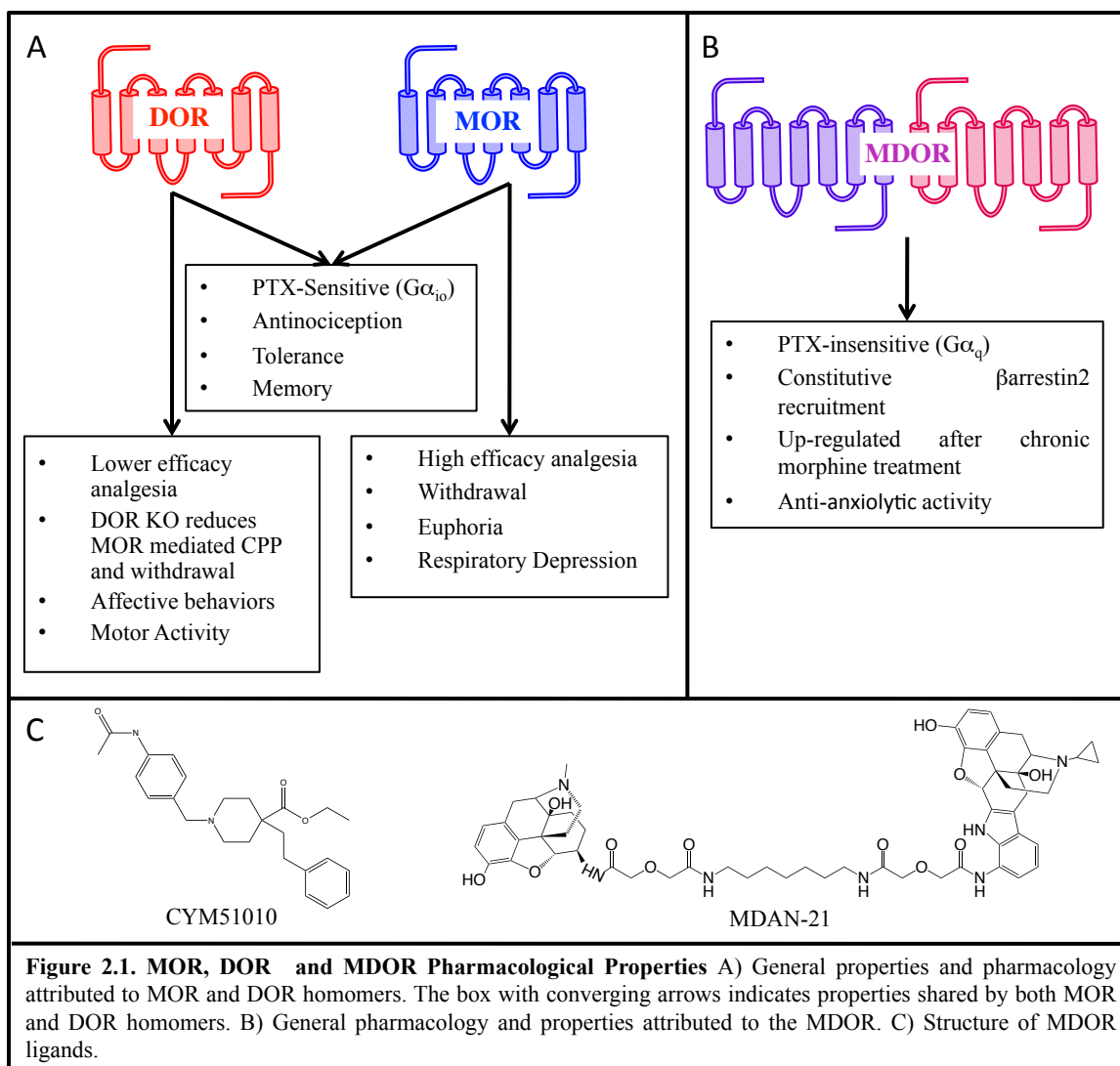
## **PART I: INTRODUCTION**

### *2.1.1 GPCR Heterodimerization*

FRET, BRET, and Co-IP methodologies show different GPCRs co-expressed in the same cell may physically interact and alter binding properties at the respective receptor. Traditionally, demonstrating that two protomers (individual GPCRs) form a heterodimer requires three criteria (see review [41]):

1. First, the two protomers must co-localize and physically interact.
2. The heteromer and protomers must show distinct pharmacological properties such as alterations in ligand binding, signaling, etc.
3. Disrupting the heteromer leads to loss of the distinct pharmacological properties observed in criteria (2).

An array of first generation tools – such as low selectivity ligands, heteromer-selective antibodies, and knockout animals – demonstrated the importance of GPCR heteromers. However, the absence of highly selective heteromer agonists and antagonists makes studying *in vivo* behaviors and signaling profiles difficult because homomer agonists cannot differentiate between protomer and heteromer activities. Consequently, the design of second-generation tools with improved selectivity and detailed pharmacological characterizations is required. Initial studies show that MOR and DOR (MDOR) heterodimerize *in vitro* and may induce distinct behavioral consequences *in vivo*.



### 2.1.2 Mu-Delta Synergy and Heterodimers as Distinct Signaling Units

*In vivo* and *in vitro* studies demonstrate that MOR and DOR interact with one another as knock-out (KOs) or selective ligands at one receptor modify the others' function (Figure 2.1, left). For example, modulating DOR enhances morphine's therapeutic profile. In DOR knockout (KO) mice, morphine produces less tolerance [27] and increases morphine-induced locomotor activity after continual treatment compared to wild-type (WT) [103]. DOR KO and pretreatment with the irreversible DOR antagonist 5' naltrindole isothiocyanate (5'-NTII) reduces morphine-mediated withdrawal [104] and

conditioned place preference (CPP), suggesting reduced abuse liability [103]. In MOR KO mice, DPDPE (a DOR selective agonist) retains its median effective dose (ED<sub>50</sub>) for tail flick antinociception [105] and reduces Deltorphin-II (DOR selective agonist) mediated respiratory depression relative to WT [106]. Collectively, these studies indicate MOR or DOR selective ligands mediate antinociception through their respective receptor. However side effect profiles – such as withdrawal, tolerance reward and respiratory depression – involves both receptors.

Co-treatment with selective MOR and DOR ligands reveals several synergistic interactions. For example, antinociception of MOR-selective agonists DAMGO and morphine is potentiated by non-antinociceptive doses of the DOR selective agonists DPDPE and Deltorphin-II [107, 108]. ICV co-administration of morphine with DOR agonists shifts antinociceptive potency and efficacy; DPDPE increases morphine potency and improved efficacy upon increased stimulus – a shift that was reversible by the DOR selective antagonist ICI 174,864 [107]. Co-treatment of MOR agonists and DOR antagonists reduces tolerance, dependence [99] and drug-seeking behavior [109]. These synergistic interactions between MOR and DOR formed the basis to design multivalent drug candidates with both MOR and DOR activity.

The subsequently identified multifunctional compounds with MOR agonist activity and DOR agonist/antagonist activity show promising pre-clinical profiles (Reviewed [16, 110]). In general, mixed activity profiles produce analgesia with reduced respiratory depression, constipation and physical dependence, suggesting a therapeutic profile for producing antinociception with fewer withdrawal symptoms than traditional

opioids. However, whether these benefits arise from MOR and DOR interactions at the molecular, cellular or circuitry level remains an open question.

### 2.1.3 MOR and DOR Physical Interaction and Co-Localization

A plethora of *in vitro* evidence shows MOR and DOR heterodimerize to form MDOR *in vitro*. BRET studies shows MOR and DOR induce a specific and saturable physical proximity consistent with heterodimerization [111]. To study MDOR in tissue, a specific antibody was developed to label and quantify MDOR [98]. Using this antibody, studies revealed chronic morphine treatment up regulates MDOR in the medulla and other pain regulatory brain regions suggesting a potential role for MDOR in tolerance. The epitope requires proximal MOR and DOR sequences demonstrating the two receptors physically interact in tissue and that chronic opioid treatment modulates MDOR levels.

MOR and DOR are frequently co-expressed throughout the central nervous system. Double knock-in mice with mCherry-MOR and GFP-DOR found 43% of neurons expressing GFP-DOR co-express mCherry-MOR[100], and 35% of mcherry-MOR receptors express GFP-DOR[100]. Neurons co-expressing MOR and DOR occurred in important regulatory pain regions such as the medulla, periaqueductal gray (PAG), and pons in the brain. The ability of this system to elucidate physical interactions was validated with Co-IP in the hippocampus, showing MOR and DOR physically interact in some native tissue and that MDOR could occur in these regions. While co-localization meets heteromer criteria #1 (Section 2.0.1), the functional consequences of MDOR remain difficult to dissect. Convincing evidence of criteria #2 and #3 is lacking

due to a lack of specific pharmacological tools (i.e. selective agonists and antagonists) that limit directly studying MDOR behaviors.

#### *2.1.4 MOR, DOR and MDOR Distinct Pharmacological Properties and MDOR Disruption*

Importantly, MOR and DOR co-expression generates a novel pharmacological target with unique receptor binding properties [97, 112] and distinct signaling scaffolds compared to MOR or DOR alone [113]. In cells co-expressing MOR and DOR, DAMGO (a MOR agonist) affinity is lower than in MOR only cells which was partially restored by truncation of the DOR C-terminus – a putative interface of MDOR heterodimerization [114]. Concurrently, MOR and DOR co-expression cause Deltorphin-II cAMP inhibition to switch from a  $G\alpha_{i/o}$  PTX-sensitive to a  $G\alpha_z$  PTX-insensitive mechanism. Additional *in vitro* studies shows MDOR constitutively recruits  $\beta$ arrestin2 providing further evidence that MDOR represents a unique pharmacological target [97]. Taken together, these studies indicate MDOR induces a unique pharmacological profile that is distinct from either MOR or DOR alone.

The available genetic, chemical, and immunochemical methodologies offer compelling evidence that MDOR modulates fundamental opioid effects including tolerance [48], drug-seeking behavior [43], withdrawal [99], antidepressant-like [45], anxiolytic-like [45], and anti-nociceptive effects [47] (*see sec. 1.3.1* for MDOR in disease). Usually, MDOR is studied *in vivo* by disrupting MDOR via MOR or DOR KO, or an antibody with uncertain pharmacological consequences. Several labs also identified peptide disruptor sequences such as the first transmembrane region of MOR

(MOR<sup>TM1</sup>)[46], to indicate MDOR disruption can enhance morphine analgesia while reducing tolerance. Together, these studies suggest MDOR contributes to tolerance and opposes opioid analgesia.

### 2.1.5 Background of MDOR Selective Ligands

The aforementioned indirect methods – KO, co-expression, disruptor sequences, an antibody, etc. – to study MDOR led several groups to pursue MDOR selective ligands. Conceptually, heterodimer selective ligands can be classified two ways: 1) A single molecule consisting of two pharmacophores separated by an appropriate length spacer promoting simultaneous binding to both active sites or, 2) a single molecule which prefers one (or both) protomer(s) in the heterodimer conformation. While these distinctions aren't necessarily mutually exclusive, they provide a useful framework for understanding heteromer ligands. Option 1 exploits the chemical phenomenon of *avidity* – in which binding the first site promotes binding to the second site. *Avidity* is a general ligand development strategy to improve compound selectivity by targeting two proximal sites in fields ranging from kinase inhibitors to GPCRs (reviewed [115, 116]). Option 2 may improve heteromer affinity through enhanced re-binding – when the ligand disassociates from one protomer it can rebind the second easier. Additionally, these single pharmacophores may show improved selectivity for either or both protomer conformations specific to the heteromer.

A few MDOR-preferring agonists suggest MDOR's therapeutic potential. CYM51010 was identified by screening a small molecule library in a  $\beta$ arrestin2 recruitment assay to show a modest 1:4:6 MDOR: MOR: DOR potency selectivity and

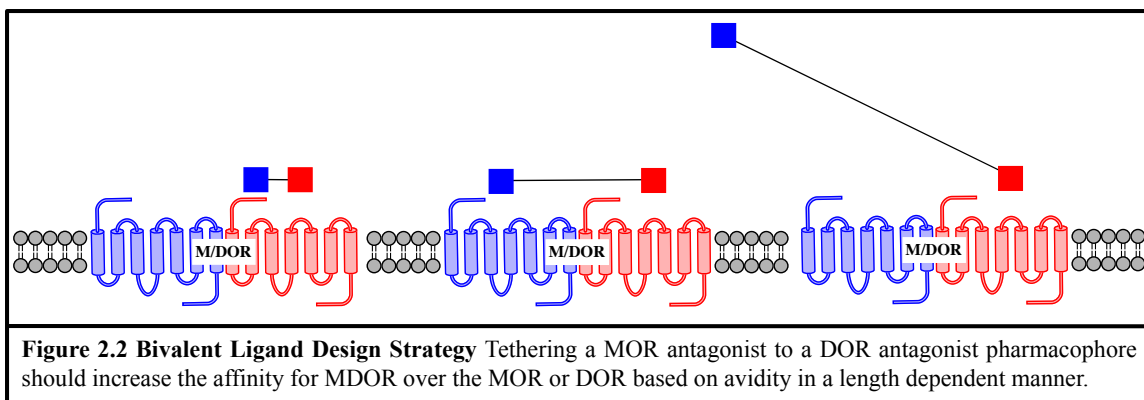
greater efficacy in cells co-expressing MOR and DOR versus MOR or DOR alone [47]. Similarly, eluxodoline preferentially activates signal transduction in cells co-expressing MOR and DOR, and recently passed Phase II clinical trials for treating irritable bowel syndrome disorder (IBS-d) [117-119]. Eluxodoline is a mixed MOR agonist and DOR antagonist, meaning the study of its *in vivo* profile requires careful consideration of three distinct targets – MOR, DOR, and MDOR. Unfortunately, multiple targets and mixed activities make interpreting eluxodoline results difficult. Without an MDOR selective antagonist, differentiating between downstream and heteromer-mediated effects is tenuous, at best. Nonetheless, these studies suggest MDOR selective drugs may provide useful therapeutics.

Portoghese and colleagues developed bivalent ligands containing the MOR agonist oxymorphone linked to the DOR antagonist naltrindole separated by a spacer. All bivalent ligands in this series showed enhanced analgesia and reduced tolerance relative to morphine, with spacer length correlating to increased potency and decreased tolerance [48]. The longest spacer tested of 21 atoms (MDAN-21) showed the highest potency and greatest reduction in tolerance. Follow-up studies reveal that MDAN-21 reduced MDOR internalization relative to mixed or single treatment with the parent pharmacophores, indicating reduced MDOR internalization may limit *in vivo* tolerance to opioids [120].

Differentiating between MOR, DOR and MDOR mediated effects remains difficult even with MDAN-21 and disruptor peptides (Section 2.0.4) because their uncertain pharmacology limits clear interpretations of the results. For example, MDAN-21 may disrupt the heteromer and the compounds selectivity *in vitro* have not been reported (to our knowledge). On the other hand, disruptor sequences may block one

MDOR interface but allow other contact points to facilitate MDOR formation. Most importantly to future drug development, the mechanism of MDOR effects are not understood because 1) most MDOR compounds show less than 10 fold *in vitro* selectivity (if tested *in vitro*), and 2) the functional consequences of connecting an MOR agonist to a DOR antagonist remains unclear. Specifically, the simultaneous occupation of an agonist and antagonist at MDOR produces an unclear change in OR signaling. Consequently, differentiating between MOR, DOR and MDOR mediated effects remains particularly difficult, especially *in vivo*. While CYM51010 is a useful lead compound and MDAN-21 a useful potential therapeutic, more selective tools, particularly antagonists, are required to elucidate the role of MDOR.

A MDOR selective antagonist would enable MDOR studies using classical pharmacological models and methodologies to explore MDOR mediated effects. Furthermore, an MDOR selective antagonist may provide a useful therapeutic target to treat addiction [43], withdrawal [121] and opioid tolerance [48]. Thus, a selective MDOR antagonist is needed to 1) differentiate between MDOR, MOR, and DOR-mediated consequences, which is currently difficult, especially *in vivo*; 2) offer a pharmacological tool to investigate MDOR function *in vivo*; and 3) determine the therapeutic potential of an MDOR antagonist for treating opioid tolerance and drug seeking behavior.

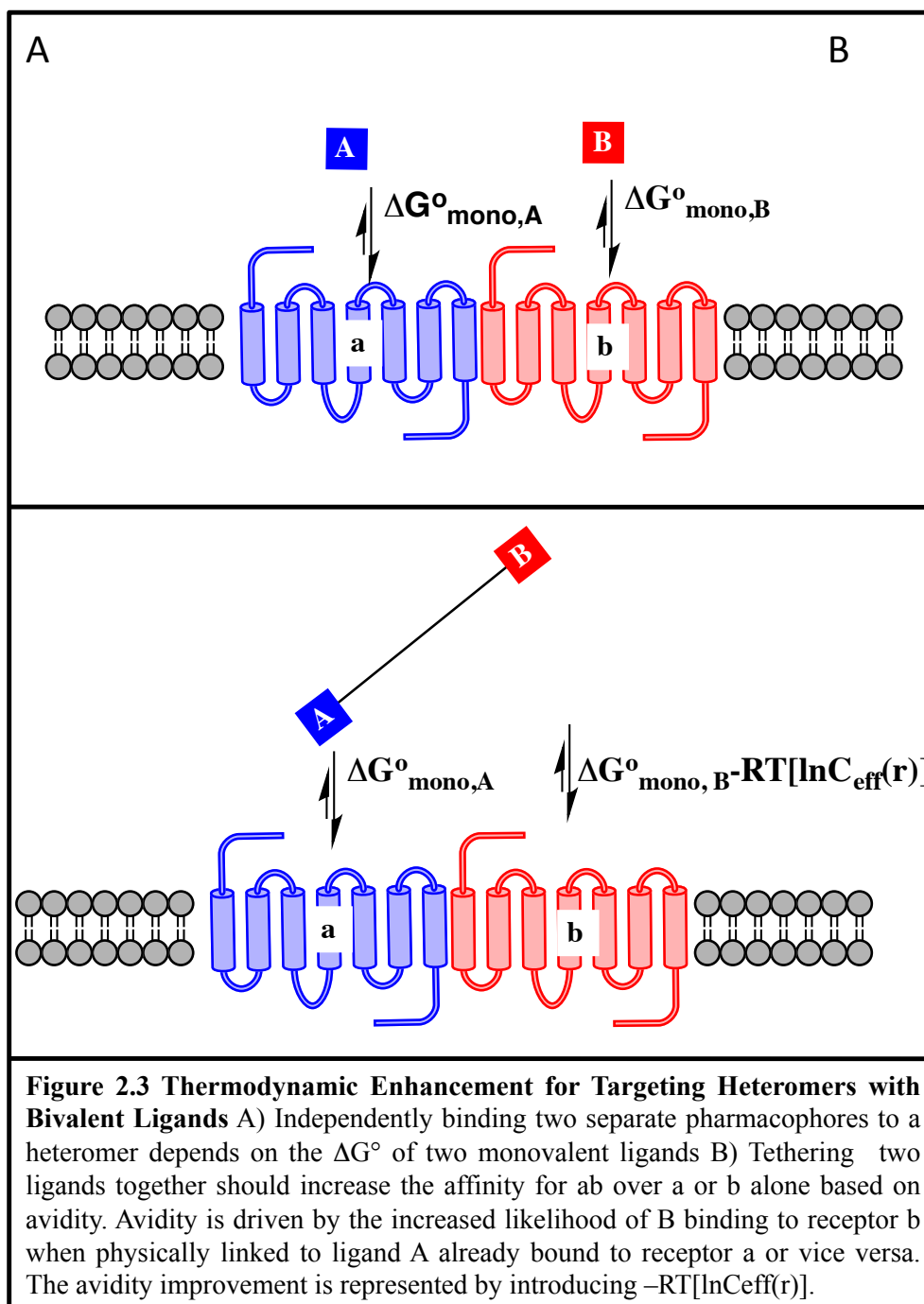


### 2.1.6 Bivalent Ligand Rationale and Design

To address this need, we synthesized a series of hetero-bivalent ligands consisting of a DOR antagonist and MOR antagonist pharmacophore physically linked by a spacer. We hypothesized that *avidity* – a phenomenon in which the binding of one pharmacophore promotes the binding of a physically linked second pharmacophore [101] – would imbue MDOR selectivity (Figure 2.2). Using this strategy, we connected a moderate affinity DOR antagonist pharmacophore [Tyr-Tic-OH][122] to a low-affinity MOR antagonist pharmacophore [H-Tyr-Pro-Phe-D1Nal-NH<sub>2</sub>][123] separated by polyamide spacers of 15 to 41 atoms in length.

‘Bivalent ligands’ simultaneously bind both receptors with pharmacophores separated by a spacer [116, 124]. For bivalent ligands, if the spacer is too short, the ligand cannot simultaneously occupy both sites (Figure 2.2, left), while a spacer longer than the distance between the two active sites will lose the avidity bonus (Figure 2.2, right). The chemical and pharmacological design of bivalent ligands requires careful consideration of 1) the monovalent parent pharmacophores such that attachment of the spacer does not reduce or alter activity, 2) a spacer that bridges the two protomers without causing non-specific membrane effects and 3) a spacer that does not interfere or alter pharmacophore

activity. The trade-offs between these three aspects of bivalent design are considered below in the designed MDOR bivalent ligand series.



### 2.1.6A Avidity and Bivalency

The monovalent binding interaction between pharmacophore A and its cognate receptor (a) ( $\Delta G^{\circ}_{\text{mono,A}}$ ) is primarily driven by the change in enthalpy between the bound and unbound states; the same driving force would also promote a second independent pharmacophore B to bind its cognate receptor (b) ( $\Delta G^{\circ}_{\text{mono,B}}$ ) [125] (Figure 2.3, top panel). In bivalent interactions the bound and unbound states are no longer independent – the binding of A to a alters the likelihood of B binding to receptor b (Figure 2.3, bottom panel). Binding a monovalent ligand causes a small decrease in entropy based on ligand solvation, in addition to reduced rotational and translational entropy. In comparison, binding of the second pharmacophore of bivalent ligands is entropically favorable once the first pharmacophore is bound. Generally, the entropic bonus persists even when losses in the spacer's translational and rotational entropy are included. The entropy  $\Delta S$  of binding to the first site is generally not favored, while binding to the second site is improved as expressed by the Gibbs Free Energy summation of bivalent ligand binding:

$$\Delta G^{\circ}_{\text{div}} = \Delta G^{\circ}_{\text{mono,A}} + \Delta G^{\circ}_{\text{mono,B}} - RT \ln[C_{\text{eff}}(r)] \quad [126]$$

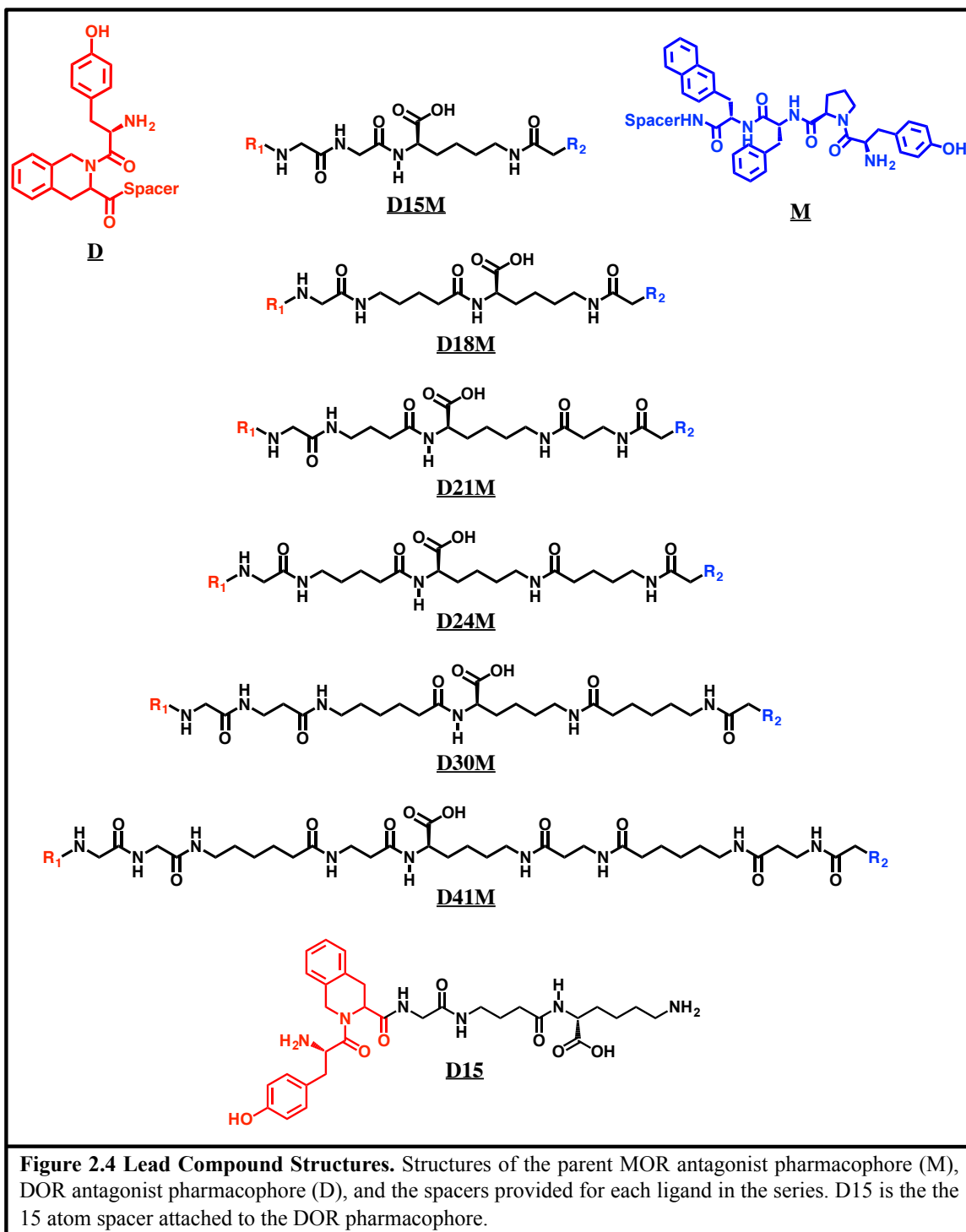
Where,  $\Delta G^{\circ}_{\text{div}}$  is the free energy for the hetero-bivalent interaction;  $\Delta G^{\circ}_{\text{mono,A}}$  is the free energy of binding for the monovalent pharmacophore A to receptor a;  $\Delta G^{\circ}_{\text{mono,B}}$  is the free energy of binding for the monovalent pharmacophore B and receptor b; and  $-RT \ln[C_{\text{eff}}(r)]$  is the effective concentration which compares the likelihood pharmacophore A and B are a specific distance (r) apart, based on the confined allowable area of the spacer. R is the ideal gas constant, and T is the temperature. The function  $-RT$

$\ln[C_{\text{eff}}(r)]$  contains two terms contributing to  $\Delta S$  of bivalent ligands (see [126] for derivation). It includes a favorable term by increasing the local concentration of pharmacophore B and one unfavorable term - the loss of conformational entropy of the spacer. This model works well for most bivalent ligand interactions, however, one can add other parameters, such as cooperativity of binding ( $\Delta G^{\circ}_{\text{coop}}$ ) or interactions between the spacer and the receptor ( $\Delta H^{\circ}_{\text{linker}}$ ). Nonetheless neither is necessary to explain avidity and in most cases  $-RT \ln[C_{\text{eff}}(r)]$  reasonably approximates improved affinity.

### *2.1.6B Choice of Pharmacophores*

Often, bivalent ligand design uses high selectivity and high affinity pharmacophores to retain binding after spacer attachment. In short, use of high-affinity ligands is used to compensate for potential reductions in  $\Delta H$  of the parent pharmacophore upon modification [127]. However, the use of high-affinity ligands, which are typically very conformationally restrained, may limit the avidity bonus. First, these highly constrained structures were developed for the homomeric GPCR conformations, not the conformation specific to the heterodimer (see sec. 2.0.2). Thus conformational rigidity may reduce the enhancement ratio if the ligand weakly recognizes the heteromer conformation relative to the different homomer conformation. Experimentally, high-affinity starting points often show relatively limited selectivity ratios. Our lab [128] previously showed that homo-bivalent ligands with two identical low-affinity pharmacophores produced greater than 10-fold improvements at the multimeric system. On the other hand, high-affinity ligands produce modest 2-3 fold improvements at the heteromer over the more potent homomer pharmacophore.

Considering the thermodynamic and logistical restrictions, we chose the well-studied H-Tyr-Tic-OH DOR antagonist pharmacophore [122, 129] (see reviews: [130, 131]) and the MOR antagonist – H-Tyr-Pro-Phe-D1Nal-NH<sub>2</sub> for the bivalent ligands (Figure 2.4) [123, 132-134]. Both sequences were chosen because of their: 1) modest affinity at DOR and MOR, respectively [122, 129, 135]; 2) established structure activity relationships (SAR) enabling straight forward future modifications [123, 130-132, 134-136]; 3) linear sequences using commercially available amino acids enabling simpler synthesis; 4) (relatively) unconstrained sequences to ensure the ligands' conformational freedom to bind unique MOR or DOR conformations within MDOR and; 5) previous modification of parent structures to the C-terminus indicating adding a spacer would not significantly alter activity or affinity [137-139]. These parameters were selected to maximize the avidity bonus while simultaneously enhancing selectivity for MDOR over MOR and DOR.



### 2.1.6C Chemical Properties of Spacer

The free energy model for binding of bivalent ligands assumed that the spacer did not have a meaningful interaction with the receptor (see Sec. 2.1.6A). In practice, this is not necessarily true, and spacer design must account for how a spacer's chemical properties can influence affinity and activity. It is particularly important to minimize potential confounding effects of one spacer within the series as bivalent compounds typically display length dependence during heteromer evaluation. If one spacer evaluating selectivity for the heteromer.

The most obvious spacer variable to test is length, which dictates the distance separating the two pharmacophores. Based on the previous MDAN studies and other GPCR bivalent ligands (see Sec. 2.0.5) a 21-atom spacer was used as a center point for our bivalent ligands [48]. We designed spacers of 15, 18, 21, 24, 30, and 41 atoms to establish a clear length dependence vs. activity relationship in the MDOR antagonist series (Figure 2.4). Traditionally, demonstrating the spacer's length dependence on heteromer affinity (or activity) supports the direct interaction with the heterodimer complex. After selecting spacer lengths, the parameters of rigidity and hydrophilicity

Spacer Length	Hydrophilicity		Rigidity		
	cLogP spacer	cLogP spacer + pharmacophores	Rotatable Bonds	Non-Rotatable Bonds	R:N
15	-3.8	1.15	12	3	4
18	-4.0	1.00	15	3	5
21	-3.8	1.20	17	4	4.25
24	-4.7	0.29	20	4	5
30	-4.0	0.99	25	5	5
41	-5.2	-0.30	33	8	4.125

**Table 2.1 Spacer Properties** <sup>a</sup>cLogP values calculated for spacer and pharmacophore using ChemDraw Professional 15.0

were maintained as close to equal as possible to minimize confounding effects independent of spacer length (Table 2.1).

The second major consideration was spacer hydrophobicity, which can significantly alter membrane interactions and receptor pharmacology [140, 141]. Differences in spacer hydrophobicity within a series can change solubility – particularly as the spacer length increases – as well as promoting non-specific membrane interactions and possible synthetic difficulties [116]. Importantly, beginning a series of very hydrophobic compounds can hinder future optimization or therapeutic development if not considered early in development [116], as most SAR modifications, particularly for antagonists, increase compound hydrophobicity. Starting with a highly hydrophobic linker can severely limit solubility in biological assays after one or a few modifications. Thus we chose the moderately hydrophilic polyamide spacers (Figure 2.4), and constrained all spacer to cLogP values within  $\sim 1$  of one another (Table 2.1), to minimize any potential membrane interactions of the spacer. cLogP spacer is the value of the spacer alone while cLogP is the calculated value of the final ligands including pharmacophores. Additionally, using polyamide sequences enabled using commercially available glycine,  $\beta$ -alanine,  $\gamma$ -amino butyric acid, valeric acid and amino hexanoic acid substituents, enabling easy synthetic adjustment of linker length. Furthermore, this approach enabled easy modification of spacer flexibility and length making this strategy particularly appealing.

The second major consideration for spacer influence on bivalent ligand activity is rigidity. We chose to assess rigidity by using the ratio of rotatable:non-rotatable (R:N) bonds for comparison of spacers with different lengths [102]. All of our designed spacers

(Figure 2.4, Table 2.1), maintained an R:N ratio between 4 and 5 to insure changes in rigidity did not provide a confounding variable. We started with flexible spacers for the initial series because the orientation of the two pharmacophores relative to MDOR was not known. Rigid spacers, which can improve avidity enhancements, in the initial series may have precluded the pharmacophores from the active site if oriented improperly relative to the MDOR contact points. After designing the bivalent ligands, we synthesized and evaluated these compounds for MOR, DOR and MDOR activity and affinity *in vitro*.

## PART II: MATERIALS AND METHODS

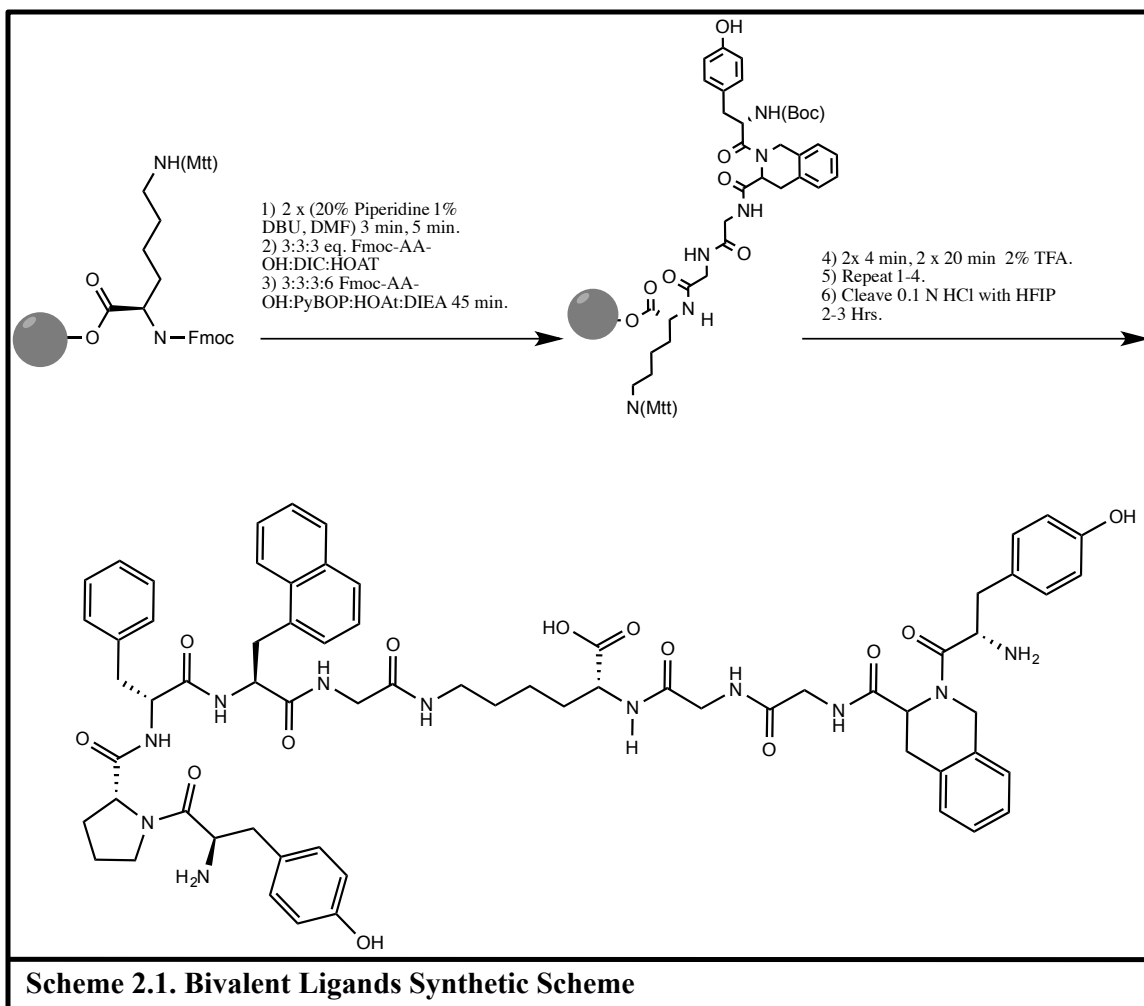
### 2.2.1 Reagents and Materials

For peptide synthesis, amino acids, reagents, and resins were purchased from Advanced Chem Tech (Louisville, KY), Chem-Impex International (Wood Dale, IL), AAPPTec (Louisville, KY), Chem-Impex International (Wood Dale, IL) and NovaBiochem (Darmstadt, Germany). DMF, DCM, NMP and other solvents were purchased from Aldrich (St. Louis, MO) and EMD (Darmstadt, Germany). All other materials were purchased from VWR (West Chester, PA).

### 2.2.2 Solid-Phase Peptide Synthesis (SPPS)

#### 2.2.2A Bivalent Ligand Synthesis

Two series of syntheses using different synthetic strategies were assessed to determine the best synthetic route for the robust synthesis of these bivalent compounds. The bivalent antagonists were synthesized using solid phase peptide synthesis (SPPS) using the following strategy unless otherwise noted. For D41M and D30M Fmoc-Lys(Mtt) was loaded onto a ChemMatrix polyethylene glycol with a Wang-linker using degassed DMF and swelled in 9:1 DCM: DMF (dry and degassed) for 1 hour. Fmoc-Lys(Mtt)-OH, DIC, HOBt, and DMAP, were dissolved in degassed and dry DMF at a 3:3:3:0.1 equivalents for 3 hours under a drying tube. Residual hydroxyl groups were capped with 2:2 acetic anhydride: pyridine. Resins were washed 3x DMF, 3x DCM, and 3x MeOH and vacuum dried overnight. For the shorter linker length compounds Fmoc-Lys(Mtt)-OH was loaded onto a 1-2% DVB polystyrene resin, 200-400 mesh in a two-step procedure. First 1.5 eq of  $\text{SOCl}_2$  in dry DCM was mixed with the Wang resin for 45

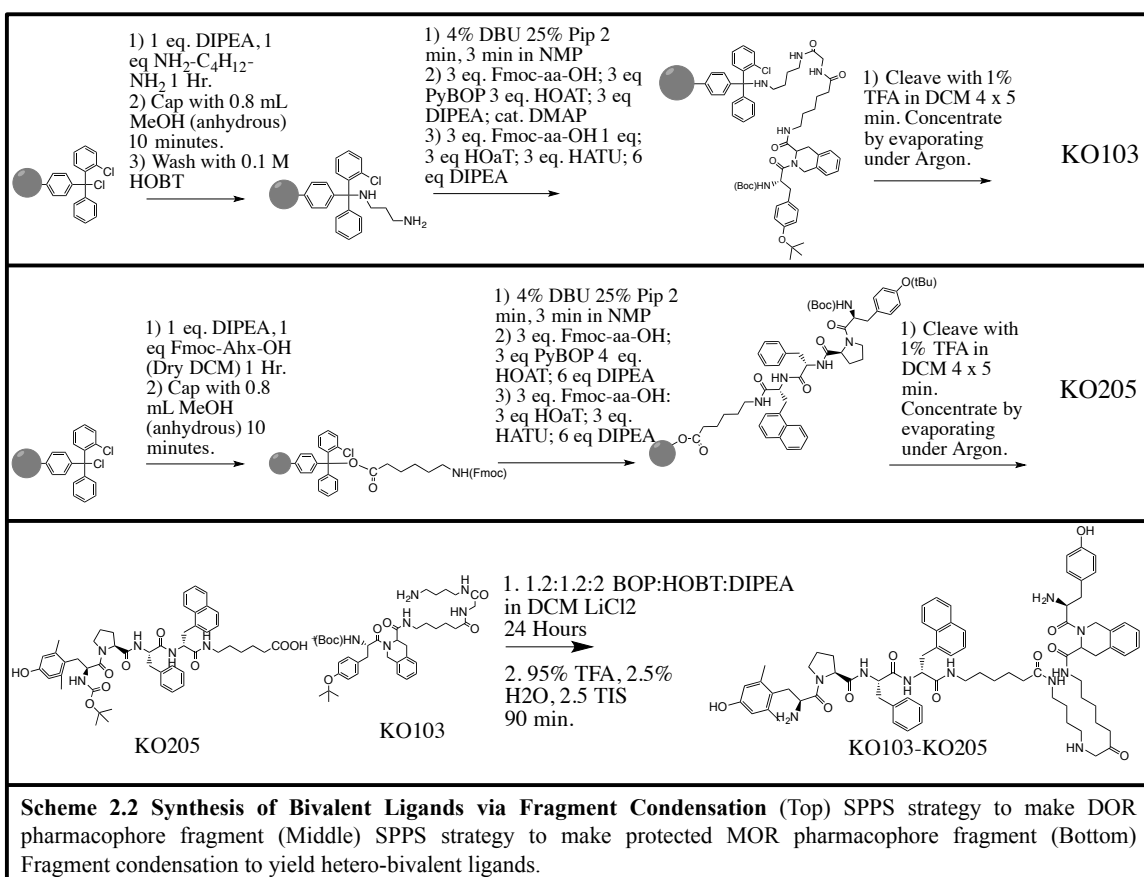


minutes at 4°C. Then Fmoc-Lys(Mtt)-OH, DIEA and KI were added and mixed at room temperature for 18-24 hours [142]. Residual hydroxyl groups were capped with 2:2 acetic anhydride: pyridine and halogen groups with MeOH. Resins were washed 3x DMF, 3x DCM and 3x MeOH and vacuum dried overnight.

In a general methodology, the spacer and the DOR pharmacophore were extended from the  $\alpha$ -amino terminus using standard Fmoc(tBu/Boc) chemistry with PyBOP+HOAt+DIEA or DIC+HOAt as coupling reagents (Scheme 2.1). The terminal DOR Tyr is protected with (Boc/tBu), enabling quasi-orthogonal Mtt deprotection with 2-3%TFA in DCM 2 x 20 minutes (for longer amino acids an additional 2 x 5 minutes step was included first to enable diffusion to the core), followed by analogous Fmoc chemistry

to extend the spacer and MOR pharmacophore. Compounds were cleaved with HFIP and 0.1 N HCl, and precipitated in cold isopropyl ether (Scheme 2.1). Reactions were monitored via the Kaiser test or chloranil [143] colorimetric analysis, incomplete couplings were coupled with - PyBROP – or Microwave assisted synthesis where appropriate.

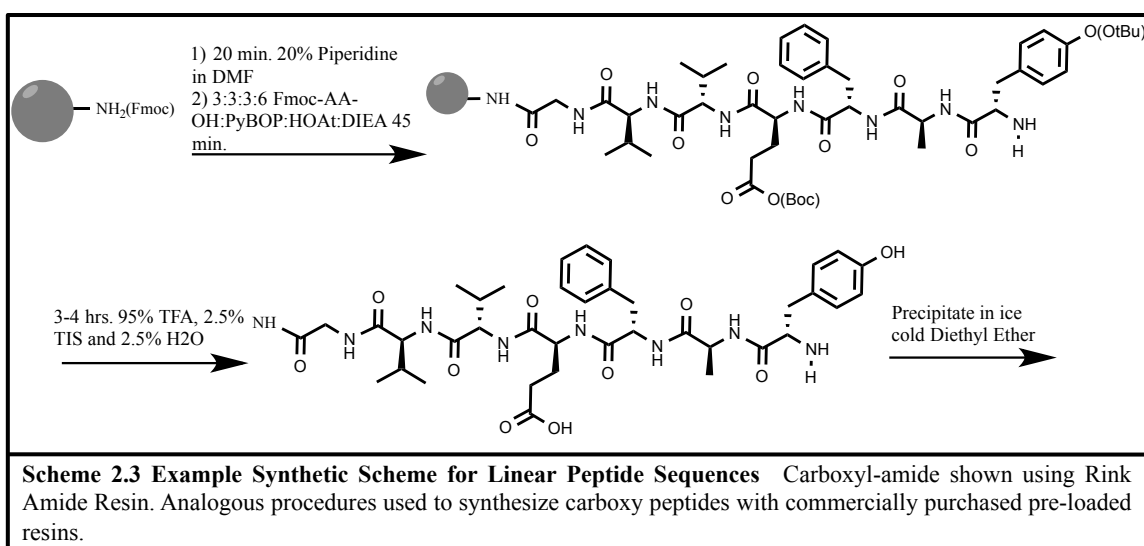
The second series of bivalent ligands used SPPS to make two separate MOR and DOR parent pharmacophores and spacers, followed by cleavage from the resin and solution phase condensation (Scheme 2.2). Further details regarding specific synthetic strategies and difficulties are discussed in the results section (Section 2.2.1).



### 2.2.2B Linear Peptide Synthesis

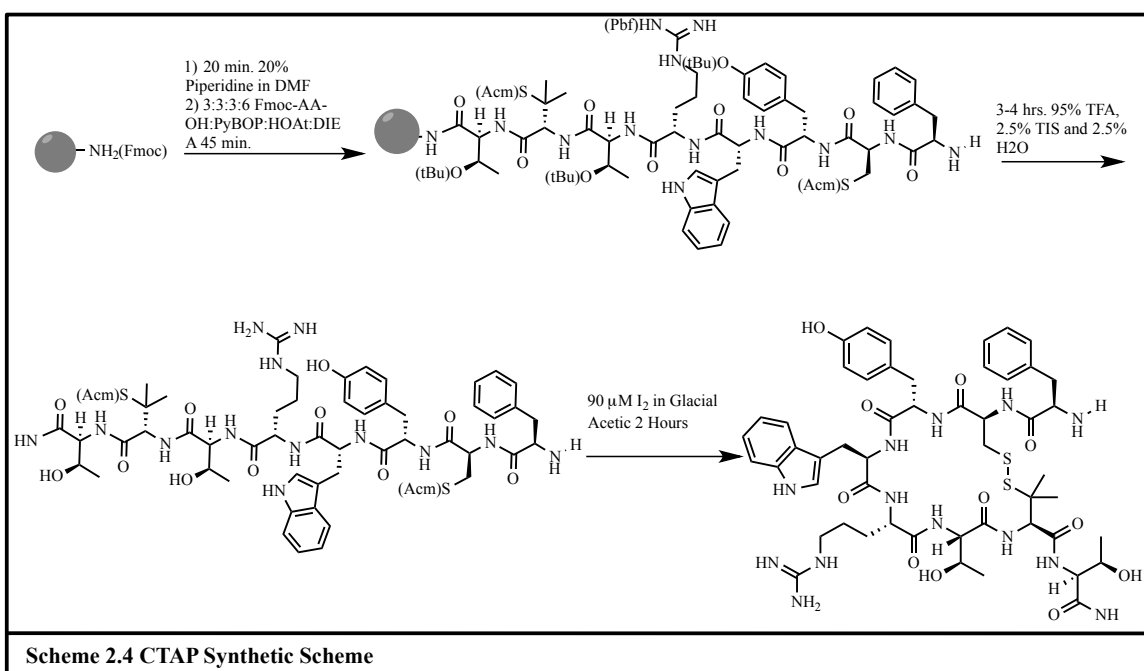
Endomorphin-2 was synthesized using the same methodology as above, starting with deprotection of Rink Amide resins and deprotection 5% DBU:20% piperidine in DMF. This was followed by subsequent coupling with 3:3:3:6 eq. PyBOP: HOAt:Fmoc-AA-OH:DIEA and DIEA at 0.25 M (or 0.5 M DIEA) in DMF. Reaction progress was monitored via the Kaiser test [143]. Cleavage proceeded via 95% TFA, 2.5% TIS and 2.5% H<sub>2</sub>O.

Deltorphin-II was synthesized using standard Fmoc/tBu chemistry. A representative protocol briefly follows, Wang resins were commercially purchased and Fmoc groups were deprotected with 5% DBU:20% piperidine in DMF and coupled with 3:3:3:6 eq. HATU:HOAt:Fmoc-AA-OH:DIEA at 0.25 M (or 0.5 M DIEA) in NMP. Reaction progress was monitored via the Kaiser test [143]. Cleavage proceeded via 95% TFA, 2.5% TIS and 2.5% H<sub>2</sub>O (Scheme 2.3) The crude product was precipitated in ice-cold ether and washed 3 additional times with ether.



### 2.2.2C Disulfide Cyclization

Peptides containing a disulfide bond – CTAP – were synthesized using standard Fmoc/tBu chemistry on Rink Amide Resin. Fmoc groups were deprotected with 20% piperidine in DMF for 20 minutes and coupled with 3:3:3:6 eq. PyBOP:HOAt:Fmoc-AA-OH:DIEA at 0.25 M (0.5 M DIEA) in DMF. Cleavage proceeded via 95% TFA, 2.5% TIS and 2.5% H<sub>2</sub>O. The acm protecting groups on Cys or Penicillamine were deprotected and cyclized with I<sub>2</sub> and precipitated in ether (Scheme 2.4) [144].



### 2.2.2D H-DMT-Tic-Ala-OH Synthesis

H-DMT-Tic-Ala-OH was synthesized with a pre-loaded Fmoc-Ala-Wang (Mesh 200-400; 1-2% DVB). Deprotections proceeded 1% DBU:20% piperidine in DMF at 75° C in a CEM Discover microwave incubator. Subsequent coupling with 3:3:3:6 eq. PyBOP: HOAt:Fmoc-Tic-OH:DIEA in NMP proceeded for 5 minutes and repeated.

(Boc)-DMT-OH was coupled with 3:3:3 eq. DIC:HOAt:Boc-DMT-OH for 10 minutes at 60° C in a microwave incubator. Temperatures were monitored via IR probe for the course of the reaction and reaction progress was monitored via the Kaiser test [143]. Cleavage proceeded via 95% TFA, 2.5% TIS and 2.5% H<sub>2</sub>O.

### *2.2.3 Peptide Purification and Analysis*

The crude product was precipitated in ice-cold isopropyl ether; purified by C18 RPLC and new compounds were analyzed via High-Resolution MS-MS while previously established compounds were characterized via Low-Resolution MS-MS. Some peptides were purified using Thermofisher (Finnigan) LCQ. After purification, compounds were dissolved in 0.1 N HCl and lyophilized. This process was repeated 2-3 times to facilitate the exchange of the TFA salt for the HCl salt, improving compound solubility.

### *2.2.4 Cell Culture*

The cell line co-expressing Myc-DOR and Flag-MOR has been previously used in the literature for MDOR studies and was a kind gift of Dr. Jia Bei Wang at the University of Maryland [145]. Chinese Hamster Ovary (CHO) cells stably expressing HA-DOR, MOR or Flag-MOR and Myc-DOR were grown in 50:50 F12K: DMEM with 10% FBS, 1% PS and 500 µg per mL of G418. The Flag-MOR and Myc-DOR cells were supplemented with 250 µg per mL Hygromycin [145]. Cells were incubated at 37° C under a 5% CO<sub>2</sub> atmosphere. For competition binding and [<sup>35</sup>S]-GTPγS coupling studies, membrane preparations were made from cells grown on 15 cm<sup>2</sup> culture treated plates. Upon reaching confluence cells were treated with 5 mM EDTA in PBS for 30 minutes or

until the cells lifted from the plate, and centrifuged at 3,000 g at 4°C for 5 minutes. The supernatants were removed, and pellets were frozen at -80°C until used.

Previously frozen pellets were homogenized with a glass-Teflon Dounce homogenizer suspended in 10 mM Tris-HCl pH 7.4, 100 mM NaCl and 1 mM EDTA. Then pellets were spun down at 15,000 g for 60 minutes at 4°C. The supernatant was removed and membranes re-suspended in the appropriate buffer indicated in section 2.2.5-2.2.6, followed by homogenization with the glass-Teflon Dounce.

### 2.2.5 [<sup>35</sup>S]GTP $\gamma$ S Coupling – Antagonist Activity

Assays were performed as previously described [62]. After making pellets, membranes were resuspended in 50 mM Tris-HCl, pH 7.4, 100 mM NaCl, 5 mM MgCl<sub>2</sub>, 1 mM EDTA, 40  $\mu$ M GDP with a Teflon-on-glass Dounce and protein quantity assessed using a modified Lowry Assay. Protein was adjusted to 15  $\mu$ g membrane protein per reaction, pre-incubated with antagonist or vehicle for 5 minutes and 100 pM [<sup>35</sup>S]GTP $\gamma$ S (PerkinElmer), then treated with 1  $\mu$ M CYM51010. Plates were incubated at 30°C for 75 minutes. Reactions were terminated by rapid filtration using a 96-well plate Brandel cell harvester (Brandel, Gaithersburg, MD) onto GF/B plates. Bound [<sup>35</sup>S]GTP $\gamma$ S was measured using a Microbeta2 scintillation counter.

Data was normalized to vehicle (0%) and 1  $\mu$ M CYM51010 (100%) stimulation. Bivalent compounds fit a biphasic dose-response curve in the MDOR line, producing an IC<sub>50HIGH</sub> representing the higher potency site and an IC<sub>50LOW</sub> for the low potency site. The Frac<sub>HIGH</sub> is the % of response attributable to the high site. All curves were assessed using a 3-variable (one site) fit and a biphasic (two-site) fit using GraphPad Prism 6.0, and a

two-ANOVA comparing one site and two site fits was performed to determine the better fit. All bivalent ligands revealed p-values <0.05 for biphasic curve fits except D30M (p = 0.067), which was attributed to the incomplete curve.

### 2.2.6 [<sup>3</sup>H]-Diprenorphine Competition Binding

Membrane preparations were made from pellets of CHO cells expressing MOR, HA-DOR or Myc-DOR and Flag-MOR as above. Protein was adjusted to 30-40 µg/rxn of protein in a 50 mM Tris-HCl pH 7.4. Candidate compounds were competed against 1-2 nM [<sup>3</sup>H]-Diprenorphine and fit to a one site competition-binding model or biphasic model as in section 2.2.5. A typical experiment involves 1) adding a fixed concentration of [<sup>3</sup>H]-diprenorphine and varying compound doses to membrane preparations, 2) incubating the mixture for 80 minutes at room temperature, 3) separating bound and unbound ligand via a 96 well GF/B filter plate, 4) and acquiring the data using a 96 well format scintillation counter. Data is normalized to the specific binding induced by [<sup>3</sup>H]-diprenorphine alone.

Candidate compounds fit a two-site model in the MDOR line, producing a  $K_{I\text{HIGH}}$  representing the higher affinity site and a  $K_{I\text{LOW}}$  for the low-affinity site. The  $\text{Frac}_{\text{HIGH}}$  is the % of response attributable to the high site, which ranges from 10-20% for binding and 35-45% for functional activity (Example in Figure 3A). The  $K_i$  was calculated using the determined concentration and  $K_D$  of [<sup>3</sup>H]-Diprenorphine in the MOR, DOR, and MDOR lines. Previously saturation binding vs [<sup>3</sup>H]-Diprenorphine at DOR and MOR determined the  $K_D = 2.4$  nM and  $K_D = 4.4$  nM, respectively.  $B_{\text{max}}$  values at DOR and MOR were 0.81 and 5.4 pmol/mg, respectively.

### 2.2.7 [<sup>35</sup>S]GTPγS Mixed Membrane D24M Antagonist Activity

MOR CHO and HA-DOR CHO pellets and reaction preparations were made as described in Section 2.2.5 with the following modifications. After protein quantitation, using the B<sub>MAX</sub> of MOR CHO and HA-DOR CHO cell lines, the membranes were mixed in an equal ratio to the expression in the MDOR cell line. The 8:1 DOR: MOR ratio was used a total protein concentration of 40 μg membrane protein per reaction.

### 2.2.8 Tail-flick Anti-nociceptive Assay

All animal procedures were performed following the policies and recommendations of the International Association for the Study of Pain, the National Institutes of Health, and with approval from the Animal Care and Use Committee of the University of Arizona for the handling and use of laboratory animals. A mouse model of acute pain (tail flick test) was used measuring the latency of tail withdrawal from a 52°C water bath. A maximum cutoff of 10 seconds was used to prevent tissue damage. Antagonist (or vehicle) was administered by ICV injection 5 minutes before CYM51010 agonist injection at the indicated concentrations. All compounds were dissolved in 10% Tween80 in sterile H<sub>2</sub>O. Briefly, 0.1 nmol/mouse, 0.32 nmol/mouse and 1.0 nmol/mouse of D24M were injected ICV. After a 5-minute pre-treatment 3.2 nmol/mouse CYM51010 was injected and tail-flick latencies were reassessed every 15 minutes for 2 hours in a 52 °C water bath.

## PART III: RESULTS

### 2.3.1 Synthesis and Characterization of MDOR Antagonists

The current MDOR studies aimed to achieve greater than 10-fold selectivity over both protomers, which has not been previously observed for most bivalent ligand studies in our lab [137, 146-149]. Further, the presence of two N-terminal pharmacophores required the development of a new synthetic strategy, as prior studies were synthesized C-terminal to N-terminal using standard SPPS techniques [137]. Thus we aimed to develop a robust and high yield synthetic scheme for bivalent ligands with two N-termini. Further, the scheme had to couple hydrophobic/sterically-hindered sequences, facilitate spacer and SAR modifications and ideally was capable of automation while using commercially available reagents.

Broadly speaking, two different synthetic strategies were pursued to construct the designed bivalent ligands (Figure 2.4). The first scheme synthesized two independent fragments via SPPS; one pharmacophore had an amino terminus substituted for the

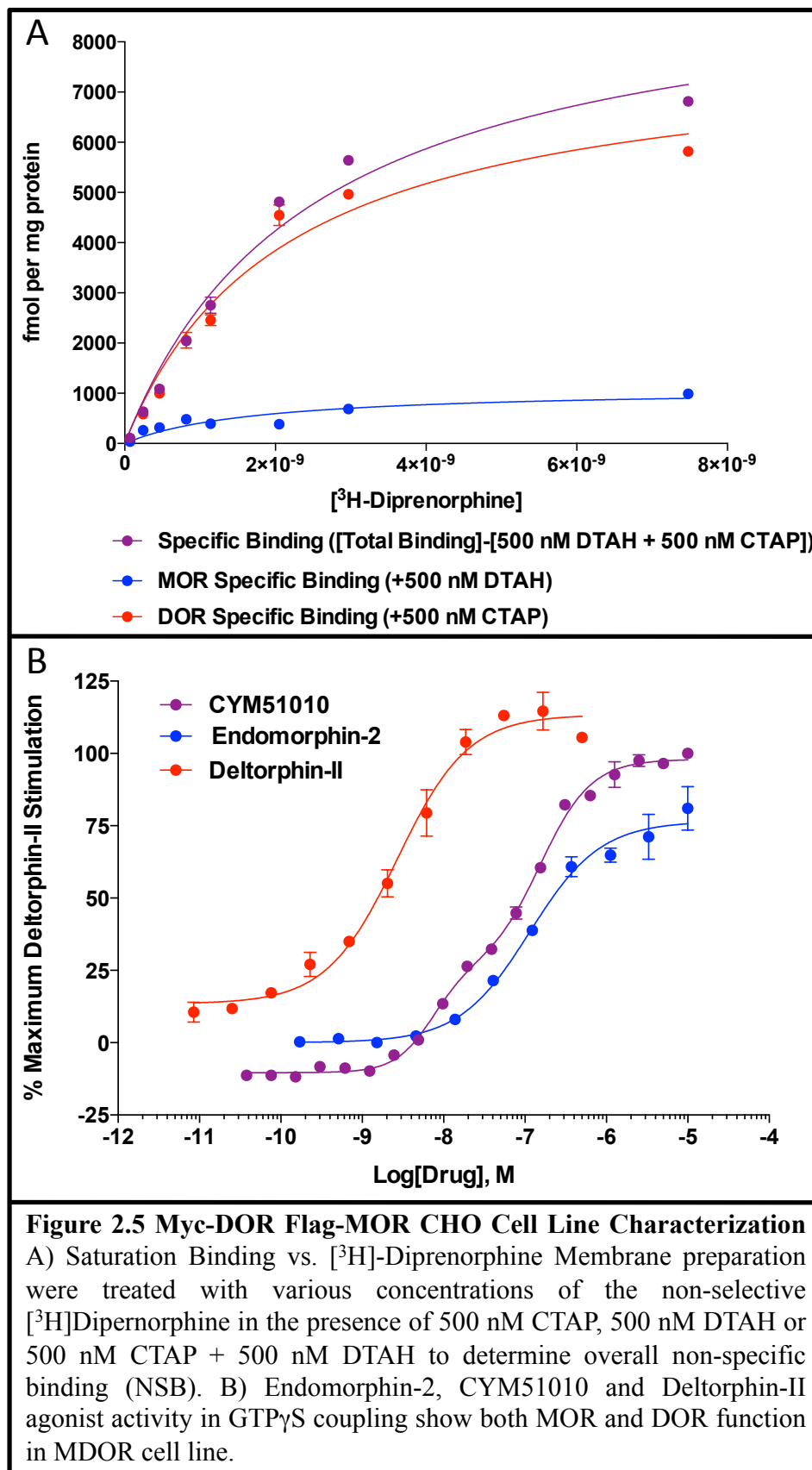
Analytical Data		HRMS <sup>b</sup>				HPLC <sup>c</sup>		%	LRMS <sup>b</sup>	
Cmpd.	Molecular Formula	Observed [M+H]	Observed [M+H] <sup>2</sup>	Calcd.	error (PPM)	R <sub>f</sub> (min)	% Purity	Yeild	Obs. [M+H]	Calcd.
M	C <sub>36</sub> H <sub>39</sub> N <sub>5</sub> O <sub>5</sub>					21.3	>95%	81%	622	622
D	C <sub>19</sub> H <sub>20</sub> N <sub>2</sub> O <sub>4</sub>					19.1	>95%	87%	341	341
D15	C <sub>31</sub> H <sub>42</sub> N <sub>6</sub> O <sub>7</sub>	611.3192		611.3193	0.20	18.9	>95%	78%		
DTAH	C <sub>24</sub> H <sub>29</sub> N <sub>3</sub> O <sub>5</sub>					27.8	>95%	51%	440	440
D15M	C <sub>67</sub> H <sub>77</sub> N <sub>11</sub> O <sub>13</sub>	1242.5622	848.39738	1242.5624	0.17	24.7	>95%	77%		
D18M	C <sub>70</sub> H <sub>83</sub> N <sub>11</sub> O <sub>13</sub>	1285.6172		1285.6172	-0.01	25.1	>95%	73%		
D21M	C <sub>72</sub> H <sub>86</sub> N <sub>12</sub> O <sub>14</sub>	1343.6444		1343.6465	1.54	25.2	>95%	54%		
D24M	C <sub>75</sub> H <sub>92</sub> N <sub>12</sub> O <sub>14</sub>	1385.6949	693.39	1385.6934	-1.03	25.5	>95%	61%		
D30M	C <sub>80</sub> H <sub>101</sub> N <sub>13</sub> O <sub>15</sub>	1484.7600		1484.7618	1.24	25.6	>95%	44%		
D41M	C <sub>88</sub> H <sub>114</sub> N <sub>16</sub> O <sub>18</sub>	1683.8744		1683.8575	-10.02	25.5	>95%	43%		
CTAP	C <sub>51</sub> H <sub>68</sub> N <sub>12</sub> O <sub>12</sub> S <sub>2</sub>					24.8	>95%	25%	1105	1105
KO103-205	C <sub>74</sub> H <sub>94</sub> N <sub>10</sub> O <sub>10</sub>	1283.7242		1283.7233	-0.73	33.1	>95%	11%		

**Table 2.2 Physical Constants and Characterization of Compounds** [a] (M+H)<sup>+</sup>, ESI (Finnigan, Thermolectron, LCQ classic); [b] (M+H)<sup>+</sup>, FAB-MS (JEOL HX110 sector instrument), or MALDI-TOF (Bruker Ultraflex III). [c] Hewlett Packard 1100 (C-18, Microsorb-MVTM, 4.6 mm x 250 mm, 5 μm) using a gradient system (10-90% acetonitrile containing 0.1% TFA within 40 mins, 1 mL/min). d negative ESI mode

carboxy terminus while the second pharmacophore had the traditional carboxy terminus. The protected peptide fragments were cleaved, followed by solution phase fragment condensation (Scheme 2). Several variations of Scheme 2 were assessed, and several candidate ligands such as KO103-205 and KO102-204 were made in the process (Scheme 2). Despite changes in solvents, coupling reagents and coupling temperature these methods produced low crude yields (<10%) and purity (<10%). Cleaving the protecting fragments proved particularly difficult due to the protected ligands high hydrophobicity. After SPPS of the individual fragments, products were soluble in diethyl ether, isopropyl ether and partially soluble in hexanes, likely leading to greatly reduced yields.

In addition, minor changes in the linker or pharmacophore composition altered solubility, requiring different solvents for precipitation and condensation of each product. Attempts at different linker lengths and diamino or hydrazine C-terminal modifications did not significantly ease encumbered synthetic strategies. Crude products were weakly soluble in 75:25 DCM: DMF with 0.1 M LiCl<sub>2</sub>, at low concentrations, requiring 24-hour time periods for the condensation step (Scheme 2, Bottom). The condensed heterobivalent ligands were then deprotected with TFA for 2 hours and evaporated under N<sub>2</sub> to oil. This synthetic methodology, while producing a few ligands, proved insufficiently robust with low yields and difficult to purify. Furthermore, the products' high hydrophobicity could lead to solubility problems in the biological assays down the line, particularly in future SAR studies. This consideration is particularly important because most SAR modifications increase hydrophobicity, particularly for antagonists. Due to synthetic difficulties and the high hydrophobicity of these compounds, these methodologies were abandoned.

The second methodology pursued the use of asymmetric synthetic methodologies in combination with standard SPPS techniques for complete bivalent ligand synthesis in the solid phase (Scheme 1). The removal of the fragment condensation step minimized synthetic difficulties introduced by the hydrophobicity of protected fragments. After optimization of coupling reagents, deprotection conditions, solvent, cleavage cocktail, resin loading and lysine protecting groups, a synthetic scheme with yields ranging from 50-80% and crude purity in the 40-80% range was obtained. Novel peptide sequence identities were confirmed using high-resolution mass spectrometry (HR-MS), and final purities exceeded 95% (Table 2.2). Previously reported structures and methods were confirmed via low-res mass spectrometry (LRMS). CTAP and DTAH, used for MDOR saturation binding, were also synthesized and characterized.



### 2.3.2 Evaluation of the MDOR cell line

We first validated the MDOR cell line by performing saturation binding experiments with [<sup>3</sup>H]-Diprenorphine in the presence of either a MOR-selective antagonist (CTAP) or DOR selective antagonist H-DMT-Tic-Ala-OH (DTAH) (Figure 2.5A). The combination of MOR and DOR yielded a  $B_{MAX} = 9.5$  pmol per mg and was determined by subtracting the non-specific binding (NSB) [500 nM CTAP + 500 nM DTAH] from total binding [vehicle]. The specific binding of MOR was determined in the presence of 500 nM DTAH – a high selectivity and affinity antagonist – which yielded a  $B_{MAX} = 1.1$  pmol per mg for Flag-MOR. Similarly, 500 nM CTAP – a high selectivity and affinity MOR ligand – was used to block all Flag-MOR sites and yielded the specific binding of DOR with a  $B_{MAX} 7.9$  pmol per mg (Table 2.3).  $K_D$  values ranged from 1.7-2.5 in the three experimental conditions but did not significantly differ from one another. These results indicate an approximate 8:1 DOR: MOR ratio and confirmed expression of both MOR and DOR subtypes.

Next, to establish functional activity of MOR, DOR and MDOR in the MDOR cell line [<sup>35</sup>S]GTP $\gamma$ S coupling assays were performed with Endomorphin-2 (MOR-selective), Deltorphin-II (DOR selective) and CYM51010 (MDOR preferring) agonists. CYM51010 showed a closely overlapping biphasic curve (Figure 2.5B). Furthermore the CYM51010 selectivity for MDOR:

Components	$B_{MAX}$ (SEM) fmol/mg	$K_D$ (SEM) nM
MDOR (+ Vehicle)	9500 (500)	2.5 (0.31)
MOR (+ 500 nM DTAH)	1100 (140)	1.7 (0.53)
DOR (+ 500 nM CTAP)	7900 (470)	2.1 (0.28)

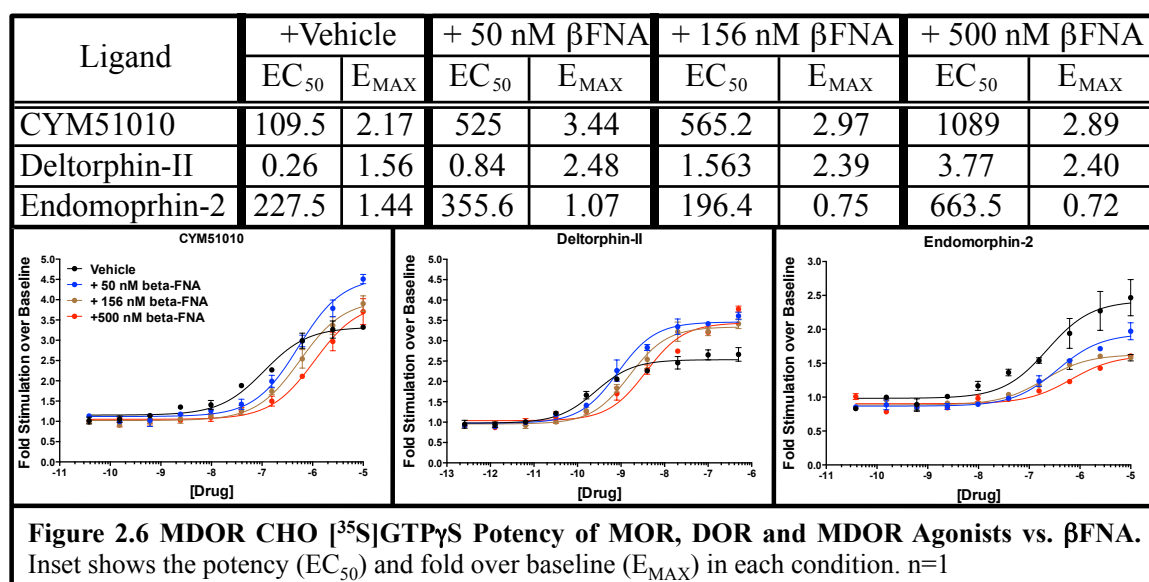
**Table 2.3 MDOR [<sup>3</sup>H]-Diprenorphine Saturation Binding** -  $B_{MAX}$  and  $K_D$  values for MDOR, MOR or DOR vs. [<sup>3</sup>H] Diprenorphine in CHO cells co-expressing Myc-DOR and Flag-MOR.

Ligand	<sup>35</sup> S]-GTPγS Agonist Activity								
	EC <sub>50</sub> <sub>DOR</sub>	E <sub>MAX</sub> <sub>DOR</sub>	EC <sub>50</sub> <sub>MOR</sub>	E <sub>MAX</sub> <sub>MOR</sub>	EC <sub>50</sub> <sub>HIGH</sub>	F <sub>HIGH</sub>	EC <sub>50</sub> <sub>LOW</sub>	E <sub>MAX</sub> <sub>MDOR</sub>	EC <sub>50</sub> <sub>HIGH</sub> :EC <sub>50</sub> <sub>DOR</sub>
CYM51010	220	75	600	53	7.2	0.31	160	100	31

**Table 2.4** CYM51010 MOR, DOR and MDOR [<sup>35</sup>S]-GTPγS Coupling in MOR, DOR and MDOR Cell Lines n=1; r<sup>2</sup> > 0.95 for all experiments.

MOR:DOR cell lines in the [<sup>35</sup>S]GTPγS agonist assays match previous reports [47] (Table 2.4). In this biphasic agonist model, the EC<sub>50</sub><sub>LOW</sub> and EC<sub>50</sub><sub>DOR</sub> were comparable (85 nM and 141 nM respectively). Our evaluation and the prior reports with this cell line indicate the co-expression and presence of the MDOR.

Next, we assessed whether a MOR irreversible antagonist (β-FNA) could disrupt MDOR activity and abolish all MOR activity. MDOR cells were pre-treated with 50 nM, 156 nM, and 500 nM β-FNA for 2 hours then pelleted and assayed for [<sup>35</sup>S]GTPγS coupling as in section 2.2.5 (Figure 2.6). β-FNA shifts Endomorphin-2 (MOR agonist activity) rightward with reduced efficacy. While 500 nM β-FNA does not completely abolish MOR efficacy, this is common with irreversible antagonists tested in systems with significant spare receptors [150]. Unfortunately, due to high receptor reserves – as



expected with an MOR  $B_{MAX} = 1.1$  pmol per mg (Table 2.3, Figure 2.5A) –  $\beta$ -FNA could not completely abolish MOR activity within its MOR: DOR selectivity range.

Initially, the irreversible antagonist experiments aimed to serve as a control for lead antagonist compounds. However, increasing  $\beta$ -FNA concentrations shifts the MDOR preferring agonist CYM51010 potency (Figure 2.6) by nearly 10-fold. This 10-fold shift in CYM51010 potency would make comparing the  $IC_{50}$  of lead compounds meaningless upon  $\beta$ -FNA treatment. By shifting the agonist's  $EC_{50}$  any antagonist  $IC_{50}$  values determined against that agonist also shift. Due to these limitations, neither  $\beta$ -FNA nor 5'-NTII (DOR selective irreversible antagonist) treatments were used for control experiments.

Interestingly, 50 nM  $\beta$ -FNA pretreatment increases both CYM51010 and Deltorphin-II efficacy (Figure 2.6). While the CYM51010 efficacy improvements diminish as  $\beta$ -FNA increases, Deltorphin-II efficacy improvements remain stable. The increased Deltorphin-II efficacy suggests  $\beta$ -FNA acts as an allosteric modulator of DOR – by shifting potency and efficacy. The initial efficacy increase of CYM51010 parallels the DOR agonist Deltorphin-II, while the decreased efficacy with increased  $\beta$ -FNA parallels the MOR agonist Endormorphin-2. That is, the CYM51010 vs.  $\beta$ -FNA dose response behaviors is a combination of the MOR and DOR agonists. These studies confirming  $\beta$ -FNA attenuates MOR efficacy and modulates DOR activity further supports MDOR formation and interaction in our system.

### 2.3.3 Candidate Compounds [<sup>35</sup>S]-GTPγS Antagonist Activity

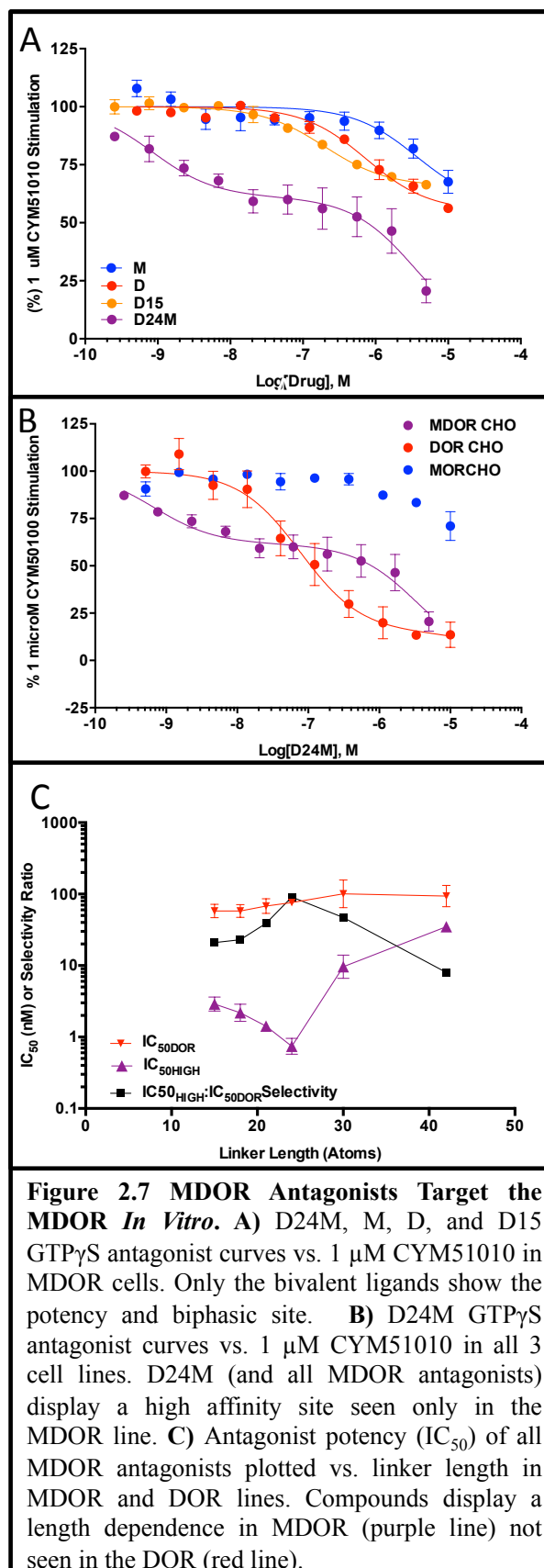
Each candidate compound (Figure 2.4) was assessed for [<sup>35</sup>S]-GTPγS antagonist activity vs. 1 μM CYM51010 in CHO cells stably expressing human MOR, DOR, or MDOR (Table 2.5). All bivalent ligands induced a biphasic antagonist response in the MDOR but not in the MOR or DOR homomeric lines; a representative example is shown in Figure 2.6B. In the MDOR line, the high potency site (IC<sub>50HIGH</sub>) is shifted relative to DOR IC<sub>50DOR</sub> between 8 and 91 fold (Table 2.5). The IC<sub>50HIGH</sub> (Figure 2.7C) shows a clear length-dependence, indicating 24 atoms is the optimal spacer length between the two pharmacophores, while no such length dependence is observed in the DOR (Figure 2.7C) or MOR lines (Table 2.5). This length dependence produces a U-shape in Figure

Ligand	GTPγS Antagonist Activity vs. 1 μM CYM51010					Competition Binding vs. [ <sup>3</sup> H]-Diprenorphine				K <sub>IHIGH</sub> : K <sub>IDOR</sub>
	IC <sub>50DOR</sub> (SEM)	IC <sub>50MOR</sub> (SEM)	IC <sub>50HI</sub> GH (SEM)	F <sub>HIGH</sub> (SEM)	IC <sub>50HIGH</sub> : IC <sub>50DOR</sub>	K <sub>IDOR</sub> (SEM)	K <sub>IMOR</sub> (SEM)	K <sub>IHIGH</sub> (SEM)	F <sub>HIGH</sub> (SEM)	
<i>D15M</i>	58 (14)	>1 μM	2.8 (0.58)	0.49 (.05)	21	270 (67)	>1 μM	2.5 (.83)	.12 (.02)	110
<i>D18M</i>	58 (13)	>1 μM	2.5 (0.70)	0.42 (.08)	23	120 (33)	>1 μM	2.0 (.36)	.12 (.02)	58
<i>D21M</i>	68 (18)	>1 μM	1.7 (0.19)	0.48 (.07)	39	98 (40)	>1 μM	1.3 (1.1)	.09 (.02)	78
<b><i>D24M</i></b>	<b>76 (5.4)</b>	<b>&gt;1 μM</b>	<b>.84 (0.32)</b>	<b>0.28 (.07)</b>	<b>91</b>	<b>84 (17)</b>	<b>&gt;1 μM</b>	<b>0.63 (.14)</b>	<b>.11 (.01)</b>	<b>133</b>
<i>D30M</i>	100 (56)	>1 μM	2.2 (0.30)	0.48 (.04)	47	290 (68)	>1 μM	8.1 (4.42)	.15 (.03)	35
<i>D41M</i>	94 (38)	>1 μM	12 (0.80)	0.43 (.02)	8	230 (77)	>1 μM	16 (8.1)	.12 (.03)	15
<i>D15</i>	ND	ND	200 (10)	0.34 <sup>1</sup>	-	250 (83)	NC	ND	-	-
<i>D</i>	100 (33)	NC	250 (45)	0.44 <sup>1</sup>	-	230 (45)	NC	ND	-	-
<i>M</i>	NC	>1 μM	>1 μM	[0.43] <sup>2</sup>	-	NC	>1 μM	ND	-	-

**Table 2.5 Functional [<sup>35</sup>S]GTPγS Antagonist Activity and [<sup>3</sup>H] Diprenorphine Competition Binding of Potential MDOR Selective Antagonists** ND = Not Determined; NC = No Convergence; <sup>1</sup> I<sub>MAX</sub> values indicated for D15, D and M for single site partial antagonist values observed. <sup>2</sup> Maximum inhibition at 10 μM. n = 3-4

2.7C and is consistent with spacer lengths of other GPCR bivalent ligands [120, 151]. Taken together, the length dependence of selectivity and activity in MDOR but not MOR or DOR line is consistent with selective targeting of MDOR.

To confirm that neither parent pharmacophore nor the linker caused the  $IC_{50HIGH}$  site, D, M and D15 were assayed for [ $^{35}S$ ]-GTP $\gamma$ S antagonist activity vs. 1  $\mu$ M CYM51010 activity at MDOR (Figure 2.7A). Neither M nor D alone produce a high potency  $IC_{50}$  in MDOR cells indicating neither pharmacophore explains the high potency site observed for D24M and other candidate compounds (Figure 2.7A). Furthermore, D (H-Tyr-Tic-OH) produces a similar potency in DOR cells ( $IC_{50}$  = 100) nM and MDOR cells ( $IC_{50}$  = 250 nM) (Figure 2.7B) while the potency for M is greater than 1  $\mu$ M

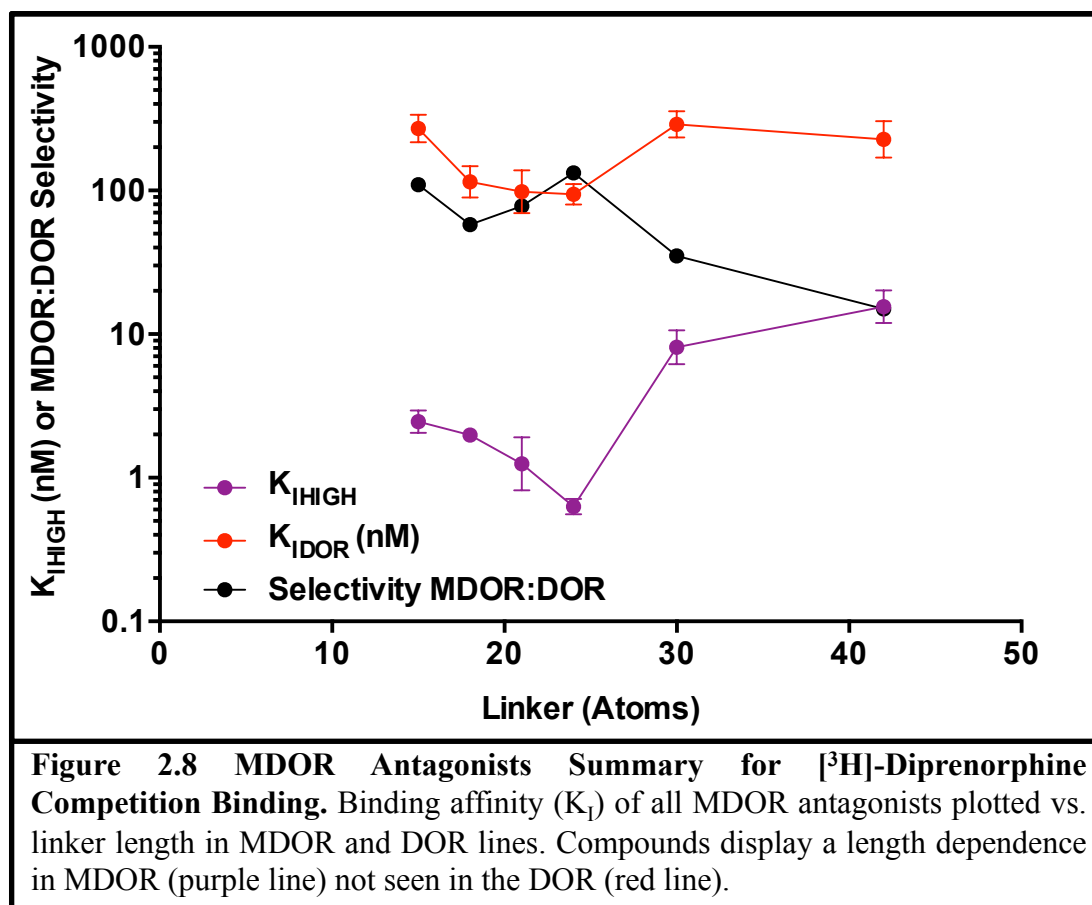


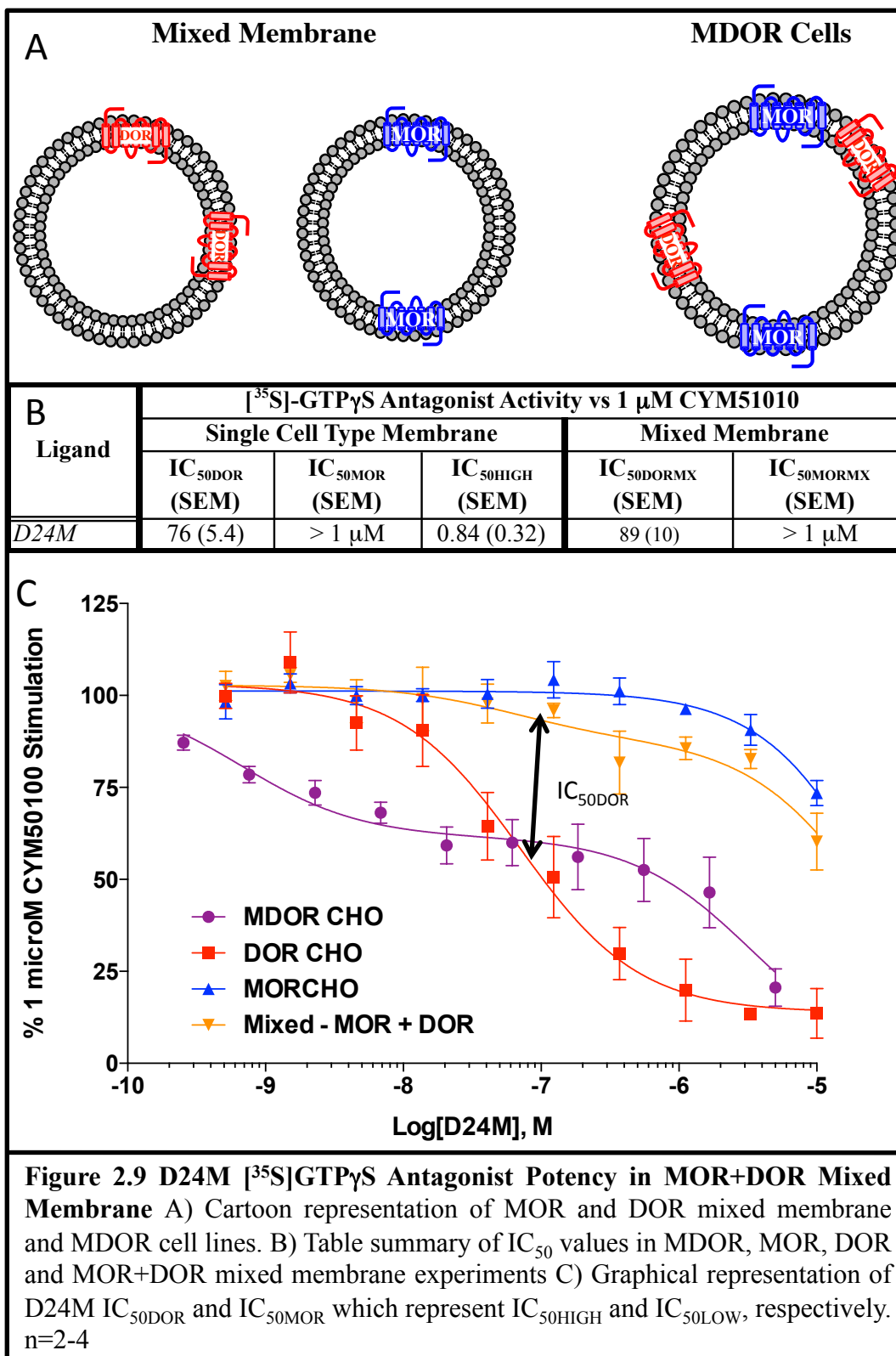
in both MOR and MDOR. D15 has an  $IC_{50}$  of 200 nM in MDOR cells (Figure 2.7A) that is comparable to D potency in MDOR indicating the spacer + pharmacophore does not explain the observed features of the bivalent ligands. Taken together, these experiments indicate the bivalent compounds likely selectively target the MDOR heteromer and D24M produces the highest potency and selectivity at the  $IC_{50HIGH}$  site in MDOR (Figure 2.7C).

#### 2.3.4 Candidate Compounds [ $^3H$ ]-Diprenorphine Binding

Next, each candidate compound was assessed for [ $^3H$ ]-Diprenorphine competition binding in MOR, DOR, or MDOR cell lines. Competition binding experiments using the non-selective [ $^3H$ ]-Diprenorphine reveals biphasic curves in the MDOR line but not in the MOR or DOR lines (Table 2.5). The fraction of ligand bound ( $Frac_{HIGH}$ ) reflects the receptor quantity to the high-affinity site ( $K_{HIGH}$ ). Importantly,  $Frac_{HIGH}$  matches the expected MDOR population predicted from saturation binding studies (Table 2.3 and Figure 2.5A). Since the MOR: DOR ratio is 8:1, the highest MDOR population possible is if all MOR is in MDOR. This prediction matches MDOR trafficking studies in which simultaneous MOR and DOR expression induces co-trafficking to the membrane together and co-internalization together in response to MOR or DOR agonists [112]. However, if MOR and DOR expression occur at different time points, a stable MDOR unit does not form as only DOR internalizes in response to a DOR agonist and only MOR internalizes to an MOR agonist [112]. Since this suggests MDOR forms a stable unit, and our system expresses significantly more DOR than MOR, all MOR likely remains constituted in MDOR.

The individual pharmacophores (D and M) show significantly reduced affinity in MDOR cells, and do not display a biphasic response, nor does the non-selective opioid antagonist naloxone (Table 2.5).  $K_{I\text{HIGH}}$  shows a clear length-dependence, supporting the optimal length between the two pharmacophores is 24 atoms. As for function (section 2.3.3), no such dependence is observed in the DOR or MOR homomer line (Table 2.5). This length dependence produces a U-shape curve (Figure 2.8) and is consistent with spacer lengths of other GPCR bivalent ligands [120, 151].

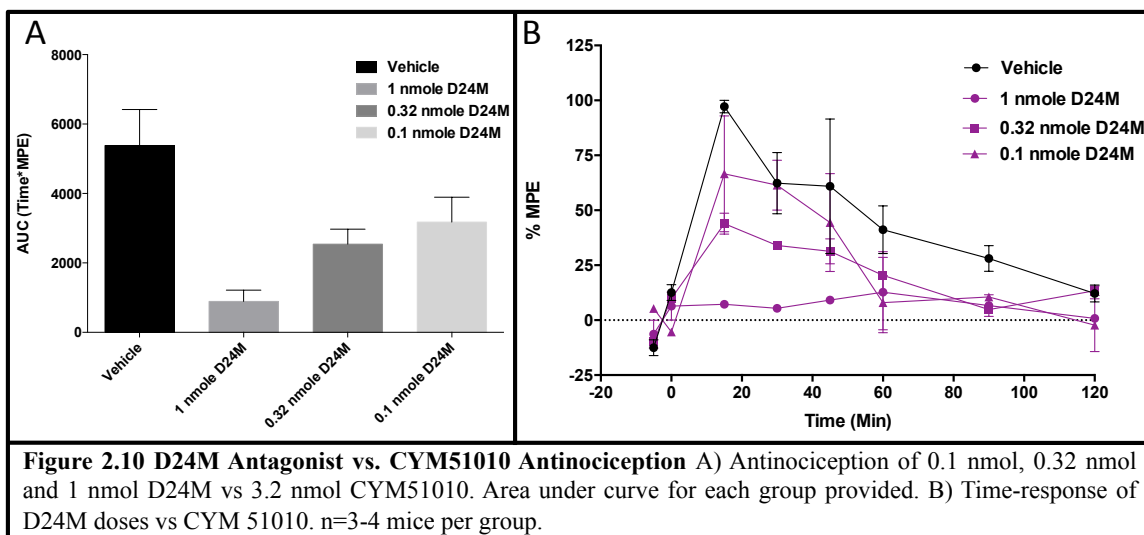




### 2.3.5 Mixed Membrane Control – [<sup>35</sup>S]-GTPγS Antagonist Activity

To show that the IC<sub>50HIGH</sub> site requires co-expression of MOR and DOR on the same membrane, we assessed the lead compound – D24M – for functional [<sup>35</sup>S]GTPγS antagonist activity in mixed membrane preparations (Figure 2.9A). First, membrane preparations from MOR and DOR singly expressing lines were mixed together in same ratio to the MDOR cell line prior to the [<sup>35</sup>S]GTPγS antagonist assay vs. 1 μM CYM51010 experiment. Mixed membrane experiments produce a biphasic curve similar to that in the MDOR, with one important difference. The high potency site in the mixed membrane (IC<sub>50DORMX</sub> = 89 nM) is comparable with that of the DOR only line (IC<sub>50DOR</sub> = 76 nM) (Figure 2.9B). Most notably, these two potencies do not reflect the high potency site observed in the co-expressed MDOR cell line (Figure 2.9C).

The additive nature of the mixed membrane experiment (that is stacking the MOR cell line signal on top of the DOR cell line signal) means the Frac<sub>HIGH</sub> is dependent on the relative assay window of the MOR and DOR lines, where in the MDOR line the assay window is dependent on the activation within the same line. The relatively small Frac<sub>HIGH</sub> approximately matches the expected Frac<sub>HIGH</sub> based on the DOR and MOR assay windows alone (not shown). Importantly, this experiment demonstrates that co-expression of both MOR and DOR on the same membrane is required for D24M to show subnanomolar potency, consistent with activity at the MDOR site.



### 2.3.6 Preliminary *in vivo* assessment of D24M

D24M activity *in vivo* was measured using the 52° C tail-flick antinociception assay in the presence of 3.2 nanomoles CYM51010 injected ICV (Figure 2.10). A single dose of CYM51010 was chosen to account for the low selectivity of CYM51010. 0.1 nanomole, 0.32 nanomole, and 1 nanomole D24M attenuated CYM51010 mediated antinociception with decreasing area under the curve (AUC) relative to the vehicle-treated animals (Figure 2.10A). As CYM51010 has been previously reported to mediate antinociception via the MDOR heteromer, these preliminary experiments suggest D24M effectively blocks MDOR activity *in vivo*.

## PART IV: DISCUSSION AND FUTURE DIRECTIONS

The current studies demonstrate the identification of a first-in-class MDOR selective antagonist; preliminary *in vivo* experiments support D24M's ability to block MDOR antinociception *in vivo*. The first MDOR selective antagonist will enable studying MDOR pharmacology *in vivo* pharmacology, particularly in the role of tolerance and withdrawal. This tool will be particularly important to help resolve conflicting reports regarding MDOR's role in tolerance, as reports of MDOR disruption can lead to reduced morphine tolerance while MDOR agonists also produce reduced tolerance. Depending on the results with D24M, we will consider future studies designing MDOR antagonists for therapeutic applications to reduce side effects of opioid therapy, drug addiction, and drug-seeking behavior.

### 2.4.1 In Vitro D24M Activity Discussion

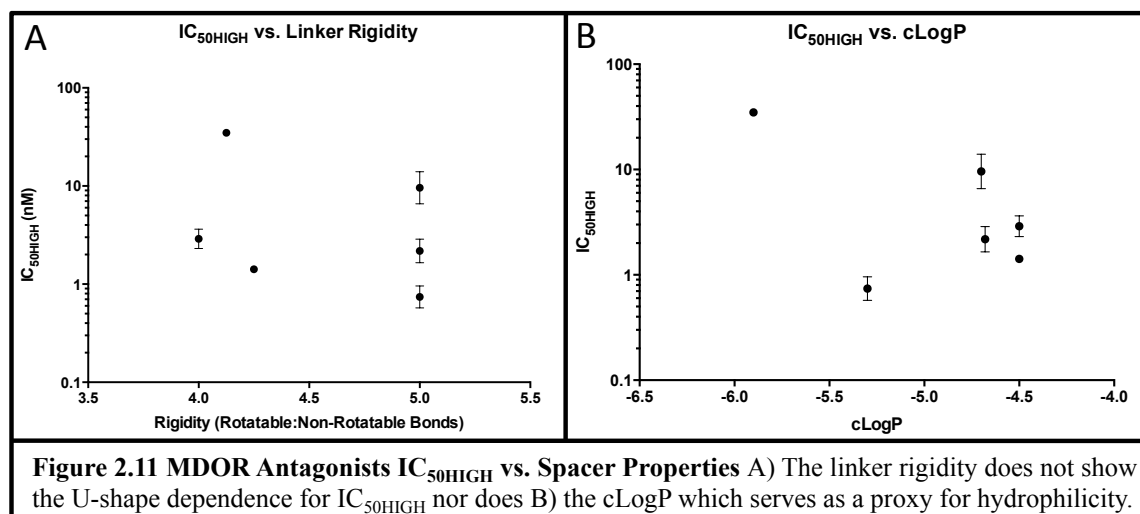
The currently designed bivalent ligands using low to medium affinity pharmacophores showed 91-fold activity improvement for MDOR over DOR and > 1,000 fold improvement over MOR antagonist activity (Table 2.5). Typically, when our lab and others started with two high-affinity ligands, bivalent ligands produced 10-100 fold improvement over one protomer, but only a 2-3x fold improvement over the second [137, 146-149, 152]. In contrast, our approach produced a 133-fold affinity improvement in the first generation of compounds.

A good strategy to target heteromers is utilizing a spacer length slightly longer than the distance between the two active sites [153]. Thus we designed, synthesized and evaluated the length-dependence of bivalent ligands with 15, 18, 21, 24, 30 and 41 atom

length spacers on MDOR activity and affinity (section 2.2.4). A spacer length of 24 atoms provided the highest potency, affinity, and most selective ligand (Table 2.4). The 24 atom spacer length is comparable to the Portuguese MDOR compound, MDAN-21. MDAN-21 contains the MOR agonist oxymorphone linked to the DOR antagonist naltrindole separated by a spacer of 21 atoms [48]. For MDAN-21 length dependence was observed using  $ED_{50}$  values for tail-flick antinociception, and increasing spacer length improved the tolerance profile of these ligands. It's worth noting, 21 atoms was the longest spacer tested by the Portuguese report, meaning longer linker lengths could show further enhancements. Furthermore, this selectivity was not assessed with molecular pharmacological approaches. Other bivalent ligands including KOR-DOR [154] have lengths of 21-26 atoms and similar distances [154, 155]. Thus our spacer length is consistent with bivalent ligands at MDOR and other GPCRs.

#### 2.4.2 Influence of Bivalent Ligand Spacer Properties on Activity

As noted in section 2.0.6 spacer chemical properties – including lipophilicity and flexibility – can alter bivalent ligand activity if not carefully considered [140, 141]. To



show that spacer length and not other properties were responsible for the U-shape dependence curve, we plotted high potency antagonist activity ( $IC_{50HIGH}$ ) vs. flexibility and cLogP values (Figure 2.11). Figure 2.11A shows that spacer rigidity R: N – the ratio of rotatable to non-rotatable bonds – does not correlate to improved  $IC_{50HIGH}$ . The lack of a clear relationship demonstrates that minor differences in linker rigidity were negligible (Figure 2.11A). Similarly, Figure 2.11B shows cLogP does not produce length dependence indicating hydrophilicity is not driving the bivalent ligand activity. Thus, minor differences in spacer composition were not responsible for the high potency sites and validated the spacer length and design of D24M for future optimization [116].

#### 2.4.3 D24M In Vivo Preliminary Activity Discussion

D24M activity *in vivo* was measured using the 52°C tail-flick antinociception assay vs. a constant concentration of ICV injected CYM51010 – an MDOR preferring agonist (Figure 2.10). 0.1 nmol, 0.32 nmol and 1.0 nmol per mouse D24M dose-dependently blocked CYM51010 mediated antinociception (Figure 2.10). As CYM51010 has been previously reported to mediate antinociception via the MDOR heteromer, these preliminary experiments suggest D24M effectively blocks MDOR activity *in vivo*.

While we began with ICV injection of D24M because our long-term interest involves the role of MDOR supraspinally in the regulation of tolerance, withdrawal and other opioid-mediated behaviors, final D24M characterization should consider intrathecal (IT) administration. IT injection will measure the D24M antagonist activity vs. agonists at the synapse between primary and secondary neurons, limiting any potential influence of differences in ligand distribution or neural circuitry confounding the observed results.

The first set of studies to address D24M potency should use various D24M concentrations vs. a single dose of CYM51010. Then selectivity of D24M *in vivo* can be assessed by comparing antagonist activity vs. DAMGO (MOR-selective), Deltorphin-II (DOR selective) and CYM51010 (MDOR preferring). Previous studies with DOR knockout mice demonstrated that acute antinociception in response to the MOR agonist DAMGO was unaltered [156], with a similar finding in MOR knockout mice with the DOR agonist DSLET or Deltorphin-II [157], suggesting both ligands induce acute antinociception independent of MDOR activation (other agonists are altered by knockout of MOR or DOR, suggesting MDOR activation).

The *in vivo* selectivity for CYM51010 antinociception can be addressed using analogous studies to Figure 2.6 with CYM51010 antinociception assessed in the presence of  $\beta$ -FNA (MOR-selective irreversible antagonist) and 5'-NTII (DOR selective irreversible antagonist). This study can determine to what extent CYM51010 mediates antinociception via MDOR (vehicle), MOR (+5'NTII) and DOR (+ $\beta$ -FNA). The spare receptor is not expected to be a problem as was in the *in vitro* studies as dosages of 5'NTII and  $\beta$ -FNA for antinociceptive studies have been clearly established to abolish DOR and MOR-mediated antinociception, respectively. If a D24M dose that maximally inhibits CYM51010 does not block DAMGO (MOR) or Deltorphin-II (DOR) mediated antinociception, then that concentration of D24M will be used for future selective studies. Otherwise,  $K_B$  may be determined to directly compare antagonist potency vs different agonists.

Afterward, direct *in vivo* assessment of MDOR mediated effects may be possible using D24M and/or subsequent analogs. D24M should prove more useful than other

approaches to studying MDOR using more indirect methodologies – such as ligand co-treatments, disruptor sequences or antibodies – with uncertain pharmacology at MDOR. For example, *in vitro* MDOR signals through the pertussis toxin insensitive  $G\alpha_z$  pathway. The use of disruptor sequences [45] such as MOR<sup>TM1</sup> [46] could leave precoupled  $G\alpha$  proteins intact and capable of signaling through the monomer. Furthermore, these disruptor sequences only use one interface at a time, despite modeling and disruptor sequences showing multiple contact points between MOR and DOR including MOR<sup>TM1</sup> [46], the DOR carboxyl tail and others. Disrupting one of the several interfaces may not completely disassociate MDOR leading to altered activities instead of abolished ones. D24M's use as a selective MDOR antagonist enables traditional pharmacological approaches to study MDOR, allowing greater control and easier interpretation than the disruptor, the antibody or co-treatment studies. Co-treatment and previous ligands such as MDAN-21 induce several confounding variables. MDAN-21 alters membrane trafficking of the receptors, and the presence of an agonist and antagonist pharmacophore leads to uncertain effects at the molecular level of MDOR [112]. Altering receptor levels at the membrane either through co-degradation or KO animals may alter results by inducing compensatory mechanisms independent of a direct MDOR interaction. Thus the use of D24M in MDOR studies can more clearly define its role in tolerance, withdrawal and other opioid-mediated behaviors.

#### 2.4.4 MDOR and DOR Agonists Discussion

The control experiment in MDOR cells using  $\beta$ -FNA to block MOR-mediated activity yielded interesting results – that  $\beta$ -FNA increased DOR agonist efficacy of

Deltorphin-II (Figure 2.9, lower middle panel). This relationship between an MOR antagonist and DOR agonist has not been previously reported to the author's knowledge. This relationship is particularly interesting given the constitutive recruitment of  $\beta$ -arrestin2 to MDOR [97]. Due to  $\beta$ -arrestin2's established role in receptor desensitization, these results may suggest that a MOR antagonist can increase DOR agonist efficacy by disrupting constitutive  $\beta$ -arrestin2 recruitment. Follow-up studies on MOR antagonist and DOR agonist relationships in neuropathic pain states with increased DOR membrane expression are warranted [158, 159]. The observation that a MOR antagonist increases DOR agonist efficacy *in vitro* is particularly compelling suggesting multi-functional compounds of a MOR antagonist and DOR agonist may be desirable in states with DOR upregulation if antinociception is preserved. Future *in vivo* studies would have to confirm that in appropriate pain or inflammatory models. The MOR antagonist would imbue reduced abuse liability while enhancing the DOR analgesia (putatively by disrupting constitutive arrestin recruitment).

#### 2.4.5 Future Directions and Experiments

The next step(s) in this project can be separated into four categories 1) establishment of methods and techniques for final D24M selectivity characterization *in vivo* (see section 2.4.3), 2) development of *in vitro* tools to study MDOR mediated signaling in greater detail, 3) SAR of D24M to improve selectivity and biological activity, and 4) *in vivo* assessment of MDOR mediated effects including opioid-induced tolerance, withdrawal and characterizing to what extent bivalent ligands such as

MMP2200 or biphalin (section 2.1) mediate their desirable therapeutic effects through MDOR.

#### *2.4.4A Development of In Vitro Tools to Characterize MDOR Signaling*

To further characterize D24M and better understand MDOR activity, techniques capable of monitoring only MDOR mediated signaling are required. Recently, techniques utilizing fluorescent and bioluminescent resonance transfer (FRET and BRET) technologies have been used to study signaling at a few GPCR heterodimers. Complemented donor-acceptor resonance energy transfer (CODA-RET) has been used to study heteromer specific signaling of dopamine 1 and dopamine 2 receptors (D1-D2) [160] and the Angiotensin 1 Receptor (AT1R) with the  $\alpha_{2c}$ -adrenergic receptor ( $\alpha_{2c}$ -AR) [161].

These systems triply co-transfect GPCRs, each tagged with half a split luciferase (Rluc8), and a signaling protein tagged with the mVenus fluorescent acceptor such as G $\alpha$  or  $\beta$ -arrestin. In this methodology, the Rluc8 is the donor molecule, which generates a luminescent signal only when the two receptors are proximal. The acceptor molecule mVenus is tagged to the signaling protein and can only be excited when Rluc8 is reconstituted. Thus upon treatment with a Rluc8 substrate – such as coelenterazine – one can measure the association of MOR, DOR, and a signaling protein. While this technology remains relatively new and validated in only a few systems, this technique would provide a new and powerful methodology to study the MDOR heteromer *in vitro*. Furthermore, the establishment of this technique and comparison to BRET experiments for the MOR and DOR homomers would enable confirmation of D24M selectivity.

#### 2.4.4A Future Structure-Activity-Relationships (SAR)

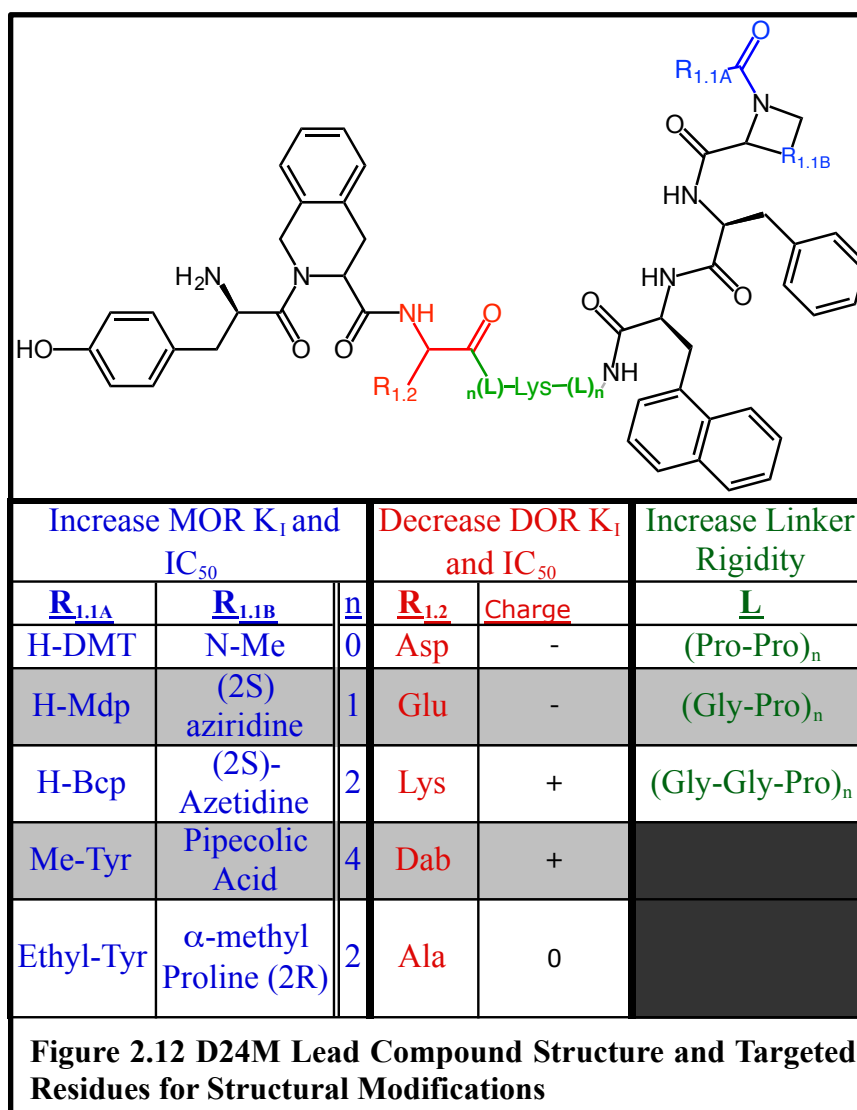
The third set of future studies involve determining the structure activity relationship (SAR) of D24M to improve MDOR selectivity by 1) decreasing DOR potency, 2) increasing MOR potency, 3) performing unique SAR and 4) increasing linker rigidity. The selectivity of our candidate compound – D24M – is practically speaking limited by the activity of the more potent DOR pharmacophore (Sec C1.0). Antagonist function and binding results indicate the MOR pharmacophore displayed significantly lower potency and affinity than the DOR pharmacophore at the respective homomers (Table 2.4). Thus increasing the MOR pharmacophore affinity may improve the MDOR:DOR:MOR selectivity ratio.

To improve MOR affinity, one can conformationally constrain the Tyrosine residue (R<sub>1.1</sub> in Figure 2.12) through introduction of 2,6-dimethyl-Tyrosine (H-DMT) and related analogs such as 4'-[N-((4'-phenyl) phenethyl) carboxamido] phenylalanine (BCP) and (2S)-2-methyl-3-(2',6'-dimethyl-4'-hydroxyphenyl)-propionic acid (MDP) to improve the MOR profile, as previously demonstrated [123, 162-164]. Additionally, a particularly pertinent modification for opioid antagonists is the removal of the N-amino charge using alkylated or des-amino analogs, which simultaneously increase potency and affinity of opioid antagonists [162, 165, 166]. Both proposed MOR modifications are synthetically straightforward and likely to improve MOR activity.

Competitive binding assays in MDOR cells show allosteric shifts upon co-treatment of MOR and DOR ligands. Additionally, ligands show subtle but clear changes in affinity in MDOR vs. MOR or DOR cells (section 2.0.4). Thus, a unique SAR of

MDOR compared to MOR or DOR is likely identifiable. A good starting place for this evaluation is the proline residue of the MOR pharmacophore (Figure 2.12). For example, substitution of Pro with N-Me [132, 133] can improve MOR antagonist potency and affinity. In fact, most opioid peptide antagonists in the literature contain N-alkylated residues at position 2, such as Aib [167], Pro [132, 168], N-Me-Phe [167], Tic [122] and N-methyl [132, 133]. A parallel SAR at position 2 could modify the number of carbons in proline analogs to establish if ring size at position 2 influences MDOR:MOR:DOR selectivity for the bivalent ligands. These modifications to position 1 and 2 of the MOR pharmacophore are likely to produce ligands with improved potency and selectivity at MDOR while exploring the unique structural requirements for heteromer affinity at each protomer.

Next, to increase selectivity one can reduce the DOR pharmacophore potency and affinity. The D24M series shows a modest 2-3 fold improvement in DOR potency relative to the parent pharmacophore (Table 2.4), with better activity than at MOR. Thus decreasing the relative DOR activity may increase MDOR selectivity. Previous SAR on the parent structures found that hydrophobicity increased DOR potency and affinity, suggesting that conversion of the COOH in H-Tyr-Tic-OH to the alkyl spacer may improve DOR potency [116]. Therefore, we hypothesize the reintroduction of a charge – specifically COOH – will decrease DOR potency leading to a more balanced ligand



profile. By decreasing DOR affinity – while evaluating negative, positive and neutral residues – we expect to observe an avidity bonus stemming from a more balanced profile of the individual pharmacophores and evaluate how R<sub>2</sub> residue composition affects the MDOR SAR (Figure 2.12).

The last SAR series begins with a relatively flexible linker to ensure the pharmacophores could correctly orient themselves within their respective binding pockets. The next SAR study could increase linker rigidity to improve MDOR selectivity by minimizing the entropic penalty of our currently flexible linker. We previously found that semi-rigid linkers with (Gly-Pro)<sub>n</sub> maximized GPCR hetero-bivalent ligand binding enhancements in other GPCR systems [137, 146, 148, 169]. Thus, future studies will determine the optimal linker rigidity for D24M by gradually increasing rigidity, using a slightly rigid (Gly-Gly-Pro)<sub>n</sub> motif and a moderately rigid (Gly-Pro)<sub>n</sub> repeat.

#### 2.4.5 Conclusions

Our lead MDOR selective antagonist is a first-in-class ligand enabling molecular and behavioral studies of MDOR *in vivo* with greater precision than previously possible. D24M and related structures will provide insight into opioid-mediated behaviors including pain, tolerance, drug seeking behavior, and analgesic drug development at MDOR, which is currently difficult to study *in vivo*. The need for these types of studies is demonstrated by the findings that MDOR is upregulated after chronic morphine treatment [98] and that MDOR disruption [46] suggests that MDOR contributes to several opioid side effects including tolerance [48], drug-seeking behavior [43], and withdrawal [99]. These studies remain unclear whether the MDOR is only active during sustained opioid

treatment, how it modulates neural circuitry in pain and dependent states, and what the precise physiological role of the MDOR is relative to MOR or DOR; our compounds will allow us to address these questions.

**CHAPTER 3:****BINDING AND FUNCTIONAL EVALUATION OF CLINICAL ANALGESICS  
AT ATYPICAL OPIOID AND NON-OPIOID PAIN TARGETS**

## PART I: INTRODUCTION

### 3.1 Clinical opioids – *in vitro* and *in vivo* efficacy and tolerance

Clinical opioids typically mediate analgesia and side effects through the MOR. However, clinicians have long appreciated subtle but significant differences between opioids. Most notably different opioids can show distinct side effect profiles and varying efficacies in different patients [76]. These observations led pharmacologists to propose different MOR opioid subtypes at numerous times, particularly in the 50s and again in the 90s [76]. Clinicians take advantage of these differences by implementing ‘opioid rotations’ in chronic pain patients. Opioid rotations switch one opioid for another every few months to minimize tolerance and maximize analgesic activity [77]. These subtle differences between clinical opioids suggest additional pharmacodynamic or pharmacokinetic contributions beyond MOR efficacy.

#### 3.1.1 Opioid efficacy and potency between assays

Modest differences in opioid efficacy can partially explain the clinical differences between opioids. Classically, ligand efficacy is defined by the magnitude of a response (i.e. measured pathway or behavior) relative to receptor occupancy for a given ligand. Operational efficacy –  $\tau$  – quantifies an agonist’s ability to produce 1) the measured response, and 2) the system’s ability to translate the stimulus into the response [150]. *In vivo*, the system’s ability to translate a stimulus (i.e. drug) into a response (i.e. antinociception) depends on the targeted receptor (i.e. MOR). Most studies correlate *in vivo* antinociception efficacy and *in vitro* MOR signaling efficacy using several different opioids to show the relationship between MOR and antinociception.

*In vivo* efficacy is estimated by using irreversible antagonists to dose-dependently reduce MOR receptor quantity to determine the receptor number required for antinociception. By gradually reducing receptor number,  $\tau$  accounts for differences in receptor density, transduction efficiency, and maximal response. Similarly, *in vitro*  $\tau$  calculations may use affinity and  $B_{MAX}$  to account for receptor density, transduction efficiency and maximal system response. Comparisons of  $\tau$  in tail-flick antinociception [80-82] and *in vitro* [ $^{35}S$ ]-GTP $\gamma$ S coupling assays reveal different rank orders for opioids (Table 3.1). For example, fentanyl has less efficacy *in vitro* than etorphine, but similar or higher efficacy *in vivo* (Table 3.1). Similarly, methadone and morphine are equiefficacious in antinociceptive assays, but morphine's  $\tau$  is nearly one-fourth of methadone *in vitro* [78] (see section 3.4.3 for further discussion). These subtle differences indicate that MOR efficacy cannot completely explain clinical opioid activity *in vivo*.

These correlation studies require careful interpretation and often overlook subtle differences between opioids. First,  $R^2$  values between *in vitro* and *in vivo* efficacy do not indicate a direct causation; statistically, correlation does not mean causation. Correlations provide a population-level analysis [78] but mask individual ligands with higher or lower efficacy than expected. Thus while intrinsic efficacy has classically explained differences between opioids [170], it fails to account for outlier cases where the *in vivo* and *in vitro* efficacy estimates do not match and nuanced differences between opioids.

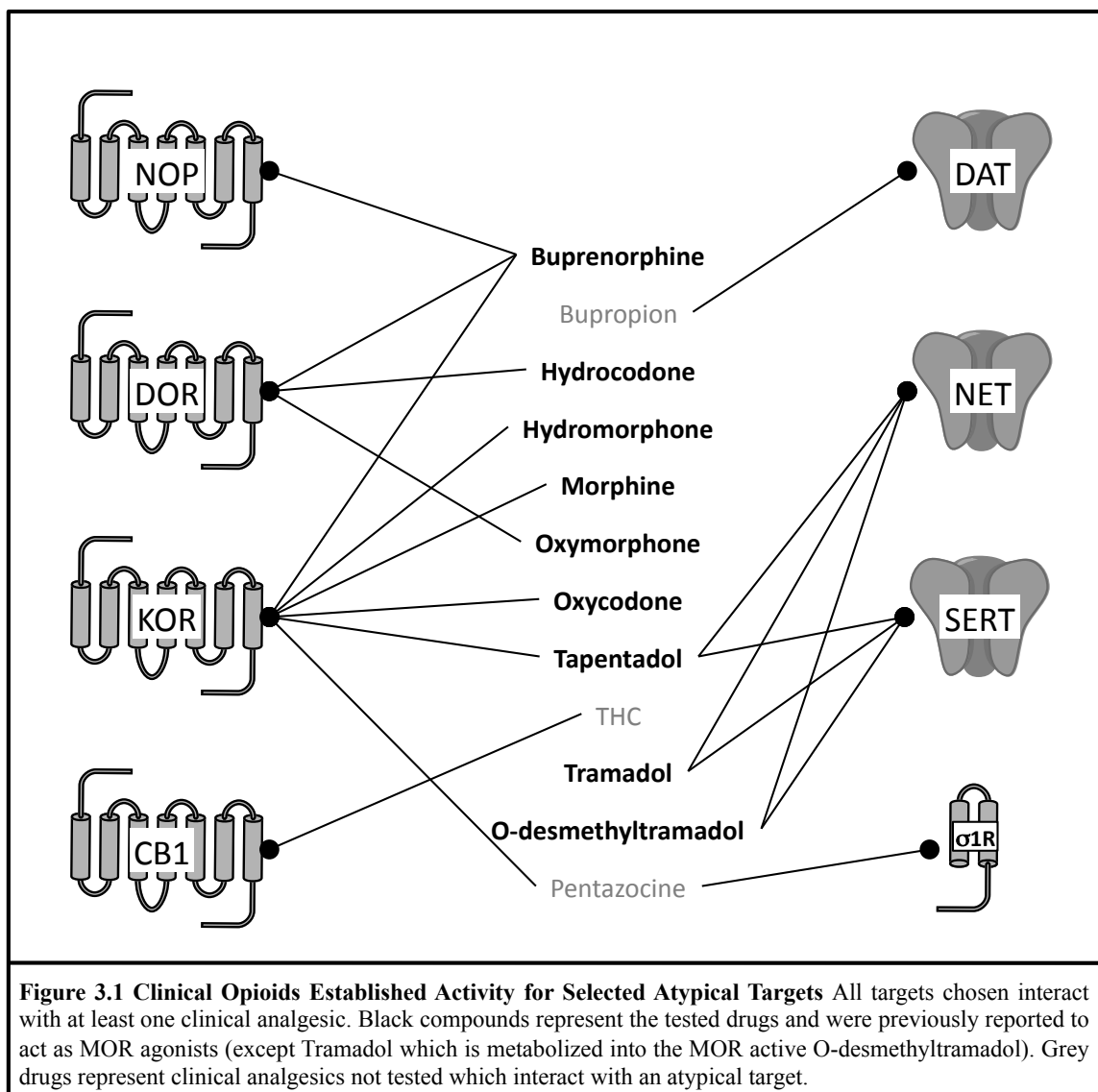
Ligand	<i>in vivo</i> Antinociception		<i>in vitro</i> [ $^{35}S$ ]-GTP $\gamma$ S	
	$\tau$	Cite	$\tau$ (SEM)	Cite
Fentanyl	54-62 <sup>a</sup>	79	12.3 (0.6)	78
Etorphine	48-57 <sup>a</sup>	80	17.5-24.9 <sup>a</sup>	80
Methadone	35-44 <sup>a</sup>	81	18.2 (0.9)	78
Morphine	38-41 <sup>a</sup>	80	2.8-3.9 <sup>a</sup>	80
Oxycodone	19-21 <sup>a</sup>	80	5.1 (0.2)	78

**Table 3.1. Relative efficacy ( $\tau$ ) of Various Clinical Opioids for *In vivo* Antinociception and *In Vitro* [ $^{35}S$ ]-GTP $\gamma$ S Coupling <sup>a</sup>95% Confidence Intervals**

### 3.1.2 Differences in opioid tolerance

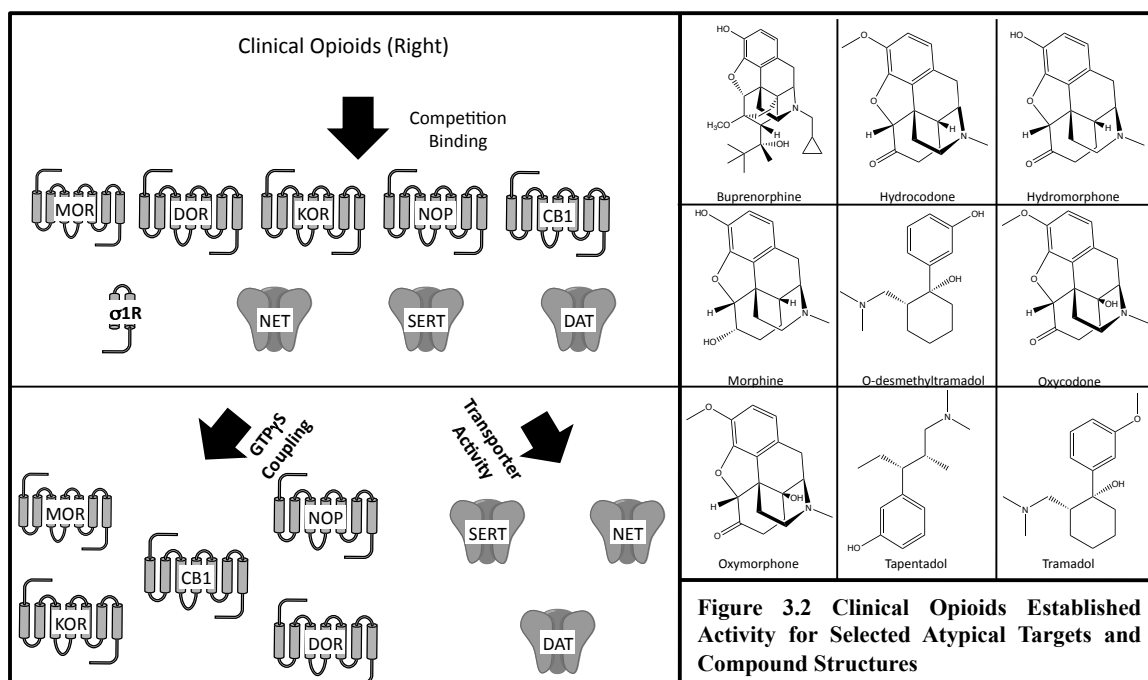
Differences in MOR efficacy may contribute to side effect profiles. Low efficacy agonists produce less respiratory depression and withdrawal in physically dependent patients [171] while high-efficacy agonists correlate with stronger analgesia. However, deeper analysis comparing ligand efficacy and system desensitization reveals subtle differences between opioids not explained by the intrinsic efficacy model. Prolonged opioid treatment *in vitro* causes receptor desensitization and shifts the agonist curves rightward – the magnitude of this shift correlating with agonist efficacy [172]. However, *in vitro* receptor desensitization and antinociceptive tolerance studies do not always correlate. For example, the high efficacy agonist etorphine produces less antinociceptive tolerance than the lower efficacy oxycodone agonists [81]. The relationship between efficacy and tolerance is further complicated by the fact that many opioids do not produce cross-tolerance. A lack of cross-tolerance is the reason opioid rotations work (see section 3.1) – even though chronic oxycodone treatment requires increasing dosages to produce the same antinociceptive effect, morphine remains antinociceptive at equipotent dosages in oxycodone tolerant and naive animals [173].

A difference between *in vitro* and *in vivo* efficacy estimates can arise if the ligand regulates antinociception by more than one receptor *in vivo*, even though only one receptor was considered *in vitro*. Additional explanations for these disparities, beyond the scope of the current studies include differences pharmacokinetics and tissue coupling efficiency. Since non-MOR targets can modulate MOR antinociception (see section 1.3.2B), the current study investigated off-target effects that may modulate *in vivo* efficacy estimates not considered for *in vitro* signaling estimates.



### 3.1.2 Rationale

Models of clinical drug activity at off-target receptors reveal many drug side effects are explained by off-target interactions [174]. Similar studies have not been reported for opioids. Due to differences in tolerance, cross-tolerance, and *in vivo* vs. *in vitro* efficacy between different opioids, we hypothesize that some clinical opioids may mediate these effects through atypical non-MOR targets. We chose eight atypical targets,



which interact with known clinical analgesics (Figure 3.1), based on our labs resources and expertise. Most of the clinical analgesics chosen (Figure 3.1, black words) – buprenorphine [78], hydrocodone, hydromorphone, morphine [78], oxymorphone, oxycodone [78], tapentadol [175], tramadol [176] and O-desmethyltramadol [175] – act as MOR agonists [7, 76, 177].

The established selectivity varies between ligands, with some showing non-MOR effects. Notably, buprenorphine interacts with DOR [178], KOR [179] and NOP [180], causing distinct changes to its *in vivo* profile. Thus, we screen all opioids against these three GPCRs, as well as CB1, which produces antinociception and analgesia from THC and related cannabinoids [181]. The three monoamine transporters – DAT, NET, and SERT – contribute to tramadol [52], tapentadol [175], and O-desmethyltramadol [182] antinociception via inhibition, while the DAT inhibitor bupropion effectively treats neuropathic pain in some patients [183]. The final target chosen –  $\sigma$ 1R – is an

intracellular protein, which was originally misidentified as an opioid receptor due to cross-reactivity of pentazocine [74, 184] and similar opioids.

Opioid activity at these atypical targets was frequently discovered in an *ad hoc* manner for individual ligands (see buprenorphine). Consequently, no unbiased screen to assess opioid activity at other targets has been reported. Such a screen will aid in understanding if differences in efficacy, tolerance, cross-tolerance, and side effects between opioids arise from unidentified atypical targets. To test this hypothesis, we screened a panel of 9 clinical analgesics at 8 non-MOR targets involved in antinociception [14, 52, 68, 71, 72, 154] (Figure 3.2; see Section 1.3.2B).

## **PART II: MATERIALS AND METHODS**

### *3.2.1 Stable Cell Line Creation*

HEK293 cells were transfected with human DAT, SERT, NET and  $\sigma$ 1R cDNA on the pEZ-M06 vector from Genecopoeia via electroporation. All constructs contained an N-terminal intracellular HA-tag. After electroporation cells recovered for 24 hours and then stably expressing clones were selected with 500  $\mu$ g per mL G418 over 5-10 passages. After recovery, expressed cells were fixed with  $-20^{\circ}$  C MeOH: Acetone 1:1 for 15 minutes on collagen treated confocal plates for immunocytochemistry (ICC) to determine receptor expression. After fixation cells were treated with anti-HA Alexa 488 in PBS + 10% goat serum for 2 hours at 1:50 dilution, treated with DAPI, then imaged on a Leica SP6 Confocal Microscope.

CHO cells (CB1, MOR, DOR, KOR and NOP) were grown as in section 2.2.4. MOR and DOR cells same as section 2.2.4. CB1 and NOP cells purchased from Perkin Elmer. HEK293 cells stably expressing DAT, NET, SERT, and  $\sigma$ 1R were grown in MEM with 10% FBS, 1% PS and 500  $\mu$ g per mL G418. SERT was grown in dialyzed FBS. All cells were split 1:2 every ~2-3 days. Previous saturation binding results were reported for MOR and DOR are reported in section 2.2.6. Analogous saturation binding vs. [ $^3$ H]-Diprenorphine at KOR determined the  $K_D = 1.8$  nM,  $B_{max} = 1.3$  pmol/mg.

### 3.2.2 Membrane Preparations

For competition binding and [<sup>35</sup>S]-GTPγS coupling studies, membrane preparations were made from cells grown on 15 cm<sup>2</sup> culture treated plates. Upon reaching confluence cells were treated with 5 mM EDTA in PBS for 30 minutes or until the cells lifted from the plate, and centrifuged at 3,000 g at 4° C for 5 minutes. The supernatants were removed, and pellets were frozen at -80° C until used. Previously frozen pellets were homogenized with a glass-Teflon Dounce homogenizer. DOR, MOR, KOR and NOP membranes were homogenized in 10 mM Tris-HCl pH 7.4, 100 mM NaCl and 1 mM EDTA. NET, DAT and SERT were homogenized in 50 mM HEPES pH 7.15, 125 mM NaCl, 3.3 mM EDTA, and both were spun down at 15,000 g for 60 minutes at 4°C. σ1R

Cell line	Binding Buffer	Radioligand	Time and Temp	Functional Activity Assay Buffer
MORCHO	50 mM TrisHCl pH 7.4, 1 mM PMSF	[ <sup>3</sup> H]-Diprenorphine	1 Hr; 30° C	50 mM Tris-HCl, pH 7.4, 100 mM NaCl, 5 mM MgCl <sub>2</sub> , 1 mM EDTA, 40 μM GDP and 1 mM PMSF.
DORCHO	50 mM TrisHCl pH 7.4, 1 mM PMSF	[ <sup>3</sup> H]-Diprenorphine		
KORCHO	50 mM TrisHCl pH 7.4, 1 mM PMSF	[ <sup>3</sup> H]-Diprenorphine		
NOPCHO	50 mM TrisHCl pH 7.4, 1 mM PMSF	[ <sup>3</sup> H]-Nociceptin		
CB1CHO	50 mM TrisHCl pH 7.4, 1 mM PMSF	[ <sup>3</sup> H]-CP55,940		20 mM HEPES pH 7.15, 200 mM NaCl, 3 mM MgCl <sub>2</sub> , 15 μM GDP
SERTHeK293	50 mM HEPES pH 7.15, 125 mM NaCl, 3.3 mM EDTA, 0.1% Ascorbic Acid	[ <sup>3</sup> H]-Mazindol	1.5 Hrs; 37° C	50 mM HEPES in Hanks Balanced Buffer Solution (HBBS) without Calcium or Magnesium
NETHEK293	50 mM HEPES pH 7.15, 125 mM NaCl, 3.3 mM EDTA, 5 mM KCl, 1x Millipore Peptidase Inhibitor	[ <sup>3</sup> H]-Mazindol		
DATHEK293		[ <sup>3</sup> H]-Mazindol		
σ1RHEK293	50mM Tris, pH 8.0	[ <sup>3</sup> H]-DTG	4 Hrs.; 37° C	

**Table 3.2 Competition Binding and Functional Assay Buffer Composition and Conditions**

was homogenized in 50 mM Tris-HCl pH 8.0 and spun down at 15,000 g for 60 minutes at 4°C. The supernatant was removed and membranes re-suspended in the appropriate buffer indicated in Table 3.2, followed by homogenization with the glass-Teflon Dounce.

### *3.2.3 Competition Radioligand Binding Assays*

Membrane preparations were adjusted to 20-40 µg of membrane protein per reaction. Unless otherwise noted, membranes were mixed with radioligand (Table 3.2) at a concentration  $< K_D$ , and competition drug. Non-specific binding (NSB) was determined with saturating concentrations of known receptor ligands as indicated in the saturation binding section, and 100% binding determined in the presence of vehicle alone. Final reactions were made to 200 µL volume and incubated at the time and temperature indicated in Table 3.2. The reaction was terminated by rapid filtration using a 96-well plate Brandel cell harvester (Brandel, Gaithersburg, MD) onto 96 well GF/B filter plates (PerkinElmer). Bound [ $^3\text{H}$ ]-radioligand was measured using a MicroBeta2 scintillation counter (PerkinElmer). Curves were fit and analyzed for  $K_I$  values as in Chapter 2.

### *3.2.4 [ $^{35}\text{S}$ ]-GTP $\gamma\text{S}$ Agonist Assays*

Unless otherwise noted, protein was adjusted to 10-15 µg of membrane protein per reaction, and mixed with 100 pM [ $^{35}\text{S}$ ]-GTP $\gamma\text{S}$  (PerkinElmer) and concentration curves of drug to 200 µL final volume as in Section 2.2 Reactions were incubated at 30 ° C for 60 minutes followed by rapid filtration using a 96-well plate Brandel cell harvester (Brandel, Gaithersburg, MD). Bound [ $^{35}\text{S}$ ] GTP $\gamma\text{S}$  was measured using a MicroBeta2 scintillation counter. Curves were fit and data analyzed as in Chapter 2.

### 3.2.5 Monoamine Transporter Activity Assays

The “Neurotransmitter Transporter Uptake Assay Kit” from Molecular Devices (Part #R8173) was used to characterize compound’s activity at NET, SERT and DAT following the manufacturer’s protocol. Briefly, 96 well clear bottom black wall plates were coated with collagen and plated at 60,000-80,000 cells per well in MEM, 10% FBS, 1X Pen/Strep and 500 µg per mL G418. For SERT, dialyzed FBS was used to minimize serotonin contributions from media. All vehicles were diluted with 0.1% BSA in HBBS, 50 mM HEPES pH 7.15. Equilibrated drug and cells were incubated for 20 min. Then the transporter dye was added and equilibrated for 45 minutes at 37°C. The plates were then read on a BioTek Plate reader with 485(20) nm excitation and 528(20) nm emission filters. The resulting data was fit using 3-variable non-linear curve regression using Prism 7.0 (GraphPad). IC<sub>50</sub> values were fit directly, and I<sub>Max</sub> values were calculated by comparison to the positive control inhibitor S-duloxetine (I<sub>Max</sub> = 100%).

## PART III: RESULTS

### 3.3.1 Evaluation of HEK293 cells expressing $\sigma$ 1R, DAT, SERT, and NET

#### 3.3.1A Stable Transfection and Immunocytochemistry of $\sigma$ 1R, DAT, SERT and NET in HEK293 Cells

HEK293 cells were transfected with  $\sigma$ 1R DAT, SERT or NET cDNA via electroporation and stable populations selected with 500  $\mu$ g per mL G418 over 5-10 passages. Receptor expression confirmed using immunocytochemistry (ICC) against the

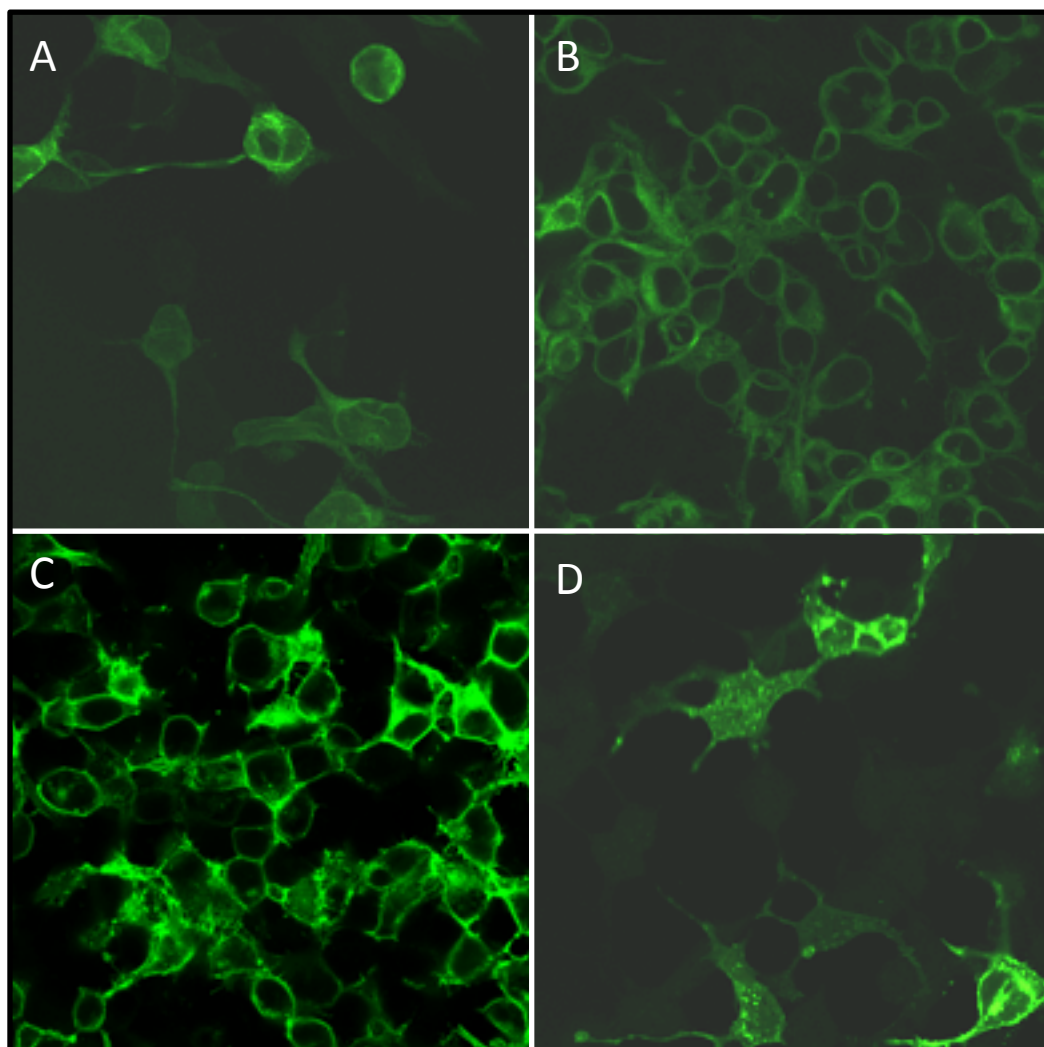


**Figure 3.3** SERT, DAT, NET and  $\sigma$ 1R ICC A-D) HEK293 cells stably transfected with cDNA encoding A)  $\sigma$ 1R B) NET-HA C) DAT-HA D) SERT-HA and imaged with anti-HA Alexa 488 and imaged via confocal microscopy.

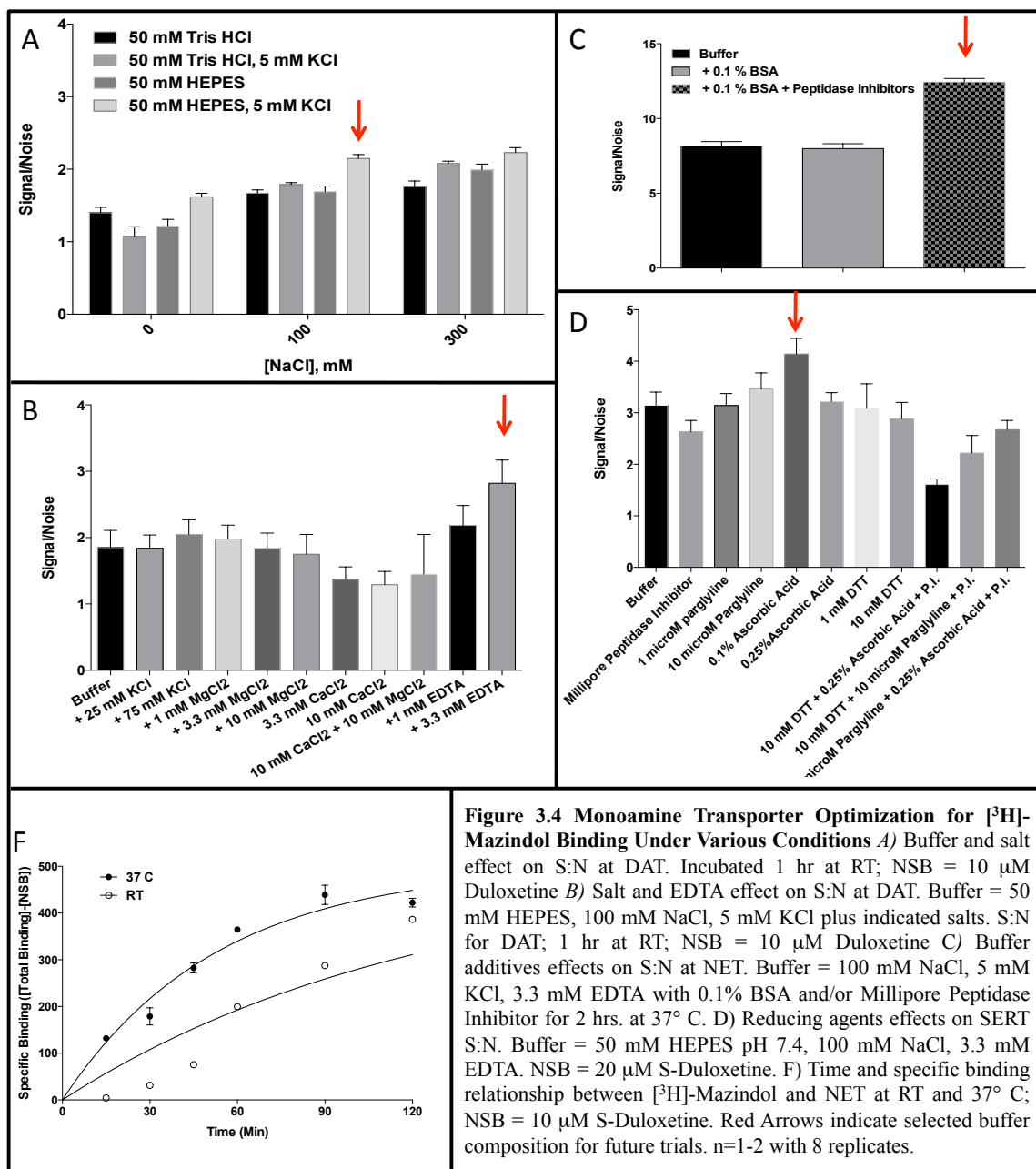


**Figure 3.4 Monoamine Transporter Optimization for [<sup>3</sup>H]-Mazindol Binding Under Various Conditions** A) Buffer and salt effect on S:N at DAT. Incubated 1 hr at RT; NSB = 10  $\mu$ M Duloxetine B) Salt and EDTA effect on S:N at DAT. Buffer = 50 mM HEPES, 100 mM NaCl, 5 mM KCl plus indicated salts. S:N for DAT; 1 hr at RT; NSB = 10  $\mu$ M Duloxetine C) Buffer additives effects on S:N at NET. Buffer = 100 mM NaCl, 5 mM KCl, 3.3 mM EDTA with 0.1% BSA and/or Millipore Peptidase Inhibitor for 2 hrs. at 37° C. D) Reducing agents effects on SERT S:N. Buffer = 50 mM HEPES pH 7.4, 100 mM NaCl, 3.3 mM EDTA. NSB = 20  $\mu$ M S-Duloxetine. E) Reducing agent combinations effects on SERT S:N. Buffer = 50 mM HEPES pH 7.4, 100 mM NaCl, 3.3 mM EDTA. NSB = 20  $\mu$ M S-Duloxetine. F) Time and specific binding relationship between [<sup>3</sup>H]-Mazindol and NET at RT and 37° C; NSB = 10  $\mu$ M S-Duloxetine. Red Arrows indicate selected buffer composition for future trials. n=1-2 with 8 replicates.

N-terminal intracellular HA-tag. Using the anti-HA Alexa 488 antibody (Figure 3.3A-D), all four lines were imaged using confocal microscopy, demonstrating a modest population of DAT,  $\sigma$ 1R, and NET with moderate expression levels and a large SERT population with high expression levels in the initial polyclonal lines. After confirming expression and membrane trafficking, each cell line was optimized for binding conditions and characterized for saturation binding.

### *3.3.1B Monoamine Transporter Radioligand Binding Optimization and Characterization*

To determine cell line feasibility for radioligand binding assays, DAT, SERT, and NET were optimized for various assay parameters against the non-selective inhibitor, [ $^3$ H]-Mazindol (Figure 3.4). First, SERT signal to noise (S:N) ratios was assessed under different buffers and salt concentrations: 50 mM HEPES or 50 mM Tris-HCl; 0, 100 or 300 mM NaCl; 0 or 5 mM KCl (Figure 3.4A). Since both 100 mM NaCl + 5 mM KCl and 300 mM NaCl + 5 mM KCl produced comparable S:N of  $\sim$ 2, we chose 100 mM NaCl + 5 mM KCl conditions (Figure 3.4A, red arrow) for future studies to minimize hypertonic effects during subsequent parameter optimization.

Next, the S:N was optimized with various concentrations of KCl, divalent cations, and EDTA (Figure 3.4B) added to the buffer. Divalent cations including MgCl<sub>2</sub> and CaCl<sub>2</sub> significantly reduced the counts per minute (CPM) signal (data not shown) and attenuated the S:N. Conversely, 1.0 mM and 3.3 mM EDTA increased the assay window and S:N (Figure 3.4B, red arrow). Finally, the buffer (50 mM HEPES pH 7.14, 100 mM NaCl, 5 mM KCl, 3.3 mM EDTA) S:N was maximized with additives to reduce NSB and maximize signal. At NET, the inclusion of 0.1% BSA and 1x Millipore peptidase

inhibitor produced a S:N of ~11 after a 2-hour incubation at 37° C (Figure 3.4C, red arrow).

Independently, SERT conditions were optimized to maximize S:N and assay window size. To enhance [<sup>3</sup>H]-Mazindol binding S:N, various reductants were added to the previously optimized SERT buffer – 50 mM HEPES pH 7.14, 100 mM NaCl (data not shown) (Figure 3.4D). DTT and pargyline reduced S:N, but 0.1% ascorbic acid improved S:N by reducing NSB. Furthermore, the Millipore peptidase inhibitor reduced the signal and thus was not used for SERT assays (Figure 3.4D).

These optimized conditions were used to determine the kinetics and equilibrium time required for [<sup>3</sup>H]-Mazindol binding, as shown for NET (Figure 3.4F). After a 90-minute incubation at 37° C, the specific binding (total binding – NSB) reached a maximum at NET, and analogous studies found the same results at SERT and DAT (data not shown). The final assay conditions (Table 3.2) produced S:N ratios of 4, 11 and 14 for SERT, NET, and DAT, respectively. These optimizations enabled the use of the polyclonal lines for compound competition binding.

Saturation binding was performed at DAT, SERT, and NET against various concentrations of [<sup>3</sup>H]-Mazindol to determine the  $K_D$  and  $B_{MAX}$  (Table 3.3). At DAT, [<sup>3</sup>H]-Mazindol produces a  $K_D = 16.2$  nM and  $B_{MAX} = 2.0$  pmol/mg; at NET the  $K_D = 7.8$  nM and  $B_{MAX} = 1.3$  pmol/mg; at SERT the  $K_D = 23$  nM and  $B_{MAX} = 1.7$  pmol/mg.

<b>Receptor</b>	<b>SERT</b>	<b>NET</b>	<b>DAT</b>	<b>σ1R</b>	<b>CB1</b>	<b>NOP</b>
$B_{MAX}$ ( <i>pmol/mg</i> )	2.0 (0.3)	1.3 (.12)	1.7 (0.1)	10.1 (0.4)	9.1 (0.5)	0.75 (0.02)
$K_D$ nM	23 (4.8)	7.8 (2.1)	16 (1.9)	13.4 (1.1)	0.92 (0.10)	0.075 (0.01)

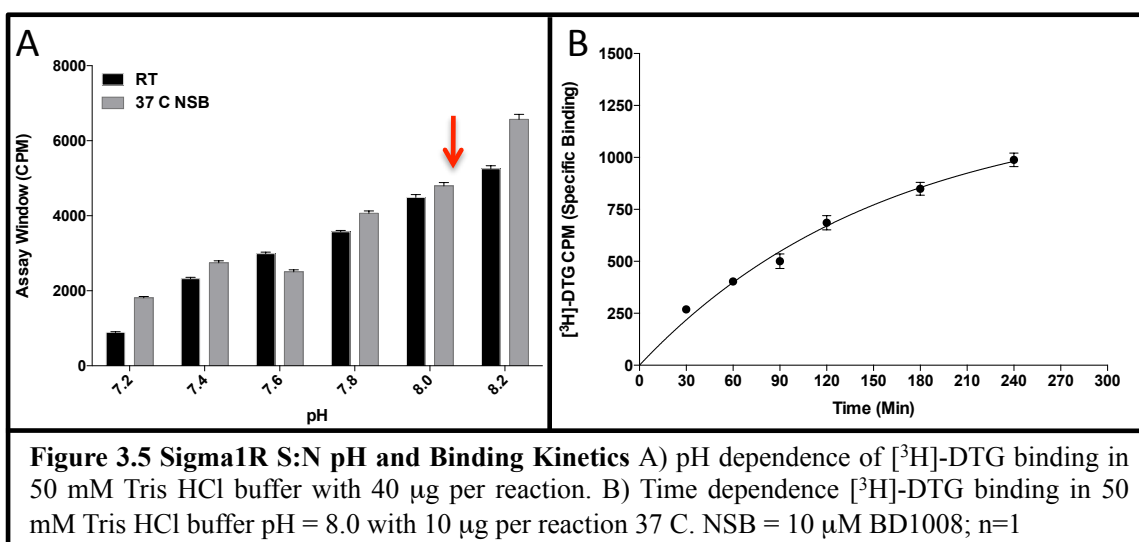
**Table 3.3 Saturation Binding of Transfected (SERT, NET, DAT and σ1r) and Commerical (CB1 and NOP) Cell Lines**

Previous saturation binding experiments at DOR, MOR and KOR vs. [ $^3\text{H}$ ]-Diprenorphine are reported in sections 2.2.5 and 3.2.1.

### 3.3.1C $\sigma 1\text{R}$ Receptor Radioligand Binding Optimization and Characterization

Previous reports of binding at  $\sigma 1\text{R}$  used basic assay conditions (pH = 8.0), so we first optimized the S:N against various pH levels (7.2-8.2) at RT and 37° C [185]. The total binding was determined against ~10 nM [ $^3\text{H}$ ]-DTG and NSB was determined against 1  $\mu\text{M}$  BD1008. All conditions produced large assay windows between 2000-6000 CPM and increased with pH and temperature (Figure 3.5A). Subsequent experiments used a pH = 8.0 to match previously reported conditions while maximizing the buffer capacity (Tris-HCl pK<sub>a</sub> at 37° C = 7.7 [186]).

To determine the binding kinetics, [ $^3\text{H}$ ]-DTG was incubated against  $\sigma 1\text{R}$  membrane preparations for 30-240 minutes (Figure 3.5B) against 5 nM [ $^3\text{H}$ ]-DTG. Specific binding plateaued around 240 minutes (Figure 3.5B). Subsequent saturation and competition binding experiments were incubated for 4.5 hours to ensure equilibrium



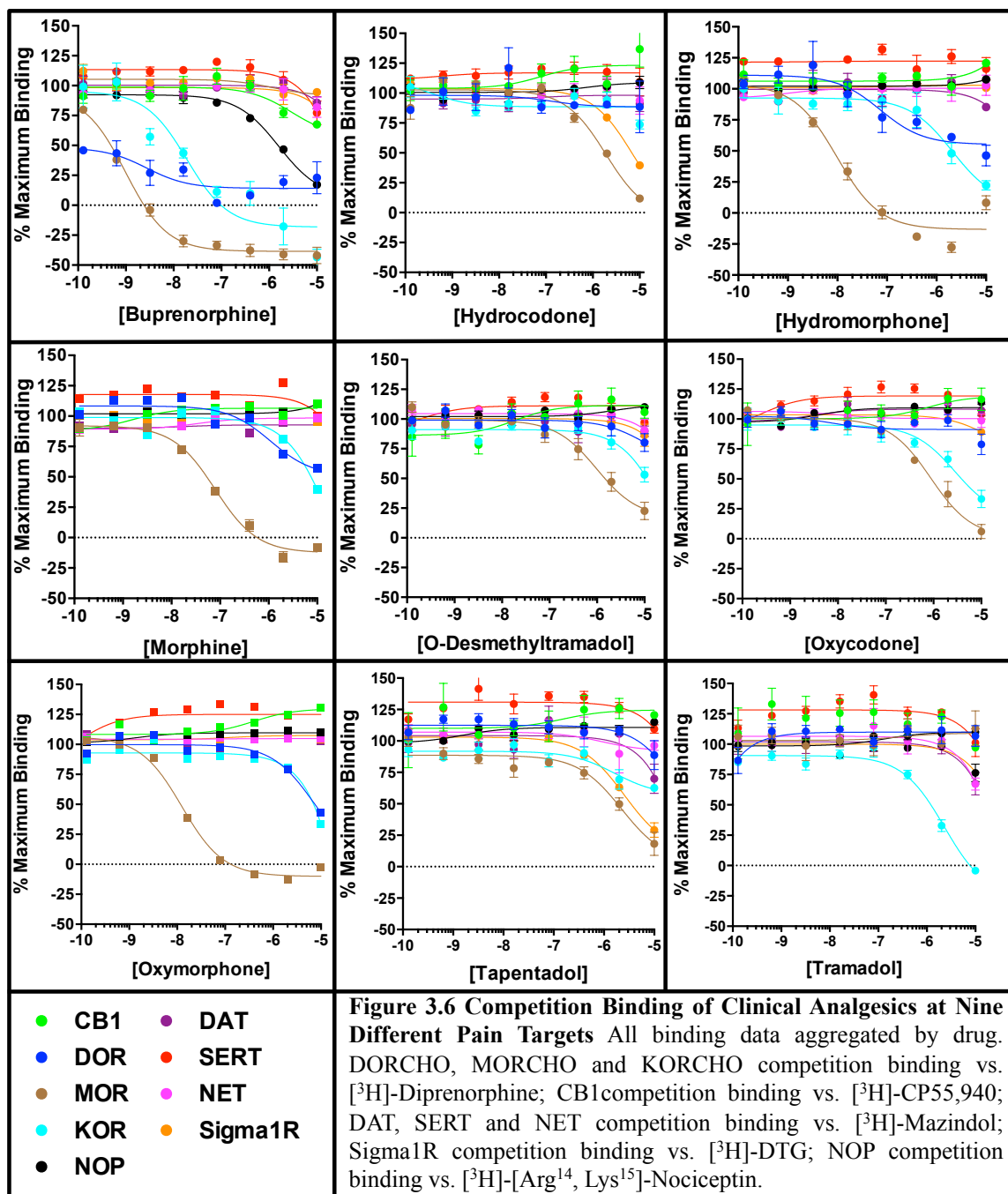
conditions. [<sup>3</sup>H]-DTG saturation binding at σ1R showed high receptor expression with a  $B_{MAX} = 10.1$  pmol per mg and a  $K_D = 13.4$  nM (Table 3.3). These assay conditions – 50 mM Tris-HCl pH = 8.0 for 4.5 hours at 37° C – produced excellent S:N ratios and assay windows for analyzing the competition binding studies.

### *3.3.1D CB1 and NOP Saturation Binding*

Lastly, we assessed PerkinElmer's stable cannabinoid receptor 1 (CB1) and nociceptin opioid receptor (NOP) CHO cell lines for saturation binding. A rigorous optimization was not performed, and saturation binding experiments proceeded using the PerkinElmer protocols adjusted for our lab setup. CB1 saturation binding was performed with varying concentrations of [<sup>3</sup>H]-CP55,940 with 10 μM WIN55,212-2 to determine NSB, yielding  $B_{MAX} = 9.1$  pmol per mg and  $K_D = 0.92$  nM (Table 3.3). NOP saturation binding was performed with varying concentrations of [<sup>3</sup>H]-Nociceptin with 200 nM [<sup>14</sup>Arg, <sup>15</sup>Lys] Nociceptin used to determine NSB, yielding  $B_{MAX} = 0.75$  pmol per mg and  $K_D = 0.071$  nM.

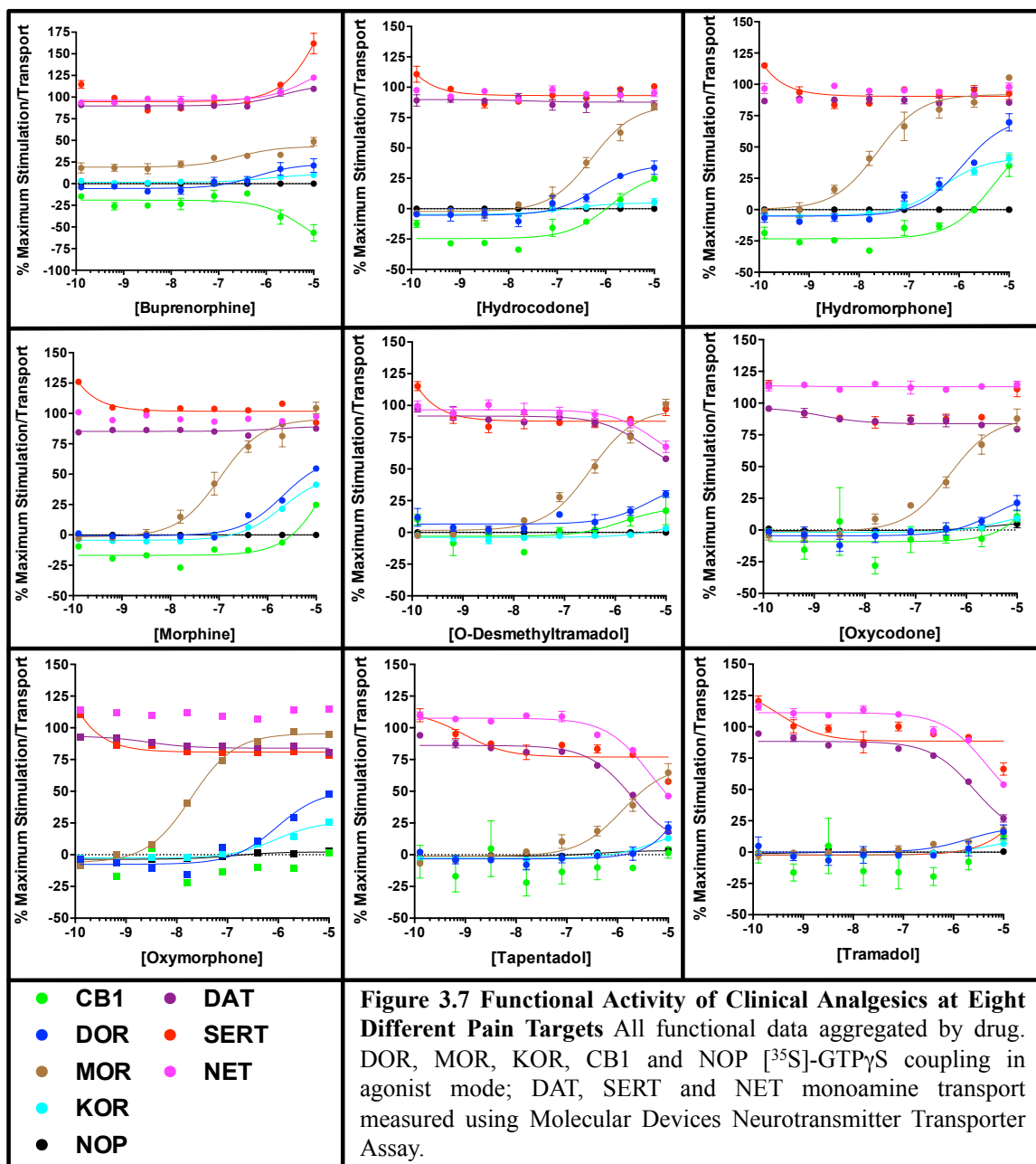
Ligand	MOR	MOR Ref.		DOR	KOR	NOP	CBI	o1R	NET	DAT	SERT
	K <sub>i</sub> (SEM)	K <sub>i</sub>	Ref.	K <sub>i</sub> (SEM)							
Buprenorphine	0.91 (0.10)	0.2157	14	34 (27)	27 (13)	430 (100)	>2,000	NC	NC	>2,000	>2,000
Hydrocodone	1800 (470)	41.58	14	>2000	NC	NC	NC	4000 (1300)	NC	NC	NC
Hydromorphone	9.4 (2.6)	0.3654	14	300 (150)	1580 (720)	NC	NC	NC	NC	NC	NC
Morphine	74 (18)	1.168	14	2500 (720)	>2000	NC	NC	NC	NC	NC	NC
O-Desmethyltramadol	1300 (290)	3190	38	NC	>2000	NC	NC	NC	NC	NC	NC
Oxycodone	780 (171)	25.87	14	NC	>2000	NC	NC	NC	NC	NC	NC
Oxymorphone	11 (1.8)	0.4055	14	>2000	>2000	NC	NC	NC	NC	NC	NC
Tapentadol	2100 (84)	160	13	NC	>2000	NC	NC	2700 (410)	NC	>2,000	NC
Tramadol	NC	12,486	14	NC	890 (33)	NC	>2,000	NC	NC	>2,000	>2,000
Naloxone	14 (1.9)	-	-	520 (110)	270 (46)	-	-	-	-	-	-
Noiceptin	-	-	-	-	-	0.71 (0.25)	-	-	-	-	-
Win [55,212-2]	-	-	-	-	-	-	33 (4.8)	-	-	-	-
BD1008	-	-	-	-	-	-	-	0.81 (0.32)	-	-	-
S-Duloxetine	-	-	-	-	-	-	-	-	110 (9.7)	51 (10)	520 (68)

**Table 3.4 Competition Binding of Clinical Analgesics at MOR and 8 Atypical Pain Targets** MOR, DOR and KOR competed against [<sup>3</sup>H]-Diprenorphine; NOP competed against [<sup>3</sup>H]-Noiceptin; CBI competed against CP55,940; o1R competed against [<sup>3</sup>H]-DTG and; NET, DAT and SERT binding competed against [<sup>3</sup>H]-Mazindol. NC = No Convergence; - = Not Tested; n = 3



Ligand	MOR		Literare MOR EC <sub>50</sub> (E <sub>MAX</sub> )	Ref.	DOR		KOR		NOP		CBI	
	EC <sub>50</sub> (SEM)	E <sub>MAX</sub> (SEM)			EC <sub>50</sub> (SEM)	E <sub>MAX</sub> (SEM)						
Buprenorphine	< 0.10	36 (3.9)	0.08 (38%)	17	1700 (520)	25 (8.9)	1100 (310)	9.7 (2.9)	NC	NC	>2,000	[-41]
Hydrocodone	470 (52)	90 (1.9)	1,500 (54%)	37	1400 (550)	42 (6.9)	NC	NC	NC	NC	1400 (690)	59 (5.8)
Hydromorphone	39 (22)	97 (1.4)	30 (58%)	37	1900 (430)	84 (9.2)	460 (100)	47 (5.4)	NC	NC	>2,000	[64]
Morphine	130 (47)	99 (4.3)	190 (70%)	37	2100 (290)	68 (7.5)	>2000 (3.3)	55 (3.3)	NC	NC	>2,000	[45]
O-Desmethyl/tramadol	360 (110)	100 (4.3)	860 (52%)	39	360 (240)	38 (14)	NC	NC	NC	NC	NC	NC
Oxycodone	460 (100)	93 (7.6)	1,400 (67%)	37	NC							
Oxymorphone	23 (4.5)	100 (6.4)	48 (64%)	37	2000 (500)	61 (24)	970 (190)	30 (2.0)	NC	NC	NC	NC
Tapentadol	1300 (520)	76 (7.4)	670	13	NC	NC	>2000 (1.8)	13	NC	NC	NC	NC
Tramadol	>10,000	[26.4]	NC	13	NC							
Endomorphin-2	200 (31)	100 (2.3)	-	-	-	-	-	-	-	-	-	-
DPDPE	-	-	-	-	17 (3.7)	100 (3.3)	-	-	-	-	-	-
U50,488	-	-	-	-	-	16 (4.2)	100 (1.6)	-	-	-	-	-
Noiceptin	-	-	-	-	-	-	-	0.26 (0.03)	100 (0.2)	-	-	-
Win55,212	-	-	-	-	-	-	-	-	-	-	52 (15)	100 (3.1)

**Table 3.5** [<sup>35</sup>S]-GTPγS Coupling of Clinical Analgesics at MOR, DOR, KOR, NOP and CBI GPCRs. NC = No Convergence; - = Not Tested; [ ] = Maximum inhibition at 10 μM; n = 3



### 3.3.2 *In Vitro* Competition Binding and Functional Activity

Buprenorphine, hydrocodone, hydromorphone, morphine, O-Desmethyltramadol, oxycodone, oxymorphone, tapentadol and tramadol affinity was determined via radioligand competition binding at MOR, DOR, KOR, NOP, CB1,  $\sigma$ 1R, NET, DAT and SERT (Table 3.4; Figure 3.6). At the MOR, buprenorphine has the highest affinity ( $K_I = 0.9$  nM) while tramadol shows no appreciable binding; hydrocodone, tapentadol, and o-desmethyl tramadol have low affinity with  $K_I$ 's of 1800 nM, 2100 nM and 1300 nM, respectively (Table 3.4). Oxycodone, oxymorphone, and hydromorphone showed moderate  $K_I$  values. The apparent affinities ( $K_I$ ) and [ $^{35}$ S]GTP $\gamma$ S coupling potencies ( $EC_{50}$ ) matched within an order of magnitude (Figure 3.6-3.7, Table 3.4-3.5). A few compounds – hydrocodone, O-desmethyltramadol, and tramadol – produce ~4-fold greater potency than the affinity with  $K_I/EC_{50} = 1800/470$ ,  $1300/360$  nM, NC/3100, respectively, indicative of different intrinsic efficacies [170] as further discussed in 3.4.1.

Buprenorphine has varying non-MOR interactions at DOR, KOR and NOP (Table 3.4, 3.5). Buprenorphine displays potent partial agonist activity at MOR and DOR. Furthermore, buprenorphine has moderate affinity for NOP, though no NOP agonist activity was observed in the [ $^{35}$ S]-GTP $\gamma$ S coupling assay, as previously reported [180]. The MOR, DOR, KOR and NOP affinity was already previously reported [179, 180, 187-189]. Buprenorphine was not analyzed at NOP in antagonist mode because previous reports show weak micromolar agonist activity [180].

The current studies reveal buprenorphine has low affinity or potency at CB1, DAT, NET, and SERT (Table 3.4 and 3.5). At high concentrations, buprenorphine is a weak inverse agonist at CB1 and a positive modulator of transport at DAT, NET, and

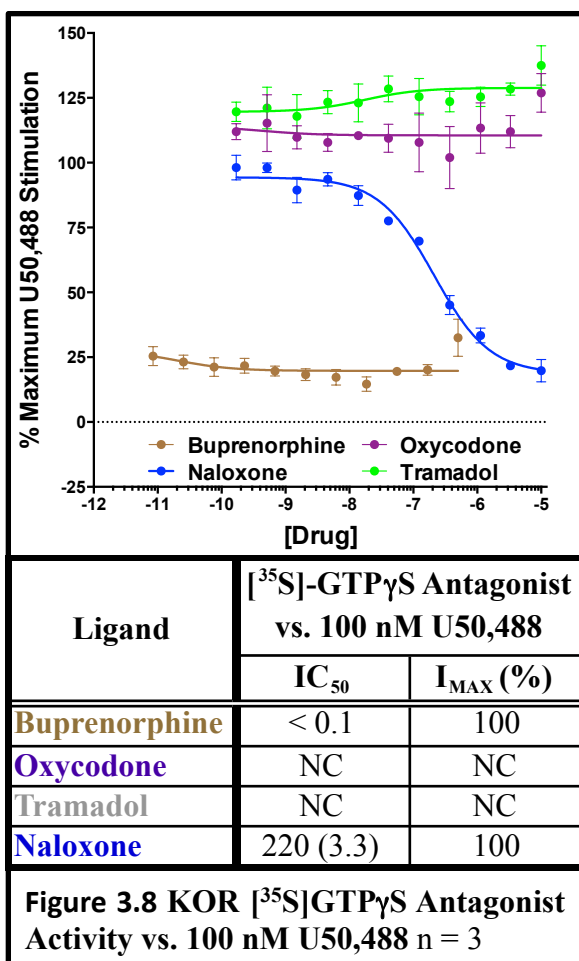
SERT. At DAT it increases transport by 67% over the vehicle at 10  $\mu$ M (Table 3.6). Despite these relatively low potencies, these novel interactions show potencies similar to NOP, which previous reports indicate contribute to buprenorphine's complex pharmacology, as discussed further in section 3.4.3D [68, 187].

Another previously unreported interactions includes hydrocodone's weak affinity at  $\sigma$ 1R that was only ~2-fold lower than MOR with  $K_I$ 's of 1800 nM and 4000 nM, respectively (Table 3.4). No  $\sigma$ 1R functional assay was performed since most assays require tissue preparations and was beyond the scope of the current assessment.

Ligand	NET		SERT		DAT	
	IC <sub>50</sub> (SEM)	I <sub>MAX</sub> (SEM)	IC <sub>50</sub> (SEM)	I <sub>MAX</sub> (SEM)	IC <sub>50</sub> (SEM)	I <sub>MAX</sub> (SEM)
Buprenorphine	>2,000	[-27]	>2,000	[-20]	>2,000	[-67]
Hydrocodone	NC	NC	NC	NC	NC	NC
Hydromorphone	NC	NC	NC	NC	NC	NC
Morphine	NC	NC	NC	NC	NC	NC
O-Desmethyltramadol	>2,000	[68]	>2,000	[34]	NC	NC
Oxycodone	NC	NC	NC	NC	NC	NC
Oxymorphone	NC	NC	NC	NC	NC	NC
Tapentadol	>2,000	[46]	>2,000	[68]	>10,000	[19]
Tramadol	>2,000	[54]	>2,000	[62]	>10,000	[22]
S-Duloxetine	140 (9.0)	100	-	-	520 (68)	100
GBR12909	-	-	180 (12)	100	-	-

**Table 3.6 Monoamine Transporter Inhibition Functional Assay for Clinical Analgesics at DAT, SERT and NET.** NC = No Convergence [ ] = Maximum inhibition at 10  $\mu$ M

## 3.3.3 .....B

*buprenorphine, Hydrocodone and Tramadol Antagonist Activity at KOR*

Buprenorphine has a high affinity for the KOR, while oxycodone and tramadol showed moderate to low affinity (Table 3.4). Since none of these compounds show KOR agonist activity (Table 3.5), they were tested for KOR antagonist activity in the presence of 100 nM U50,488 (Figure 3.8). Buprenorphine has high antagonist potency (IC<sub>50</sub> < 0.1 nM) and affinity activity matching prior *in vitro* [190] and *in vivo* studies of buprenorphine as a KOR antagonist [179]. On the other hand, oxycodone and tramadol show no significant antagonist

activity at KOR (Figure 3.8). The apparent differences between these weak affinities and apparent activity are likely driven by different assay conditions or low efficacy, as discussed in section 3.4.1.

## **PART IV: DISCUSSION AND FUTURE PERSPECTIVES**

### **3.4 Clinical Analgesics at Atypical Pain Targets**

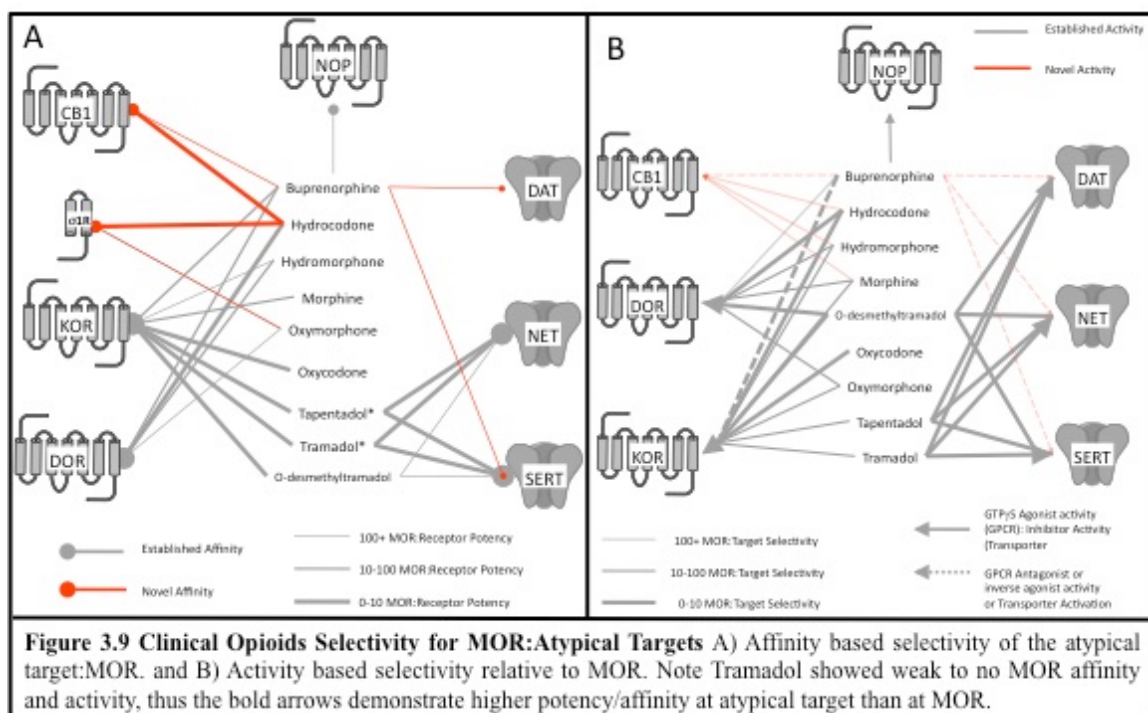
Nine clinical analgesics were assessed for binding affinity and activity at the MOR and 8-9 atypical targets involved in analgesia to determine whether therapeutic differences between clinical opioids may arise from non-MOR targets.

#### *3.4.1 Potency, Affinity, and Efficacy at MOR Discussion*

At MOR, potency and affinity values match previous reports within two log units of one another (Table 3.4) [175, 176, 178, 191-193]. Several opioids show modest differences in affinity and potency at MOR. For example, o-desmethyltramadol and hydrocodone have  $EC_{50}$  values ~4 times higher than their respective  $K_I$  at MOR (Table 3.4-3.5), while tramadol shows no binding (Table 3.4) but weak agonist activity at 10  $\mu$ M in [ $^{35}$ S]-GTP $\gamma$ S coupling at MOR (Table 3.5). Hydromorphone, on the other hand, shows 4-fold less potency than affinity at MOR. These modest differences in affinity and potency are frequently observed and generally explained by differences in intrinsic efficacy.

Whereas affinity measures receptor occupancy, intrinsic efficacy indicates an agonist's ability to translate occupancy into activation. The difference between affinity and intrinsic efficacy is an important consideration in over-expressed systems with a significant spare receptor reserve – or the number of extra receptors not required to elicit a full response. For example, a compound that produces a full GTP $\gamma$ S stimulation by activating 10% of receptors results in a higher potency than affinity – since affinity measures half receptor occupancy. The higher a compound's intrinsic efficacy, the larger the difference between affinity and potency. Furthermore, the reported affinity for

morphine and other clinical compounds at MOR varies by up to 3 orders of magnitude[176], and thus minor differences between potency and affinity were not pursued further.



### 3.4.2 Differences in Clinical and In Vitro Efficacy

The likelihood an atypical target contributes to a clinical opioid's *in vivo* profile was assessed in two different ways. First, the MOR: Atypical target selectivity ratio was calculated for both competition binding (Table 3.7, Top) and functional activity (Table 3.7, Bottom). Figure 3.9 visually represents the binding and functional data, with novel interactions (to the best of our knowledge) in red and established interactions in gray; thicker lines represent a lower MOR: Atypical Target selectivity ratio. All tested compounds act through ORs showing partial or complete naloxone reversible

antinociception and most act through MOR. Therefore, *in vitro* MOR: Atypical target selectivity ratio's closer to 1 indicate the highest likelihood interactions at *in vivo* doses.

Ligand	MOR:Atypical Target Selectivity for Competition Binding									
	MOR:DOR	MOR:KOR	MOR:NOP	MOR:CB1	MOR:NET	MOR:DAT	MOR:SERT	MOR:σ1R		
Buprenorphine	38	30	481	2222	-	2222	2222	2222	-	-
Hydrocodone	> 3	-	-	-	-	-	-	-	-	2.3
Hydromorphone	33	168	-	-	-	-	-	-	-	-
Morphine	34	27	-	-	-	-	-	-	-	-
O-Desmethyltramadol	-	1.5	-	-	-	-	-	-	-	-
Oxycodone	-	2.6	-	-	-	-	-	-	-	-
Oxymorphone	182	182	-	-	-	-	-	-	-	240
Tapentadol	-	0.94	-	-	-	-	0.94	-	-	-
Tramadol	-	<1.0	-	-	-	-	-	-	-	-
	<b>MOR:Atypical Target Selectivity for Functional Assays</b>									
Ligand	MOR:DOR	MOR:KOR	MOR:NOP	MOR:CB1	MOR:NET	MOR:DAT	MOR:SERT			
Buprenorphine	17000	11000	-	20000	10000	10000	10000	10000	-	-
Hydrocodone	2.9	-	-	3.1	-	-	-	-	-	-
Hydromorphone	48	12	-	51	-	-	-	-	-	-
Morphine	16	15	-	16	-	-	-	-	-	-
O-Desmethyltramadol	1.0	5.6	-	-	2.8	-	2.8	-	-	-
Oxycodone	-	4.3	-	-	-	-	-	-	-	-
Oxymorphone	86	42	-	-	-	-	-	-	-	-
Tapentadol	-	1.5	-	-	0.75	-	0.75	0.75	0.75	-
Tramadol	-	-	-	-	0.33	-	0.33	0.33	0.33	-

**Table 3.7 MOR:Atypical Target Selectivity for Competition Binding (Top) and Functional Assessment (Bottom)**

The second analysis compared each compound's clinical potency from an equianalgesic dose table [194] and *in vitro* MOR [<sup>35</sup>S]-GTPγS potency (EC<sub>50</sub>) values from Table 3.5 (Table 3.8). This comparison (roughly) estimates to what extent clinical analgesia is explained by MOR activation. All dose values were normalized to morphine, such that a compound 5X more potent than morphine produces 'Drug/Morphine Ratio' = 0.2 and a drug 5X less potent produces a 'Drug/Morphine Ratio' = 5.0 for both clinical and *in vitro* ratios. The 'Clinical/*In Vitro* Ratio' divides the clinical and *in vitro* dose ratios. Thus, a compound with a 'Clinical/*In Vitro* Ratio' > 1 is less potent clinically than expected based on the *in vitro* MOR potency and a compound with a 'Clinical/*In Vitro* Ratio' < 1 is more potent clinically than predicted by the *in vitro* assays. Compounds

<b>Drug</b>	<b>Clinical Ratio</b>	<b><i>In Vitro</i> - MOR GTPγS</b>	<b>Clinical/ <i>In vitro</i></b>
	<u>Drug/Morphine</u>	<u>Drug/Morphine</u>	
	<u>Ratio<sup>1</sup></u>	<u>Ratio<sup>2</sup></u>	
Hydrocodone	0.95	3.66	0.26
Hydromorphone	0.20	0.30	0.67
Morphine	1.00	1.00	1.00
Oxycodone	0.45	3.61	0.13
Oxymorphone	0.57	0.18	3.17
Tapentadol	3.22	10.12	0.32
Tramadol*	10.83	10000	<0.12

**Table 3.8 Clinical Anti-nociception and *In Vitro* MOR [<sup>35</sup>S]-GTPγS Potency Comparison of Selected Clinical Analgesics**

The clinical ratio represents an equimolar comparison for analgesic dose from clinical ratio tables taken from <sup>1</sup>clinicalc.com/opioids/. <sup>2</sup>*In vitro* MOR GTPγS values taken from table 3.5. All values normalized to morphine = 1.00. Clinical/*In vitro* ratio is the quotient of the Clinical Ratio and *In vitro* ratio. Thus values <1 indicate a drug more potent clinically than *in vitro*. Red > 3 fold more potent *in vivo* than *in vitro*. Black is ~equipotent *in vivo* and *in vitro*. Green is less potent *in vivo* and *in vitro* \*10,000 nM used as a proxy for its incomplete convergence

with a 'Clinical/*In Vitro* Ratio' less than 1 indicate greater analgesia than predicted by the *in vitro* MOR potency. These differences may arise from pharmacokinetics, efficacy or atypical targets may enhance the *in vivo* analgesia.

As expected, this methodology identifies established multi-functional drugs as clinically more potent than expected from *in vitro* MOR potency. Both tramadol and tapentadol act as SERT and NET inhibitors, in addition to MOR *in vivo* (see section 1.3) to mediate antinociception [175, 195]. Both drugs have a 'Clinical/*In Vitro* Ratio' < 1, indicating a higher clinical potency than expected based on *in vitro* MOR [<sup>35</sup>S]-GTP $\gamma$ S coupling alone (Table 3.8). Thus this analysis can identify compounds with atypical targets *in vivo*.

Oxycodone has a 'Clinical/*In Vitro* Ratio' of 0.12 (Table 3.8) with limited 1:4.3 MOR: KOR agonist selectivity (Table 3.7). These findings match previous reports indicating KOR agonist activity contributes to oxycodone antinociception [196]. Furthermore, this increased *in vivo* potency has been traditionally attributed to oxycodone's active transport across the blood-brain barrier (BBB) resulting in 3 times higher concentration in the brain than the blood [197]. Since these effects explain oxycodone's increased *in vivo* potency, we considered this further validation as a means to identify non-MOR contributions to antinociception.

### 3.4.3 Clinical Opioid Affinity and Activity at Atypical Targets

#### 3.4.3A Equianalgesic Potency of Hydromorphone and Morphine in the Clinic and In Vitro

Hydromorphone and morphine are approximately equipotent in both the clinic and *in vitro* evaluations with a ‘Clinical/*In Vitro* Ratio’ of 0.67 and 1.00, respectively. This indicates that neither potentiates antinociception through an atypical target *in vivo* or both potentiate antinociception to similar extents (not necessarily through the same mechanism). Based on the *in vitro* selectivity comparison (Table 3.7), hydromorphone shows partial KOR agonist activity with 12:1 KOR:MOR selectivity (Table 3.5); similarly, morphine shows 16 and 15 DOR:MOR and KOR:DOR selectivity (Table 3.7).

If both equally enhance antinociception at an atypical target, then a DOR antagonist should reduce morphine antinociceptive potency. In fact, mice treated with the DOR selective antagonist NTI show a slight, but not statistically significant 1.2-fold decrease in morphine antinociceptive potency [198], indicating minimal DOR contribution to morphine antinociception. Because morphine’s 16:1 DOR:MOR *in vitro* selectivity (Table 3.7) does not significantly improve antinociception, it is assumed we need a selectivity ratio lower than 16:1 for *in vivo* effects for full agonists.

#### 3.4.3B Hydrocodone CBI Activity and $\sigma 1R$ Affinity

Clinically, morphine and hydrocodone are roughly equipotent (Table 3.8), but hydrocodone is 5-fold less potent *in vitro*. Unlike oxycodone, bioavailability does not explain this 5-fold difference as morphine oral bioavailability is ~30-40% [199] compared to hydrocodone’s bioavailability of ~60% [200]. Hydrocodone demonstrated

several atypical interactions including weak CB1 agonist activity; DOR partial agonist activity (Figure 3.7); and  $\sigma$ 1R affinity (Figure 3.6) that may improve *in vivo* potency relative to *in vitro* activity. Hydrocodone is weakly selective at MOR over DOR and CB1 selectivity ratios of 2.9, and 3.1, respectively (Table 3.7). These low selectivity ratios indicate good candidates for *in vivo* activity and both could contribute to hydrocodone Clinical/*In Vitro* Ratio' of 0.26 (Table 3.8). The DOR selective agonists DPDPE and Deltorphin-II potentiate MOR-mediated antinociception of DAMGO and morphine [107, 108]. A similar synergy exists between CB1 and MOR [201]. Future studies will test these activities *in vivo*, by testing if hydrocodone antinociception is (at least partially) reversible by a DOR or CB1 antagonist.

Lastly, hydrocodone shows a MOR: $\sigma$ 1R affinity selectivity of 2.1 (Table 3.7), indicating likely  $\sigma$ 1R activity *in vivo*.  $\sigma$ 1R is a chaperone protein with agonists producing inhibition of  $\text{Ca}^{2+}$ ,  $\text{K}^{+}$ ,  $\text{Na}^{+}$  voltage-gated ion channels [72] and potentiating SK channels, NMDA and  $\text{IP}_3$  receptors. Under pathological conditions,  $\sigma$ 1R is transferred from the endoplasmic reticulum (ER) to the plasma membrane to produce high cytosolic  $\text{IP}_3$  concentrations and reduce ER  $\text{Ca}^{2+}$  [184, 202]. Since  $\sigma$ 1R amplifies or modulates signaling opposed to direct signal alteration [184, 202],  $\sigma$ 1R functional assays were not further pursued in this project. As the  $\sigma$ 1R antagonist haloperidol increases morphine and DPDPE antinociception [74, 75], future studies will explore if hydrocodone  $\sigma$ 1R antagonist activity enhances its *in vivo* potency. Therefore, a  $\sigma$ 1R agonist should reduce hydrocodone antinociception if hydrocodone activity is enhanced by  $\sigma$ 1R. Similarly, an  $\sigma$ 1R antagonist should not increase hydrocodone antinociception. These antinociception

assays should be compared to a control non- $\sigma$ 1R MOR agonist such as oxymorphone to validate the specificity of hydrocodone's effect at  $\sigma$ 1R.

#### 3.4.3C Oxymorphone Lower Potency in the Clinic than In Vitro

Oxymorphone produces a 'Clinical/*In Vitro* Ratio' of 3.2 indicating oxymorphone is clinically less potent than expected from the *in vitro* MOR assay (Table 3.8). Oxymorphone did not show selectivity for any atypical target less than 10 (Table 3.7), indicating no tested atypical targets likely attenuates oxymorphone antinociception. Serendipitously, this 2.6 fold difference is equal to the ratio in bioavailabilities between oxymorphone with 10-11% oral bioavailability [203, 204] and morphine with ~30-40% oral bioavailability [199, 205]. Thus, oxymorphone's 3.2 'Clinical/*In Vitro* Ratio' is explained by morphine's higher bioavailability than oxymorphone.

#### 3.4.3D Buprenorphine Activity and Atypical Targets

Buprenorphine shows high affinity and potency at MOR, in addition to numerous atypical interactions with relatively low selectivity  $> 1,000$  (Table 3.7). However, buprenorphine weak partial agonist at MOR ( $E_{MAX} = 36\%$ ) leads to overestimating MOR: Atypical target selectivity. According to traditional receptor theory – to produce equianalgesic activity *in vivo* buprenorphine must occupy more receptors than a full agonist – thus reducing the effective selectivity *in vivo* (Figure 3.7). Thus, despite low selectivity ratios, these atypical interactions could contribute to buprenorphine's complex pharmacology.

A 'Clinical/*In Vitro* Ratio' for buprenorphine was not calculated because buprenorphine is administered transdermally instead of Per os (PO) and different routes of administration prohibit direct comparison due to PK effects. Nonetheless, buprenorphine produces unexpected positive transport at SERT, DAT and NET (Figure 3.7; Table 3.7) at micromolar concentrations. Buprenorphine induced positive transport at all 3 transporters most notably with an  $E_{MAX} = -67\%$  (at 10  $\mu\text{M}$ ) for DAT (Table 3.7). *In vivo*, this activity should reverse antinociception, as SERT, NET and DAT inhibitors cause antinociception [57]. Fittingly, *in vivo* antinociception of buprenorphine shows a bell-shaped curve, in which antinociception increases followed by reduced efficacy at higher doses [188]. Part of bell-curve is attributed to buprenorphine's KOR antagonist and NOP agonist activity [187, 189]. However, differentiating between NOP and monoamine transporters can be difficult, as microdialysis studies show the NOP agonist Orphanin FQ decreases extracellular 5-HT levels in the dorsal raphe nucleus (DRN) and the nucleus accumbens (NAcc) [206], which is reversed by the NOP antagonist [Nphe<sup>1</sup>]Nociceptin(1-13)NH<sub>2</sub>. The models studying buprenorphine with NOP KO or antagonist may reduce basal or tonic 5-HT removal from the synapse by blockade of NOP. Thus buprenorphine's NOP and SERT-mediated effects may synergize from cross talk in the same cell.

Furthermore, buprenorphine is used to treat cocaine, opioid and alcohol addiction [207-209] and poly-addiction. Numerous studies have synthesized buprenorphine analogs to improving its use as a poly-addiction treatment [210, 211] by modulating KOR and NOP activity. The novel DA influx activity of buprenorphine reported here indicates an important and unappreciated target in poly-addiction treatments. DA release in the

NuAcc plays a well-established role in addiction [212]. While KOR and NOP agonists decrease DA in the NuAcc [213, 214], the current studies suggest buprenorphine's effectiveness as a poly-drug treatment arises from DAT interactions. This is particularly compelling as buprenorphine is a KOR antagonist (Figure 3.8), and analogs increasing buprenorphine's NOP agonist activity did not explain the reduced reward in cocaine reward models [215].

Follow-up studies should determine the *in vivo* full dose response curve of buprenorphine in these lines and its reversibility with a reuptake inhibitor at SERT, NET and/or DAT. Since selective serotonin reuptake inhibitors (SSRIs) can enhance antinociception, one would expect the serotonin positive modulation to induce a pronociceptive effect. Furthermore, the monoamine transporter activity likely contributes to buprenorphine *in vivo* profile, despite its low potency. The positive influx at SERT, NET and DAT showed higher potency than buprenorphine's NOP agonist potency (Tables 3.4 and 3.5), which has been previously reported to contribute to buprenorphine's *in vivo* pharmacological profile [68, 216].

#### 3.4.4 Conclusions

Nine clinical analgesics were assessed for affinity and activity at MOR, DOR, KOR, NOP, CB1,  $\sigma$ 1R (affinity only), NET, DAT and SERT (Table 3.4; Figure 3.6). Buprenorphine and hydrocodone showed several interactions at atypical (non-MOR) targets involved in pain regulation. Buprenorphine's unreported positive influx at the monoamine transporters may explain its unique pharmacology *in vivo*. Additionally, hydrocodone's comparable  $\sigma$ 1R and MOR affinities indicate  $\sigma$ 1R may enhance

hydrocodone antinociception *in vivo*. Future studies will test whether the identified atypical targets contribute to each drug's *in vivo* pharmacology.

**CHAPTER IV:****EVALUATION OF ENDOGENOUS OPIOID COMPOUNDS FOR  
FUNCTIONALLY SELECTIVE SIGNALING AT OPIOID RECEPTORS**

## PART I: INTRODUCTION

### 4.1.1 Neuropeptides and Signal Modulation

Neuropeptides – such as the endogenous opioid peptides – modulate the neuronal activity of ‘classical’ small molecule neurotransmitters over longer time periods – minutes compared to seconds – rather than inducing basal level changes on their own [217]. However, many questions remain concerning neuropeptide:receptor interactions. For example,  $\beta$ endorphin (1-27) acts as an antagonist for  $\beta$ endorphin (1-31) induced analgesia, despite both ligands putatively acting as partial agonists of the MOR and DOR [218]. Such discrepancies indicate ligand:receptor interactions are more complex than traditional receptor theory may posit.

Classically, different endogenous opioid families mediate their effects by activating the MOR, DOR or KOR – with each receptor assigned a putative endogenous role based on modest receptor subtype selectivity and *in vivo* co-localization experiments [219-222]. These studies imagined the receptor as the control node to modulate downstream consequences; different ligands – so long as they similarly bound to and activated the receptor – were more or less interchangeable [223]. However, the opioidergic system consists of more than 20 endogenous opioid peptides [219] but only three genetic subtypes – MOR, DOR and KOR. Binding affinity studies indicate most [219] endogenous opioid peptides bind at least two (and often all three) subtypes with low nM affinity; this low subtype selectivity suggests most peptides can activate multiple receptors *in vivo*. During the 80s and 90s this was attributed to biological redundancy. However, recent reports of several peptides as biased agonists at MOR [224, 225] –

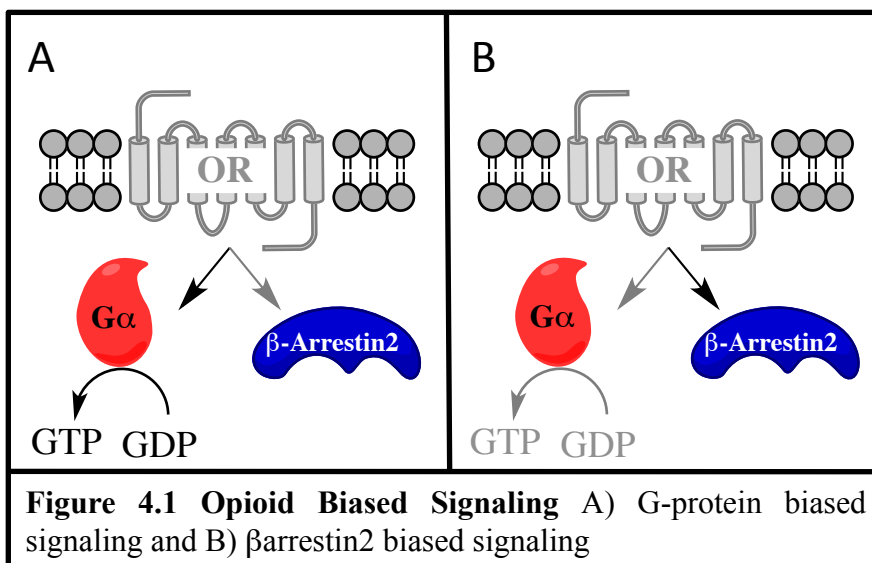
which favor one signaling pathway over another – call the biological redundancy hypothesis into question.

#### 4.1.2 Opioids and Biased Signaling

Recent drug discovery efforts identified several biased opioid agonists [63, 83, 226], which activate  $G\alpha$  signaling but do not recruit  $\beta$ arrestin2, or vice versa (Figure 4.1). These biased agonists generate intriguing and desirable pharmacological properties, such as reduced tolerance or limited dysphoria in animal models [2, 94, 225, 227-229]. These drug discovery approaches indicate that the ligand can also control receptor signaling and physiological function.

#### 4.1.3A KOR Biased Signaling

At KOR  $\beta$ arrestin2 can mediate dysphoria and aversion, suggesting biased agonists that activate  $G\alpha$  signaling but not  $\beta$ arrestin2 could cause analgesia without dysphoria and aversion [230, 231]. Several KOR biased agonists including 6'-



guanidinonaltrindole (6'GNTI) and RB-64 produce some of the predicted results [232-238]. For example, RB-64 produces anti-nociception while avoiding anhedonia and motor dysfunction. However RB-64 still produced CPA indicating that dysphoria remains in at least some biased KOR agonists [235]. Depending on the system,  $\beta$ arrestin signaling can provide positive therapeutic benefits for biased drugs [225].

#### *4.1.3B MOR Biased Signaling*

$\beta$ arrestin2 knockout (KO) mice treated with morphine produce enhanced anti-nociception [84] with reduced tolerance, respiratory depression, constipation, dependence, and tolerance [85, 86]. Interestingly full agonists such as fentanyl or high doses of morphine overcame the reduction in side effects. Subsequent screening studies identified several MOR biased ligands [89-91, 239].

*In vitro* assays show that TRV130, PZM21 and other ligands do not appreciably recruit  $\beta$ arrestin2, but stimulate typical  $G\alpha$  signaling. Nonetheless, these biased compounds have replicated some of the expected findings from the  $\beta$ arrestin2 KO studies. PZM21 and TRV130 both showed reduced constipation and reduced respiratory depression in mice and rats [91, 94, 239]. PZM21 may have reduced abuse liability as it didn't induce conditioned place preference [92]. Overall there are some caveats and limitations to  $\beta$ arrestin2 as a drug discovery target, including the lack of a structure-activity relationship (SAR) for arrestin bias [92]. Endomorphin-2 (Tyr-Pro-Phe-Phe-NH<sub>2</sub>) was identified as a biased agonist favoring  $\beta$ arrestin recruitment over G-protein signaling at MOR. Functionally, endomorphin-2 displayed a lower operational efficacy for GIRKs (G protein dependent) relative to desensitization ( $\beta$ arrestin dependent)[224]. The ability

to activate G-proteins without  $\beta$ arrestin2 recruitment has been suggested to offer a target for analgesics with reduced side effects such as tolerance and addiction. Despite encouraging preclinical results, an in-depth investigation of endogenous opioid peptides and biased signaling at non-MORs remains absent.

#### *4.1.3 Rationale*

Opioid receptors (ORs) are G-protein Coupled Receptors (GPCRs) which mediate analgesia, tolerance, withdrawal, and slow GI transit. Classically, ORs couple inhibitory  $G\alpha_{i/o}$  proteins and recruit  $\beta$ arrestin2 – a multifaceted scaffold molecule implicated in opioid mediated effects including tolerance, constipation, dysphoria and nausea. Upon activation,  $\beta$ arrestin2 and  $G\alpha_{i/o}$  induce downstream signaling responses such as reduced cAMP levels. Recent drug discovery efforts identified several functionally selective exogenous opioids which prefer certain signaling pathways at a given receptor – such as  $G\alpha$  stimulation – to others – such as  $\beta$ arrestin2 recruitment, and generate desired pharmacological properties. Noting that most of the 20+ endogenous opioid peptides are non-selective and some opioids display functional selectivity, two important points emerge. First, endogenous and exogenous ligands – such as those used during studies – do not necessarily generate the same effects. Second, two different endogenous opioid peptides may differentially activate a given receptor. Thus, we ask: Can different Dynorphins, Enkephalins, Endorphins and Endomorphins induce biased signaling at the MOR, DOR or KOR? If so, do these differences result in modulated receptor regulation or differential control between different endogenous peptides? Could biased signaling

make up for low receptor selectivity of the endogenous peptides to impart specific physiological roles to each peptide?

Relative to exogenous ligands, the characterization of endogenous biased signaling remains understudied. The inherent properties of endogenous ligands – limited subtype selectivity, difficult *in vivo* evaluation, limited bioavailability and bioactive cleavage products – make demonstrating *in vivo* bias a distinct experimental problem from identifying potential therapeutics. However, understanding if and how natural functional selectivity works should assist in the development of better drugs.

## PART II: MATERIALS AND METHODS

### 4.2.1 Reagents and Assay Materials

$\beta$ -endorphin(1-31),  $\alpha$ -endorphin(1-17) were commercially purchased.

### 4.2.2 SPPS

Dynorphin A (1-17), Dynorphin B (1-13), Leu-enkephalin, Met-enkephalin, Endomorphin-1, and Endomorphin-2 were synthesized using standard Fmoc/tBu chemistry. Briefly, preloaded resins were deprotected with 20% piperidine in DMF 20 minutes then coupled with 3:3:3:6 eq. PyBOP, HOAt, Fmoc-AA-OH and DIEA at 0.25 M (or 0.5 M DIEA) in NMP. Reaction progress was monitored via Kaiser. Cleavage proceeded via 95% TFA, 2.5% TIS and 2.5% H<sub>2</sub>O. The crude product was precipitated in ice-cold ether, purified via RP-HPLC and characterized via mass spectrometry.

Analytical Data		HPLC <sup>a</sup>		LRMS <sup>b</sup>	
Cmpd.	Molecular Formula	% Purity	% Yield	Observed [M+H]	Calcd.
Met-Enkephalin	C <sub>27</sub> H <sub>35</sub> N <sub>5</sub> O <sub>7</sub> S	>95%	65%	574	574.2
Leu-Enkephalin	C <sub>28</sub> H <sub>38</sub> N <sub>5</sub> O <sub>7</sub>	>95%	77%	556	556.3
Endomorphin-1	C <sub>34</sub> H <sub>38</sub> N <sub>6</sub> O <sub>5</sub>	>95%	51%	611	611.3
Endomorphin-2	C <sub>32</sub> H <sub>37</sub> N <sub>5</sub> O <sub>5</sub>	>95%	44%	440	440.2
DynorphinA(1-17)	C <sub>99</sub> H <sub>155</sub> N <sub>31</sub> O <sub>23</sub>	>95%	15%	1074.6 <sup>[M+2H]</sup>	2148.2
DynorphinB(1-13)	C <sub>70</sub> H <sub>109</sub> N <sub>20</sub> O <sub>15</sub>	>95%	25%	1470	1469.8

**Table 4.1 Physical constants and characterization of compounds** <sup>a</sup> Hewlett Packard 1100 (C-18, Microsorb-MVTM, 4.6 mm x 250 mm, 5  $\mu$ m) using a gradient system (10-90% acetonitrile containing 0.1% TFA within 40 mins, 1 mL/min). <sup>d</sup> negative ESI mode

<sup>b</sup> (M+H)<sup>+</sup>, FAB-MS (JEOL HX110 sector instrument), or MALDI-TOF (Bruker Ultraflex III).

#### *4.2.3 Peptide Purification and Characterization*

See section 2.2.3 for experimental details and Table 4.1 for peptide characterization results.

#### *4.2.4 [<sup>35</sup>S]-GTPγS G protein Coupling Assay*

See section 2.2.5. OR-CHO cells and their culture conditions are also described in section 2.2.

#### *4.2.5 βarrestin2 Recruitment Assay*

PathHunter<sup>®</sup> β-Arrestin assays were used to measure recruitment in U2OS cells expressing the DOR, KOR and MOR (DiscoverX, Fremont, CA) according to the manufacturer's protocol. Cells were treated with agonist for 90 min prior to luminescence reading on a Synergy 2 plate reader (BioTek, Winooski, VT). For antagonist experiments, the cells were incubated with the antagonist for 60 min prior to agonist addition. All measurements were made in duplicate. For the "preliminary results" 6-point curves in duplicates were run. The data was analyzed as described in section 2.2.5.

#### *4.2.6 Forskolin Stimulated cAMP Inhibition*

For the cAMP assays, CHO cells expressing the DOR were stimulated with forskolin 15 min. prior to opioid treatment. cAMP concentrations were measured using a competitive [<sup>3</sup>H]cAMP binding assay, as previously described [240], with the following modifications. Briefly, HA-DOR-CHO cells were plated in 96 well plates at 50,000 cell/well and serum starved for 24 hours. Cells were incubated in 100 μL of Earle's balanced

salt solution with 500  $\mu\text{M}$  isobutylmethylxanthine (IBMX) for 15 minutes at 37°C.

The media was removed and drugs diluted in MEM (+100  $\mu\text{M}$  Forskolin, 500  $\mu\text{M}$  IBMX, + 1% Pen/Strep) were incubated for 15 min at 37°C. The reaction was stopped via aspiration and 60  $\mu\text{L}$  of ice-cold Tris/EDTA buffer was added to each well, and plates boiled for 10 minutes to lyse the cells. Lysates were spun down for 10 min at 4,000 RPM @ 4°C. Lysate was added to 50 pmol [ $^3\text{H}$ ]-cAMP and 100  $\mu\text{L}$  protein kinase A (PKA) buffer (40 mM Tris, 1 mM EDTA, 60  $\mu\text{g}/\text{mL}$  PKA and 0.1% BSA) in an ice bath for 2–3 h. A standard cAMP dilution between 0 and 32 pmol cAMP was made. Reactions were filtered through 1.0  $\mu\text{m}$  glass fiber filters in MultiScreen-FB 96-well plates (Millipore, Billerica, MA). The total [ $^3\text{H}$ ]-cAMP was measured by a MicroBeta2 scintillation counter (PerkinElmer Life Science, Boston, MA).  $\text{IC}_{50}$  values were determined by fitting the data using a 3-variable nonlinear curve fit on GraphPad Prism 4 (GraphPad Software, San Diego, CA).

#### 4.2.7 AC Superactivation

AC super activation was measured as previously described [241] with the following considerations. Cells were treated with MEM buffer (control) or ligand in MEM buffer + 50  $\mu\text{M}$  opiorphin as a enkephalase inhibitor [242] for 24 hours. Buffer including ligand and enkephalinase inhibitor was replaced every 8 hours to minimize degradation. 100  $\mu\text{M}$  water-soluble forskolin was used to stimulate AC activity. [ $^3\text{H}$ ]-cAMP concentrations were measured as in the cAMP inhibition assay, previously described. Percentage of basal cAMP level increase after dosage or vehicle was measured.

## PART III: RESULTS

## 4.3.1 Biased Signaling of Endogenous Opioid Peptides at MOR, DOR and KOR

Ligand	DOR				KOR				MOR			
	$[^{35}\text{S}]\text{GTP}\gamma\text{S}$		$\beta$ -arrestin2 Recruitment		$[^{35}\text{S}]\text{GTP}\gamma\text{S}$		$\beta$ -arrestin2 Recruitment		$[^{35}\text{S}]\text{GTP}\gamma\text{S}$		$\beta$ -arrestin2 Recruitment	
	EC <sub>50</sub>	E <sub>MAX</sub>	EC <sub>50</sub>	E <sub>MAX</sub>	EC <sub>50</sub>	E <sub>MAX</sub>	EC <sub>50</sub>	E <sub>MAX</sub>	EC <sub>50</sub>	E <sub>MAX</sub>	EC <sub>50</sub>	E <sub>MAX</sub>
DynorphinA(1-17)	455	100	210	89	1.6	100	13	100	240	100	>1000	[85]
DynorphinB(1-13)	64	100	570	95	9.2	100	16	100	240	87	>1000	[77]
Leu-Enkephalin	3.7	100	19	100	>1000	[25]	NC		190	96	>1000	[71]
Met-Enkephalin	16	100	10	100	>1000	[30]	NC		40	100	900	100
$\alpha$ -endorphin	230	88	130	72	>1000	[30]	NC		620	68	>1000	[59]
$\beta$ -endorphin (1-31)	370	76	280	75	>1000	[30]	>1000	[30]	370	62	>1000	[83]
Endomorphin-1	NC				NC				200	62	150	68
Endomorphin-2	NC				NC				93	79	190	64

**Table 4.2 Preliminary Screen of Endogenous Opioid Activity at MOR, DOR and KOR** n = 1-3 except Dynorphins and Leu-Enkephalin at DOR where n=3, [ ] = stimulation at 10  $\mu\text{M}$ ; NC = No convergence; NT = Not Tested

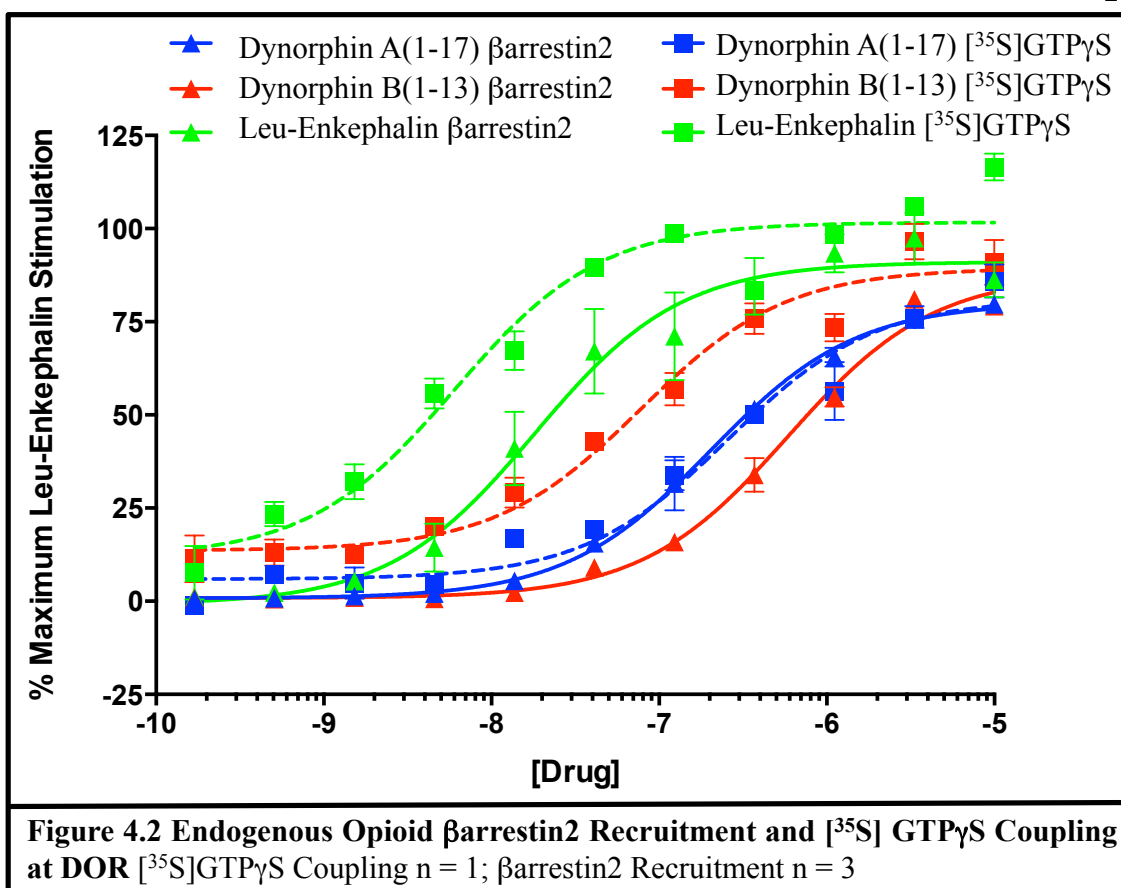
Combining the preclinical promise of biased agonists with an appreciation for the opioidnergic system's varied cellular and behavioral responses, we investigated endogenous OR peptides for  $\beta$ arrestin2 or  $G\alpha_{i/o}$  signaling at MOR, DOR and KOR. Dynorphin A/B, Met-/Leu-Enkephalin, Endomorphin1/2 and  $\alpha$ -/ $\beta$ -endorphin were assessed for  $[^{35}\text{S}]\text{-GTP}\gamma\text{S}$  coupling and  $\beta$ arrestin2 recruitment assays in CHO and U20S cells (Table 4.2).

At MOR only Endomorphin-1 and Endomorphin-2 recruit  $\beta$ arrestin2 with an EC<sub>50</sub> below 900 nM (Table 4.2), while stimulating  $[^{35}\text{S}]\text{GTP}\gamma\text{S}$  coupling with moderate potencies of EC<sub>50</sub> = 200 nM and 93 nM, respectively. The Endomorphins did not produce signals at KOR or DOR and were the only ligands selective for one receptor. Unfortunately this bias was previously reported and none of the other Enkephalins, Endorphins or Dynorphins produced stark differences from one another in either assay [224]. All four opioid families acted as agonists at MOR with most ligands, outside the

endomorphins, stimulating moderate [<sup>35</sup>S]-GTPγS coupling and weak βarrestin2 recruitment.

KOR was the only receptor displaying strong selectivity for a peptide family, the classical Dynorphin A and Dynorphin B. Both peptides produced potent [<sup>35</sup>S]-GTPγS coupling responses and strong βarrestin2 recruitment. Since both Dynorphin A (1-17) and Dynorphin B (1-13) produced similar profiles in both pathways, it appears neither is biased toward either pathway and were not further pursued.

The enkephalins, endorphins and dynorphins all showed modest to strong potency at DOR (Table 4.2). The enkephalins and endorphins were approximately equipotent and efficacious in both [<sup>35</sup>S]-GTPγS coupling and βarrestin2 recruitment assays. However, Dynorphin A (1-17) favors βarrestin2 over [<sup>35</sup>S]-GTPγS coupling,  $EC_{50arr} = 210$   $EC_{50G} = 455$ . Dynorphin B (1-13) modestly favors [<sup>35</sup>S]-GTPγS coupling at DOR over βarrestin2 recruitment,  $EC_{50arr} = 570$   $EC_{50G} = 64$  (Table 4.2, highlighted in red; Figure 4.2). This shift in potency rank order for [<sup>35</sup>S]-GTPγS coupling and βarrestin2 recruitment suggests Dynorphin A (1-17) and Dynorphin B (1-13) induce distinct DOR receptor conformations.



#### 4.3.2 Dynorphin and DOR cAMP Regulation

To investigate if these putative conformational differences propagated different downstream events, Dynorphin A (1-17), Dynorphin B (1-13) and Leu-Enkephalin (as a reference compound) were assessed for forskolin-induced cAMP inhibition – a well-established  $G\alpha$  dependent pathway. Acute studies revealed comparable Dynorphin A (1-17) and Leu-enkephalin  $\text{IC}_{50}$  values of 21 nM and 5.3 nM, respectively (Table 4.3). However, Dynorphin B (1-13) produces a ~6-fold weaker potency ( $\text{IC}_{50} = 120$  nM) than Dynorphin A (1-17). Dynorphin B (1-13) is a less potent agonist in the forskolin-induced cAMP inhibition compared to Dynorphin A (1-17) and Leu-enkephalin. On the other

hand, Dynorphin A (1-17) was less potent than Dynorphin B (1-13) in [<sup>35</sup>S]-GTPγS coupling. Furthermore, Dynorphin A (1-17) and Dynorphin B (1-13) produced sub-maximal I<sub>MAX</sub> values of 51-53% for forskolin stimulated cAMP activity whereas Leu-Enkephalin produced an I<sub>MAX</sub> = 100 %. These qualitative differences between ligand potency and efficacy at each pathway were quantitatively analyzed for β (bias factor).

#### 4.3.3 Dynorphin and DOR β Factors

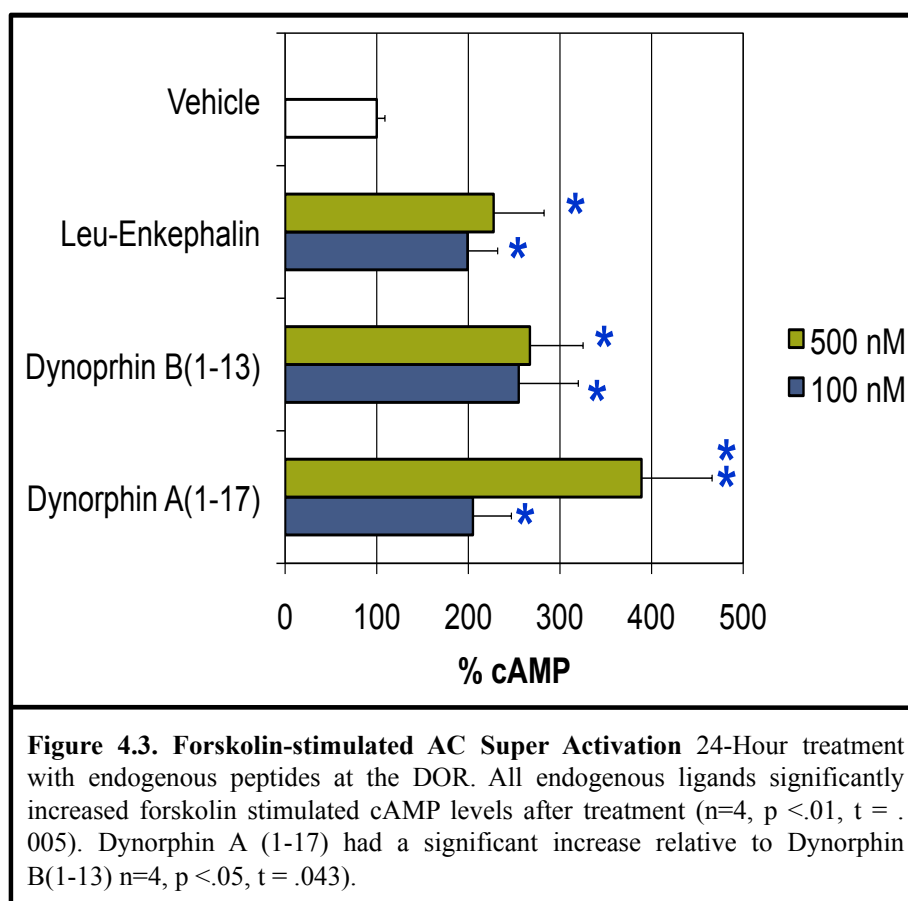
Ligand	<sup>35</sup> S]GTPγS			β-arrestin2 Recruitment			cAMP		β - Bias Factor		
	EC <sub>50</sub>	E <sub>MAX</sub>	Hill Slope	EC <sub>50</sub>	E <sub>MAX</sub>	Hill Slope	IC <sub>50</sub>	I <sub>MAX</sub>	GTPγS vs. βarrestin2	βarrestin2 vs. cAMP	GTPγS vs. cAMP
Leu-Enkephalin	3.7	100	0.73	19	100	1.00	5.3	100	0.00	0.00	0.00
Dynorphin A (1-17)	450	100	0.54	210	89	0.98	21	51	-0.99	-0.20	-1.19
Dynorphin B (1-13)	64	100	0.50	570	95	0.90	120	53	0.27	0.13	0.40

**Table 4.3 Bias Factors (β) for Dynorphin A (1-17), Dynorphin B (1-13) and Leu-Enkephalin at DOR in [<sup>35</sup>S]GTPγS, βarrestin2 and cAMP Signaling** Dynorphin B is about 10 fold better at activating GTPγS signaling vs β-arrestin recruitment and Dynorphin A is about 10 fold better at activating arrestin recruitment over [<sup>35</sup>S]-GTPγS coupling. β-arrestin2 Recruitment n = 3; [<sup>35</sup>S]GTPγS n = 1-2

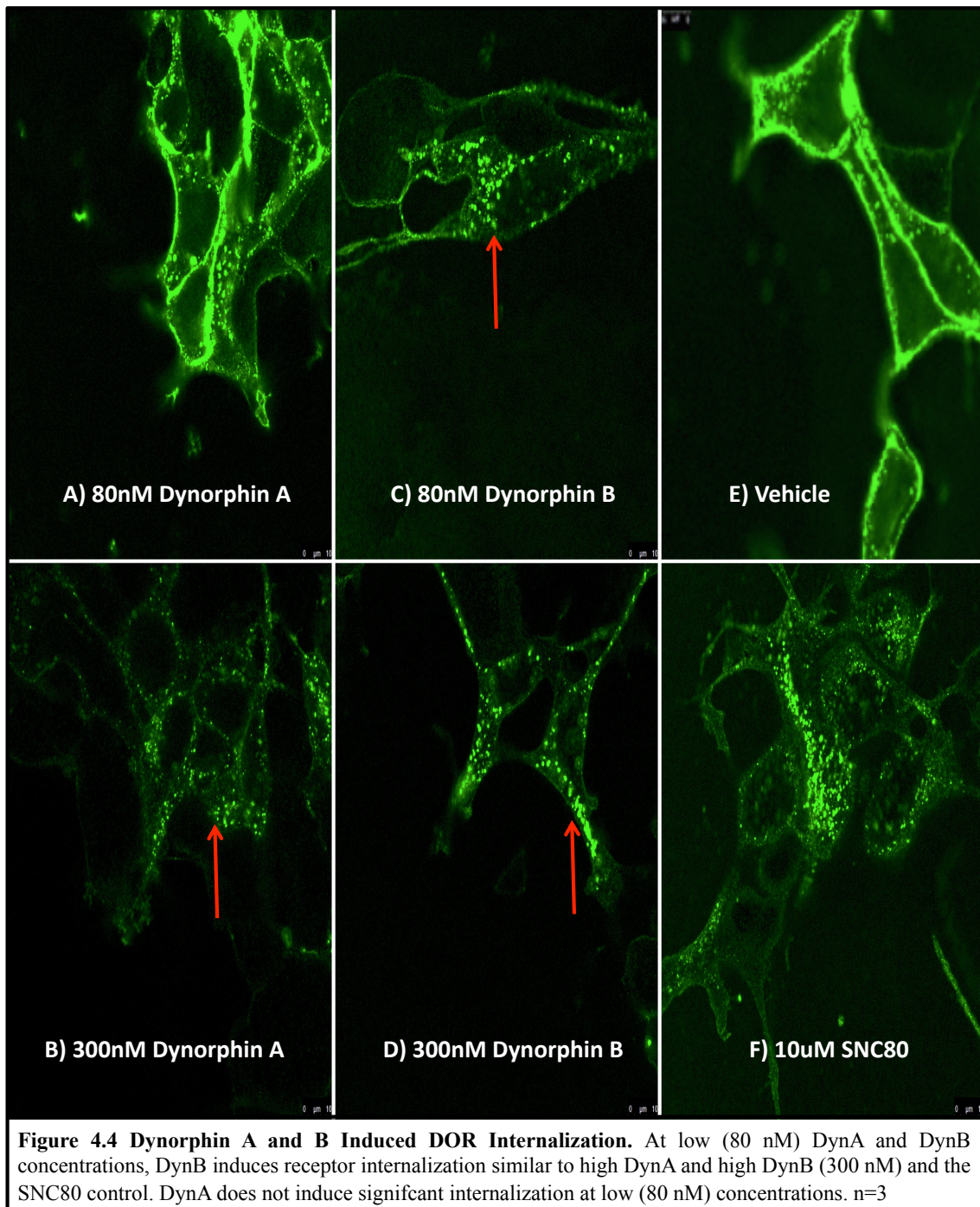
We calculated a bias factor (β) to compare forskolin-stimulated cAMP inhibition, [<sup>35</sup>S]-GTPγS coupling and βarrestin2 recruitment to one another for each ligand (Table 4.2), as previously described [243]. Leu-enkephalin was the standard ‘unbiased’ agonist at DOR for each pathway and thus produces a β = 0. A positive β indicates the ligand favors the pathway named first; a negative value indicates the ligand favors the pathway named second. Further β is a log function, meaning a difference of one β unit represents a 10-fold difference in relative activity between the two pathways. The bias factor quantitatively reveals the same story as was observed qualitatively in the preliminary screening data.

Dynorphin A (1-17) strongly favors cAMP inhibition over [<sup>35</sup>S]-GTP $\gamma$ S coupling ( $\beta = -1.19$ ), whereas Dynorphin B (1-13) modestly favors [<sup>35</sup>S]-GTP $\gamma$ S coupling over cAMP inhibition ( $\beta = 0.40$ ). The difference in  $\beta$  between Dynorphin A and Dynorphin B is 1.49, indicating a nearly 30-fold shift in relative activity between these two ligands. The second largest difference in  $\beta$  is the swapped potency rank order between [<sup>35</sup>S]-GTP $\gamma$ S coupling and  $\beta$ arrestin2 recruitment. Dynorphin A (1-17) is biased against [<sup>35</sup>S]-GTP $\gamma$ S coupling ( $\beta = -0.99$ ) and Dynorphin B (1-13) displays a modest bias toward [<sup>35</sup>S]-GTP $\gamma$ S coupling ( $\beta = 0.27$ ). Dynorphin A (1-17) favors  $\beta$ arrestin2 recruitment over [<sup>35</sup>S]-GTP $\gamma$ S coupling activity by nearly 20-fold (difference in  $\beta = 1.28$ ).

These



differences in signaling activity and putative receptor conformations



suggest that these ligands may differentially regulate downstream DOR signaling.

#### *4.3.4 Dynorphin A (1-17) and Dynorphin B (1-13) Induced Receptor Regulation at DOR*

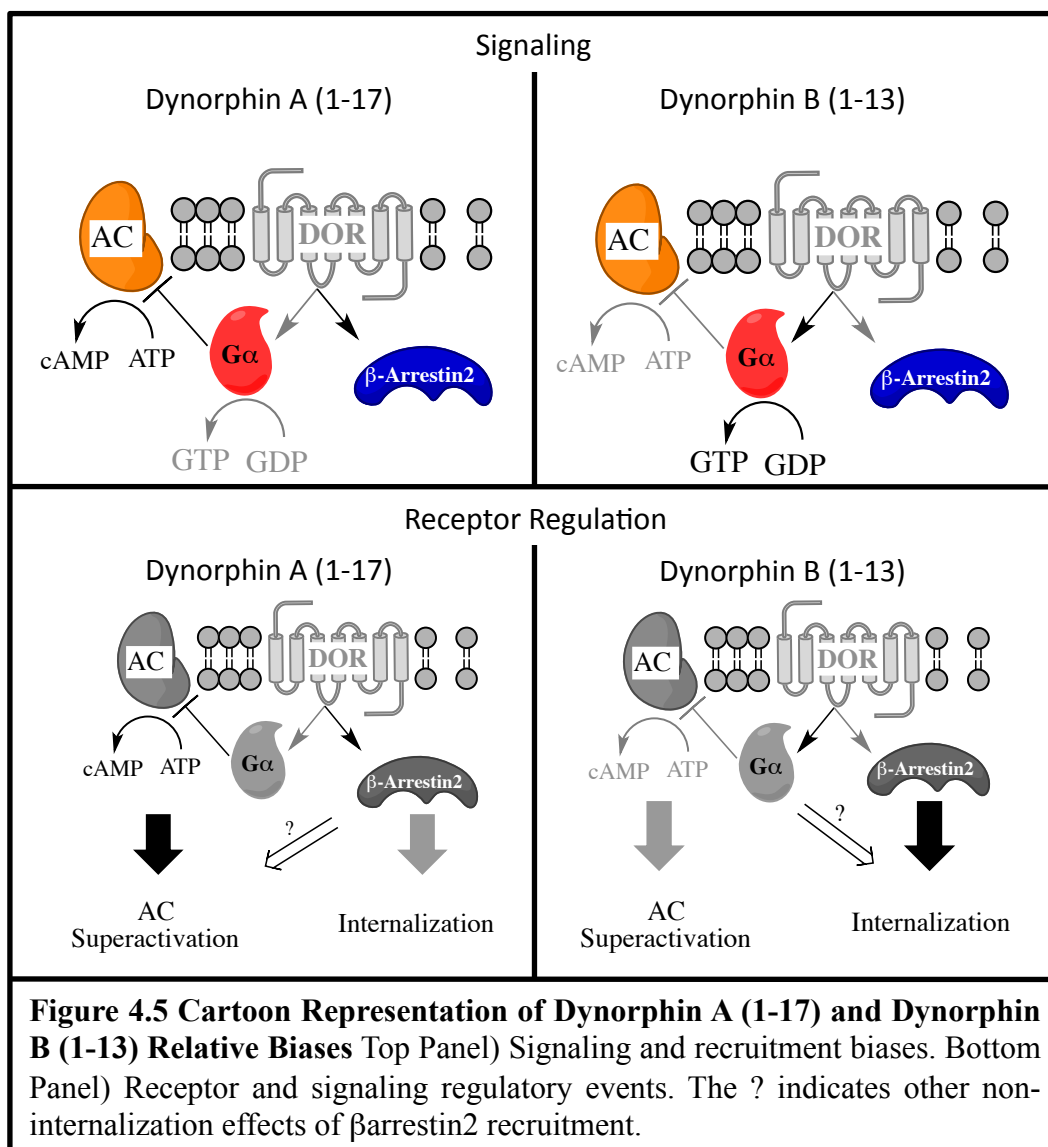
At the DOR, chronic opioid treatment causes a compensatory increase in forskolin-stimulated cAMP levels [241] referred to as Adenylyl Cyclase (AC) super activation, which may play a physiological role in developing opioid tolerance, dependence and withdrawal [244]. Chronic treatment with Dynorphin A (1-17) produced significantly greater cAMP super activation than Leu-Enkephalin, with an increase of 400% over baseline relative to 210% or 201% at high doses of 500 nM ligand with Leu-Enkephalin and Dynorphin B (Figure 4.3). This upregulation in forskolin-stimulated cAMP indicates that Dynorphin A (1-17) and Dynorphin B (1-13) regulate receptor signaling in distinct ways. It's important to note that the more potent and efficacious Leu-enkephalin produced less cAMP superactivation than Dynorphin A (1-17), so the results cannot be simply explained by potency or efficacy.

Dynorphin A (1-17) and Dynorphin B (1-13) also differentially regulate DOR-mediated internalization (Figure 4.4). At low doses (80 nM) of Dynorphin A (1-17) (Figure 4.4A), no appreciable internalization over the vehicle treatment occurs (Figure 4.4E). However, at the same low 80 nM dose Dynorphin B (1-13) induced robust internalization (Figure 4.4C). Upon higher 300 nM treatments, both Dynorphin A (1-17) and Dynorphin B (1-13) produced robust internalization, comparable to the positive control SNC80 (Figure 4.4B, D and F). Taken together, this suggests that Dynorphin B (1-13) modulates DOR signaling by receptor internalization and Dynorphin A (1-17) modulates DOR signaling by AC superactivation. These different methods of receptor

modulation indicate that not all endogenous opioids activate the receptors in an equal way.

## PART IV: DISCUSSION AND FUTURE PERSPECTIVES

Investigations studying opioid mechanisms and drug development independently revealed most endogenous neuropeptides bind to and activate most opioid subtypes, and that several exogenous ligands can act as biased agonists. However, whether or not endogenous opioid peptide-receptor pairs can display biased signaling remains largely unanswered in the literature, particularly at the DOR.



#### 4.4.1 Bias Factor ( $\beta$ ) of [ $^{35}$ S]-GTP $\gamma$ S Coupling, $\beta$ arrestin2 recruitment and cAMP

##### *Inhibition*

To address this question, we assessed a variety of endogenous opioids – Endomorphin-1, Endomorphin-2, Met-Enkephalin, Leu-Enkephalin,  $\beta$ endorphin (1-31),  $\alpha$ endorphin, Dynorphin A (1-17) and Dynorphin B (1-13) for G $\alpha$  signaling and  $\beta$ arrestin2 recruitment at MOR, DOR and KOR to test for functional selectivity. Our studies indicate that Dynorphin A (1-17) preferentially recruits  $\beta$ arrestin2 and Dynorphin B (1-13) preferentially signals via G-protein coupling at the DOR (Figure 4.2; Table 4.3). Figure 4.5 shows a cartoon schematic of the observed biased signals between Dynorphin A (1-17) and Dynorphin B (1-13) at the DOR, with black arrows indicating that pathway is favored and gray arrows indicating it is less favored.

Initially these signaling differences appear modest; Dynorphin A (1-17) is ~2-fold more potent for  $\beta$ arrestin2 than [ $^{35}$ S]-GTP $\gamma$ S coupling at DOR; Dynorphin B (1-13) is about ~9-fold more potent for [ $^{35}$ S]-GTP $\gamma$ S coupling than  $\beta$ arrestin2 recruitment at DOR (Table 4.3). If neither Dynorphin A (1-17) nor Dynorphin B (1-13) displayed biased signaling, or the potency differences were assay dependent, then the potencies should scale approximately equally between assays, relative to the control Leu-Enkephalin ligand. However, the changes in potency rank order suggest that Dynorphin A (1-17) and Dynorphin B (1-13) induce two distinct DOR conformations. Calculated bias factors for [ $^{35}$ S]-GTP $\gamma$ S coupling vs.  $\beta$ arrestin2 recruitment is -0.66 for Dynorphin A (1-17) and 0.49 for Dynorphin B (1-13).

Dynorphin A (1-17) strongly favors cAMP inhibition over [<sup>35</sup>S]-GTPγS coupling ( $\beta = -1.19$ ), whereas Dynorphin B (1-13) modestly favors [<sup>35</sup>S]-GTPγS coupling over cAMP inhibition ( $\beta = 0.40$ ). The difference in  $\beta$  between Dynorphin A and Dynorphin B is 1.49, indicating a nearly 30-fold shift in relative activity between these two ligands. cAMP inhibition is typically correlated to Based on the differences in  $\beta$  for cAMP and  $\beta$ arrestin2 signaling, we predicted these peptides would differentially affect receptor mediated G $\alpha$  regulation.

#### 4.4.2 Dynorphin A (1-17) and Dynorphin B (1-13) Regulation of DOR

At the DOR, chronic opioid treatment causes a compensatory increase in forskolin-stimulated cAMP levels [241] referred to as *Adenylyl Cyclase (AC) super activation*. AC super activation may play a physiological role in developing opioid tolerance, dependence and withdrawal [244]. This upregulation in forskolin-stimulated cAMP indicates that Dynorphin A (1-17) and Dynorphin B (1-13) regulate the receptor in different ways. While similar differences have been previously reported for exogenous ligands [244] differences between endogenous ligands may play a more fundamental role in disease and physiological function *in vivo*.

Our findings at DOR with the Dynorphins contribute to the emerging evidence that exogenous ligands can differentially signal or regulate receptor function. Dynorphin B (1-13) produced less  $\beta$ arrestin2 recruitment but more robust DOR internalization (Figure 4.4-4.5; Table 4.3). This atypical non-classical correlation between  $\beta$ arrestin recruitment and internalization has been observed for other receptors too, such as at

CCR1 where CCL23 favors internalization over  $\beta$ arrestin recruitment [243]. DOR agonists retain full antinociceptive activity when they do not internalize the receptor, as a comparison of the high internalizing (SNC80) and low internalizing (AR-M100390) [245] DOR ligands shows the former produces significant tolerance while the later does not. Due to Dynorphin up regulation in neuropathic pain states, this is an intriguing future study – if differences in Dynorphin A and Dynorphin B release modulate DOR activity *in vivo*.

Taken together, the current study and the CCR studies show that endogenous ligands can recruit  $\beta$ -arrestin2 for non-internalization purposes. This is an important distinction to make and could contribute to signaling specificity of endogenous opioids.  $\beta$ arrestin2 is a multi-faceted scaffold protein that can promote signaling of numerous kinase families independent of  $G\alpha$  signaling [246]. The potential for  $\beta$ arrestin2 mediating other effects is particularly prominent with Dynorphin A (1-17). Dynorphin A (1-17) recruits  $\beta$ arrestin2 with greater potency but does not induce internalization at low concentrations (Figure 4.4-4.5; Table 4.3), suggesting it is serving another function.

$\beta$ arrestin2 can scaffold Src (Review [247, 248]) at other GPCRs and has been found to contribute to DOR-mediated AC super activation [241]. Dynorphin A (1-17) produced greater AC super activation (Figure 4.5), and future studies *in vitro* could explore Src kinase function in this. Differences in AC super activation by endogenous ligands could play important roles in the physiological states of disease and requires

Peptide	1	2	3	4	5	6	7	8	9	10	11	12	13	14	15	16	17
<i>Leu-Enkephalin</i>	H-Tyr-	Gly-	Gly-	Phe-	Leu-OH												
<i>DynorphinA(1-17)</i>	H-Tyr-	Gly-	Gly-	Phe-	Leu-	Arg-	Arg-	Ile-	Arg-	Pro-	Lys-	Leu-	Lys-	Trp-	Asp-	Asn	Gln-OH
<i>DynorphinB(1-13)</i>	H-Tyr-	Gly-	Gly-	Phe-	Leu-	Arg-	Arg-	Gln-	Phe-	Lys-	Val-	Val-	Thr-OH				

**Table 4.4 Sequence of Endogenous Dynorphin and Leu-Enkephalin Peptides**

further *in vivo* study. Nonetheless, *in vitro* assays show endogenous opioid peptides with differing (or absent) C-terminal tails induce distinct activity profiles. Therefore, we show three endogenous opioids induce distinct signaling and regulatory outcomes *in vitro* at the DOR. Further studies are required to understand the differences in  $G\alpha$  activation, other cellular regulatory changes, and potential uses of Dynorphin A/B as peptide scaffolds for drug design [249].

#### *4.4.3 Future Directions and the Unique Challenges of Endogenous Biased Signaling*

Biased signaling studies have primarily focused on identifying drug candidates – to identify ligands that activate pathways with therapeutic potential and avoid ones with side effects. Whereas the drug development aspect has been extensively reviewed elsewhere [83], this section considers the unique challenges of endogenous biased signaling. However, endogenous ligands and drug development investigating biased signaling asks fundamentally different questions. Drug development considers: can we make a molecule that favors pathway A over pathway B? And then, does pathway A lead to desired therapeutic outcomes and pathway B lead to undesirable ones? Endogenous peptide studies consider: Does biased agonism serve as a basic neurological control mechanism with GPCR:peptide pairs serving as an additional layer of signaling specificity?

Answering the endogenous bias question requires different considerations beyond drug development approaches, because most GPCRs have numerous ligands that are determined by biology, not drug development. In addition, most exogenous systemic drugs have longer exposure times to receptor, whereas endogenous ligands are locally

available for short time periods; most endogenous ligands display limited subtype selectivity; and endogenous peptides have limited bioavailability and bioactive cleavage products that makes *in vivo* evaluation difficult. Endogenous biased ligands have distinct experimental challenges that are distinct from identifying potential small molecule therapeutics.

Peptide ligands facilitate a wide range of responses by the brain in reaction to environmental challenges contributing to complex behaviors and disease. Interestingly, GPCR systems consist of usually 2-20 receptor subtypes and up to 10x as many endogenous ligands, typically with limited subtype selectivity. Relative to exogenous ligands, the characterization of endogenous functional selectivity remains understudied. However, understanding if and how natural functional selectivity works should assist in the development of better drugs. Therefore, we propose three necessary types of evidence to identify an endogenous biased ligand:

1. *Demonstrate at least two endogenous ligands differentially activate two (or more) signaling or regulatory events at a given receptor.* This can arise from bias quantification, swaps in potency rank order, changes in efficacy, etc.
2. Show the ligand pair induces a distinct behavioral or physiological response *and* that the observed bias mechanism is the mechanism for the observed behavior *in vivo*. The observed *in vitro* differences correspond to *in vivo* consequences (such as behavioral, developmental or disease responses).

3. Demonstrate the putative biased ligands are not physiologically redundant. Evidence for non-redundancy may include tissue-specific, disease-specific or other biologically relevant states with specific expression; or change of biological function for knockout of putatively redundant ligands. That is, ligand expression is controlled in such a way that the observed *in vitro* and *in vivo* differences (1 and 2) are biologically regulated in a meaningful way. If two ligands induce distinct signals, but are always expressed at the same time, in the same tissue to produce the same biological effect that suggests those ligands may not use biased signaling as a control mechanism.

## REFERENCES

1. Gaskin, D.J. and P. Richard, *The economic costs of pain in the United States*. J Pain, 2012. **13**(8): p. 715-24.
2. *Institute of Medicine Report from the Committee on Advancing Pain Research, Care, and Education: Relieving Pain in America, A Blueprint for Transforming Prevention, Care, Education and Research*. The National Academies Press.
3. *American Diabetes Association*. Available from: <http://www.diabetes.org/diabetes-basics/diabetes-statistics/>
4. *Heart Disease and Stroke Statistics—2011 Update: A Report From the American Heart Association*. Available from: <http://circ.ahajournals.org/content/123/4/e18.full.pdf>
5. *American Cancer Society, Prevalence of Cancer*. Available from: [http://www.cancer.org/docroot/CRI/content/CRI\\_2\\_6x\\_Cancer\\_Prevalence\\_How\\_Many\\_People\\_Have\\_Cancer.asp](http://www.cancer.org/docroot/CRI/content/CRI_2_6x_Cancer_Prevalence_How_Many_People_Have_Cancer.asp)
6. Breivik, H., et al., *Cancer-related pain: a pan-European survey of prevalence, treatment, and patient attitudes*. Ann Oncol, 2009. **20**(8): p. 1420-33.
7. Moulin, D., et al., *Pharmacological management of chronic neuropathic pain: revised consensus statement from the Canadian Pain Society*. Pain Res Manag, 2014. **19**(6): p. 328-35.
8. Kroenke, K., E.E. Krebs, and M.J. Bair, *Pharmacotherapy of chronic pain: a synthesis of recommendations from systematic reviews*. Gen Hosp Psychiatry, 2009. **31**(3): p. 206-19.
9. in *Opioids in Palliative Care: Safe and Effective Prescribing of Strong Opioids for Pain in Palliative Care of Adults*. 2012: Cardiff (UK).
10. Ossipov, M.H., et al., *Spinal and supraspinal mechanisms of neuropathic pain*. Ann N Y Acad Sci, 2000. **909**: p. 12-24.
11. Noble, M., et al., *Long-term opioid management for chronic noncancer pain*. Cochrane Database Syst Rev, 2010(1): p. CD006605.
12. Jones, C.M., K.A. Mack, and L.J. Paulozzi, *Pharmaceutical overdose deaths, United States, 2010*. JAMA, 2013. **309**(7): p. 657-9.
13. *Addressing Prescription Drug Abuse in the United States Current Activities and Future Opportunities*, B.H.C.C.P.D.A.S.U.S.D.o.H.a.H. Services, Editor. 2010.
14. Abrams, D.I., et al., *Cannabinoid-opioid interaction in chronic pain*. Clin Pharmacol Ther, 2011. **90**(6): p. 844-51.
15. Riemsma, R., et al., *Systematic review of tapentadol in chronic severe pain*. Curr Med Res Opin, 2011. **27**(10): p. 1907-30.
16. Giri, A.K. and V.J. Hruba, *Investigational peptide and peptidomimetic mu and delta opioid receptor agonists in the relief of pain*. Expert Opin Investig Drugs, 2014. **23**(2): p. 227-41.
17. Largent-Milnes, T.M., et al., *Building a better analgesic: multifunctional compounds that address injury-induced pathology to enhance analgesic efficacy while eliminating unwanted side effects*. J Pharmacol Exp Ther, 2013. **347**(1): p. 7-19.
18. Deekonda, S., et al., *Design, synthesis and biological evaluation of multifunctional ligands targeting opioid and bradykinin 2 receptors*. Bioorg Med Chem Lett, 2015. **25**(19): p. 4148-52.
19. Waldhoer, M., S.E. Bartlett, and J.L. Whistler, *Opioid receptors*. Annu Rev Biochem, 2004. **73**: p. 953-90.
20. Al-Hasani, R. and M.R. Bruchas, *Molecular mechanisms of opioid receptor-dependent signaling and behavior*. Anesthesiology, 2011. **115**(6): p. 1363-81.

21. Marieb, E.N., and Hoehn, K., *Human anatomy and physiology*. 8th ed. 2010: Pearson Education Publishing.
22. Mizoguchi, H., et al., *The mu-opioid receptor gene-dose dependent reductions in G-protein activation in the pons/medulla and antinociception induced by endomorphins in mu-opioid receptor knockout mice*. *Neuroscience*, 1999. **94**(1): p. 203-7.
23. Wilkerson, R.G., et al., *The Opioid Epidemic in the United States*. *Emerg Med Clin North Am*, 2016. **34**(2): p. e1-e23.
24. Health, H.S.o.P. *The Chronic Pain Epidemic: What's to Be Done?* 2016; Available from: <https://theforum.sph.harvard.edu/events/the-chronic-pain-epidemic/>.
25. Dart, R.C., et al., *Assessment of the abuse of tapentadol immediate release: the first 24 months*. *J Opioid Manag*, 2012. **8**(6): p. 395-402.
26. Abdelhamid, E.E., et al., *Selective blockage of delta opioid receptors prevents the development of morphine tolerance and dependence in mice*. *J Pharmacol Exp Ther*, 1991. **258**(1): p. 299-303.
27. Zhu, Y., et al., *Retention of supraspinal delta-like analgesia and loss of morphine tolerance in delta opioid receptor knockout mice*. *Neuron*, 1999. **24**(1): p. 243-52.
28. Suzuki, T., et al., *Antisense oligodeoxynucleotide to delta opioid receptors attenuates morphine dependence in mice*. *Life Sci*, 1997. **61**(11): p. PL 165-70.
29. Hepburn, M.J., et al., *Differential effects of naltrindole on morphine-induced tolerance and physical dependence in rats*. *J Pharmacol Exp Ther*, 1997. **281**(3): p. 1350-6.
30. Qi, J.N., H.I. Mosberg, and F. Porreca, *Modulation of the potency and efficacy of mu-mediated antinociception by delta agonists in the mouse*. *J Pharmacol Exp Ther*, 1990. **254**(2): p. 683-9.
31. Ananthan, S., et al., *Synthesis, opioid receptor binding, and biological activities of naltrexone-derived pyrido- and pyrimidomorphinans*. *J Med Chem*, 1999. **42**(18): p. 3527-38.
32. Ananthan, S., et al., *14-Alkoxy- and 14-Acyloxy-pyridomorphinans: Mixed Mu Agonist/Delta Antagonist Opioid Analgesics with Diminished Tolerance and Dependence Side Effects*. Submitted, 2012.
33. Anand, J.P., et al., *The behavioral effects of a mixed efficacy antinociceptive peptide, VRP26, following chronic administration in mice*. *Psychopharmacology (Berl)*, 2016. **233**(13): p. 2479-87.
34. Bender, A.M., et al., *Rapid Synthesis of Boc-2',6'-dimethyl-l-tyrosine and Derivatives and Incorporation into Opioid Peptidomimetics*. *ACS Med Chem Lett*, 2015. **6**(12): p. 1199-203.
35. Harland, A.A., et al., *Effects of N-Substitutions on the Tetrahydroquinoline (THQ) Core of Mixed-Efficacy mu-Opioid Receptor (MOR)/delta-Opioid Receptor (DOR) Ligands*. *J Med Chem*, 2016. **59**(10): p. 4985-98.
36. Harland, A.A., et al., *Further Optimization and Evaluation of Bioavailable, Mixed-Efficacy mu-Opioid Receptor (MOR) Agonists/delta-Opioid Receptor (DOR) Antagonists: Balancing MOR and DOR Affinities*. *J Med Chem*, 2015. **58**(22): p. 8952-69.
37. Lowery, J.J., et al., *In vivo characterization of MMP-2200, a mixed delta/mu opioid agonist, in mice*. *J Pharmacol Exp Ther*, 2011. **336**(3): p. 767-78.
38. Stevenson, G.W., et al., *The mixed-action delta/mu opioid agonist MMP-2200 does not produce conditioned place preference but does maintain drug self-administration in rats, and induces in vitro markers of tolerance and dependence*. *Pharmacol Biochem Behav*, 2015. **132**: p. 49-55.
39. Do Carmo, G.P., et al., *Behavioral pharmacology of the mu/delta opioid glycopeptide MMP2200 in rhesus monkeys*. *J Pharmacol Exp Ther*, 2008. **326**(3): p. 939-48.

40. Lipkowski, A.W., et al., *Biological activity of fragments and analogues of the potent dimeric opioid peptide, biphalin*. Bioorg Med Chem Lett, 1999. **9**(18): p. 2763-6.
41. Gomes, I., et al., *G Protein-Coupled Receptor Heteromers*. Annu Rev Pharmacol Toxicol, 2016. **56**: p. 403-25.
42. Milligan, G., *G-protein-coupled receptor heterodimers: pharmacology, function and relevance to drug discovery*. Drug Discov Today, 2006. **11**(11-12): p. 541-9.
43. van Rijn, R.M. and J.L. Whistler, *The delta(1) opioid receptor is a heterodimer that opposes the actions of the delta(2) receptor on alcohol intake*. Biol Psychiatry, 2009. **66**(8): p. 777-84.
44. Milan-Lobo, L., et al., *Anti-analgesic effect of the mu/delta opioid receptor heteromer revealed by ligand-biased antagonism*. PLoS One, 2013. **8**(3): p. e58362.
45. Kabli, N., et al., *Antidepressant-like and anxiolytic-like effects following activation of the mu-delta opioid receptor heteromer in the nucleus accumbens*. Mol Psychiatry, 2014. **19**(9): p. 986-94.
46. He, S.Q., et al., *Facilitation of mu-opioid receptor activity by preventing delta-opioid receptor-mediated codegradation*. Neuron, 2011. **69**(1): p. 120-31.
47. Gomes, I., et al., *Identification of a mu-delta opioid receptor heteromer-biased agonist with antinociceptive activity*. Proc Natl Acad Sci U S A, 2013. **110**(29): p. 12072-7.
48. Daniels, D.J., et al., *Opioid-induced tolerance and dependence in mice is modulated by the distance between pharmacophores in a bivalent ligand series*. Proc Natl Acad Sci U S A, 2005. **102**(52): p. 19208-13.
49. Turnaturi, R., et al., *Multitarget Opioid/Non-opioid Ligands: A Potential Approach in Pain Management*. Curr Med Chem, 2016. **23**(40): p. 4506-4528.
50. Nichols, D.E. and C.D. Nichols, *Serotonin receptors*. Chem Rev, 2008. **108**(5): p. 1614-41.
51. Hammond, D.L. and T.L. Yaksh, *Antagonism of stimulation-produced antinociception by intrathecal administration of methysergide or phentolamine*. Brain Res, 1984. **298**(2): p. 329-37.
52. Fox, M.A., C.L. Jensen, and D.L. Murphy, *Tramadol and another atypical opioid meperidine have exaggerated serotonin syndrome behavioural effects, but decreased analgesic effects, in genetically deficient serotonin transporter (SERT) mice*. Int J Neuropsychopharmacol, 2009. **12**(8): p. 1055-65.
53. Basile, A.S., et al., *Characterization of the antinociceptive actions of bicifadine in models of acute, persistent, and chronic pain*. J Pharmacol Exp Ther, 2007. **321**(3): p. 1208-25.
54. Cui, M., et al., *Periaqueductal gray stimulation-induced inhibition of nociceptive dorsal horn neurons in rats is associated with the release of norepinephrine, serotonin, and amino acids*. J Pharmacol Exp Ther, 1999. **289**(2): p. 868-76.
55. Llorca-Torrallba, M., et al., *Noradrenergic Locus Coeruleus pathways in pain modulation*. Neuroscience, 2016. **338**: p. 93-113.
56. Pertovaara, A., *Noradrenergic pain modulation*. Prog Neurobiol, 2006. **80**(2): p. 53-83.
57. Bardin, L., J. Lavarenne, and A. Eschaliere, *Serotonin receptor subtypes involved in the spinal antinociceptive effect of 5-HT in rats*. Pain, 2000. **86**(1-2): p. 11-8.
58. Tai, Y.H., et al., *Amitriptyline suppresses neuroinflammation and up-regulates glutamate transporters in morphine-tolerant rats*. Pain, 2006. **124**(1-2): p. 77-86.
59. Pan, Z.Z., *mu-Opposing actions of the kappa-opioid receptor*. Trends Pharmacol Sci, 1998. **19**(3): p. 94-8.
60. Pfeiffer, A., et al., *Psychotomimesis mediated by kappa opiate receptors*. Science, 1986. **233**(4765): p. 774-6.
61. Chavkin, C., *The therapeutic potential of kappa-opioids for treatment of pain and addiction*. Neuropsychopharmacology, 2011. **36**(1): p. 369-70.

62. Zhou, L., et al., *Development of functionally selective, small molecule agonists at kappa opioid receptors*. J Biol Chem, 2013. **288**(51): p. 36703-16.
63. Dogra, S. and P.N. Yadav, *Biased agonism at kappa opioid receptors: Implication in pain and mood disorders*. Eur J Pharmacol, 2015. **763**(Pt B): p. 184-90.
64. Lambert, D.G., *The nociceptin/orphanin FQ receptor: a target with broad therapeutic potential*. Nat Rev Drug Discov, 2008. **7**(8): p. 694-710.
65. Kotlinska, J., et al., *Orphanin FQ/nociceptin but not Ro 65-6570 inhibits the expression of cocaine-induced conditioned place preference*. Behav Pharmacol, 2002. **13**(3): p. 229-35.
66. Ciccocioppo, R., et al., *The nociceptin/orphanin FQ/NOP receptor system as a target for treatment of alcohol abuse: a review of recent work in alcohol-preferring rats*. Physiol Behav, 2003. **79**(1): p. 121-8.
67. Ciccocioppo, R., et al., *Effect of nociceptin/orphanin FQ on the rewarding properties of morphine*. Eur J Pharmacol, 2000. **404**(1-2): p. 153-9.
68. Zaveri, N.T., *The nociceptin/orphanin FQ receptor (NOP) as a target for drug abuse medications*. Curr Top Med Chem, 2011. **11**(9): p. 1151-6.
69. Jensen, B., et al., *Medical Marijuana and Chronic Pain: a Review of Basic Science and Clinical Evidence*. Curr Pain Headache Rep, 2015. **19**(10): p. 50.
70. Hill, K.P., *Medical Marijuana for Treatment of Chronic Pain and Other Medical and Psychiatric Problems: A Clinical Review*. JAMA, 2015. **313**(24): p. 2474-83.
71. Baron, E.P., *Comprehensive Review of Medicinal Marijuana, Cannabinoids, and Therapeutic Implications in Medicine and Headache: What a Long Strange Trip It's Been*. Headache, 2015. **55**(6): p. 885-916.
72. Maurice, T. and T.P. Su, *The pharmacology of sigma-1 receptors*. Pharmacol Ther, 2009. **124**(2): p. 195-206.
73. Zamanillo, D., et al., *Sigma 1 receptor: a new therapeutic target for pain*. Eur J Pharmacol, 2013. **716**(1-3): p. 78-93.
74. Chien, C.C. and G.W. Pasternak, *Functional antagonism of morphine analgesia by (+)-pentazocine: evidence for an anti-opioid sigma 1 system*. Eur J Pharmacol, 1993. **250**(1): p. R7-8.
75. Chien, C.C. and G.W. Pasternak, *Selective antagonism of opioid analgesia by a sigma system*. J Pharmacol Exp Ther, 1994. **271**(3): p. 1583-90.
76. Pasternak, G.W., *Multiple opiate receptors: deja vu all over again*. Neuropharmacology, 2004. **47 Suppl 1**: p. 312-23.
77. Ballantyne, J.C. and J. Mao, *Opioid therapy for chronic pain*. N Engl J Med, 2003. **349**(20): p. 1943-53.
78. McPherson, J., et al., *mu-opioid receptors: correlation of agonist efficacy for signalling with ability to activate internalization*. Mol Pharmacol, 2010. **78**(4): p. 756-66.
79. Sirohi, S., et al., *The analgesic efficacy of fentanyl: relationship to tolerance and mu-opioid receptor regulation*. Pharmacol Biochem Behav, 2008. **91**(1): p. 115-20.
80. Pawar, M., et al., *Opioid agonist efficacy predicts the magnitude of tolerance and the regulation of mu-opioid receptors and dynamin-2*. Eur J Pharmacol, 2007. **563**(1-3): p. 92-101.
81. Madia, P.A., et al., *Dosing protocol and analgesic efficacy determine opioid tolerance in the mouse*. Psychopharmacology (Berl), 2009. **207**(3): p. 413-22.
82. Kumar, P., et al., *Hydromorphone efficacy and treatment protocol impact on tolerance and mu-opioid receptor regulation*. Eur J Pharmacol, 2008. **597**(1-3): p. 39-45.
83. Kenakin, T., *Functional selectivity and biased receptor signaling*. J Pharmacol Exp Ther, 2011. **336**(2): p. 296-302.

84. Bohn, L.M., et al., *Enhanced morphine analgesia in mice lacking beta-arrestin 2*. Science, 1999. **286**(5449): p. 2495-8.
85. Raehal, K.M. and L.M. Bohn, *The role of beta-arrestin2 in the severity of antinociceptive tolerance and physical dependence induced by different opioid pain therapeutics*. Neuropharmacology, 2011. **60**(1): p. 58-65.
86. Raehal, K.M., J.K. Walker, and L.M. Bohn, *Morphine side effects in beta-arrestin 2 knockout mice*. J Pharmacol Exp Ther, 2005. **314**(3): p. 1195-201.
87. Urban, J.D., et al., *Functional selectivity and classical concepts of quantitative pharmacology*. J Pharmacol Exp Ther, 2007. **320**(1): p. 1-13.
88. Hruby, V.J., et al., *New paradigms and tools in drug design for pain and addiction*. AAPS J, 2006. **8**(3): p. E450-60.
89. Groer, C.E., et al., *An opioid agonist that does not induce micro-opioid receptor--arrestin interactions or receptor internalization*. Mol Pharmacol, 2007. **71**(2): p. 549-57.
90. Tidgewell, K., et al., *Herkinorin analogues with differential beta-arrestin-2 interactions*. J Med Chem, 2008. **51**(8): p. 2421-31.
91. Dewire, S.M., et al., *A G protein-biased ligand at the mu-opioid receptor is potently analgesic with reduced gastrointestinal and respiratory dysfunction compared to morphine*. J Pharmacol Exp Ther, 2013.
92. Manglik, A., et al., *Structure-based discovery of opioid analgesics with reduced side effects*. Nature, 2016. **advance online publication**: p. 1-6.
93. Manglik, A., et al., *Structure-based discovery of opioid analgesics with reduced side effects*. Nature, 2016. **advance online publication**: p. 1-6.
94. Chen, X.T., et al., *Structure-activity relationships and discovery of a G protein biased mu opioid receptor ligand, [(3-methoxythiophen-2-yl)methyl]({2-[(9R)-9-(pyridin-2-yl)-6-oxaspiro-[4.5]decan- 9-yl]ethyl})amine (TRV130), for the treatment of acute severe pain*. J Med Chem, 2013. **56**(20): p. 8019-31.
95. Soergel, D.G., et al., *Biased agonism of the mu-opioid receptor by TRV130 increases analgesia and reduces on-target adverse effects versus morphine: A randomized, double-blind, placebo-controlled, crossover study in healthy volunteers*. Pain, 2014. **155**(9): p. 1829-35.
96. Soergel, D.G., et al., *First clinical experience with TRV130: pharmacokinetics and pharmacodynamics in healthy volunteers*. J Clin Pharmacol, 2014. **54**(3): p. 351-7.
97. Ong, E.W. and C.M. Cahill, *Molecular Perspectives for mu/delta Opioid Receptor Heteromers as Distinct, Functional Receptors*. Cells, 2014. **3**(1): p. 152-79.
98. Gupta, A., et al., *Increased abundance of opioid receptor heteromers after chronic morphine administration*. Sci Signal, 2010. **3**(131): p. ra54.
99. Lenard, N.R., et al., *Absence of conditioned place preference or reinstatement with bivalent ligands containing mu-opioid receptor agonist and delta-opioid receptor antagonist pharmacophores*. Eur J Pharmacol, 2007. **566**(1-3): p. 75-82.
100. Erbs, E., et al., *A mu-delta opioid receptor brain atlas reveals neuronal co-occurrence in subcortical networks*. Brain Struct Funct, 2015. **220**(2): p. 677-702.
101. Vauquelin, G. and S.J. Charlton, *Exploring avidity: understanding the potential gains in functional affinity and target residence time of bivalent and heterobivalent ligands*. Br J Pharmacol, 2013. **168**(8): p. 1771-85.
102. Berque-Bestel, I., F. Lezoualc'h, and R. Jockers, *Bivalent ligands as specific pharmacological tools for G protein-coupled receptor dimers*. Curr Drug Discov Technol, 2008. **5**(4): p. 312-8.
103. Chefer, V.I. and T.S. Shippenberg, *Augmentation of morphine-induced sensitization but reduction in morphine tolerance and reward in delta-opioid receptor knockout mice*. Neuropsychopharmacology, 2009. **34**(4): p. 887-98.

104. Abdelhamid, E.E., et al., *Selective Blockage of Delta-Opioid Receptors Prevents the Development of Morphine-Tolerance and Dependence in Mice*. Journal of Pharmacology and Experimental Therapeutics, 1991. **258**(1): p. 299-303.
105. Loh, H.H., et al., *mu Opioid receptor knockout in mice: effects on ligand-induced analgesia and morphine lethality*. Brain Res Mol Brain Res, 1998. **54**(2): p. 321-6.
106. Matthes, H.W., et al., *Activity of the delta-opioid receptor is partially reduced, whereas activity of the kappa-receptor is maintained in mice lacking the mu-receptor*. J Neurosci, 1998. **18**(18): p. 7285-95.
107. Porreca, F., et al., *Modulation of Mu-Mediated Antinociception in the Mouse Involves Opioid Delta-2 Receptors*. Journal of Pharmacology and Experimental Therapeutics, 1992. **263**(1): p. 147-152.
108. He, L. and N.M. Lee, *Delta opioid receptor enhancement of mu opioid receptor-induced antinociception in spinal cord*. J Pharmacol Exp Ther, 1998. **285**(3): p. 1181-6.
109. Snyder, S.H. and G.W. Pasternak, *Historical review: Opioid receptors*. Trends Pharmacol Sci, 2003. **24**(4): p. 198-205.
110. Ananthan, S., *Opioid ligands with mixed mu/delta opioid receptor interactions: an emerging approach to novel analgesics*. AAPS J, 2006. **8**(1): p. E118-25.
111. Wang, D., et al., *Opioid receptor homo- and heterodimerization in living cells by quantitative bioluminescence resonance energy transfer*. Mol Pharmacol, 2005. **67**(6): p. 2173-84.
112. Kabli, N., et al., *Agonists at the delta-opioid receptor modify the binding of micro-receptor agonists to the micro-delta receptor hetero-oligomer*. Br J Pharmacol, 2010. **161**(5): p. 1122-36.
113. Rozenfeld, R. and L.A. Devi, *Receptor heterodimerization leads to a switch in signaling: beta-arrestin2-mediated ERK activation by mu-delta opioid receptor heterodimers*. FASEB J, 2007. **21**(10): p. 2455-65.
114. Fan, T., et al., *A role for the distal carboxyl tails in generating the novel pharmacology and G protein activation profile of mu and delta opioid receptor hetero-oligomers*. J Biol Chem, 2005. **280**(46): p. 38478-88.
115. Murray, C.W. and D.C. Rees, *The rise of fragment-based drug discovery*. Nat Chem, 2009. **1**(3): p. 187-92.
116. Shonberg, J., P.J. Scammells, and B. Capuano, *Design strategies for bivalent ligands targeting GPCRs*. ChemMedChem, 2011. **6**(6): p. 963-74.
117. Dove, L.S., et al., *Eluxadoline benefits patients with irritable bowel syndrome with diarrhea in a phase 2 study*. Gastroenterology, 2013. **145**(2): p. 329-38 e1.
118. Wade, P.R., et al., *Modulation of gastrointestinal function by MuDelta, a mixed micro opioid receptor agonist/ micro opioid receptor antagonist*. Br J Pharmacol, 2012. **167**(5): p. 1111-25.
119. Fujita, W., et al., *Molecular characterization of eluxadoline as a potential ligand targeting mu-delta opioid receptor heteromers*. Biochem Pharmacol, 2014. **92**(3): p. 448-56.
120. Yekkirala, A.S., A.E. Kalyuzhny, and P.S. Portoghese, *An immunocytochemical-derived correlate for evaluating the bridging of heteromeric mu-delta opioid protomers by bivalent ligands*. ACS Chem Biol, 2013. **8**(7): p. 1412-6.
121. Stockton, S.D., Jr. and L.A. Devi, *Functional relevance of mu-delta opioid receptor heteromerization: a role in novel signaling and implications for the treatment of addiction disorders: from a symposium on new concepts in mu-opioid pharmacology*. Drug Alcohol Depend, 2012. **121**(3): p. 167-72.
122. Salvadori, S., et al., *Delta opioidmimetic antagonists: prototypes for designing a new generation of ultraspecific opioid peptides*. Mol Med, 1995. **1**(6): p. 678-89.

123. Fichna, J., et al., *Synthesis and characterization of potent and selective mu-opioid receptor antagonists, [Dmt(1), D-2-Nal(4)]endomorphin-1 (Antanal-1) and [Dmt(1), D-2-Nal(4)]endomorphin-2 (Antanal-2)*. J Med Chem, 2007. **50**(3): p. 512-20.
124. Pluckthun, A. and P. Pack, *New protein engineering approaches to multivalent and bispecific antibody fragments*. Immunotechnology, 1997. **3**(2): p. 83-105.
125. Mammen, M., Choi, S. K., and Whitesides, G. M., *Polyvalent Interactions in Biological Systems: Implications for Design and*
- Use of Multivalent Ligands and Inhibitors*. Agnew. Chem. Int. Ed. , 1998. **37**: p. 2754-2794.
126. Kane, R.S., *Thermodynamics of multivalent interactions: influence of the linker*. Langmuir, 2010. **26**(11): p. 8636-40.
127. Hiller, C., J. Kuhhorn, and P. Gmeiner, *Class A G-protein-coupled receptor (GPCR) dimers and bivalent ligands*. J Med Chem, 2013. **56**(17): p. 6542-59.
128. Brabez, N., et al., *Design, synthesis, and biological studies of efficient multivalent melanotropin ligands: tools toward melanoma diagnosis and treatment*. J Med Chem, 2011. **54**(20): p. 7375-84.
129. Schiller, P.W., et al., *Differential stereochemical requirements of mu vs. delta opioid receptors for ligand binding and signal transduction: development of a class of potent and highly delta-selective peptide antagonists*. Proc Natl Acad Sci U S A, 1992. **89**(24): p. 11871-5.
130. Salvadori, S., et al., *Evolution of the Dmt-Tic pharmacophore: N-terminal methylated derivatives with extraordinary delta opioid antagonist activity*. J Med Chem, 1997. **40**(19): p. 3100-8.
131. Balboni, G., et al., *Further studies on lead compounds containing the opioid pharmacophore Dmt-Tic*. J Med Chem, 2008. **51**(16): p. 5109-17.
132. Fichna, J., et al., *Novel highly potent mu-opioid receptor antagonist based on endomorphin-2 structure*. Bioorg Med Chem Lett, 2008. **18**(4): p. 1350-3.
133. Fichna, J., et al., *Novel endomorphin analogues with antagonist activity at the mu-opioid receptor in the gastrointestinal tract*. Regul Pept, 2010. **162**(1-3): p. 109-14.
134. Perlikowska, R., et al., *Design, synthesis and pharmacological characterization of endomorphin analogues with non-cyclic amino acid residues in position 2*. Basic Clin Pharmacol Toxicol, 2010. **106**(2): p. 106-13.
135. Kruszynski, R., et al., *Novel endomorphin-2 analogs with mu-opioid receptor antagonist activity*. J Pept Res, 2005. **66**(3): p. 125-31.
136. Li, T., et al., *Transformation of mu-opioid receptor agonists into biologically potent mu-opioid receptor antagonists*. Bioorg Med Chem, 2007. **15**(3): p. 1237-51.
137. Josan, J.S., et al., *Solid-Phase Synthesis of Heterobivalent Ligands Targeted to Melanocortin and Cholecystokinin Receptors*. Int J Pept Res Ther, 2008. **14**(4): p. 293-300.
138. Balboni, G., et al., *Highly selective fluorescent analogue of the potent delta-opioid receptor antagonist Dmt-Tic*. J Med Chem, 2004. **47**(26): p. 6541-6.
139. Gao, Y., et al., *Structure-activity relationship of the novel bivalent and C-terminal modified analogues of endomorphin-2*. Bioorg Med Chem Lett, 2005. **15**(7): p. 1847-50.
140. Russo, O., et al., *Synthesis of specific bivalent probes that functionally interact with 5-HT(4) receptor dimers*. J Med Chem, 2007. **50**(18): p. 4482-92.
141. Page, D., et al., *Novel C-terminus modifications of the Dmt-Tic motif: a new class of dipeptide analogues showing altered pharmacological profiles toward the opioid receptors*. J Med Chem, 2001. **44**(15): p. 2387-90.
142. Krishnara, S.a.R., B., *A protocol for racemization-free loading of Fmoc-amino acids to Wang resin*. Tetrahedron Lett, 2008. **49**(15): p. 2435-2437.

143. Amblard, M., et al., *Methods and protocols of modern solid phase Peptide synthesis*. Mol Biotechnol, 2006. **33**(3): p. 239-54.
144. Suode Zhang, F.L., Mohammed Akhter Hossain, Fazel Shabanpoor Geoffrey W. Tregear, John D. Wade, *Simultaneous Post-cysteine(S-Acm) Group Removal Quenching of Iodine and Isolation of Peptide by One Step Ether Precipitation*. International Journal of Peptide Research and Therapeutics, 2008. **14**(4): p. 301-305.
145. Rutherford, J.M., et al., *Evidence for a mu-delta opioid receptor complex in CHO cells co-expressing mu and delta opioid peptide receptors*. Peptides, 2008. **29**(8): p. 1424-31.
146. Handl, H.L., et al., *Synthesis and evaluation of bivalent NDP-alpha-MSH(7) peptide ligands for binding to the human melanocortin receptor 4 (hMC4R)*. Bioconjug Chem, 2007. **18**(4): p. 1101-9.
147. Josan, J.S., et al., *Cell-specific targeting by heterobivalent ligands*. Bioconjug Chem, 2011. **22**(7): p. 1270-8.
148. Josan, J.S., et al., *Heterobivalent ligands crosslink multiple cell-surface receptors--a step towards personal medicine*. Adv Exp Med Biol, 2009. **611**: p. 413-4.
149. Vagner, J., et al., *Heterobivalent ligands crosslink multiple cell-surface receptors: the human melanocortin-4 and delta-opioid receptors*. Angew Chem Int Ed Engl, 2008. **47**(9): p. 1685-8.
150. Kenakin, T., *Pharmacology Primer, Third Edition: Theory, Application and Methods Third* 2009: Academic Press.
151. Lensing, C.J., et al., *An in Vitro and in Vivo Investigation of Bivalent Ligands That Display Preferential Binding and Functional Activity for Different Melanocortin Receptor Homodimers*. J Med Chem, 2016. **59**(7): p. 3112-28.
152. Harvey, J.H., et al., *Tuned-Affinity Bivalent Ligands for the Characterization of Opioid Receptor Heteromers*. ACS Med Chem Lett, 2012. **3**(8): p. 640-644.
153. Krishnamurthy, V.M., et al., *Dependence of effective molarity on linker length for an intramolecular protein-ligand system*. J Am Chem Soc, 2007. **129**(5): p. 1312-20.
154. Bhushan, R.G., et al., *A bivalent ligand (KDN-21) reveals spinal delta and kappa opioid receptors are organized as heterodimers that give rise to delta(1) and kappa(2) phenotypes. Selective targeting of delta-kappa heterodimers*. J Med Chem, 2004. **47**(12): p. 2969-72.
155. Soriano, A., et al., *Adenosine A2A receptor-antagonist/dopamine D2 receptor-agonist bivalent ligands as pharmacological tools to detect A2A-D2 receptor heteromers*. J Med Chem, 2009. **52**(18): p. 5590-602.
156. Chabot-Dore, A.J., M. Millecamps, and L.S. Stone, *The delta-opioid receptor is sufficient, but not necessary, for spinal opioid-adrenergic analgesic synergy*. J Pharmacol Exp Ther, 2013. **347**(3): p. 773-80.
157. Hosohata, Y., et al., *delta-Opioid receptor agonists produce antinociception and [35S]GTPgammaS binding in mu receptor knockout mice*. Eur J Pharmacol, 2000. **388**(3): p. 241-8.
158. Gendron, L., et al., *Morphine and pain-related stimuli enhance cell surface availability of somatic delta-opioid receptors in rat dorsal root ganglia*. J Neurosci, 2006. **26**(3): p. 953-62.
159. Cahill, C.M., et al., *Up-regulation and trafficking of delta opioid receptor in a model of chronic inflammation: implications for pain control*. Pain, 2003. **101**(1-2): p. 199-208.
160. Urizar, E., et al., *CODA-RET reveals functional selectivity as a result of GPCR heteromerization*. Nat Chem Biol, 2011. **7**(9): p. 624-30.
161. Bellot, M., et al., *Dual agonist occupancy of AT1-R-alpha2C-AR heterodimers results in atypical Gs-PKA signaling*. Nat Chem Biol, 2015. **11**(4): p. 271-9.



179. Negus, S.S., M.J. Picker, and L.A. Dykstra, *Kappa antagonist properties of buprenorphine in non-tolerant and morphine-tolerant rats*. Psychopharmacology (Berl), 1989. **98**(1): p. 141-3.
180. Bloms-Funke, P., et al., *Agonistic effects of the opioid buprenorphine on the nociceptin/OFQ receptor*. Peptides, 2000. **21**(7): p. 1141-6.
181. Pertwee, R.G., *The diverse CB1 and CB2 receptor pharmacology of three plant cannabinoids: delta9-tetrahydrocannabinol, cannabidiol and delta9-tetrahydrocannabivarin*. Br J Pharmacol, 2008. **153**(2): p. 199-215.
182. Vazzana, M., et al., *Tramadol hydrochloride: pharmacokinetics, pharmacodynamics, adverse side effects, co-administration of drugs and new drug delivery systems*. Biomed Pharmacother, 2015. **70**: p. 234-8.
183. Learned-Coughlin, S.M., et al., *In vivo activity of bupropion at the human dopamine transporter as measured by positron emission tomography*. Biol Psychiatry, 2003. **54**(8): p. 800-5.
184. Su, T.P. and T. Hayashi, *Understanding the molecular mechanism of sigma-1 receptors: towards a hypothesis that sigma-1 receptors are intracellular amplifiers for signal transduction*. Curr Med Chem, 2003. **10**(20): p. 2073-80.
185. Glennon, R.A., et al., *Structural features important for sigma 1 receptor binding*. J Med Chem, 1994. **37**(8): p. 1214-9.
186. Aldrich, S. *Buffer Reference Center*. 2017; Available from: <http://www.sigmaaldrich.com/life-science/core-bioreagents/biological-buffers/learning-center/buffer-reference-center.html>.
187. Lutfy, K. and A. Cowan, *Buprenorphine: a unique drug with complex pharmacology*. Curr Neuropharmacol, 2004. **2**(4): p. 395-402.
188. Raffa, R.B., Ding, Z. , *Examination of the preclinical antinociceptive efficacy of buprenorphine and its designation as full- or partial-agonist*. Acute Pain, 2007. **9**(3): p. 145-152.
189. Tallarida, R.J., A. Cowan, and R.B. Raffa, *On deriving the dose-effect relation of an unknown second component: an example using buprenorphine preclinical data*. Drug Alcohol Depend, 2010. **109**(1-3): p. 126-9.
190. Zhu, J., et al., *Activation of the cloned human kappa opioid receptor by agonists enhances [35S]GTPgammaS binding to membranes: determination of potencies and efficacies of ligands*. J Pharmacol Exp Ther, 1997. **282**(2): p. 676-84.
191. Thompson, C.M., et al., *Activation of G-proteins by morphine and codeine congeners: insights to the relevance of O- and N-demethylated metabolites at mu- and delta-opioid receptors*. J Pharmacol Exp Ther, 2004. **308**(2): p. 547-54.
192. Lotsch, J., *Opioid metabolites*. J Pain Symptom Manage, 2005. **29**(5 Suppl): p. S10-24.
193. Gillen, C., et al., *Affinity, potency and efficacy of tramadol and its metabolites at the cloned human mu-opioid receptor*. Naunyn Schmiedebergs Arch Pharmacol, 2000. **362**(2): p. 116-21.
194. Guidelines, A.P.S. *Equivalent Opioid Calculator: Equianalgesic dosage conversion calculator*. [cited 2017; Available from: <http://clincalc.com/opioids/>].
195. Desmeules, J.A., *The tramadol option*. Eur J Pain, 2000. **4 Suppl A**: p. 15-21.
196. Ross, F.B. and M.T. Smith, *The intrinsic antinociceptive effects of oxycodone appear to be kappa-opioid receptor mediated*. Pain, 1997. **73**(2): p. 151-7.
197. Bostrom, E., U.S. Simonsson, and M. Hammarlund-Udenaes, *In vivo blood-brain barrier transport of oxycodone in the rat: indications for active influx and implications for pharmacokinetics/pharmacodynamics*. Drug Metab Dispos, 2006. **34**(9): p. 1624-31.

198. Sofuoglu, M., P.S. Portoghese, and A.E. Takemori, *Differential antagonism of delta opioid agonists by naltrindole and its benzofuran analog (NTB) in mice: evidence for delta opioid receptor subtypes*. J Pharmacol Exp Ther, 1991. **257**(2): p. 676-80.
199. Kalso, E. and A. Vainio, *Morphine and oxycodone hydrochloride in the management of cancer pain*. Clin Pharmacol Ther, 1990. **47**(5): p. 639-46.
200. Amabile, C.M. and B.J. Bowman, *Overview of oral modified-release opioid products for the management of chronic pain*. Ann Pharmacother, 2006. **40**(7-8): p. 1327-35.
201. Cichewicz, D.L., *Synergistic interactions between cannabinoid and opioid analgesics*. Life Sci, 2004. **74**(11): p. 1317-24.
202. Su, T.P., et al., *The sigma-1 receptor chaperone as an inter-organelle signaling modulator*. Trends Pharmacol Sci, 2010. **31**(12): p. 557-66.
203. Guay, D.R., *Use of oral oxymorphone in the elderly*. Consult Pharm, 2007. **22**(5): p. 417-30.
204. Prommer, E., *Oxymorphone: a review*. Support Care Cancer, 2006. **14**(2): p. 109-15.
205. Gourlay, G.K., D.A. Cherry, and M.J. Cousins, *A comparative study of the efficacy and pharmacokinetics of oral methadone and morphine in the treatment of severe pain in patients with cancer*. Pain, 1986. **25**(3): p. 297-312.
206. Tao, R., et al., *Nociceptin/orphanin FQ decreases serotonin efflux in the rat brain but in contrast to a kappa-opioid has no antagonistic effect on mu-opioid-induced increases in serotonin efflux*. Neuroscience, 2007. **147**(1): p. 106-16.
207. Greenwald, M., et al., *Buprenorphine duration of action: mu-opioid receptor availability and pharmacokinetic and behavioral indices*. Biol Psychiatry, 2007. **61**(1): p. 101-10.
208. Husbands, S.M., *Buprenorphine and Related Orvinols*. ACS Symposium Series, 2013. **1131**: p. 127-144.
209. Li, X., D. Shorter, and T.R. Kosten, *Buprenorphine in the treatment of opioid addiction: opportunities, challenges and strategies*. Expert Opin Pharmacother, 2014. **15**(15): p. 2263-75.
210. Husbands, S.M., et al., *BU74, a complex oripavine derivative with potent kappa opioid receptor agonism and delayed opioid antagonism*. Eur J Pharmacol, 2005. **509**(2-3): p. 117-25.
211. Moynihan, H., et al., *14 beta-O-cinnamoylnaltrexone and related dihydrocodeinones are mu opioid receptor partial agonists with predominant antagonist activity*. J Med Chem, 2009. **52**(6): p. 1553-7.
212. Hyman, S.E., R.C. Malenka, and E.J. Nestler, *Neural mechanisms of addiction: the role of reward-related learning and memory*. Annu Rev Neurosci, 2006. **29**: p. 565-98.
213. Di Chiara, G. and A. Imperato, *Opposite effects of mu and kappa opiate agonists on dopamine release in the nucleus accumbens and in the dorsal caudate of freely moving rats*. J Pharmacol Exp Ther, 1988. **244**(3): p. 1067-80.
214. Di Giannuario, A. and S. Pieretti, *Nociceptin differentially affects morphine-induced dopamine release from the nucleus accumbens and nucleus caudate in rats*. Peptides, 2000. **21**(7): p. 1125-30.
215. Hillhouse, T.M., Hallahan, J. E., Jutkiewicz, E. M., Husbands, S. M., and Traynor, J. R. *A buprenorphine analog attenuates drug-primed and stress-induced cocaine reinstatement*. in *Society for Neuroscience*. 2016. San Diego, CA.
216. Ciccocioppo, R., et al., *Buprenorphine reduces alcohol drinking through activation of the nociceptin/orphanin FQ-NOP receptor system*. Biol Psychiatry, 2007. **61**(1): p. 4-12.
217. Joels, M., *Modulatory actions of steroid hormones and neuropeptides on electrical activity in brain*. Eur J Pharmacol, 2000. **405**(1-3): p. 207-16.
218. Hammonds, R.G., Jr., P. Nicolas, and C.H. Li, *beta-endorphin-(1-27) is an antagonist of beta-endorphin analgesia*. Proc Natl Acad Sci U S A, 1984. **81**(5): p. 1389-90.

219. Mansour, A., et al., *The cloned mu, delta and kappa receptors and their endogenous ligands: evidence for two opioid peptide recognition cores*. Brain Res, 1995. **700**(1-2): p. 89-98.
220. Guttenberg, N.D., et al., *Co-localization of mu opioid receptor is greater with dynorphin than enkephalin in rat striatum*. Neuroreport, 1996. **7**(13): p. 2119-24.
221. Wang, H., et al., *Ultrastructural immunocytochemical localization of mu opioid receptors and Leu5-enkephalin in the patch compartment of the rat caudate-putamen nucleus*. J Comp Neurol, 1996. **375**(4): p. 659-74.
222. Svingos, A.L., et al., *Ultrastructural immunocytochemical localization of mu-opioid receptors in rat nucleus accumbens: extrasynaptic plasmalemmal distribution and association with Leu5-enkephalin*. J Neurosci, 1996. **16**(13): p. 4162-73.
223. Pasternak, G.W., *The Opiate Receptors*. 2008, New York: Huanna Press- Springer Publishing.
224. Rivero, G., et al., *Endomorphin-2: a biased agonist at the mu-opioid receptor*. Mol Pharmacol, 2012. **82**(2): p. 178-88.
225. Thompson, G.L., et al., *Biased Agonism of Endogenous Opioid Peptides at the mu-Opioid Receptor*. Mol Pharmacol, 2015. **88**(2): p. 335-46.
226. Whalen, E.J., S. Rajagopal, and R.J. Lefkowitz, *Therapeutic potential of beta-arrestin- and G protein-biased agonists*. Trends Mol Med, 2011. **17**(3): p. 126-39.
227. Rives, M.L., et al., *6'-Guanidinonaltrindole (6'-GNTI) is a G protein-biased kappa-opioid receptor agonist that inhibits arrestin recruitment*. J Biol Chem, 2012. **287**(32): p. 27050-4.
228. Schmid, C.L., et al., *Functional selectivity of 6'-guanidinonaltrindole (6'-GNTI) at kappa-opioid receptors in striatal neurons*. J Biol Chem, 2013. **288**(31): p. 22387-98.
229. Lamb, K., et al., *Antinociceptive effects of herkinorin, a MOP receptor agonist derived from salvinorin A in the formalin test in rats: new concepts in mu opioid receptor pharmacology: from a symposium on new concepts in mu-opioid pharmacology*. Drug Alcohol Depend, 2012. **121**(3): p. 181-8.
230. Bruchas, M.R. and C. Chavkin, *Kinase cascades and ligand-directed signaling at the kappa opioid receptor*. Psychopharmacology (Berl), 2010. **210**(2): p. 137-47.
231. Bruchas, M.R., et al., *Kappa opioid receptor activation of p38 MAPK is GRK3- and arrestin-dependent in neurons and astrocytes*. J Biol Chem, 2006. **281**(26): p. 18081-9.
232. Lovell, K.M., et al., *Structure-Activity Relationship Studies of Functionally Selective Kappa Opioid Receptor Agonists that Modulate ERK 1/2 Phosphorylation While Preserving G Protein Over betaArrestin2 Signaling Bias*. ACS Chem Neurosci, 2015.
233. Rives, M.L., et al., *6'GNTI is a G protein-biased kappa opioid receptor agonist that inhibits arrestin recruitment*. J Biol Chem, 2012.
234. Schmid, C.L., et al., *Functional Selectivity of 6'-guanidinonaltrindole (6'-GNTI) at Kappa Opioid Receptors in Striatal Neurons*. J Biol Chem, 2013.
235. White, K.L., et al., *The G protein-biased kappa-opioid receptor agonist RB-64 is analgesic with a unique spectrum of activities in vivo*. J Pharmacol Exp Ther, 2015. **352**(1): p. 98-109.
236. DiMattio, K.M., F.J. Ehler, and L.Y. Liu-Chen, *Intrinsic relative activities of kappa opioid agonists in activating Galpha proteins and internalizing receptor: Differences between human and mouse receptors*. Eur J Pharmacol, 2015. **761**: p. 235-44.
237. Maillet, E.L., et al., *Noribogaine is a G-protein biased kappa-opioid receptor agonist*. Neuropharmacology, 2015. **99**: p. 675-88.
238. White, K.L., et al., *Identification of novel functionally selective kappa-opioid receptor scaffolds*. Mol Pharmacol, 2014. **85**(1): p. 83-90.

239. Manglik, A., et al., *Structure-based discovery of opioid analgesics with reduced side effects*. Nature, 2016. **advance online publication**: p. 1-6.
240. Grieco, P., et al., *Design and microwave-assisted synthesis of novel macrocyclic peptides active at melanocortin receptors: discovery of potent and selective hMC5R receptor antagonists*. J Med Chem, 2008. **51**(9): p. 2701-7.
241. Varga, E.V., et al., *Converging protein kinase pathways mediate adenylyl cyclase superactivation upon chronic delta-opioid agonist treatment*. J Pharmacol Exp Ther, 2003. **306**(1): p. 109-15.
242. Rosa, M., et al., *Structure-activity relationship study of opiorphin, a human dual ectopeptidase inhibitor with antinociceptive properties*. J Med Chem, 2012. **55**(3): p. 1181-8.
243. Rajagopal, S., et al., *Biased agonism as a mechanism for differential signaling by chemokine receptors*. J Biol Chem, 2013. **288**(49): p. 35039-48.
244. Varga, E.V., et al., *Agonist-specific regulation of the delta-opioid receptor*. Life Sci, 2004. **76**(6): p. 599-612.
245. Pradhan, A.A., et al., *In vivo delta opioid receptor internalization controls behavioral effects of agonists*. PLoS One, 2009. **4**(5): p. e5425.
246. DeWire, S.M., et al., *Beta-arrestins and cell signaling*. Annu Rev Physiol, 2007. **69**: p. 483-510.
247. Lefkowitz, R.J., K. Rajagopal, and E.J. Whalen, *New roles for beta-arrestins in cell signaling: not just for seven-transmembrane receptors*. Mol Cell, 2006. **24**(5): p. 643-52.
248. Pierce, K.L., R.T. Premont, and R.J. Lefkowitz, *Seven-transmembrane receptors*. Nat Rev Mol Cell Biol, 2002. **3**(9): p. 639-50.
249. Varga, E.V., et al., *Molecular mechanisms of excitatory signaling upon chronic opioid agonist treatment*. Life Sci, 2003. **74**(2-3): p. 299-311.

**APPENDIX A:**

**Supplementary Data**

# Analytical/Biological Mass Spectrometry Core Facility Results

Request #: 217512

Sample Name: 302-15

Submitted by: Keith Olson

Operator: KK

Date Received: 7/7/2017

Date Completed: 7/11/2017

Solvent Used: ACN

Matrix Used:

Analysis notes: The sample was dissolved in 200uL ACN/H2O.  
Positive ion analysis gave M+H ions at m/z 1244.57686 and M+2H ions at m/z 622.79224 for C67H77N11O13.

## Instrument

- Bruker FT-ICR
- Bruker Amazon Ion Trap
- Bruker MALDI-TOF
- Bruker MALDI-TOF/TOF
- Thermo LCQ Ion Trap
- Shimadzu GC-MS

## Ionization Method

- Positive
- Negative
- ESI     APCI     APPI
- MALDI
- EI

## Sample Introduction

- Infusion/Flow Injection
- HPLC (ESI) or GC (EI)
- Direct Probe

## Resolution

- Accurate Mass
- Survey Mass

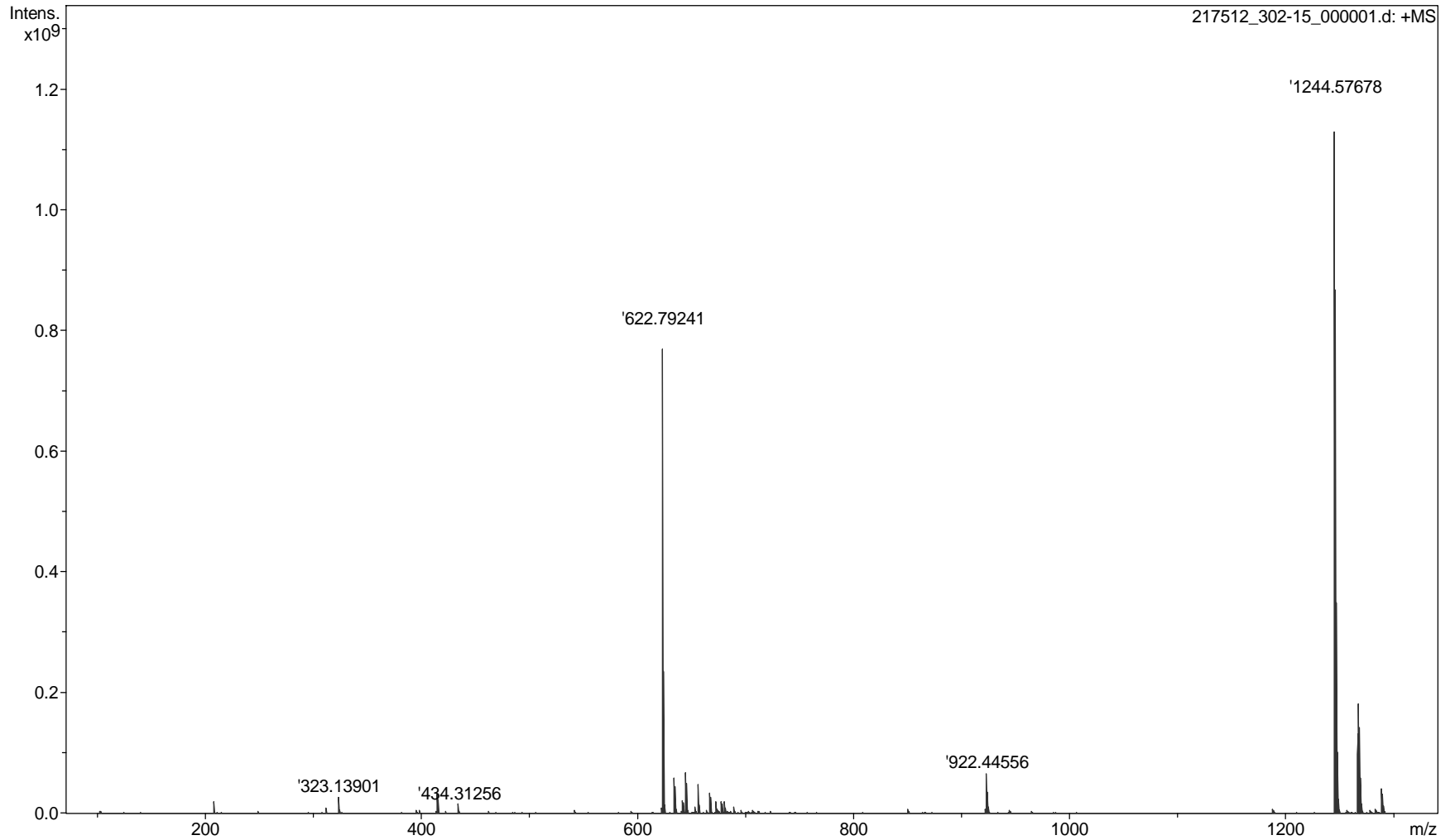
# Generic Display Report

## Analysis Info

Analysis Name D:\Data\July\_17\217512\_302-15\_000001.d  
Method April\_good\_method  
Sample Name 217512\_302-15  
Comment 217512, 302-15, dissolved in 200uL H2O/ACN

Acquisition Date 7/11/2017 1:44:21 PM

Operator  
Instrument apex-Qe



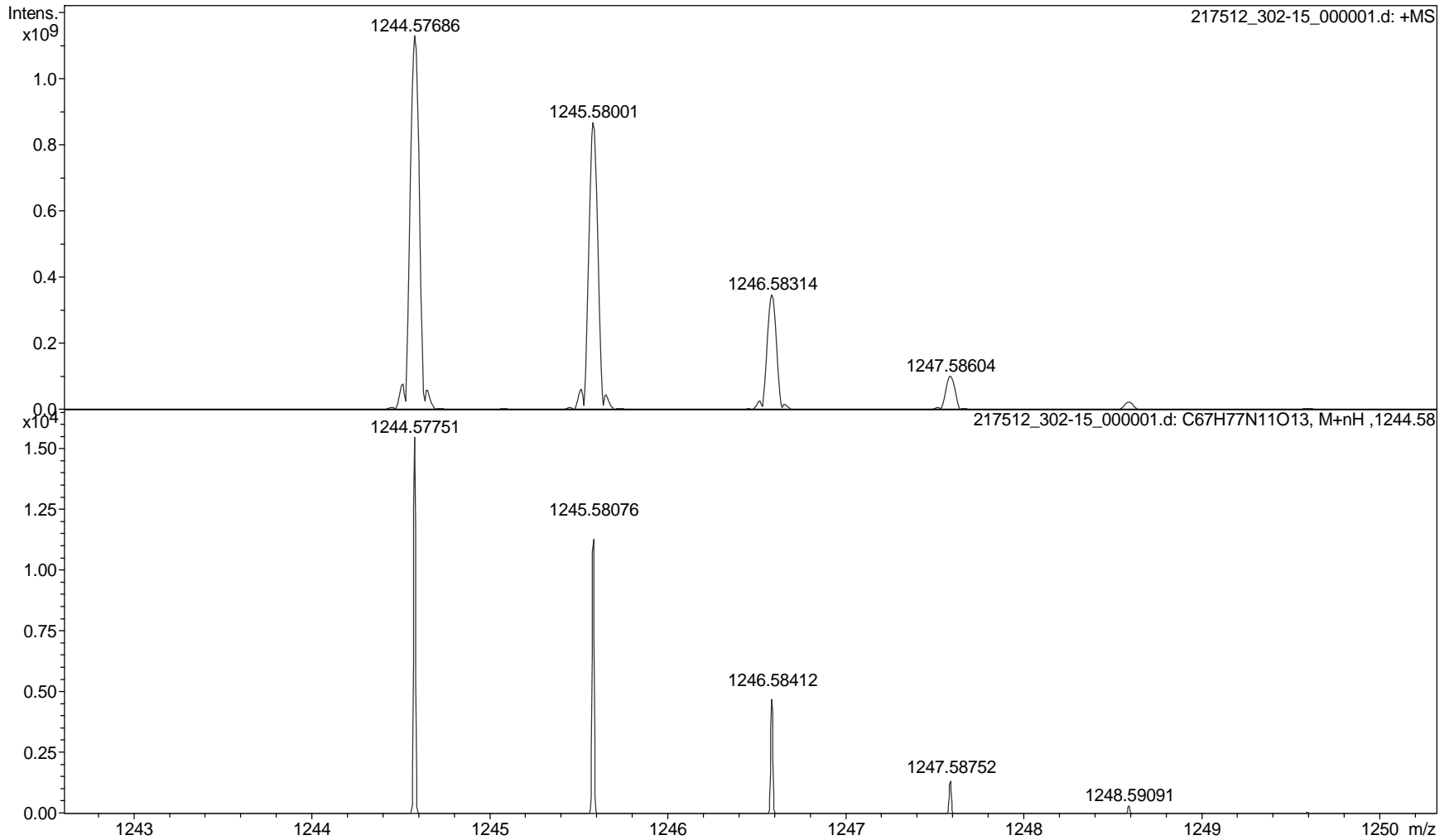
# Generic Display Report

## Analysis Info

Analysis Name D:\Data\July\_17\217512\_302-15\_000001.d  
Method April\_good\_method  
Sample Name 217512\_302-15  
Comment 217512, 302-15, dissolved in 200uL H2O/ACN

Acquisition Date 7/11/2017 1:44:21 PM

Operator  
Instrument apex-Qe



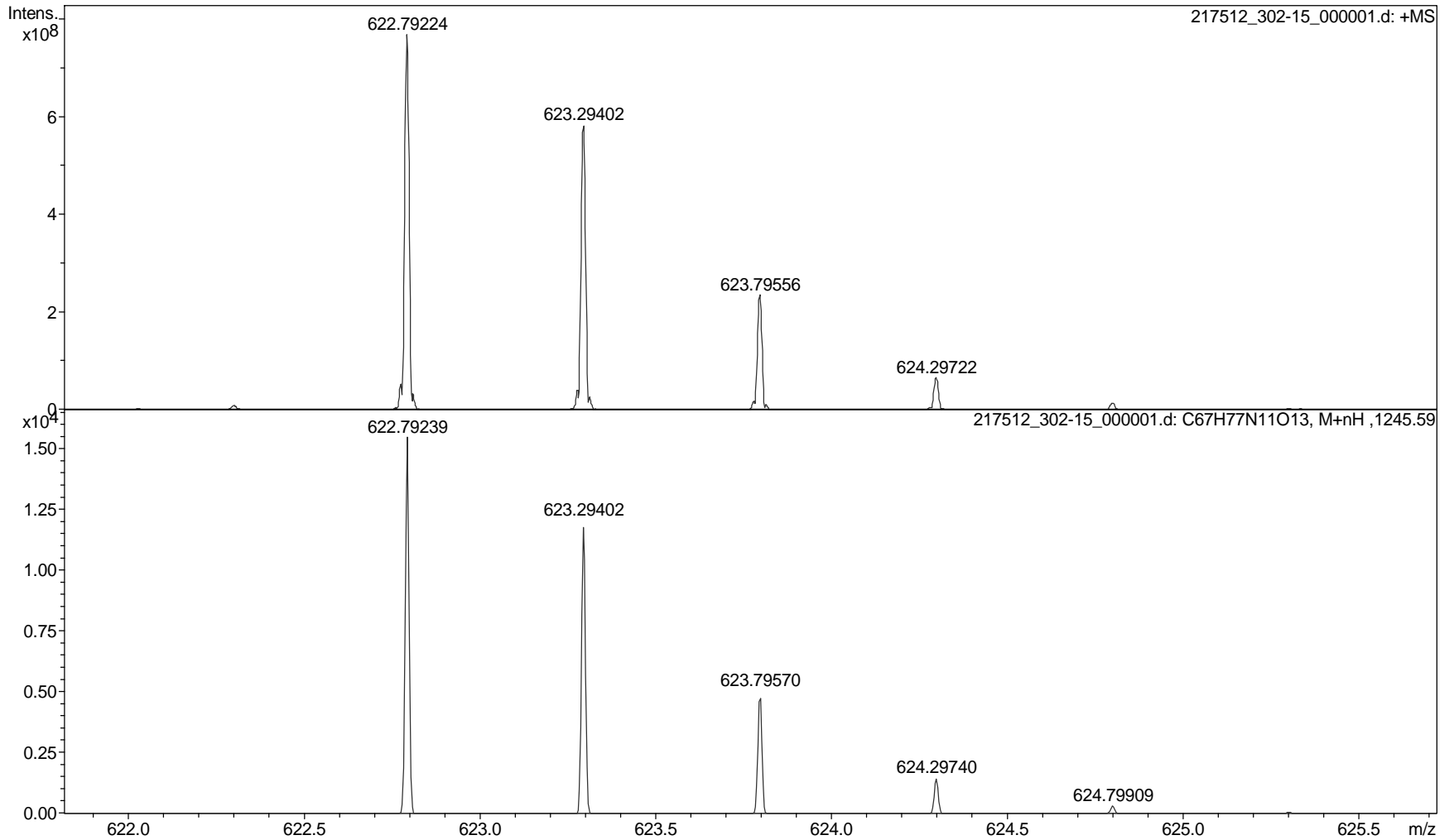
# Generic Display Report

## Analysis Info

Analysis Name D:\Data\July\_17\217512\_302-15\_000001.d  
Method April\_good\_method  
Sample Name 217512\_302-15  
Comment 217512, 302-15, dissolved in 200uL H2O/ACN

Acquisition Date 7/11/2017 1:44:21 PM

Operator  
Instrument apex-Qe



# Analytical/Biological Mass Spectrometry Core Facility Results

Request #: 217512

Sample Name: 302-18

Submitted by: Keith Olson

Operator: KK

Date Received: 7/7/2017

Date Completed: 7/11/2017

Solvent Used: ACN

Matrix Used:

Analysis notes: The sample was dissolved in 200uL ACN/H2O and diluted 10x in ACN/H2O. Positive ion analysis gave M+H ions at m/z 1286.62467 and M+2H ions at m/z 643.81629 for C70H83N11O13.

## Instrument

- Bruker FT-ICR
- Bruker Amazon Ion Trap
- Bruker MALDI-TOF
- Bruker MALDI-TOF/TOF
- Thermo LCQ Ion Trap
- Shimadzu GC-MS

## Ionization Method

- Positive
- Negative
- ESI     APCI     APPI
- MALDI
- EI

## Sample Introduction

- Infusion/Flow Injection
- HPLC (ESI) or GC (EI)
- Direct Probe

## Resolution

- Accurate Mass
- Survey Mass

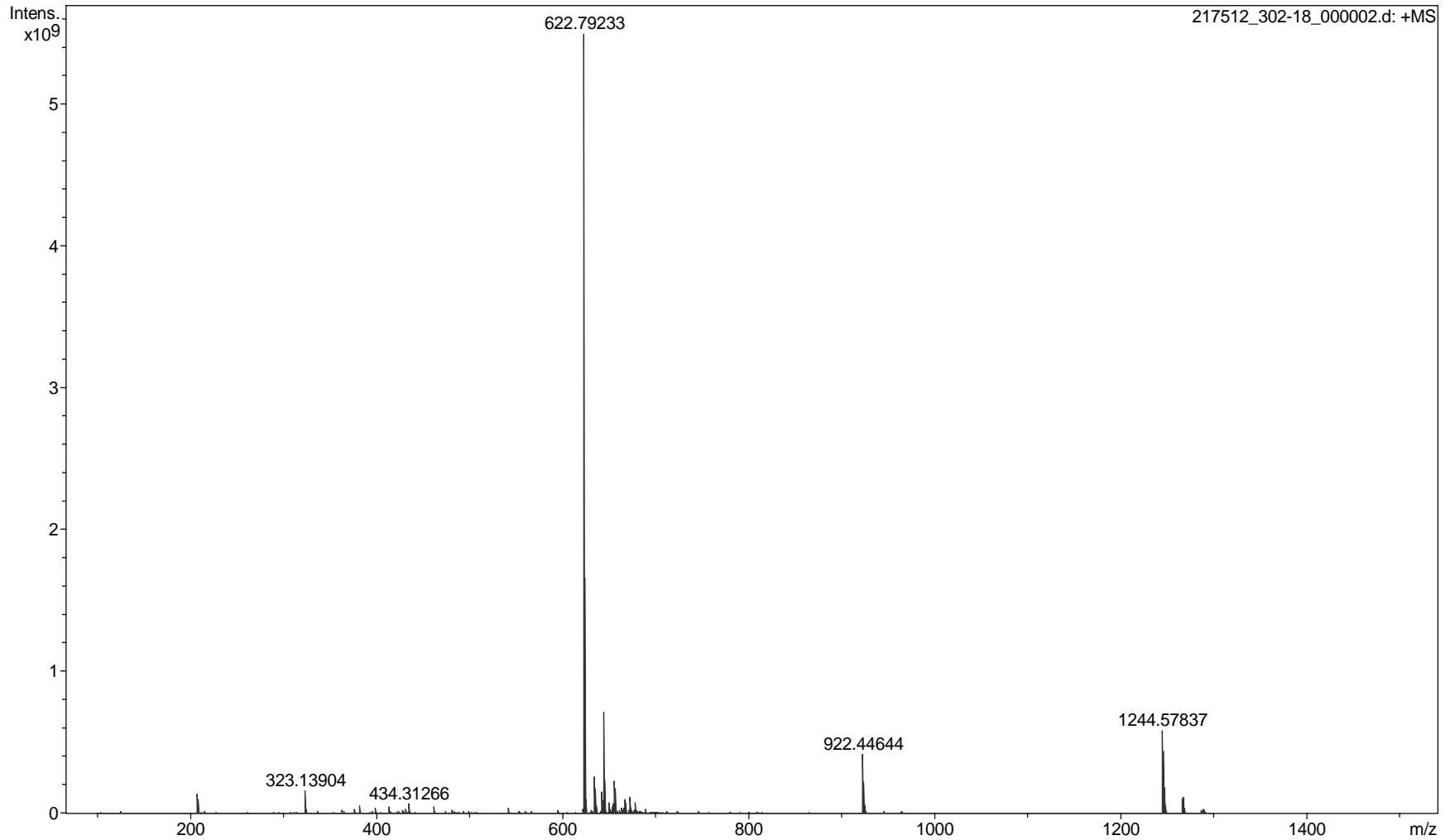
# Generic Display Report

## Analysis Info

Analysis Name D:\Data\July\_17\217512\_302-18\_000002.d  
Method April\_good\_method  
Sample Name 217512\_302-18  
Comment 217512, 302-18, dissolved in 200uL H2O/ACN, then diluted 10x in H2O/ACN

Acquisition Date 7/11/2017 2:21:52 PM

Operator  
Instrument apex-Qe



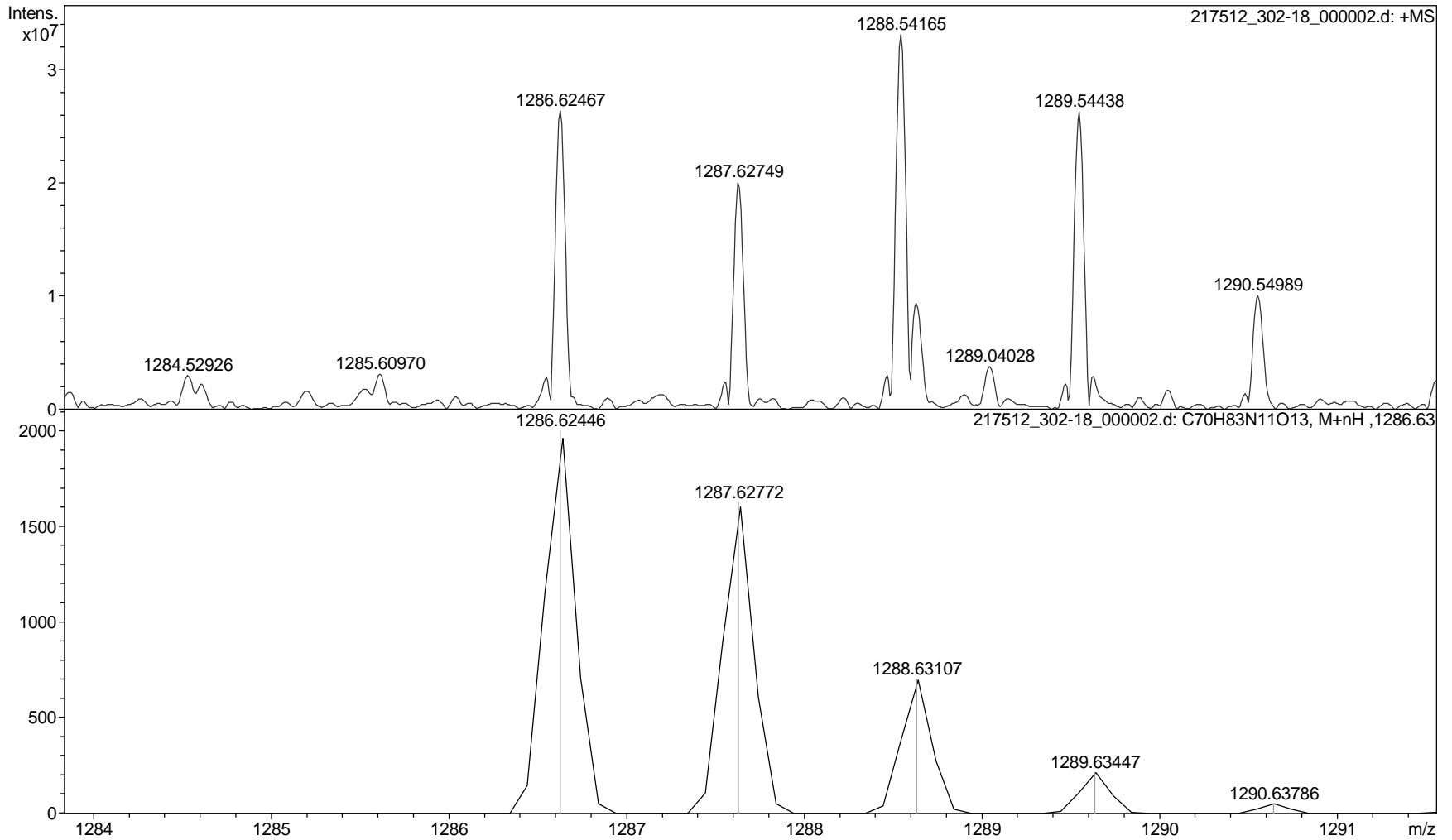
# Generic Display Report

## Analysis Info

Analysis Name D:\Data\July\_17\217512\_302-18\_000002.d  
Method April\_good\_method  
Sample Name 217512\_302-18  
Comment 217512, 302-18, dissolved in 200uL H2O/ACN, then diluted 10x in H2O/ACN

Acquisition Date 7/11/2017 2:21:52 PM

Operator  
Instrument apex-Qe



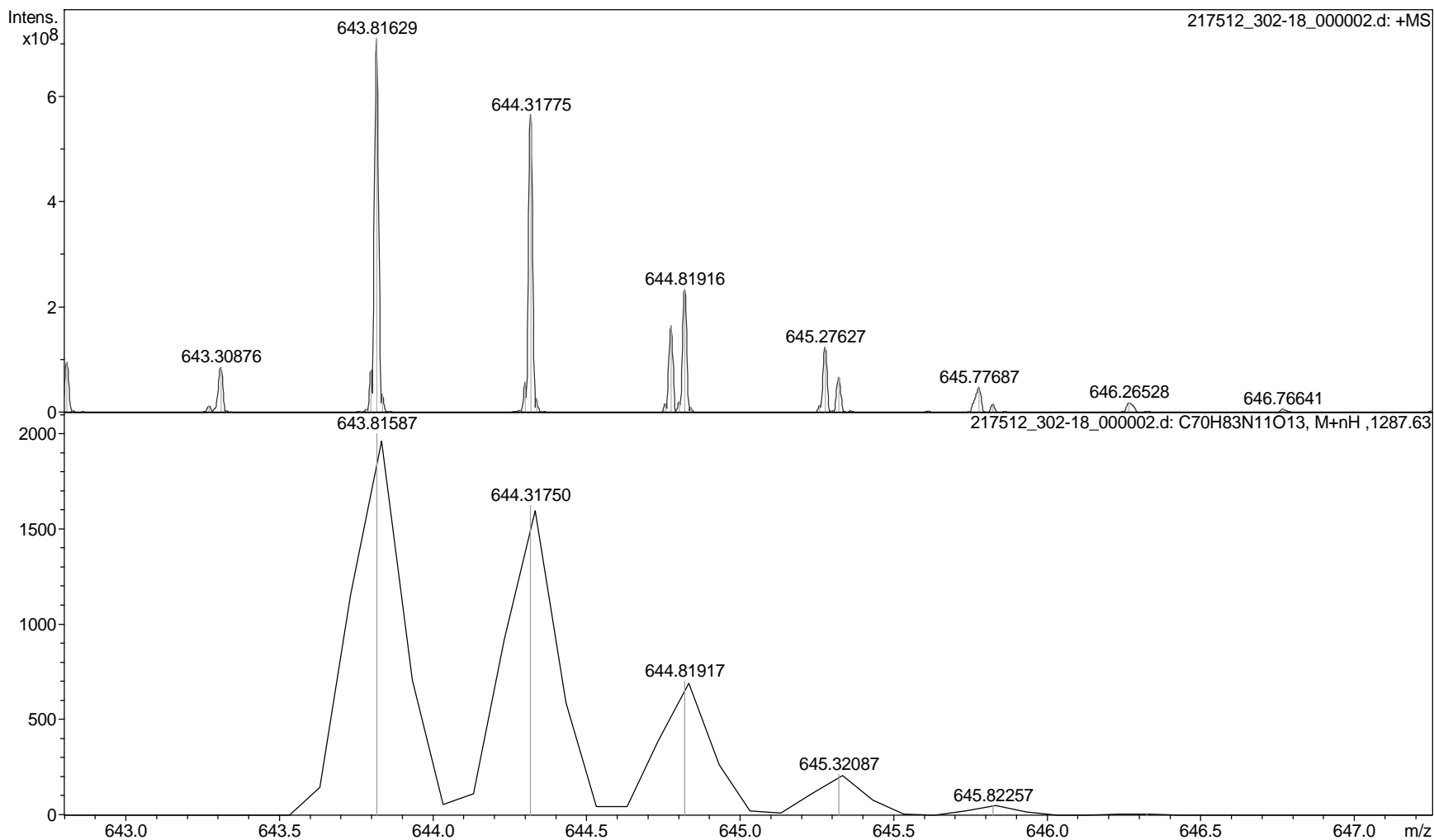
# Generic Display Report

## Analysis Info

Analysis Name D:\Data\July\_17\217512\_302-18\_000002.d  
Method April\_good\_method  
Sample Name 217512\_302-18  
Comment 217512, 302-18, dissolved in 200uL H2O/ACN, then diluted 10x in H2O/ACN

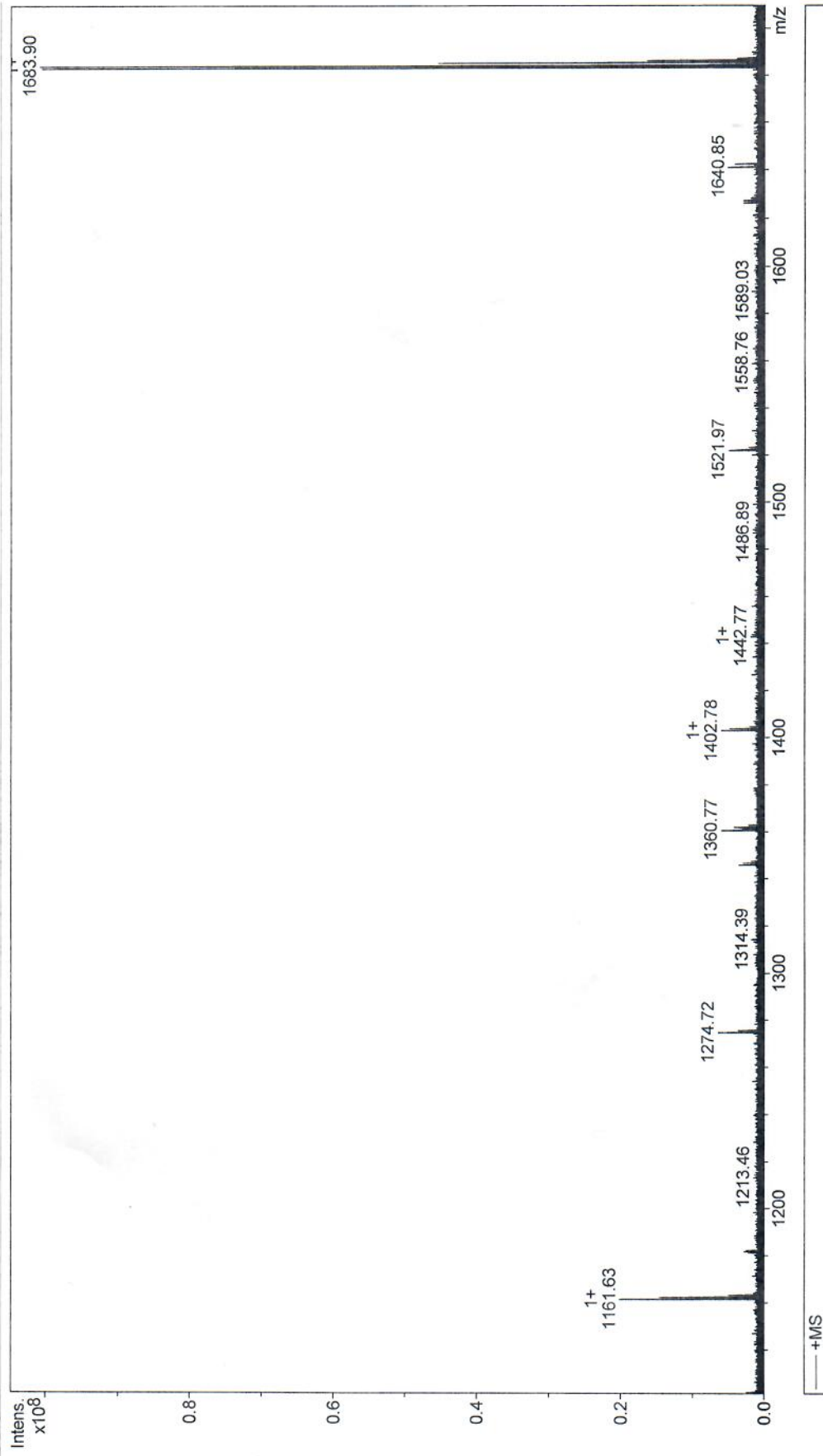
Acquisition Date 7/11/2017 2:21:52 PM

Operator  
Instrument apex-Qe



# Generic Display Report

**Analysis Info**  
Analysis Name: D:\Data\Dec\_16\15\_0830\_KO30242P2\_000002.d  
Method: April\_good\_method  
Sample Name: KO30242P2\_ESIposs  
Comment:  
Acquisition Date: 12/16/2015 2:06:13 PM  
Operator:  
Instrument: apex-Qe



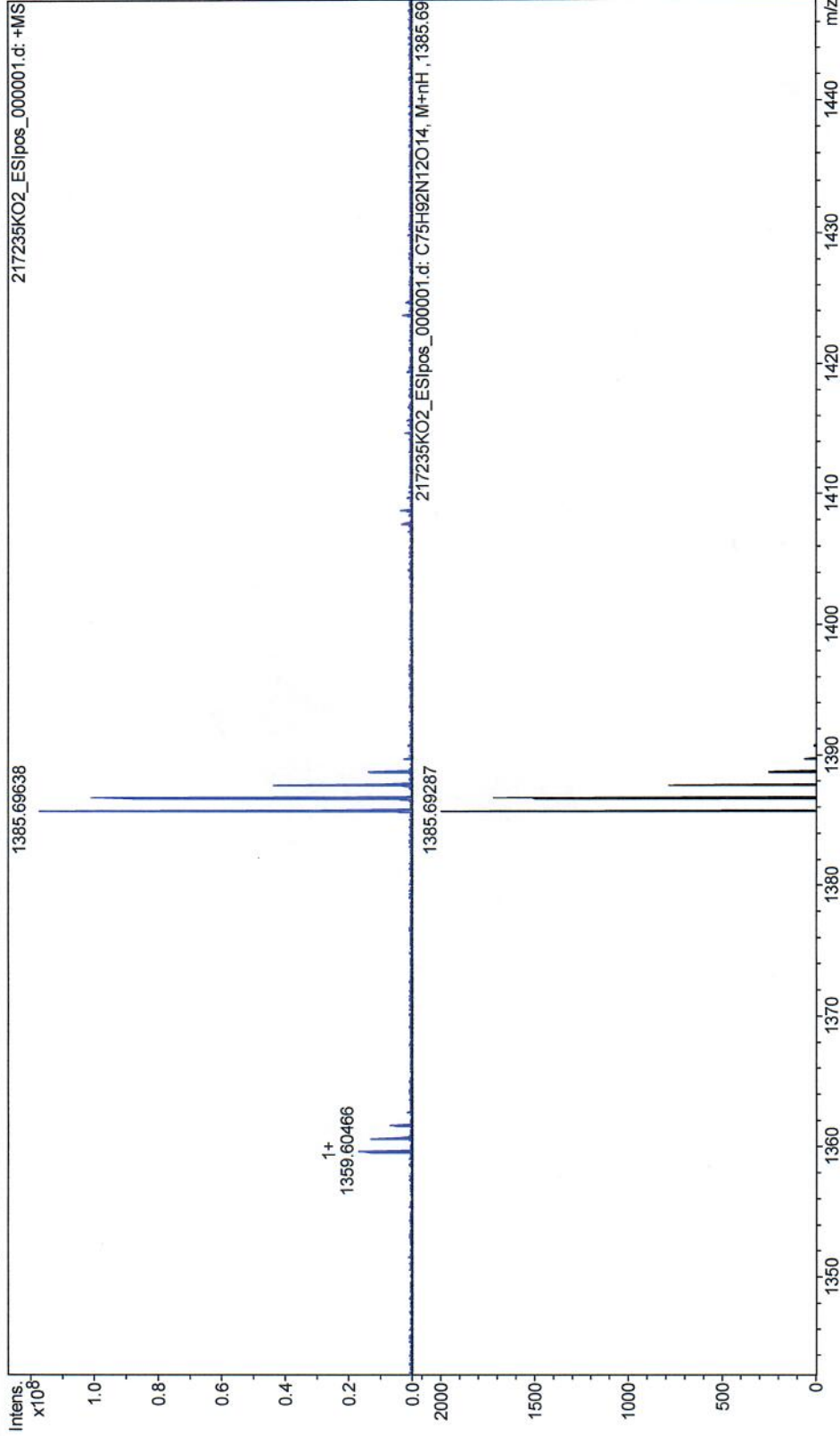
# Generic Display Report

## Analysis Info

Analysis Name D:\Data\Apr\_17\217235KO2\_ESIpos\_000001.d  
Method April\_good\_method  
Sample Name 217235KO2\_ESIpos  
Comment 217235KO2\_3022P2, dil 10x in MeOH/ACN

Acquisition Date 4/6/2017 9:31:14 AM

Operator apex-Qe  
Instrument



# Analytical/Biological Mass Spectrometry Core Facility Results

Request #: 217512

Sample Name: 302-30

Submitted by: Keith Olson

Operator: KK

Date Received: 7/7/2017

Date Completed: 7/11/2017

Solvent Used: ACN

Matrix Used:

Analysis notes: The sample was dissolved in 200uL ACN/H<sub>2</sub>O and diluted 10x in ACN/H<sub>2</sub>O. Positive ion analysis gave M+H ions at m/z 1484.76328 and M+2H ions at m/z 742.88420 for C<sub>80</sub>H<sub>101</sub>N<sub>13</sub>O<sub>15</sub>.

## Instrument

- Bruker FT-ICR
- Bruker Amazon Ion Trap
- Bruker MALDI-TOF
- Bruker MALDI-TOF/TOF
- Thermo LCQ Ion Trap
- Shimadzu GC-MS

## Ionization Method

- Positive
- Negative
- ESI     APCI     APPI
- MALDI
- EI

## Sample Introduction

- Infusion/Flow Injection
- HPLC (ESI) or GC (EI)
- Direct Probe

## Resolution

- Accurate Mass
- Survey Mass

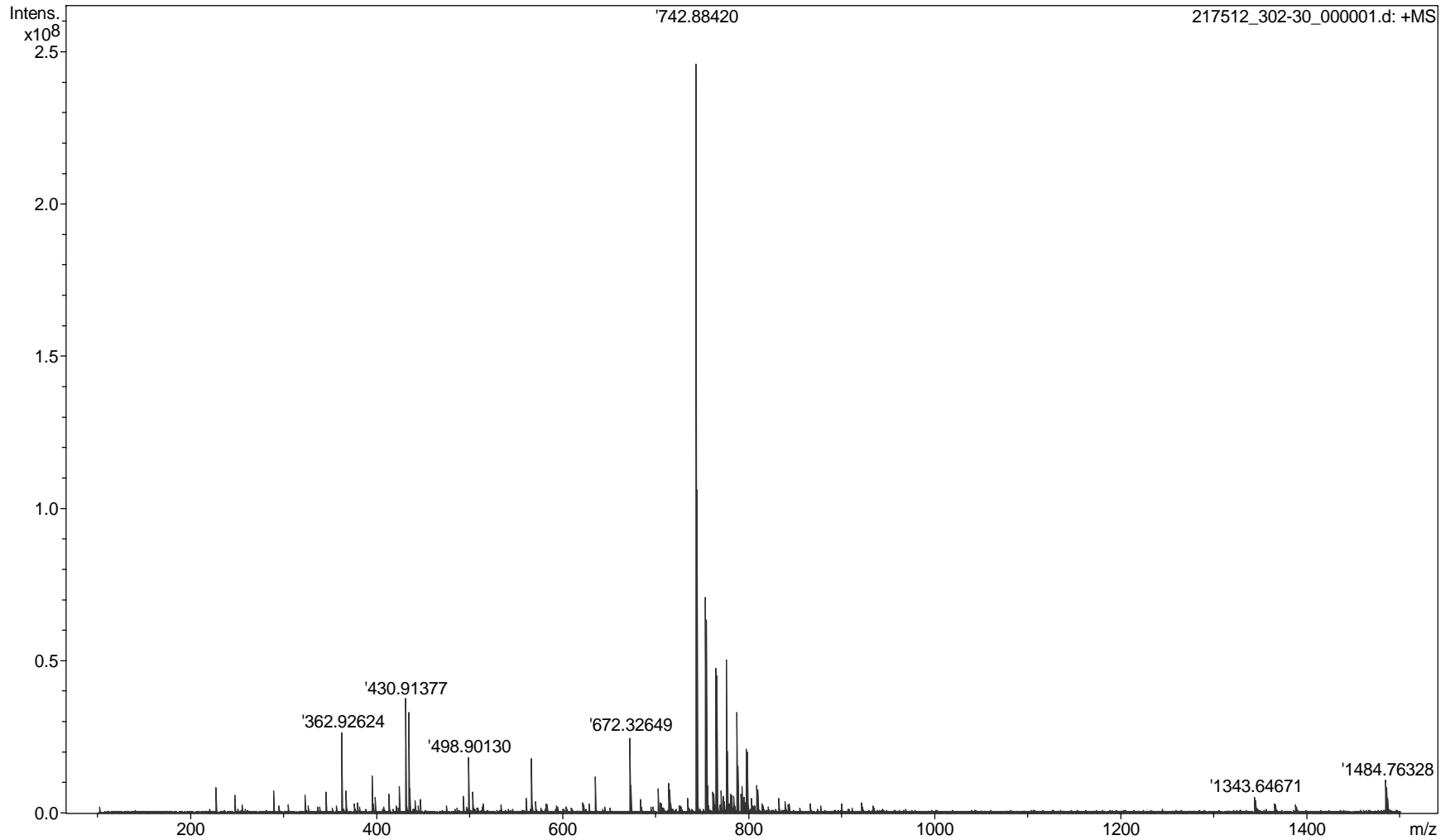
# Generic Display Report

## Analysis Info

Analysis Name D:\Data\July\_17\217512\_302-30\_000001.d  
Method April\_good\_method  
Sample Name 217512\_302-30  
Comment 217512, 302-30, dissolved in 200uL H2O/ACN, then diluted 10x in H2O/ACN

Acquisition Date 7/11/2017 3:42:08 PM

Operator  
Instrument apex-Qe



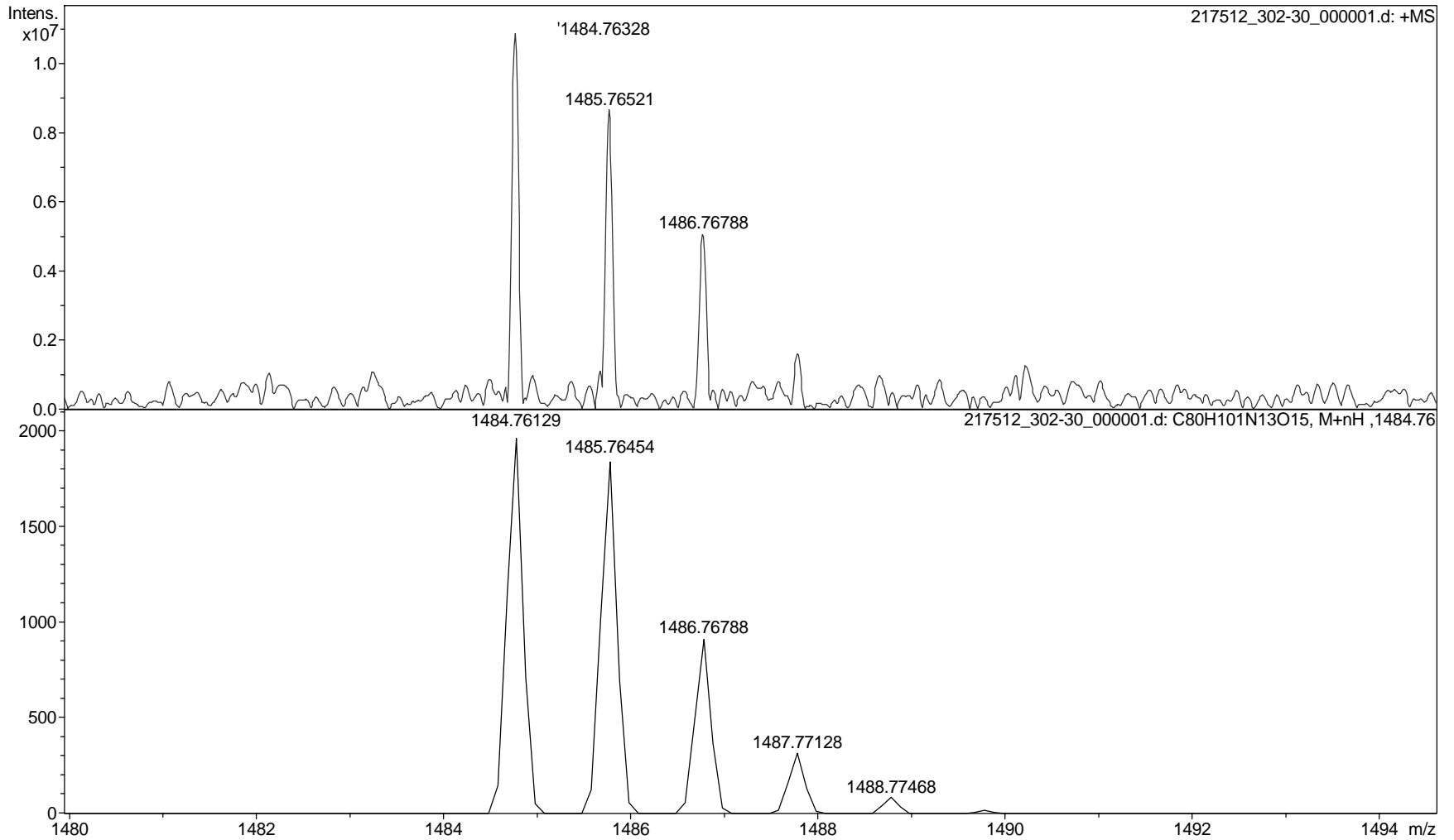
# Generic Display Report

## Analysis Info

Analysis Name D:\Data\July\_17\217512\_302-30\_000001.d  
Method April\_good\_method  
Sample Name 217512\_302-30  
Comment 217512, 302-30, dissolved in 200uL H2O/ACN, then diluted 10x in H2O/ACN

Acquisition Date 7/11/2017 3:42:08 PM

Operator  
Instrument apex-Qe



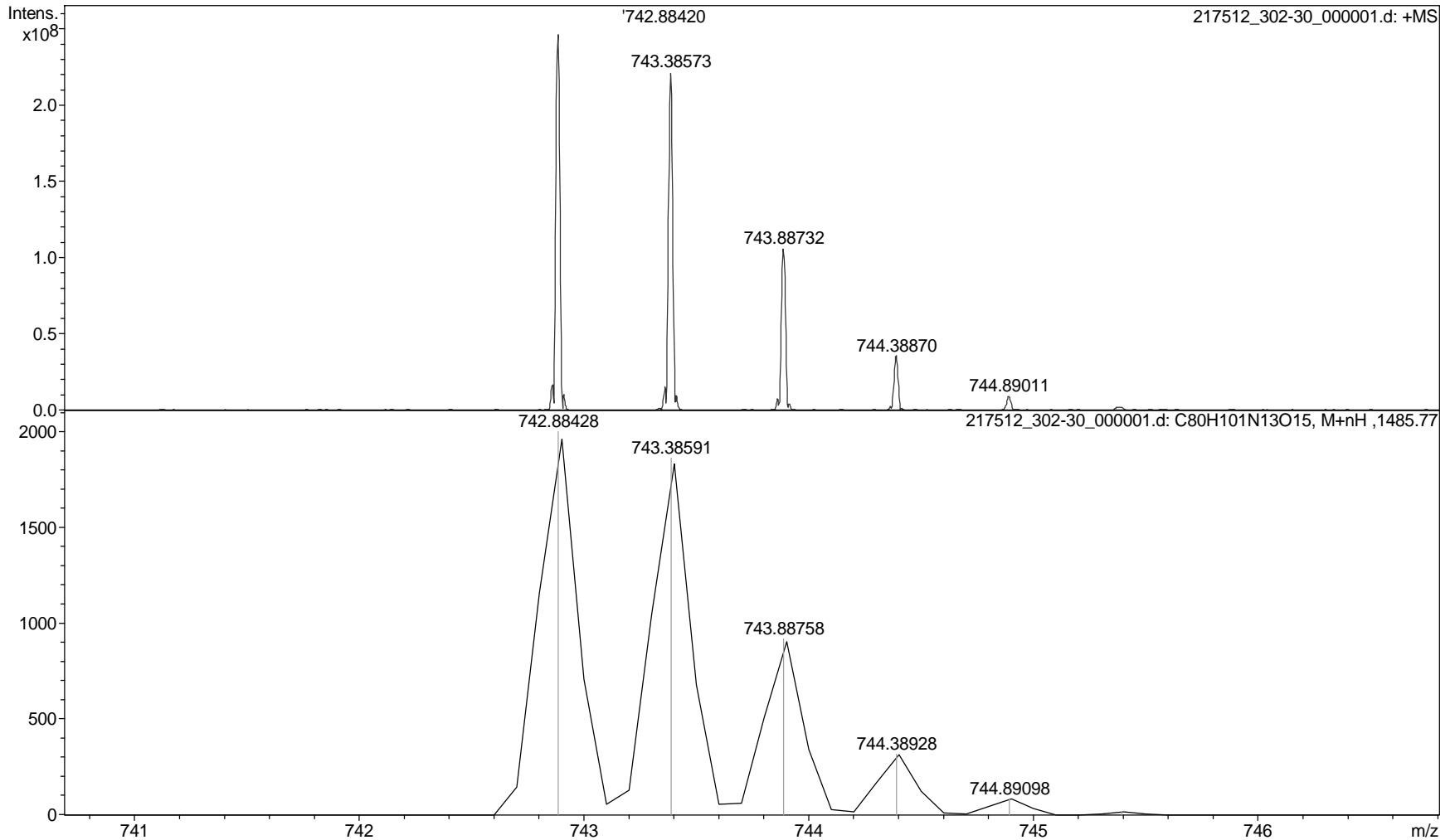
# Generic Display Report

## Analysis Info

Analysis Name D:\Data\July\_17\217512\_302-30\_000001.d  
Method April\_good\_method  
Sample Name 217512\_302-30  
Comment 217512, 302-30, dissolved in 200uL H2O/ACN, then diluted 10x in H2O/ACN

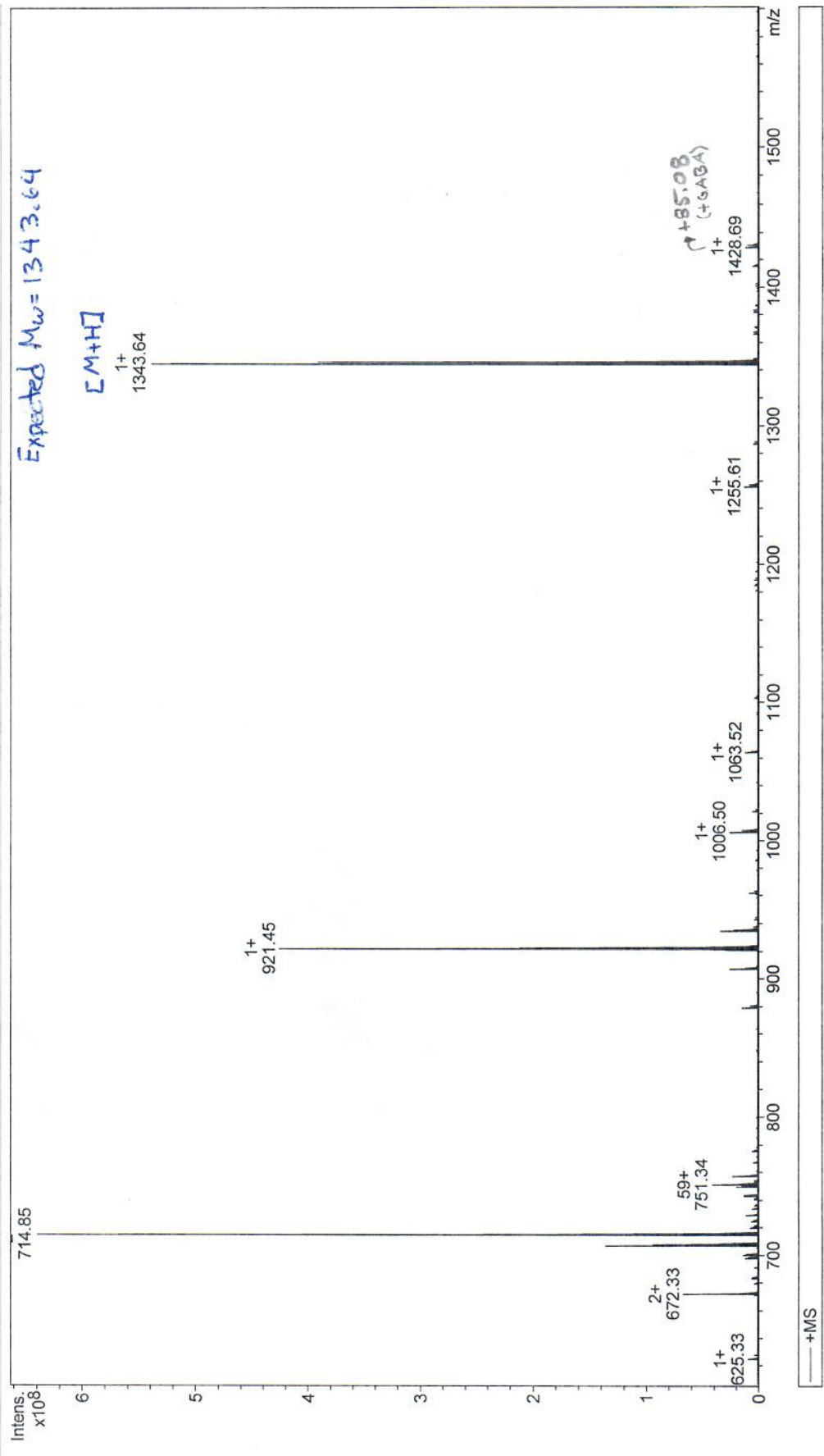
Acquisition Date 7/11/2017 3:42:08 PM

Operator  
Instrument apex-Qe



# Generic Display Report

**Analysis Info**  
Analysis Name: D:\Data\Dec\_16\15\_0830\_KO30221P2\_000004.d  
Method: April\_good\_method  
Sample Name: KO30221P2\_ESIposs NB3721  
Comment: Pg 50  
Acquisition Date: 12/16/2015 1:38:58 PM  
Operator: apex-Qe  
Instrument: apex-Qe



## ==== BIO5 Analytical Lab Report ====

C:\LabSolutions\Data\Project1\Purification\QCs\Dec17-2015\KO302-15\_pQC.lcd

Sample Name : KO302-15\_pQC

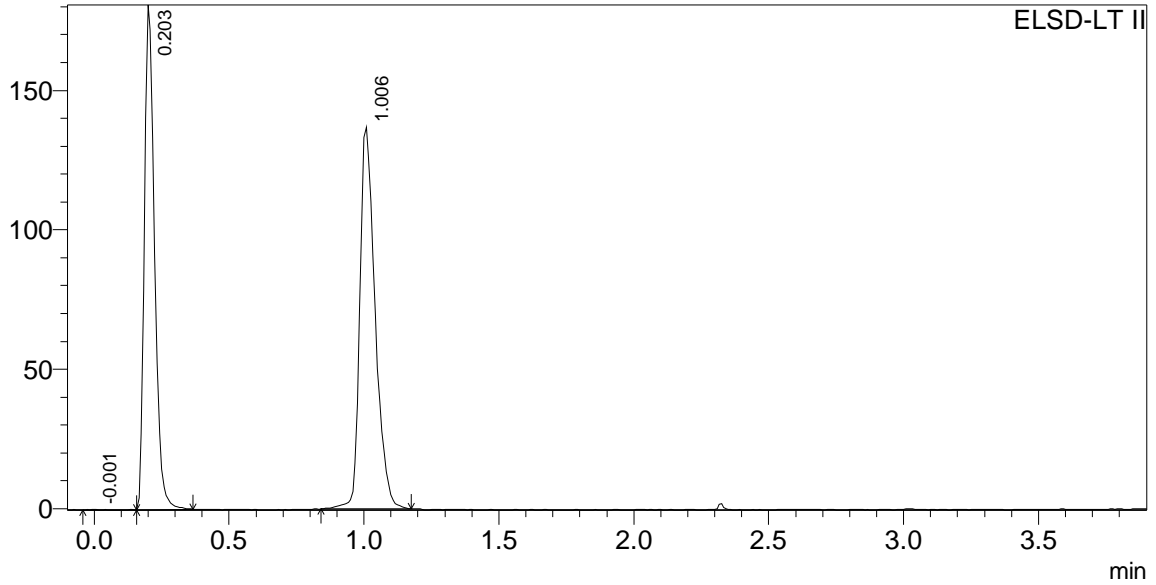
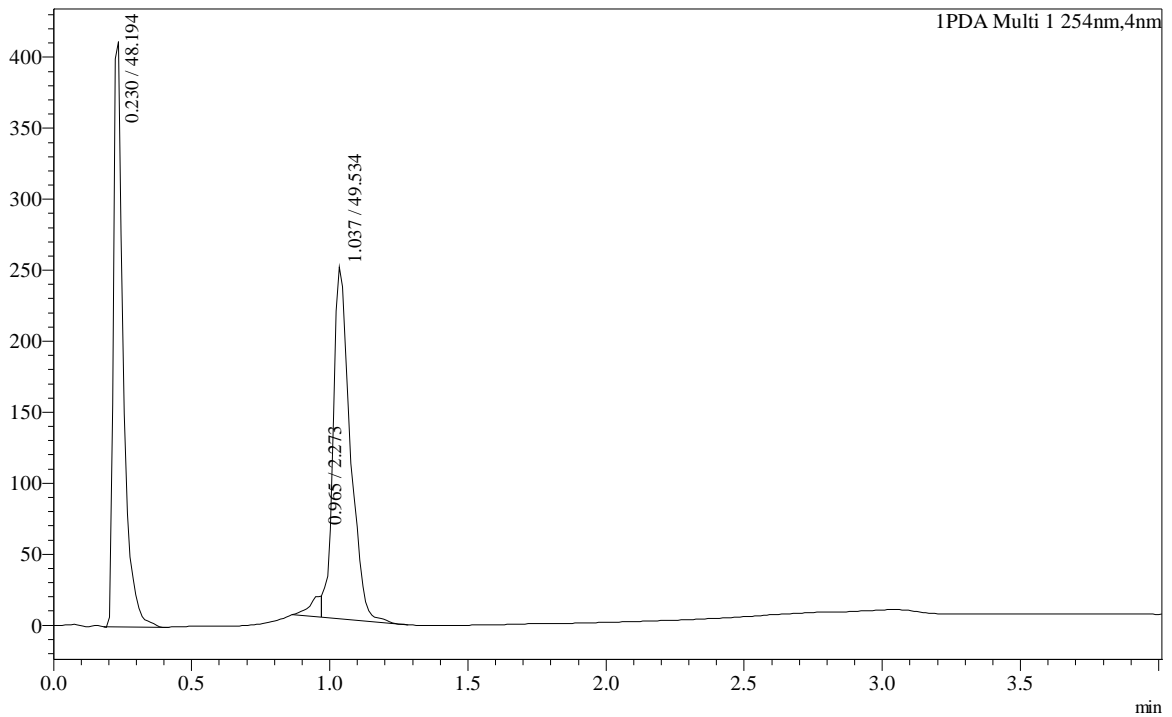
Vial# : 89

Injection Volume : 10

Data File : C:\LabSolutions\Data\Project1\Purification\QCs\Dec17-2015\KO302-15\_pQC.lcd

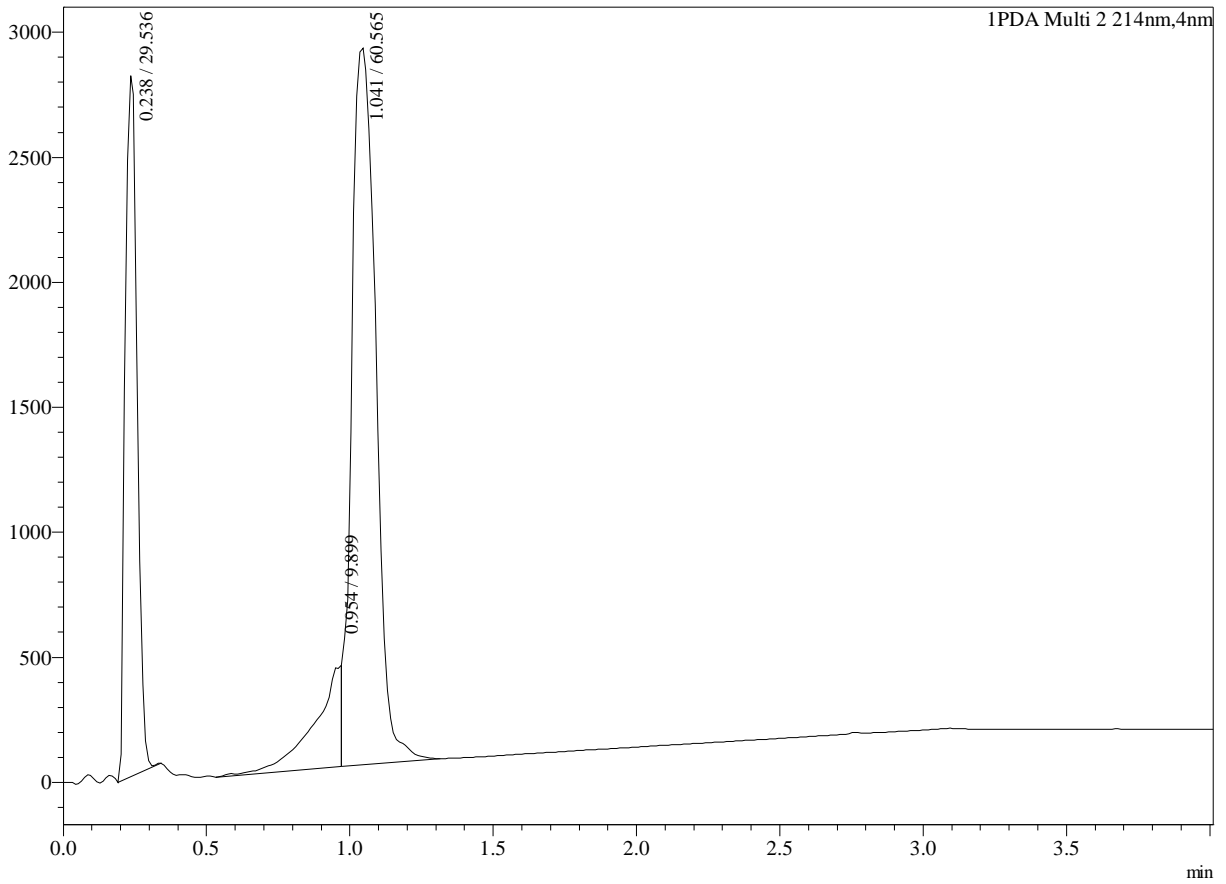
Month-Day Acquired : 12/17/2015

Original Method File : StandardRunVials.lcm

C:\LabSolutions\Data\Project1\Purification\QCs\Dec17-2015\KO302-15\_pQC.lcd  
mVmAU  
Chromatogram

mAU

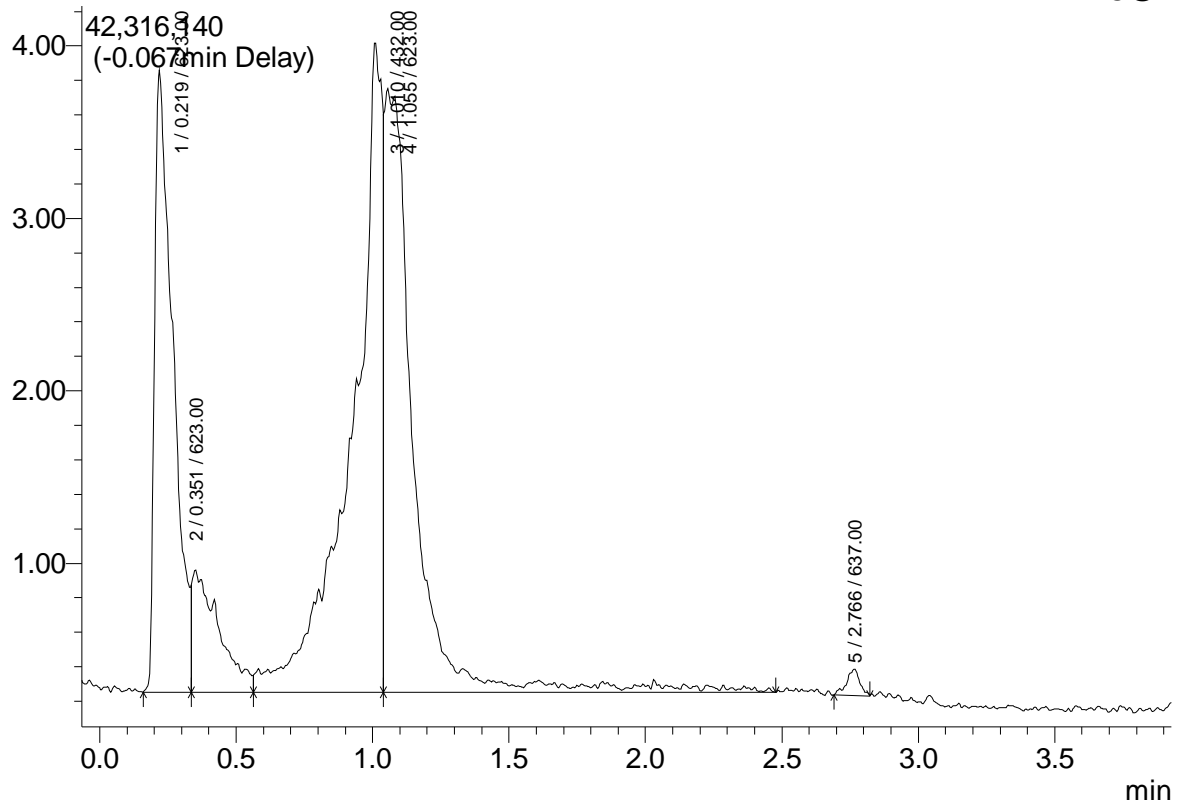
Chromatogram



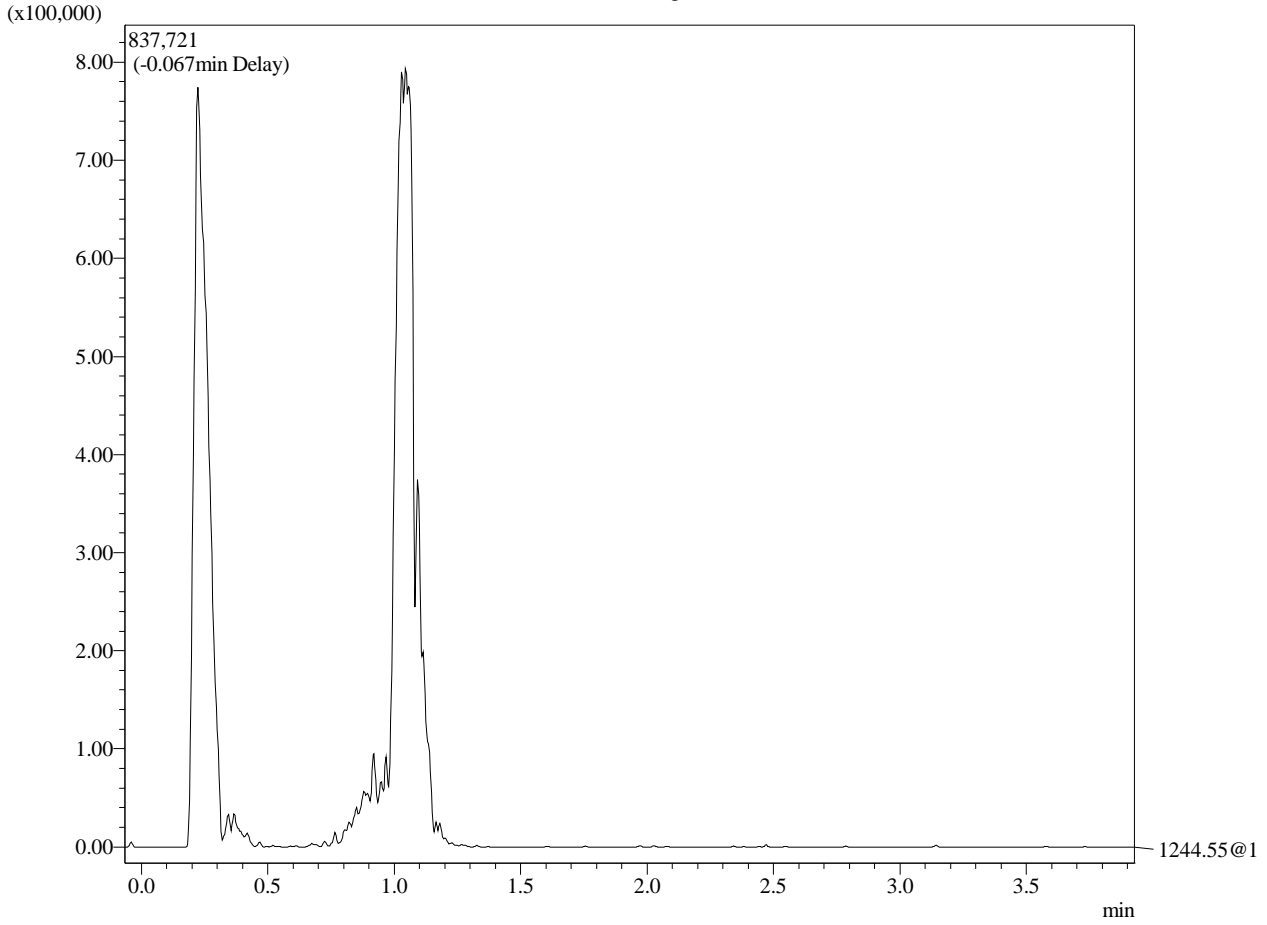
(x10,000,000)

MS Chromatogram

TIC@1

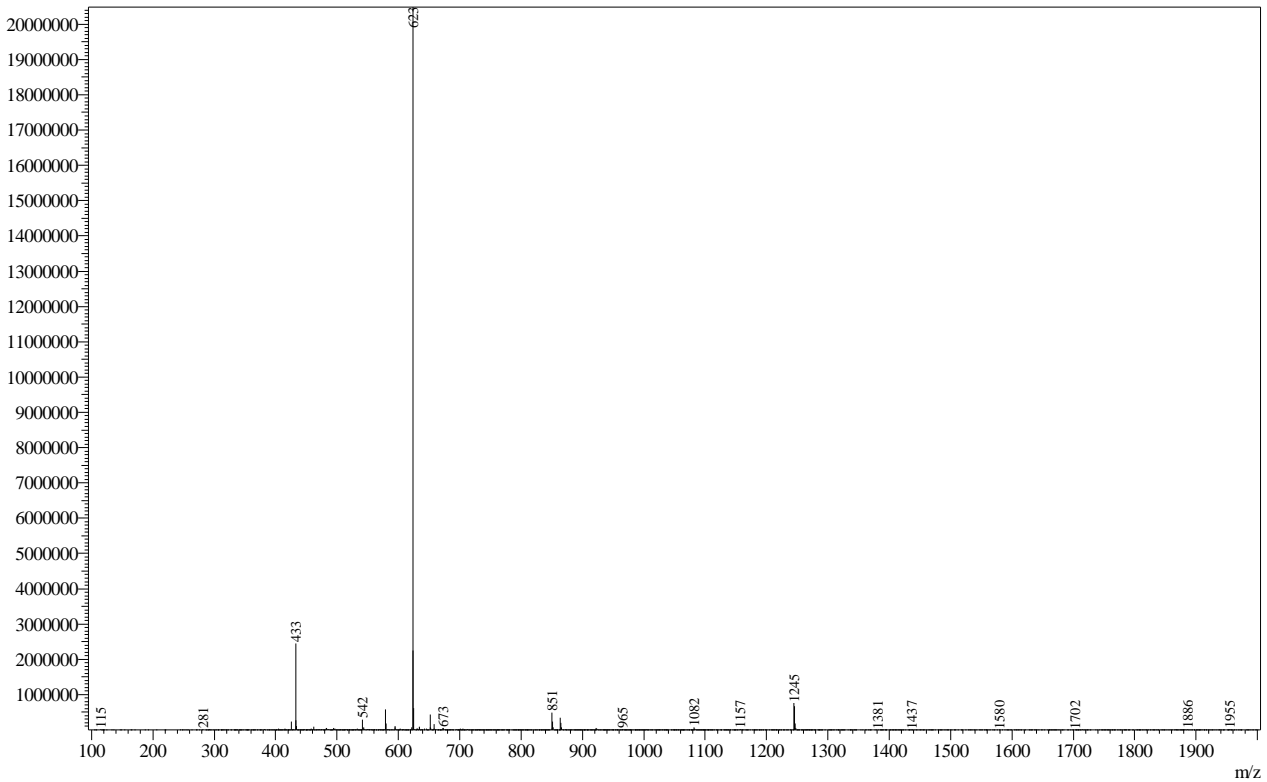


MS Chromatogram

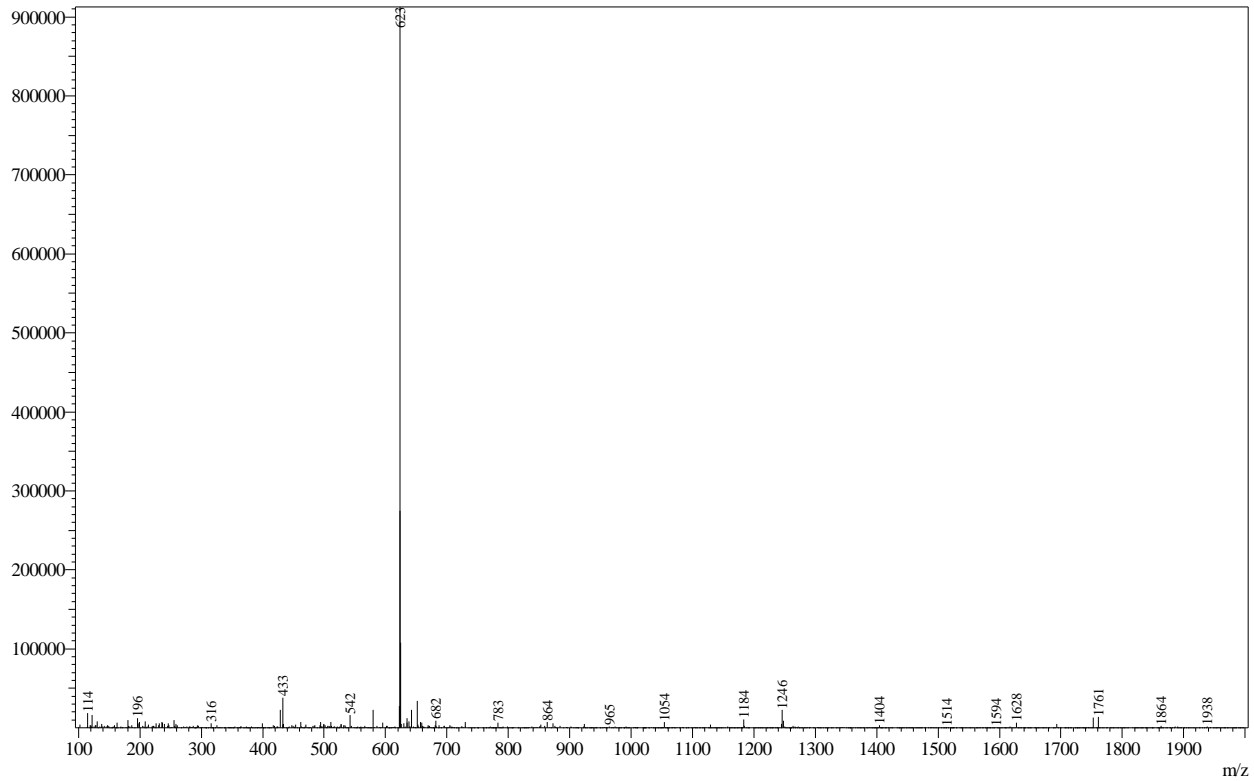


Mass Spectrum

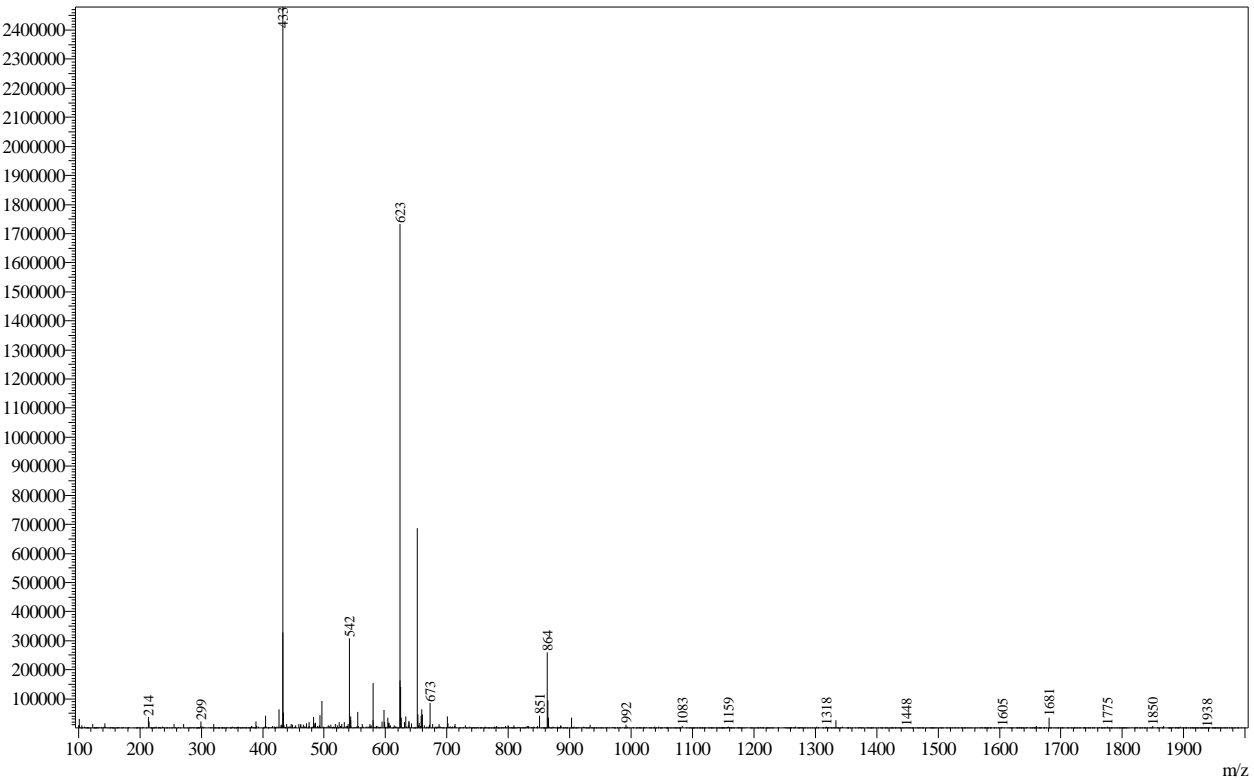
Peak#: 1 R.Time: 0.219(Scan#: 79)  
 MassPeaks: 1221  
 Spectrum Mode: Averaged 0.216-0.223(78-80)  
 BG Mode: Calc Segment 1 - Event 1



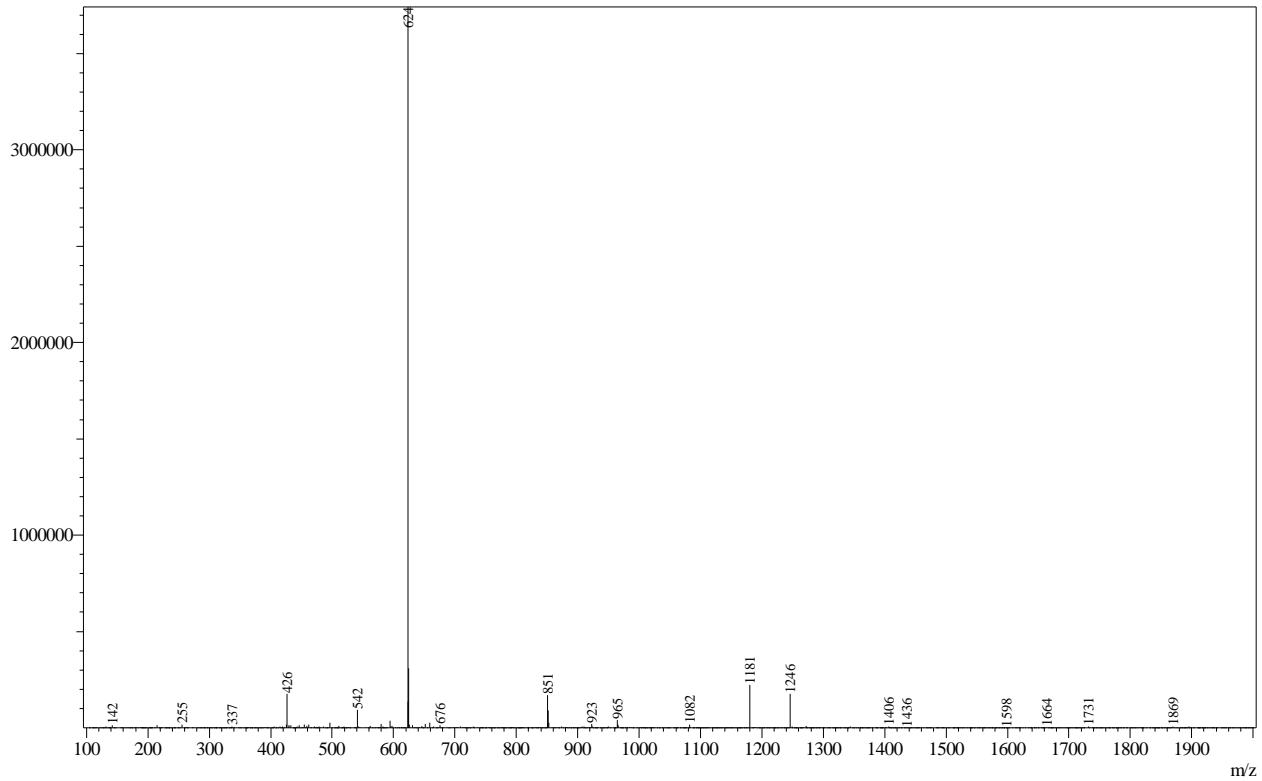
Peak#:2 R.Time:0.351(Scan#:115)  
MassPeaks:989  
Spectrum Mode:Averaged 0.348-0.355(114-116)  
BG Mode:Calc Segment 1 - Event 1



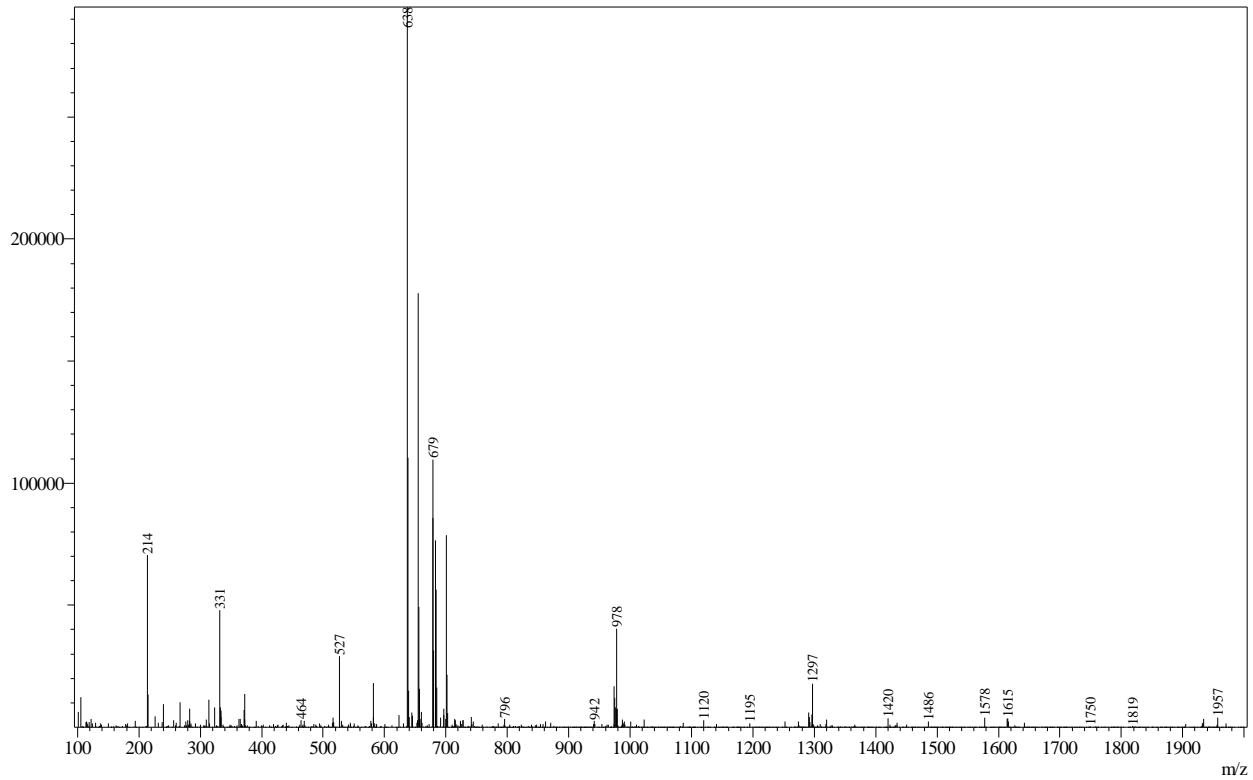
Peak#:3 R.Time:1.010(Scan#:295)  
MassPeaks:1117  
Spectrum Mode:Averaged 1.008-1.015(294-296)  
BG Mode:Calc Segment 1 - Event 1



Peak#:4 R.Time:1.055(Scan#:307)  
MassPeaks:986  
Spectrum Mode:Averaged 1.052-1.059(306-308)  
BG Mode:Calc Segment 1 - Event 1



Peak#:5 R.Time:2.766(Scan#:774)  
MassPeaks:982  
Spectrum Mode:Averaged 2.764-2.771(773-775)  
BG Mode:Calc Segment 1 - Event 1



## ==== BIO5 Analytical Lab Report ====

C:\LabSolutions\Data\Project1\Purification\QCs\Feb25-2016\KO302-18p2-4.lcd

Sample Name : KO302-18p2-4

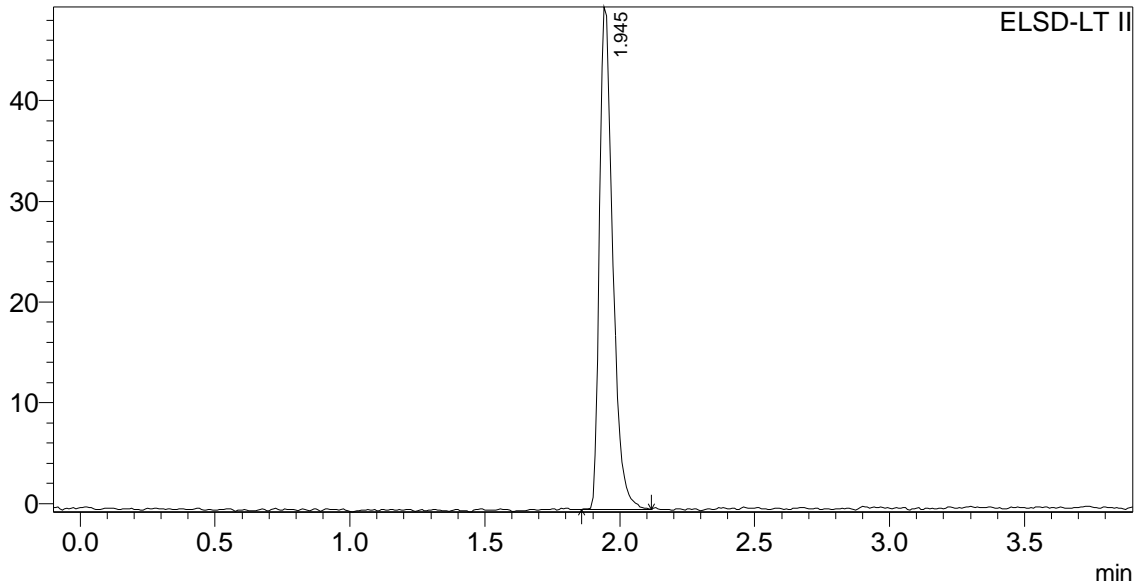
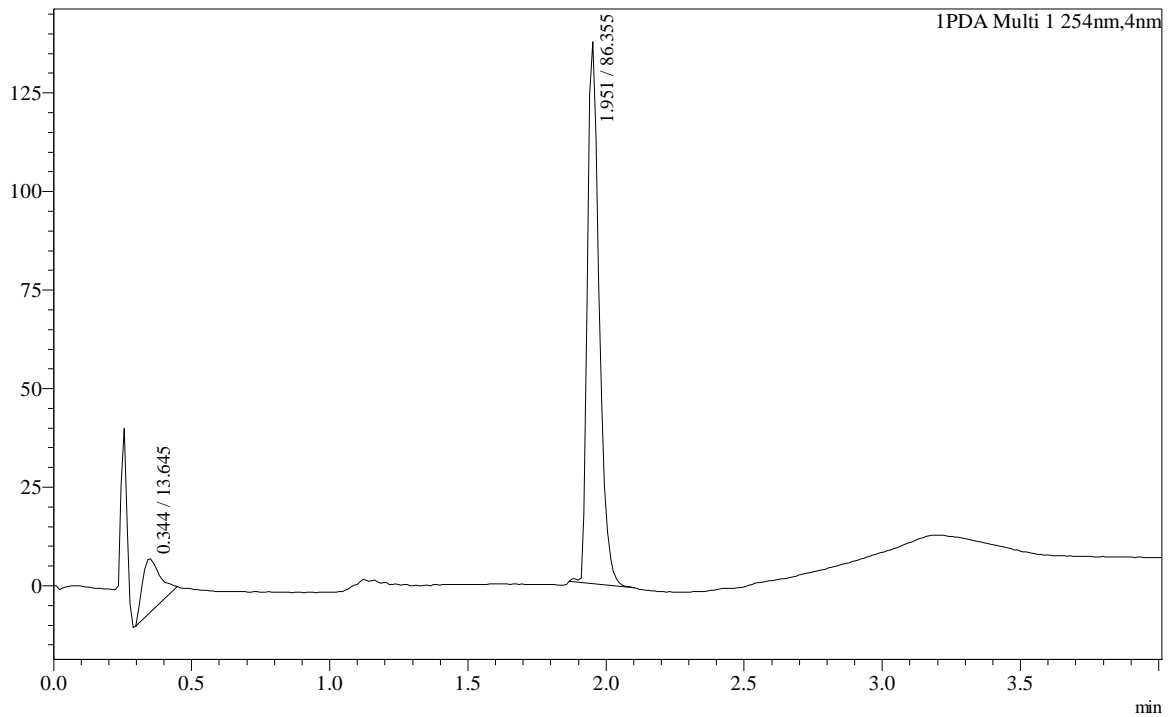
Vial# : 18

Injection Volume : 10

Data File : C:\LabSolutions\Data\Project1\Purification\QCs\Feb25-2016\KO302-18p2-4.lcd

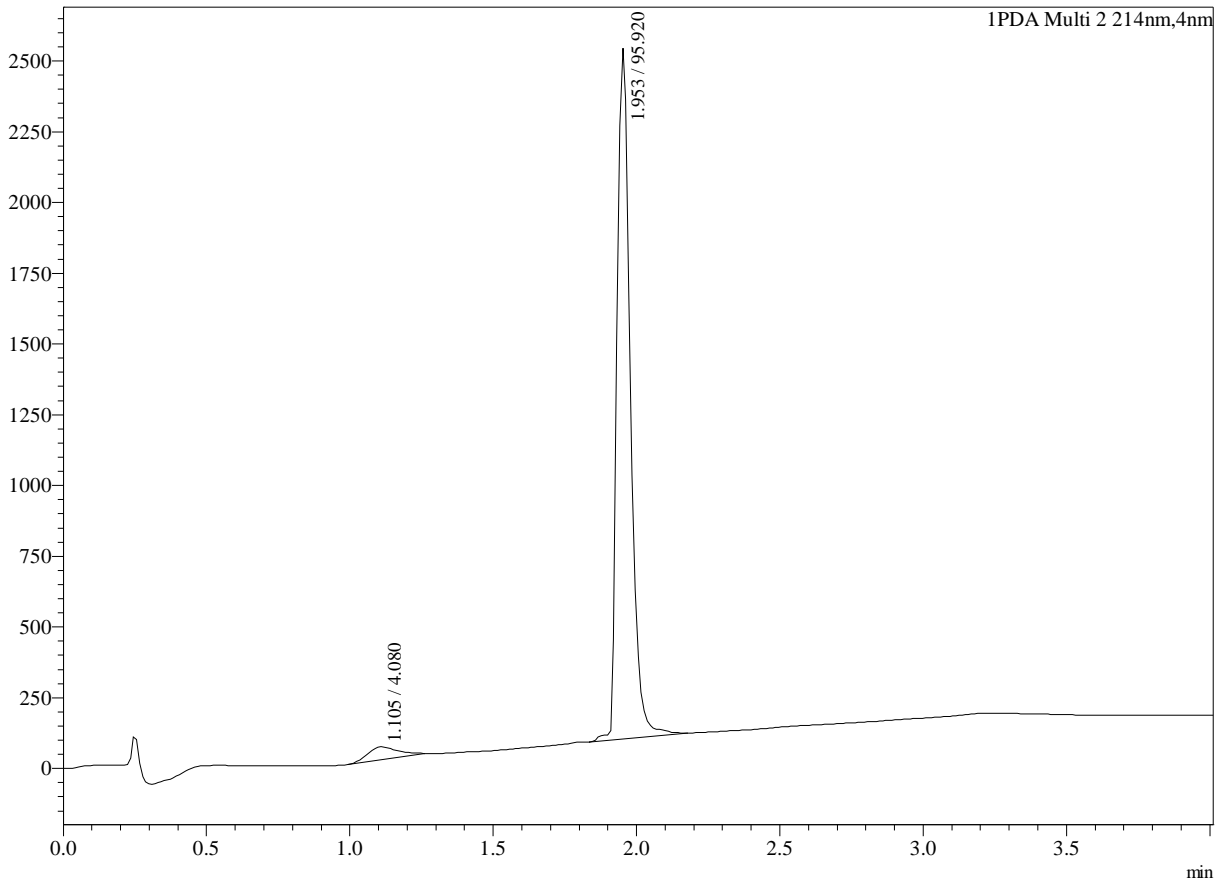
Month-Day Acquired : 2/25/2016

Original Method File : StandardRunPlates.lcm

C:\LabSolutions\Data\Project1\Purification\QCs\Feb25-2016\KO302-18p2-4.lcd  
mVmAU  
Chromatogram

mAU

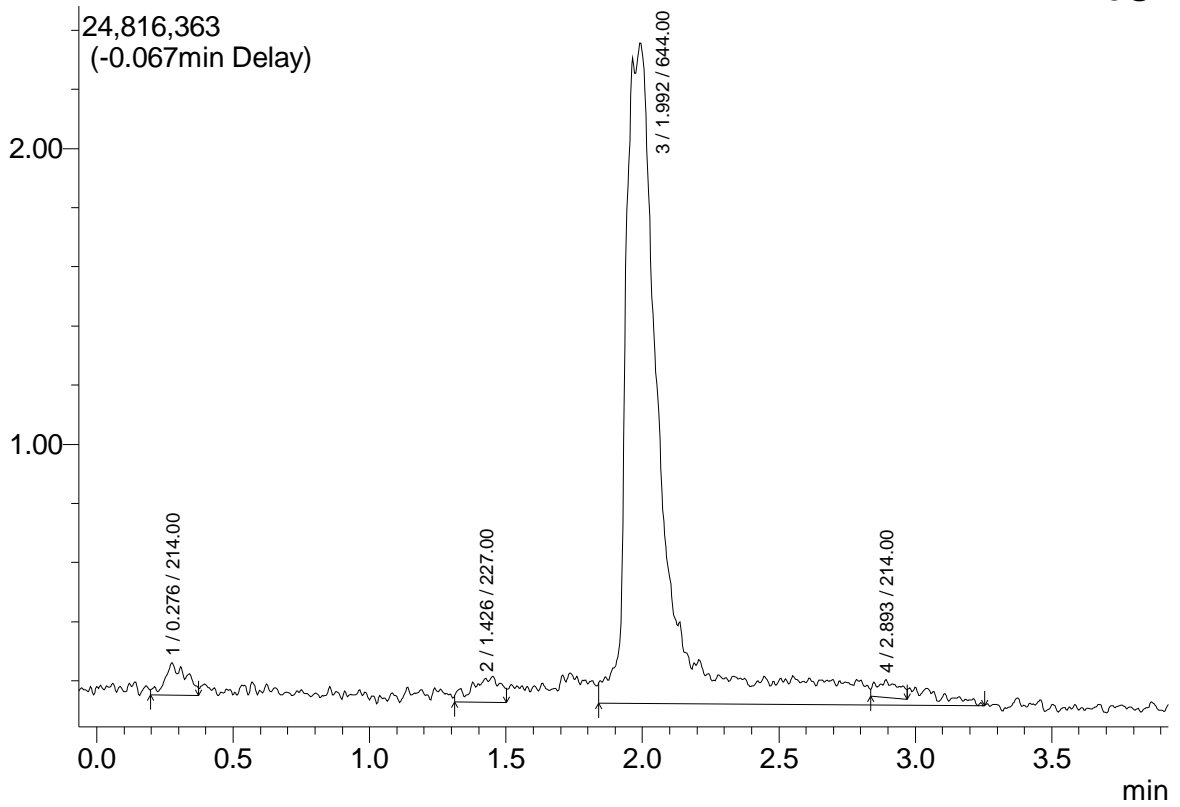
Chromatogram

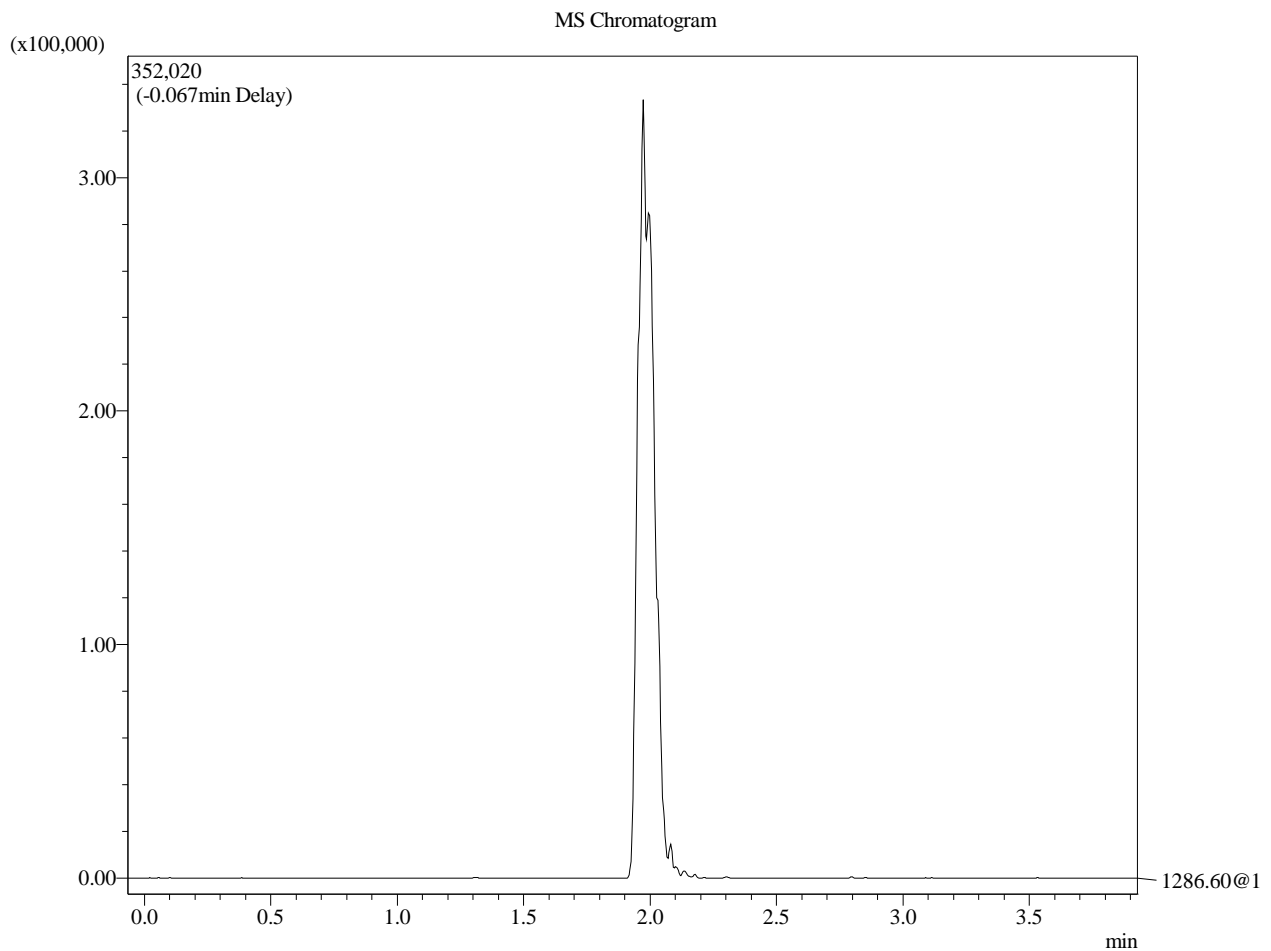


(x10,000,000)

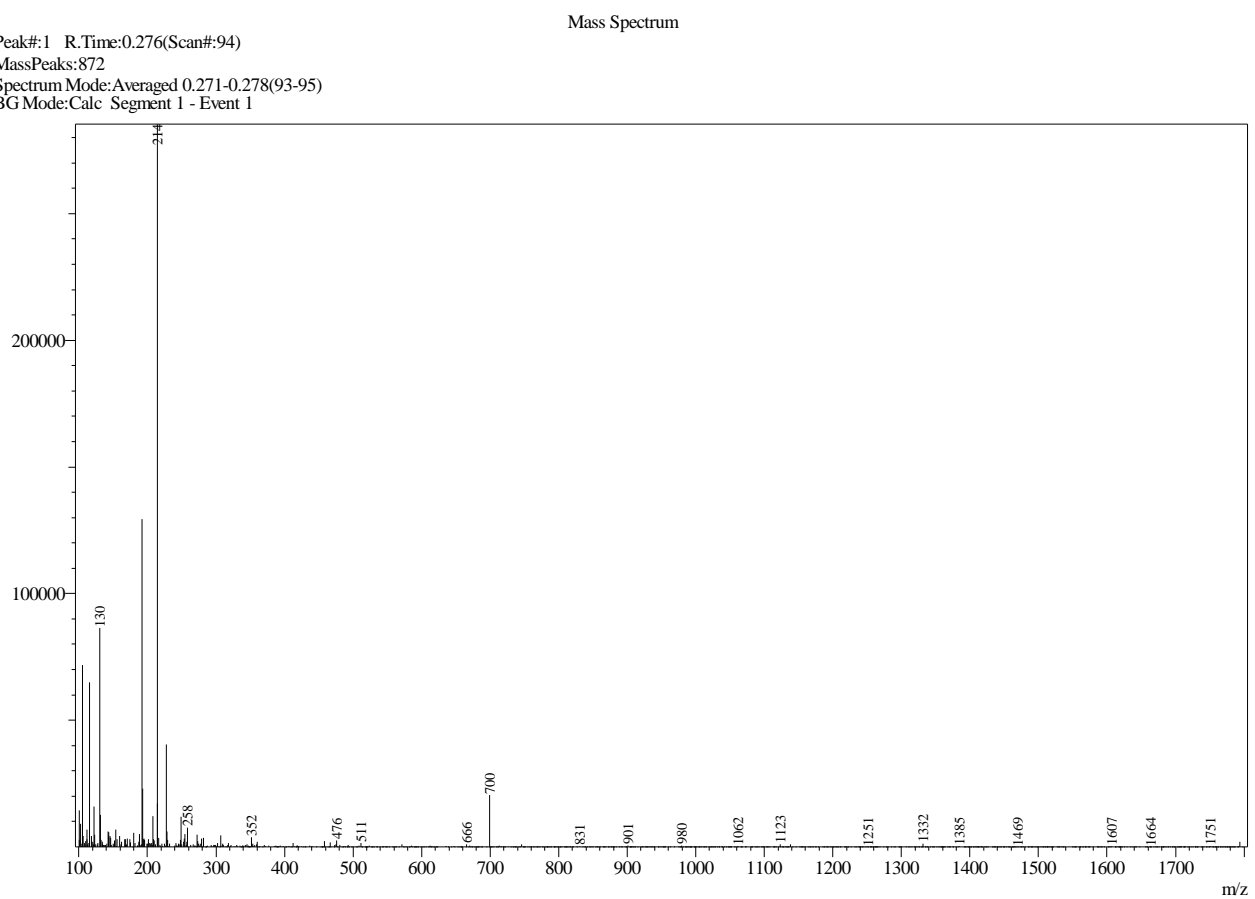
MS Chromatogram

TIC@1

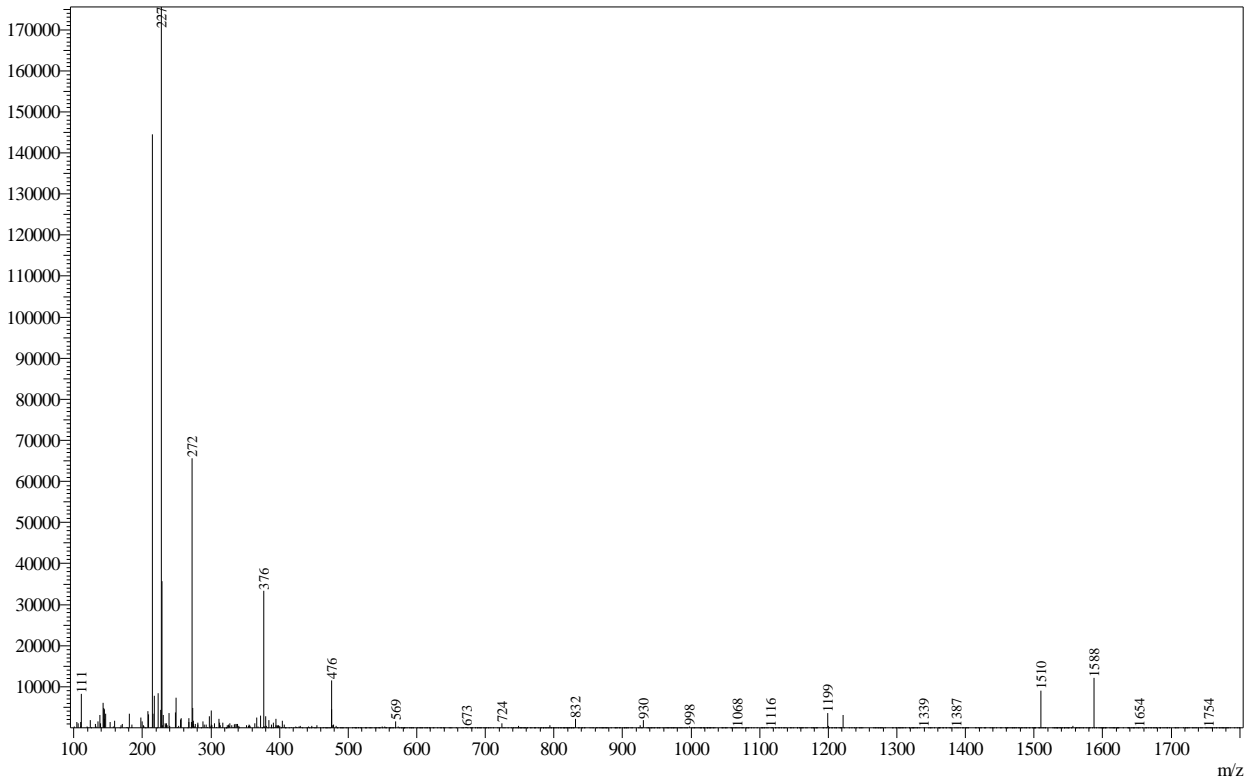




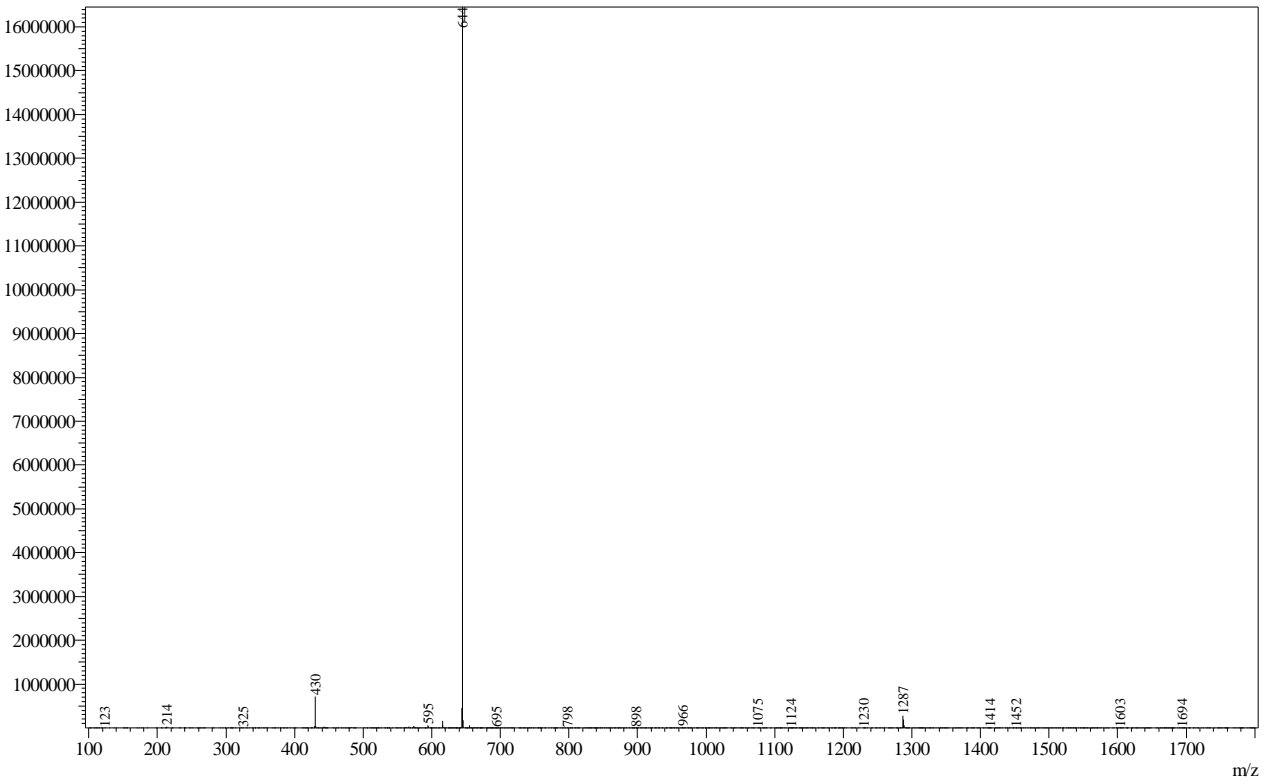
Peak#: 1 R.Time: 0.276(Scan#: 94)  
MassPeaks: 872  
Spectrum Mode: Averaged 0.271-0.278(93-95)  
BG Mode: Calc Segment 1 - Event 1



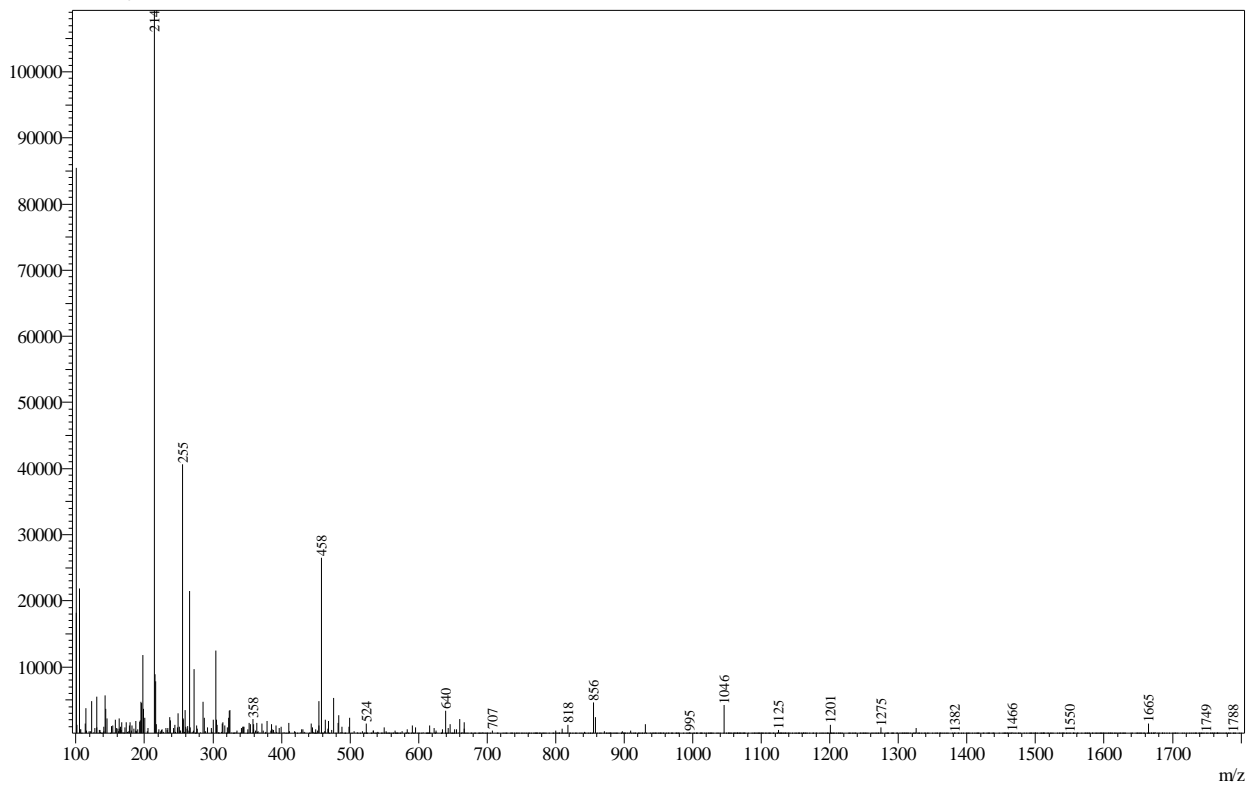
Peak#:2 R.Time:1.426(Scan#:408)  
MassPeaks:765  
Spectrum Mode:Averaged 1.422-1.429(407-409)  
BG Mode:Calc Segment 1 - Event 1



Peak#:3 R.Time:1.992(Scan#:563)  
MassPeaks:895  
Spectrum Mode:Averaged 1.990-1.998(562-564)  
BG Mode:Calc Segment 1 - Event 1



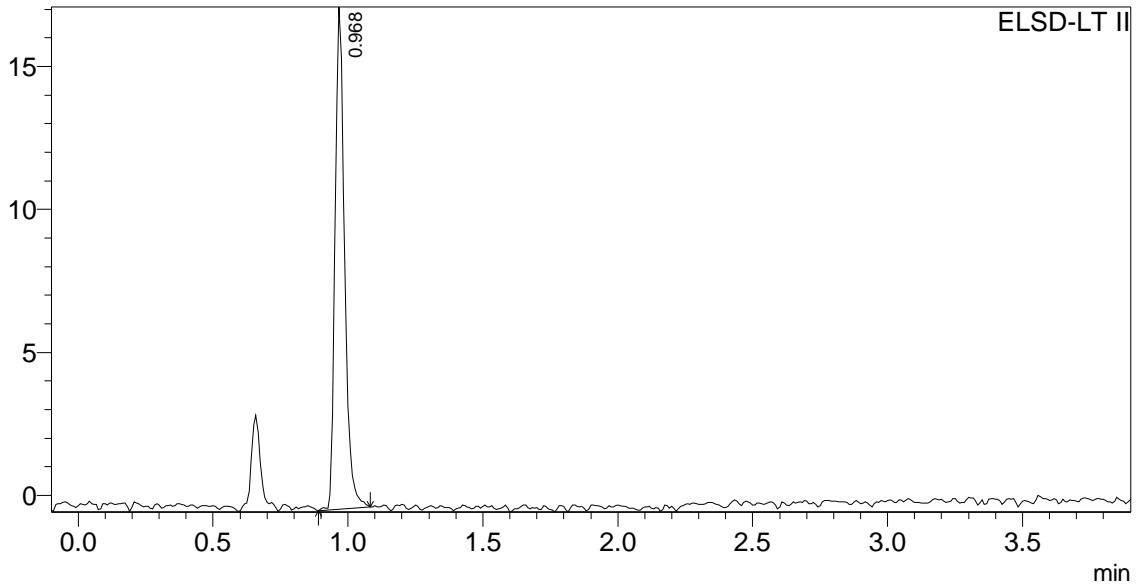
Peak#4 R.Time:2.893(Scan#:808)  
MassPeaks:834  
Spectrum Mode:Averaged 2.889-2.896(807-809)  
BG Mode:Calc Segment 1 - Event 1



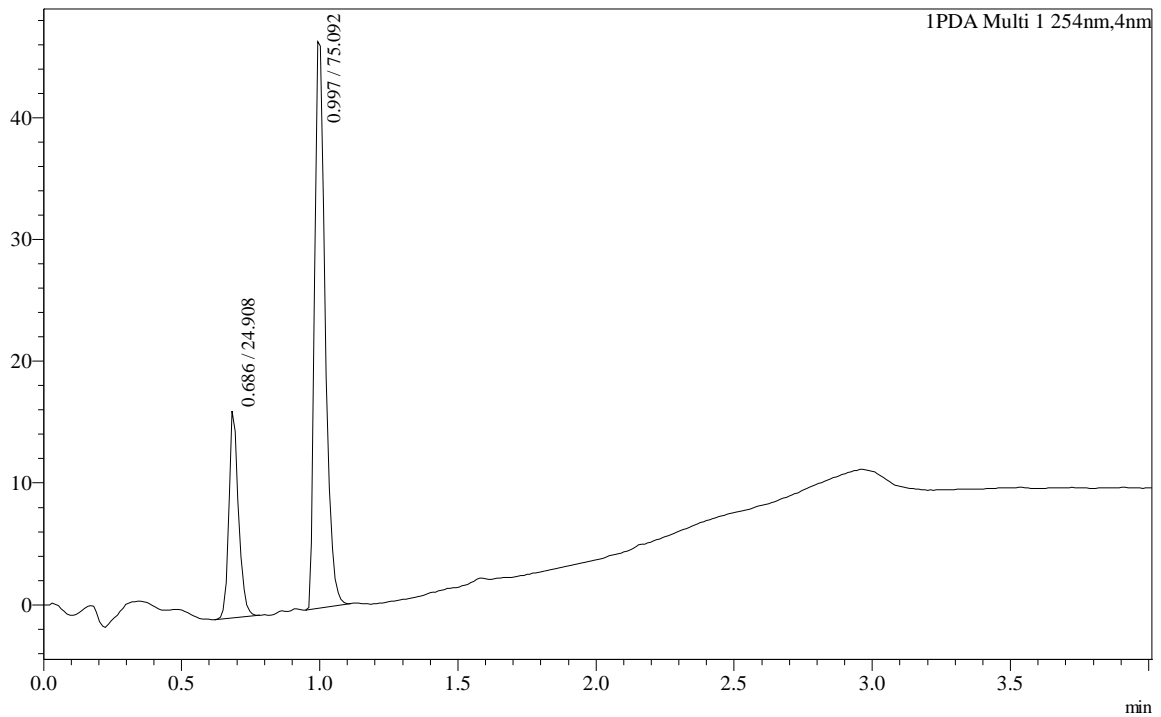
## ==== BIO5 Analytical Lab Report ====

C:\LabSolutions\Data\Project1\Purification\QCs\Feb5-2016\KO302-30\_fracQC\_004.lcd  
Sample Name : KO302-30\_fracQC\_004  
Vial# : 88  
Injection Volume : 10  
Data File : C:\LabSolutions\Data\Project1\Purification\QCs\Feb5-2016\KO302-30\_fracQC\_004.lcc  
Month-Day Acquired : 2/5/2016  
Original Method File : StandardRunPlates.lcm

mV C:\LabSolutions\Data\Project1\Purification\QCs\Feb5-2016\KO302-30\_fracQC\_004.lcd

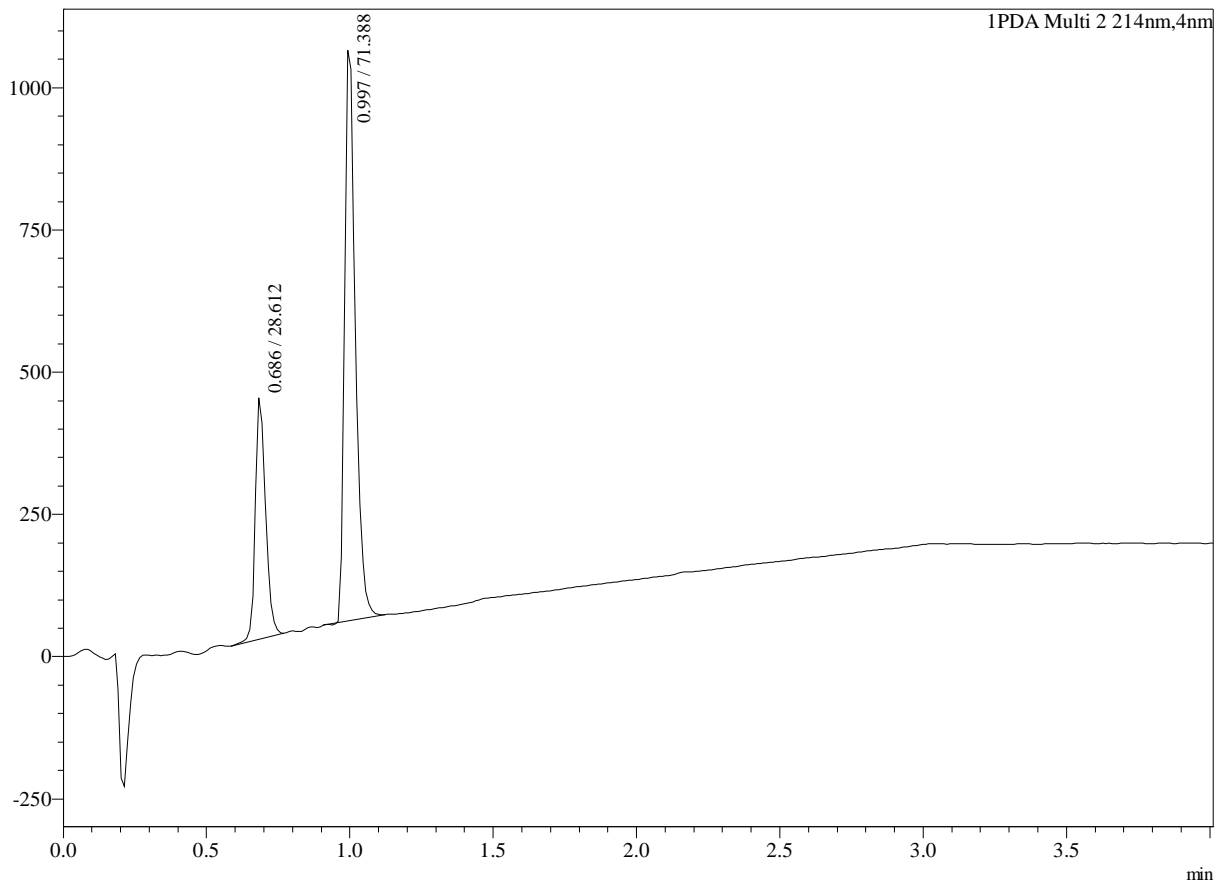


mAU Chromatogram



mAU

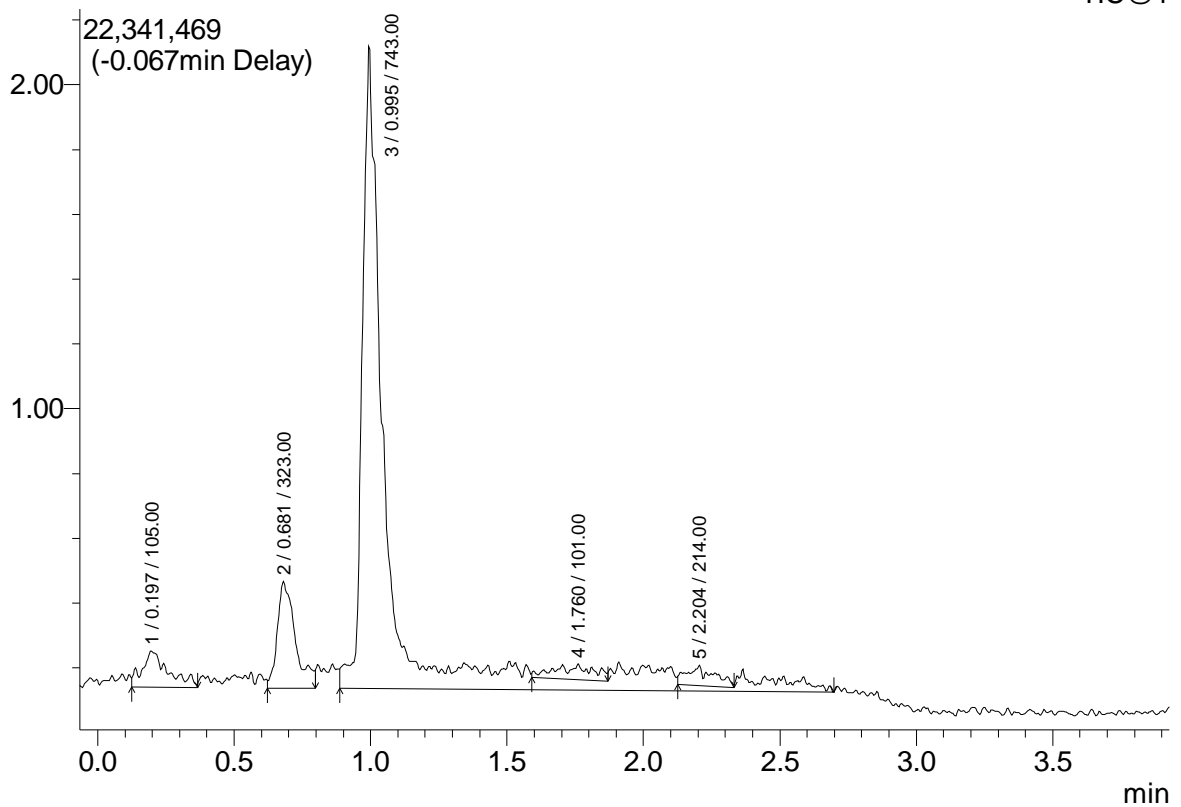
Chromatogram

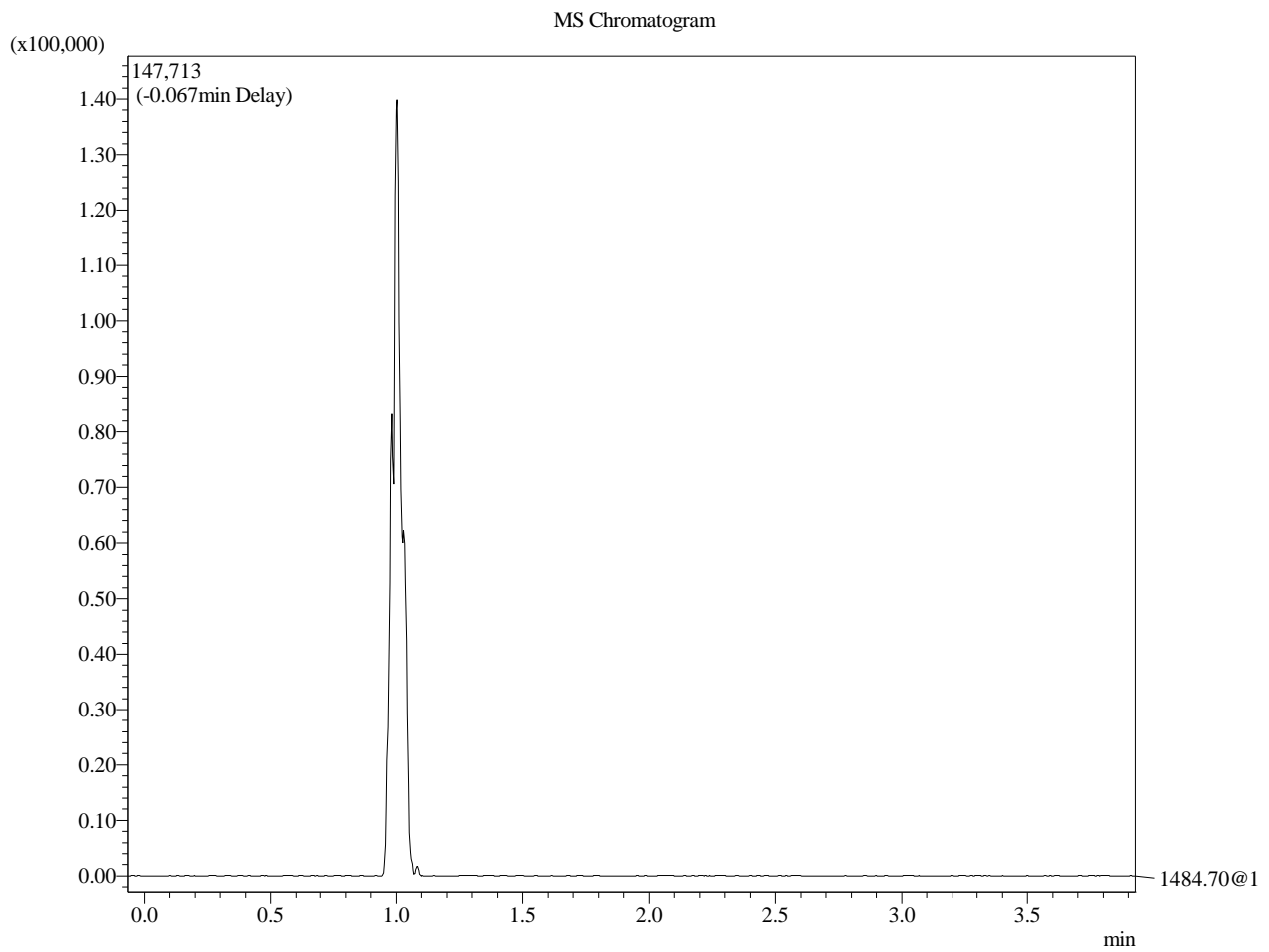


(x10,000,000)

MS Chromatogram

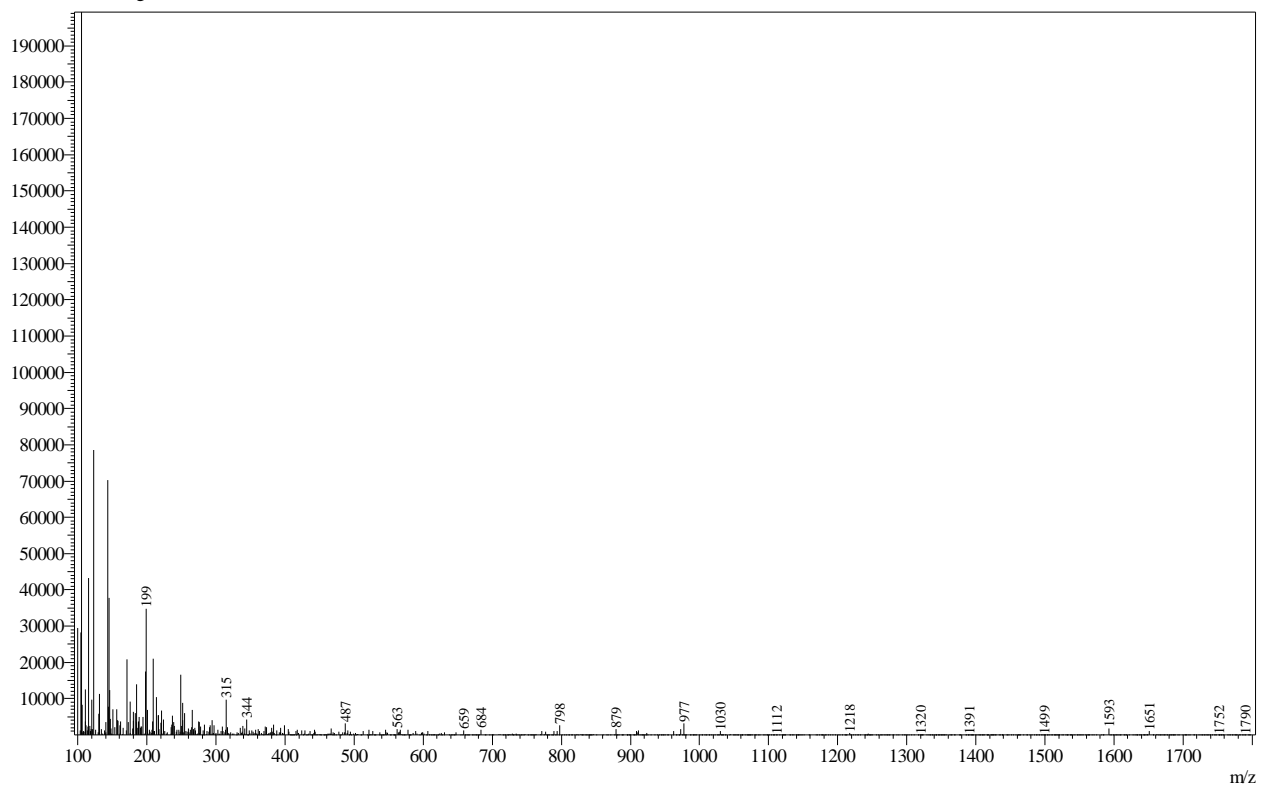
TIC@1



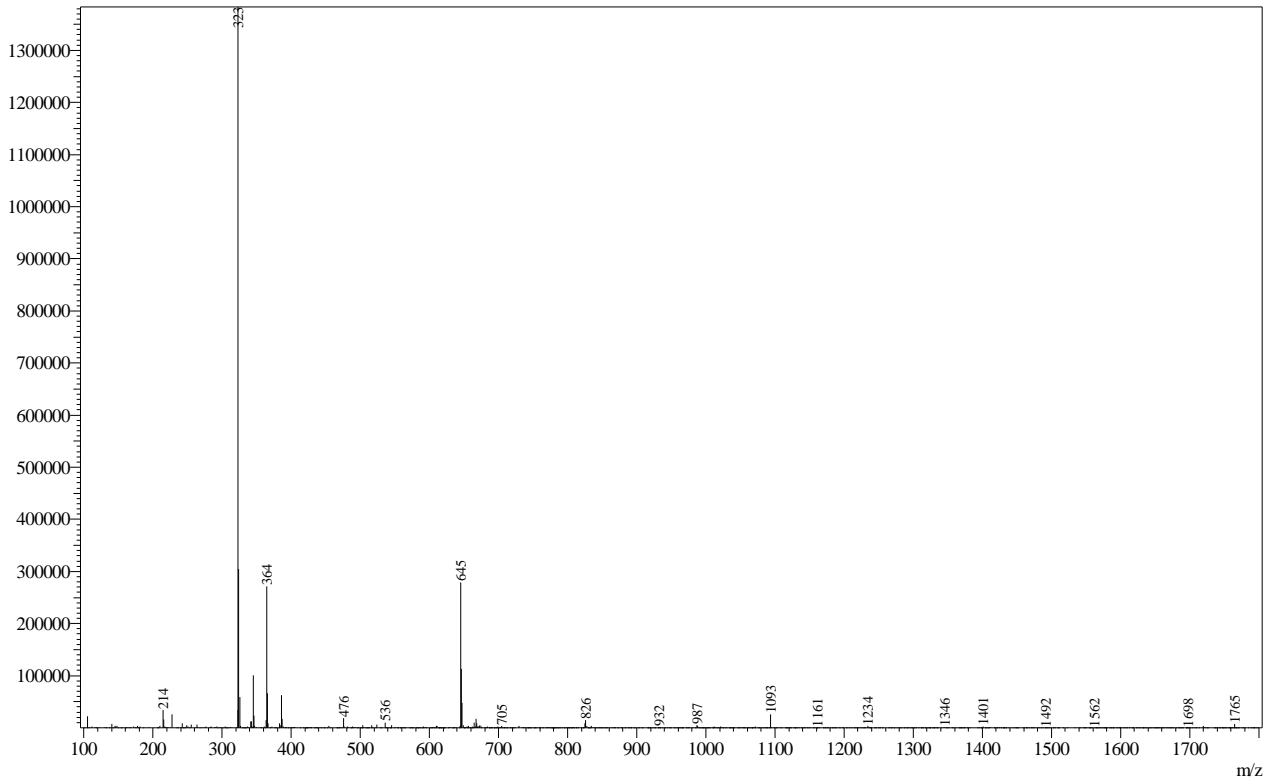


Peak#: 1 R.Time:0.197(Scan#:73)  
MassPeaks:922  
Spectrum Mode:Averaged 0.194-0.201(72-74)  
BG Mode:Calc Segment 1 - Event 1

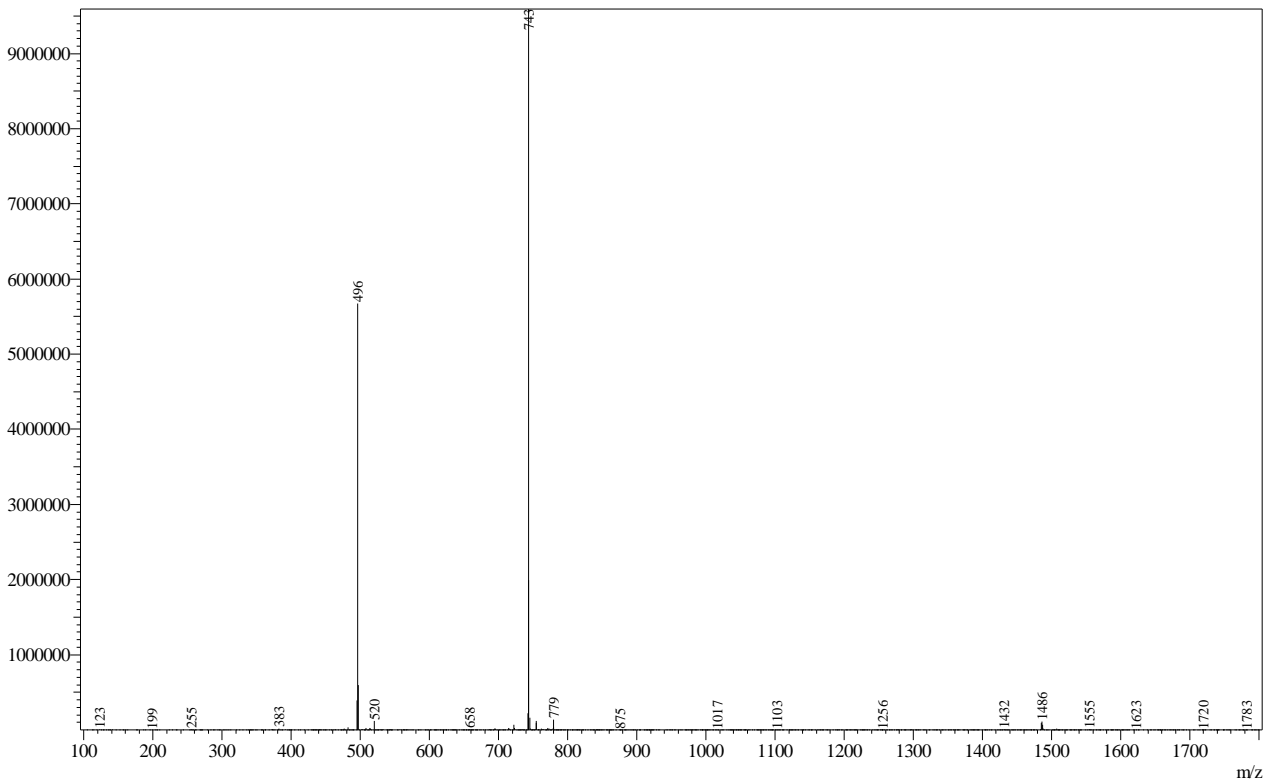
Mass Spectrum



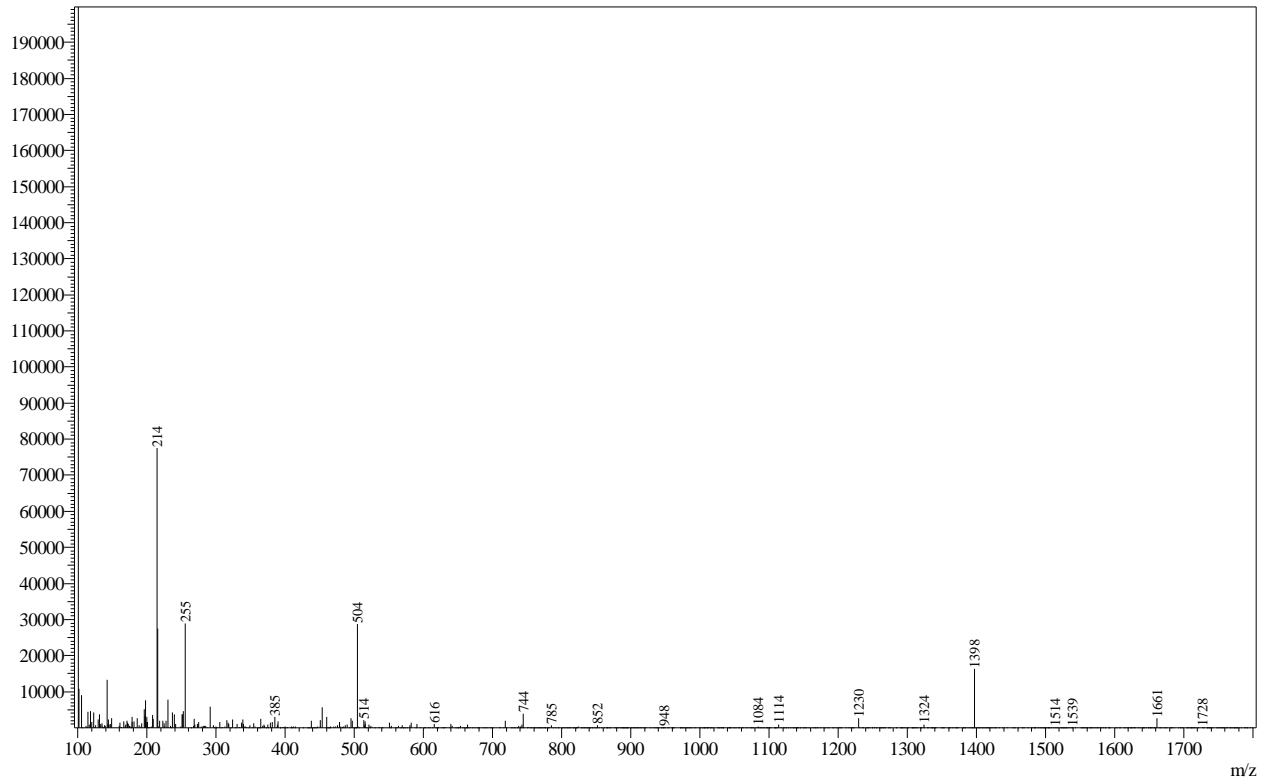
Peak#:2 R.Time:0.681(Scan#:205)  
MassPeaks:875  
Spectrum Mode:Averaged 0.678-0.685(204-206)  
BG Mode:Calc Segment 1 - Event 1



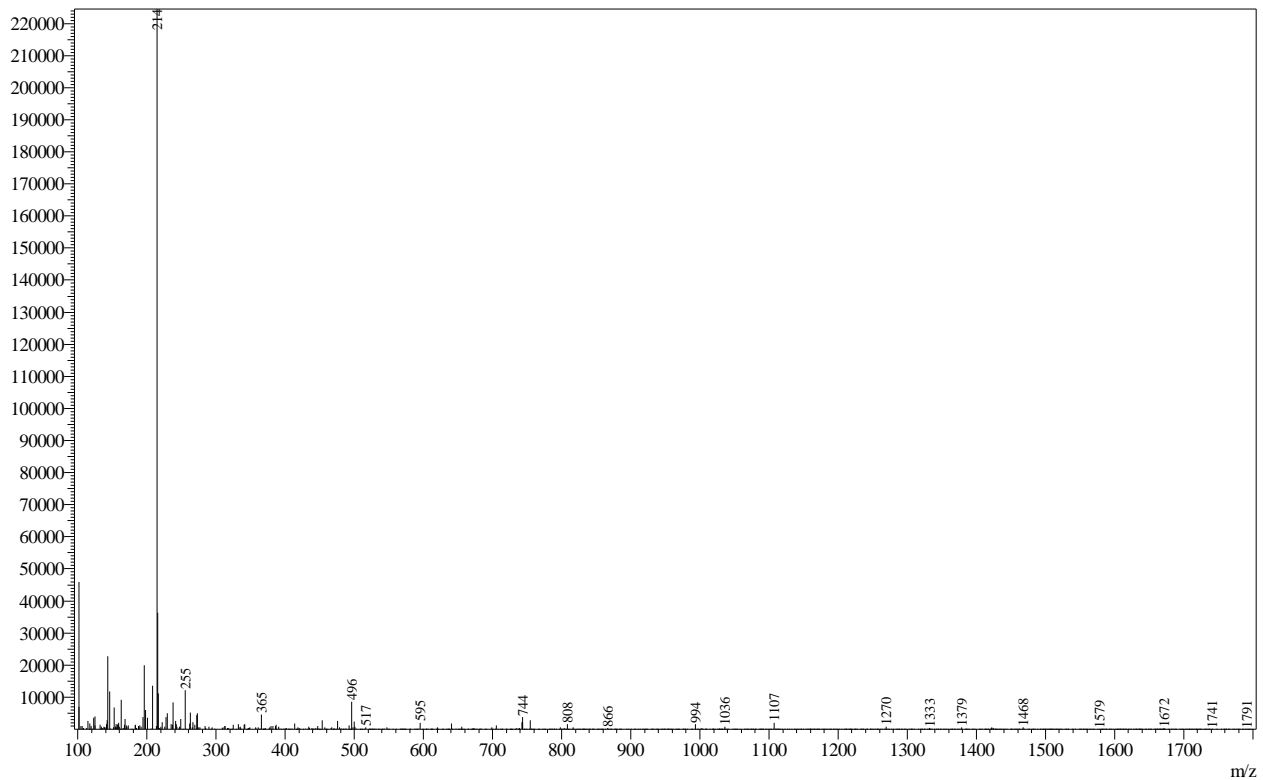
Peak#:3 R.Time:0.995(Scan#:290)  
MassPeaks:880  
Spectrum Mode:Averaged 0.989-0.997(289-291)  
BG Mode:Calc Segment 1 - Event 1



Peak#:4 R.Time:1.760(Scan#:499)  
MassPeaks:790  
Spectrum Mode:Averaged 1.756-1.763(498-500)  
BG Mode:Calc Segment 1 - Event 1

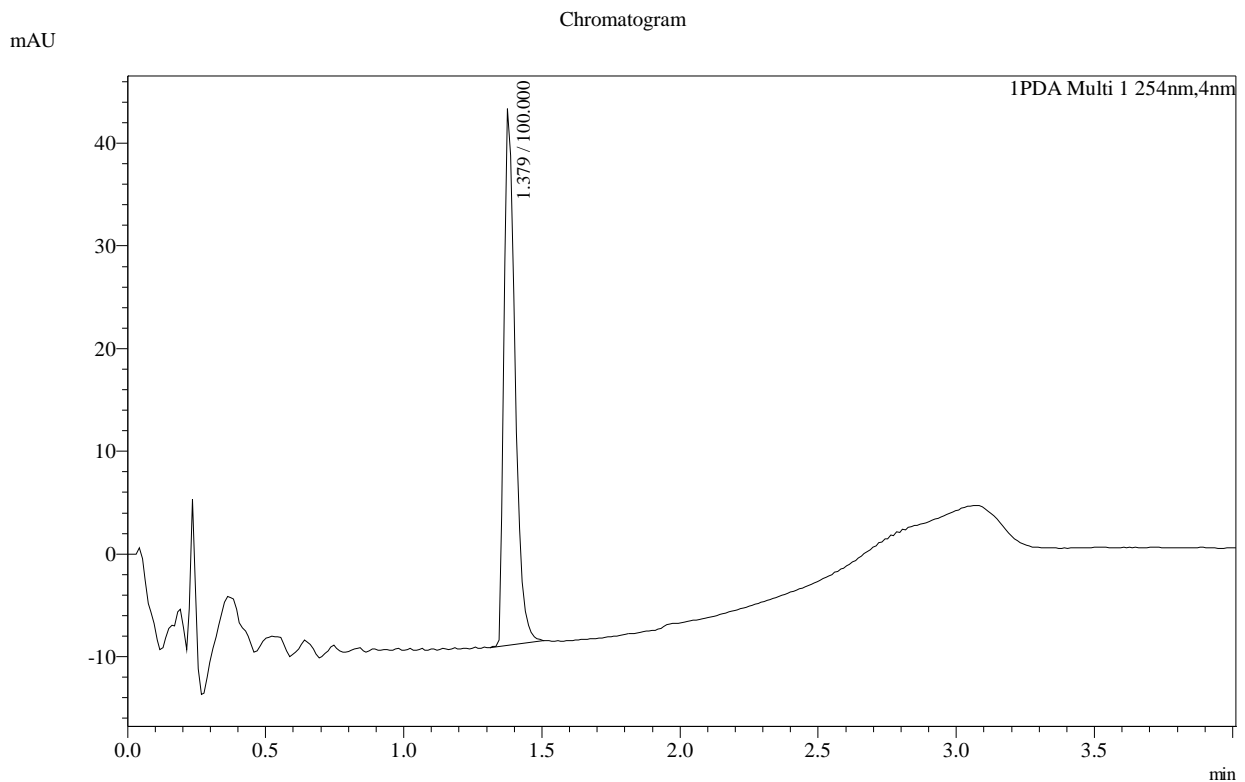
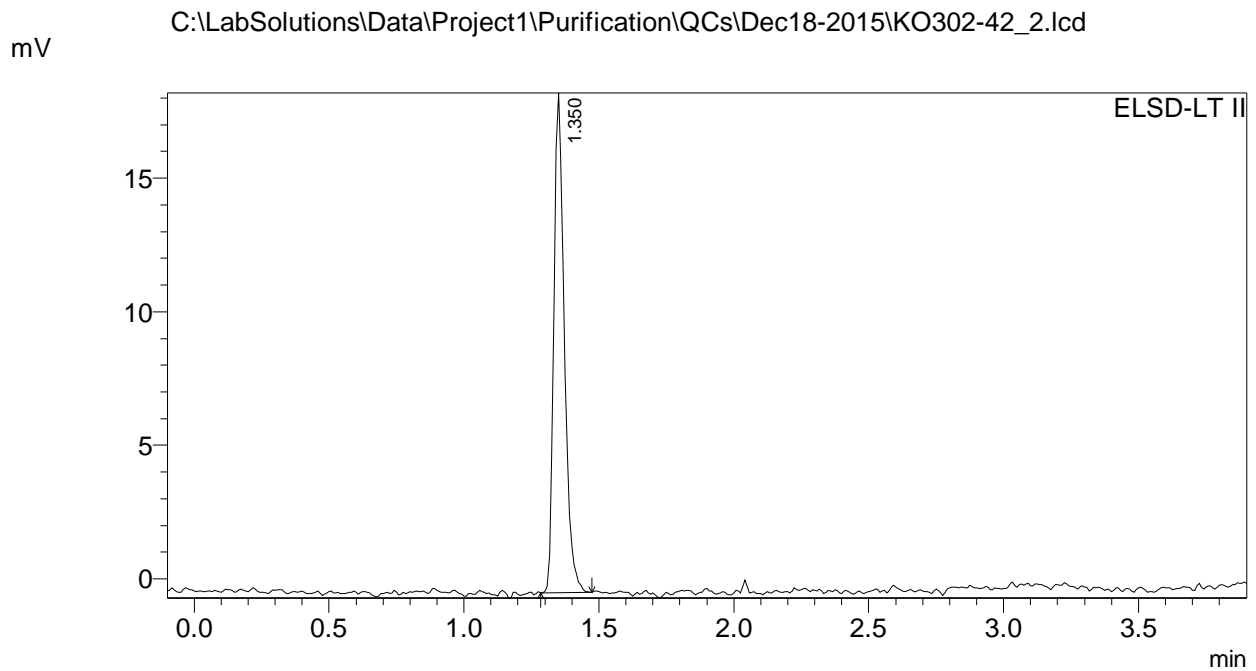


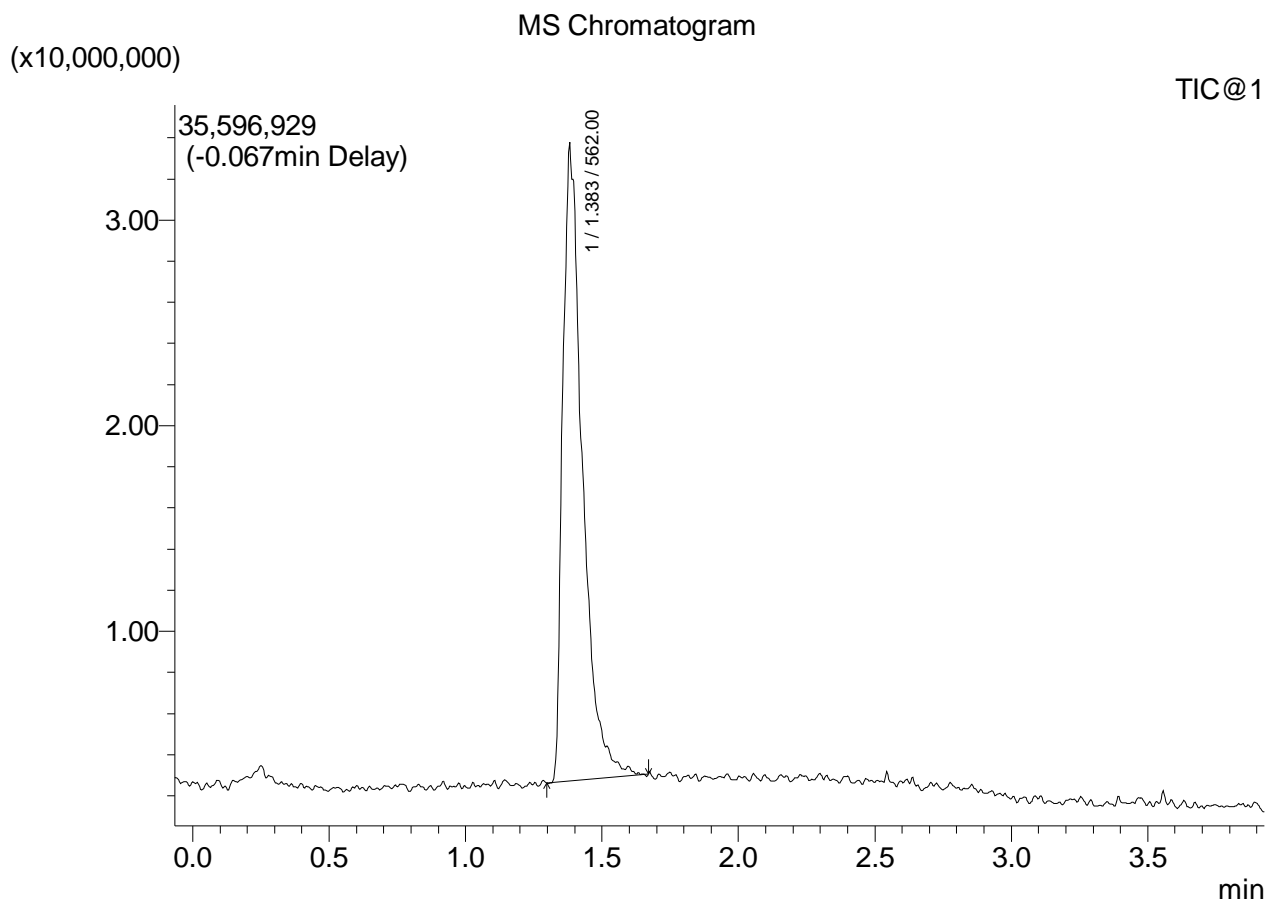
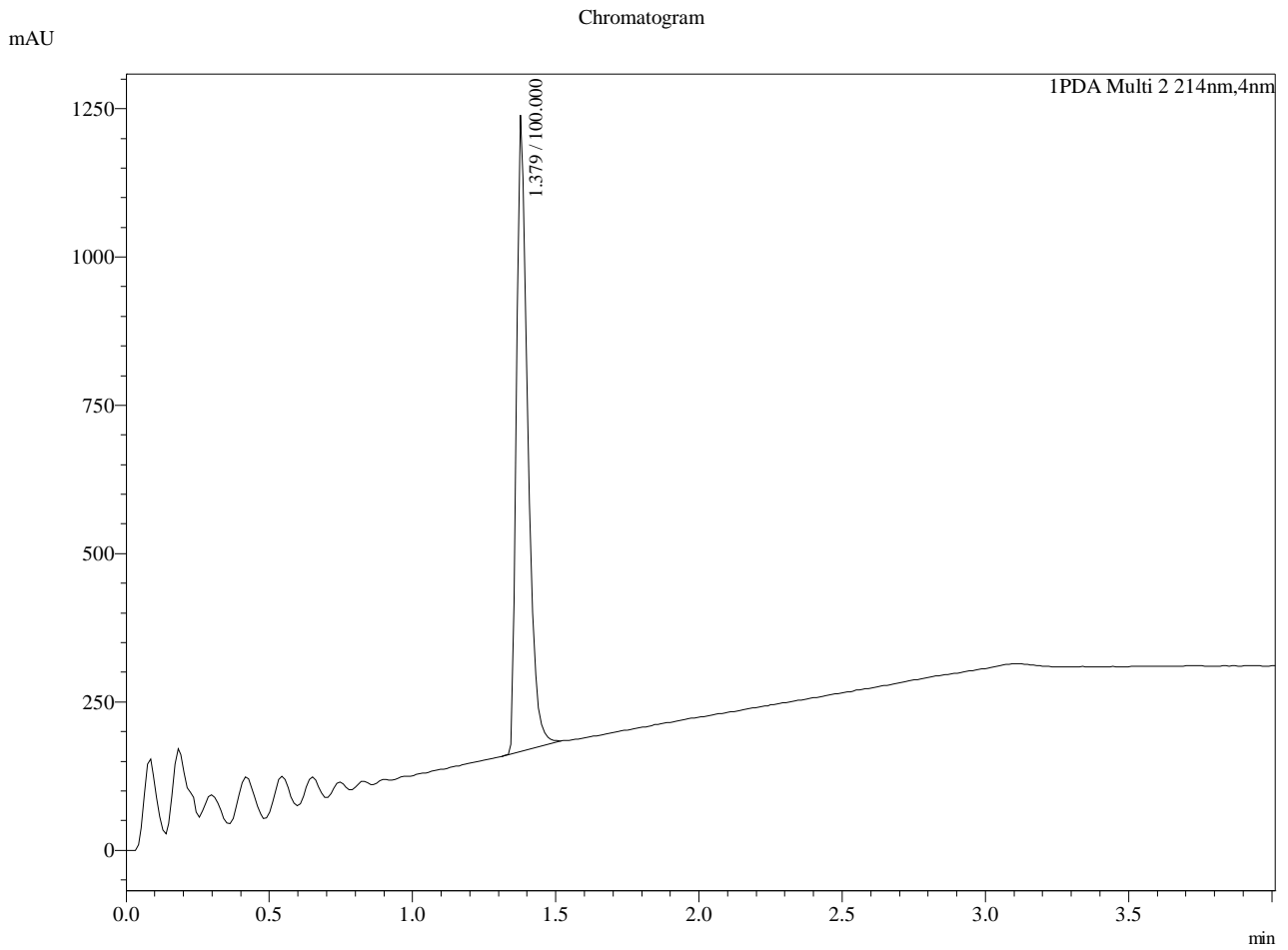
Peak#:5 R.Time:2.204(Scan#:620)  
MassPeaks:801  
Spectrum Mode:Averaged 2.199-2.207(619-621)  
BG Mode:Calc Segment 1 - Event 1

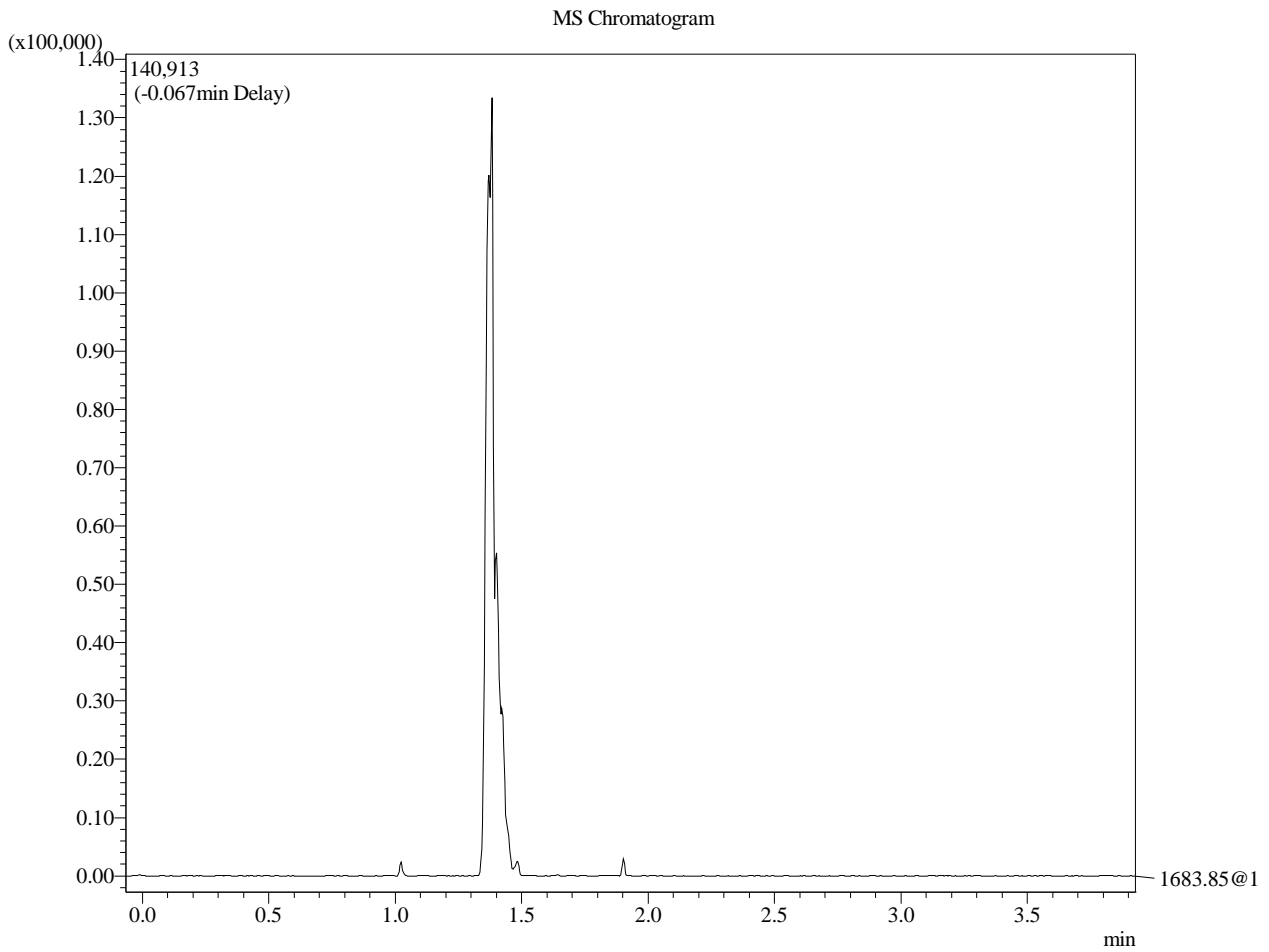


**==== BIO5 Analytical Lab Report ====**

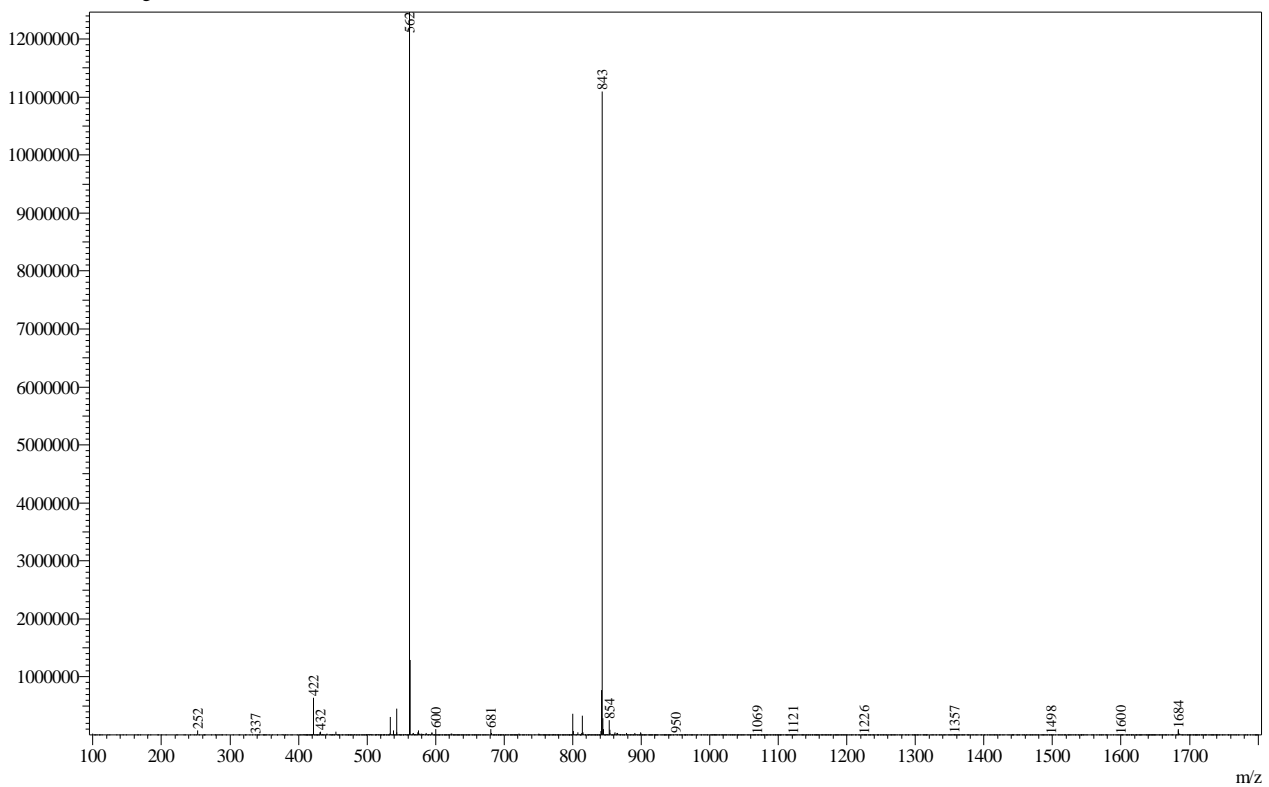
C:\LabSolutions\Data\Project1\Purification\QCs\Dec18-2015\KO302-42\_2.lcd  
Sample Name : KO302-42\_2  
Vial# : 9  
Injection Volume : 10  
Data File : C:\LabSolutions\Data\Project1\Purification\QCs\Dec18-2015\KO302-42\_2.lcd  
Month-Day Acquired : 12/18/2015  
Original Method File : StandardRunPlates.lcm







Peak#: 1 R.Time: 1.383(Scan#:396)  
MassPeaks: 1007  
Spectrum Mode: Averaged 1.378-1.385(395-397)  
BG Mode: Calc Segment 1 - Event 1



**==== BIO5 Analytical Lab Report ====**

C:\LabSolutions\Data\Project1\Purification\QCs\Jan12-2016\KO104\_fracQC\_003.lcd

Sample Name : KO104\_fracQC\_003

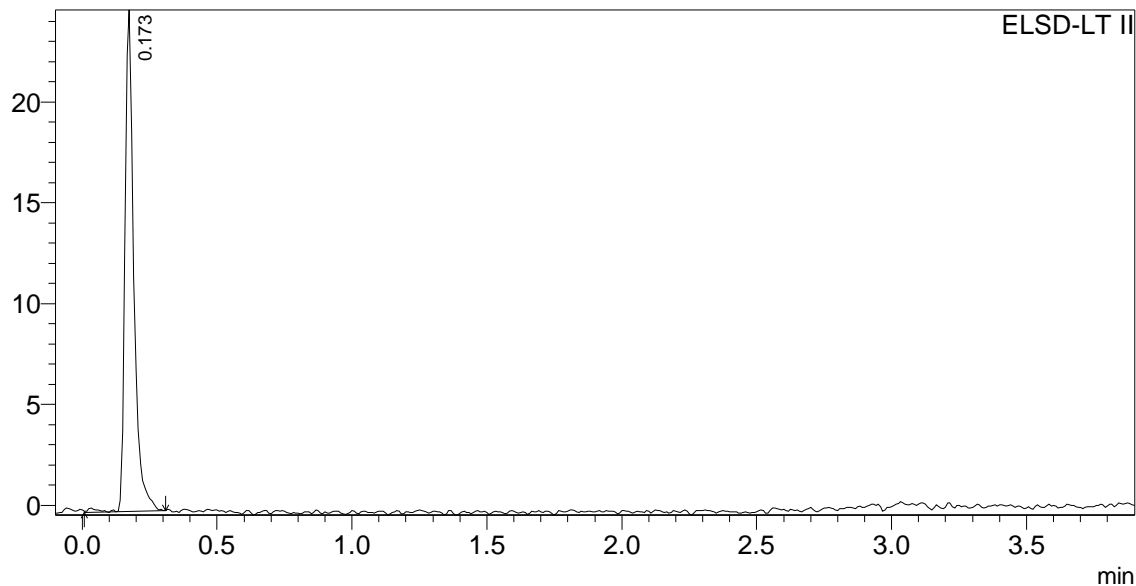
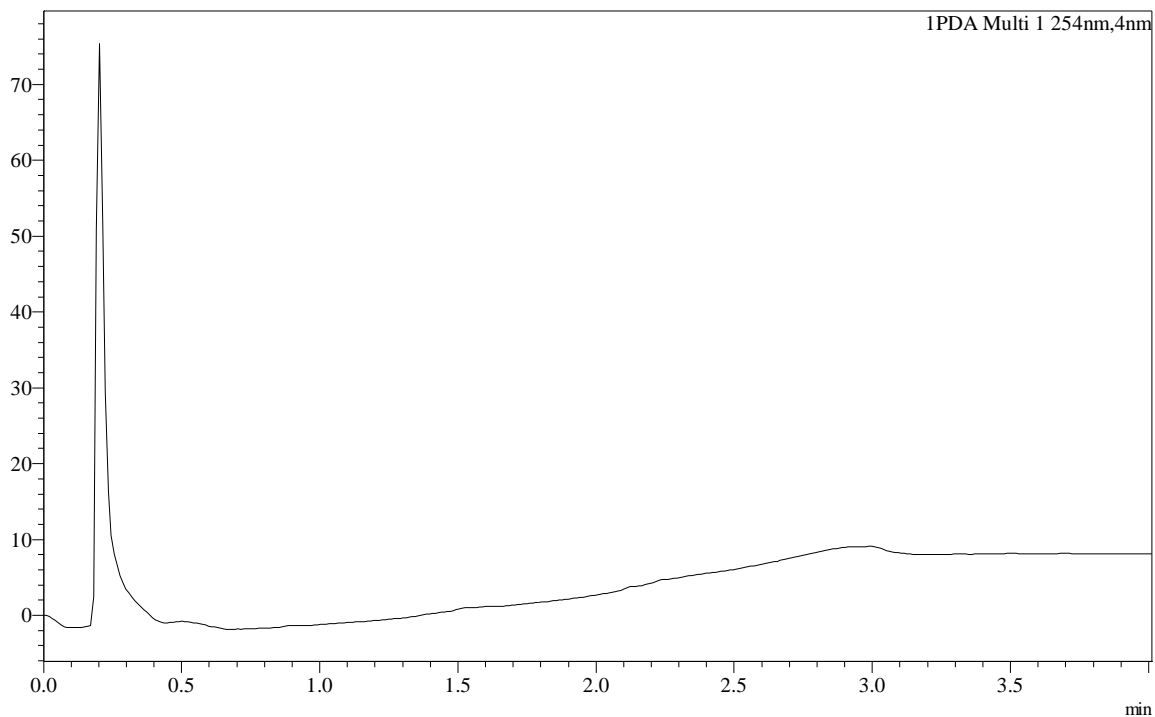
Vial# : 3

Injection Volume : 10

Data File : C:\LabSolutions\Data\Project1\Purification\QCs\Jan12-2016\KO104\_fracQC\_003.lcd

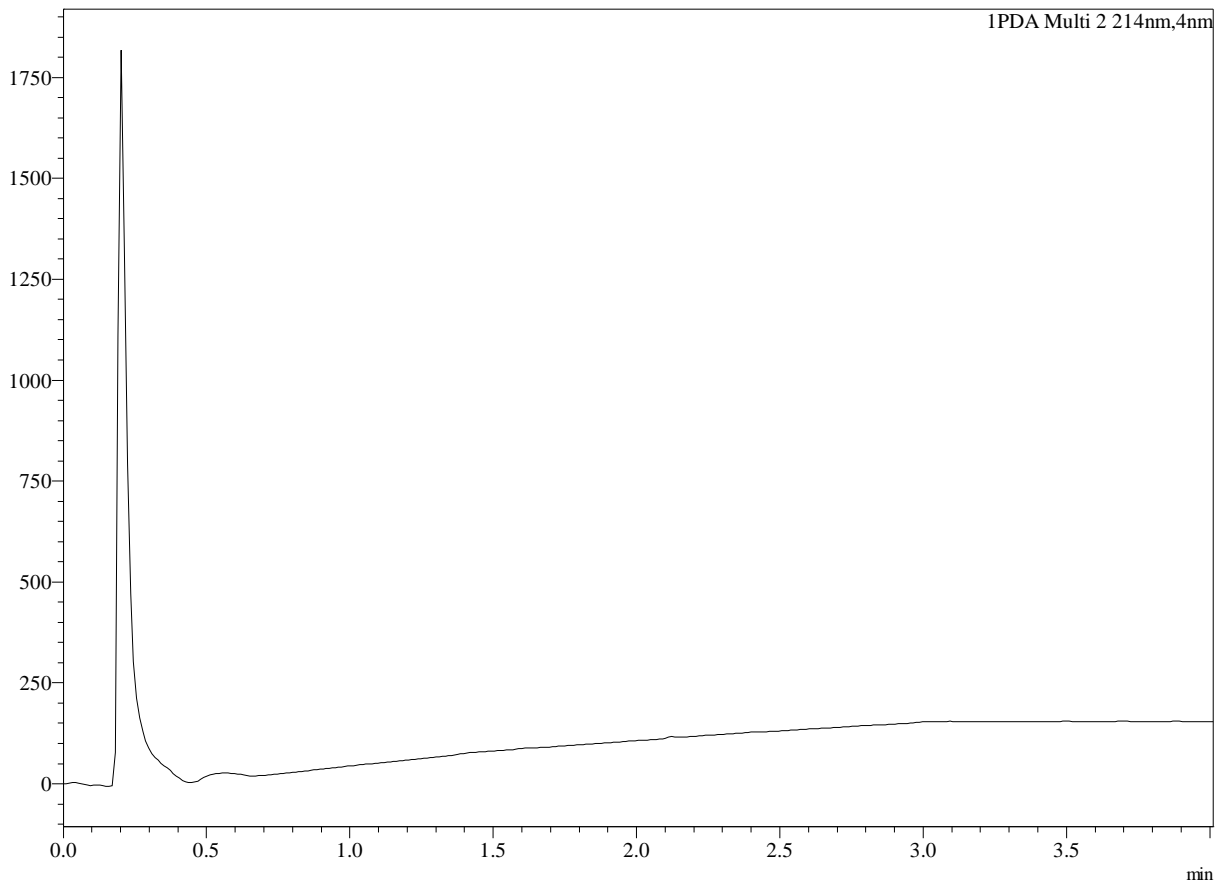
Month-Day Acquired : 1/12/2016

Original Method File : StandardRunPlates.lcm

C:\LabSolutions\Data\Project1\Purification\QCs\Jan12-2016\KO104\_fracQC\_003.lcd  
mVmAU  
Chromatogram

mAU

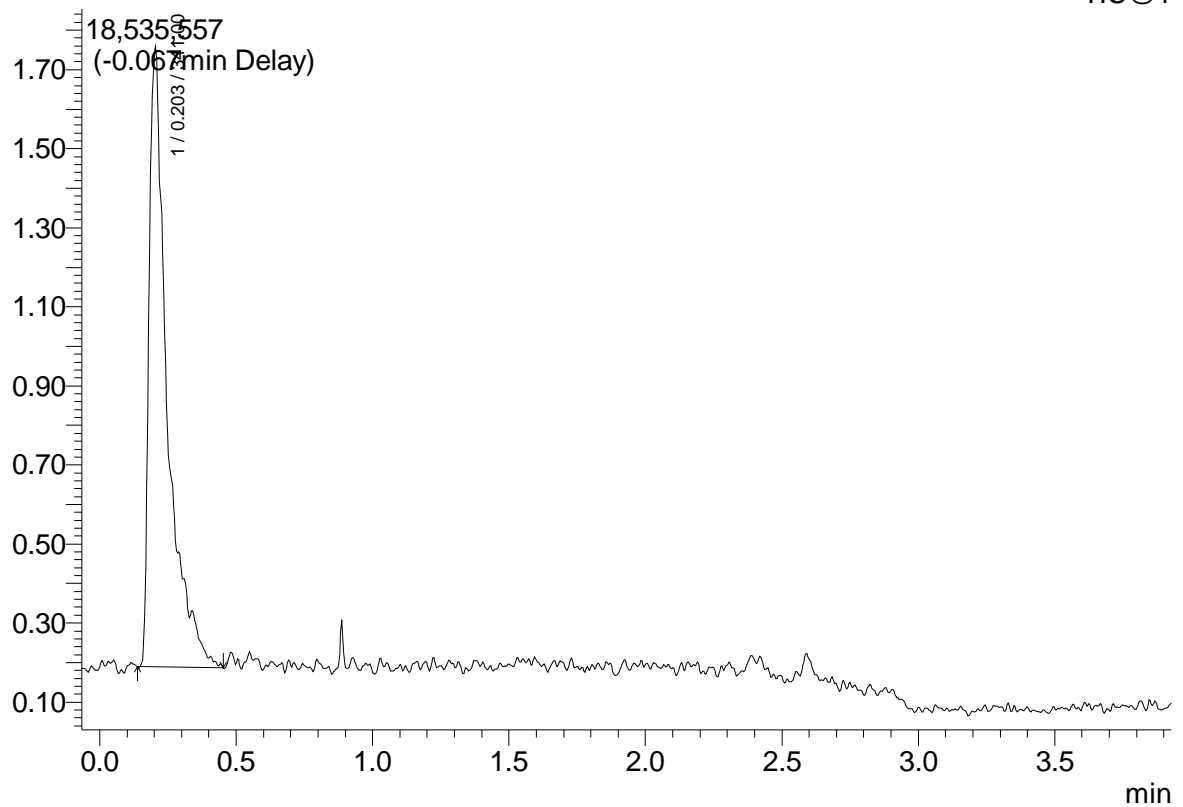
Chromatogram

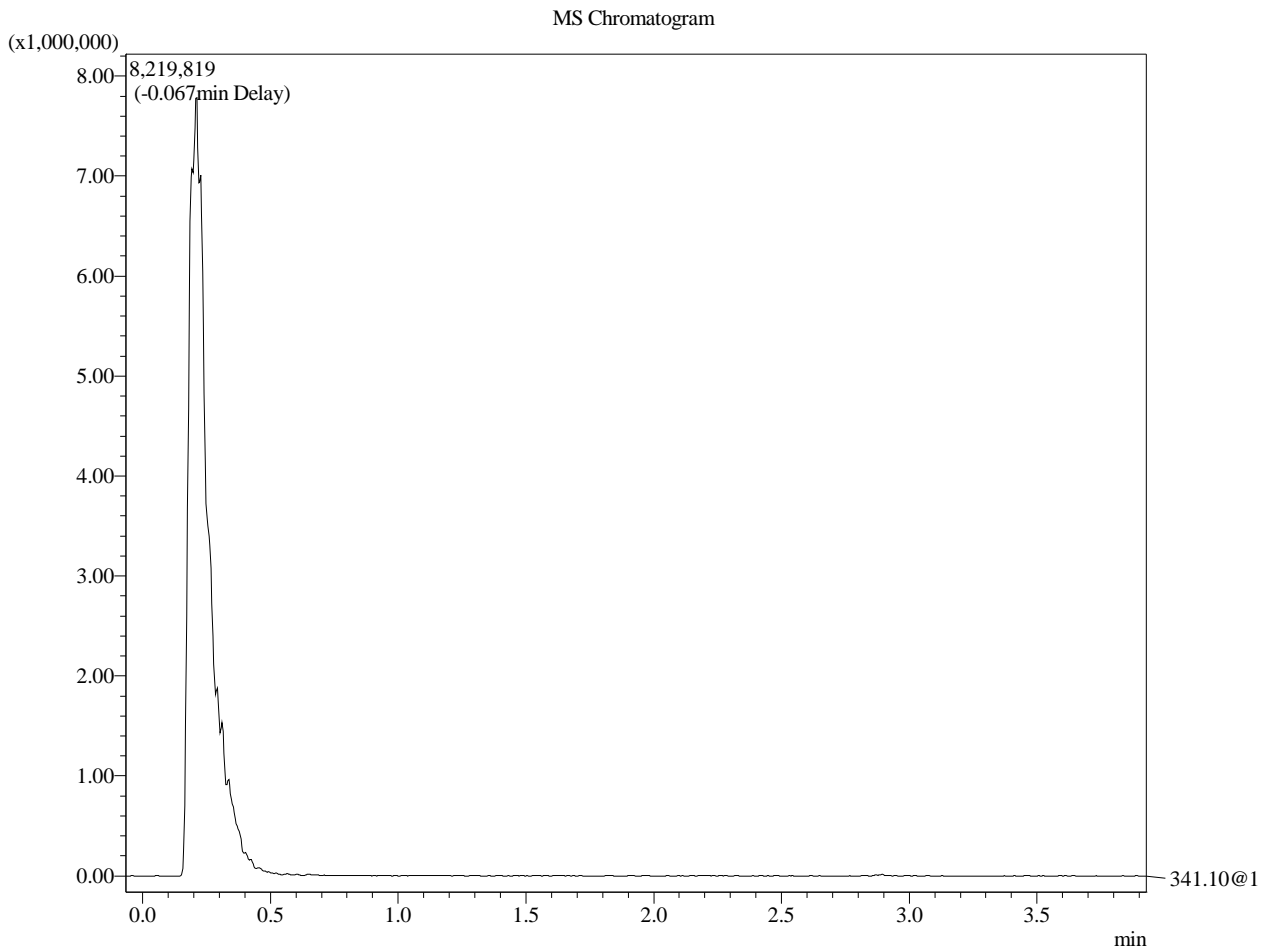


MS Chromatogram

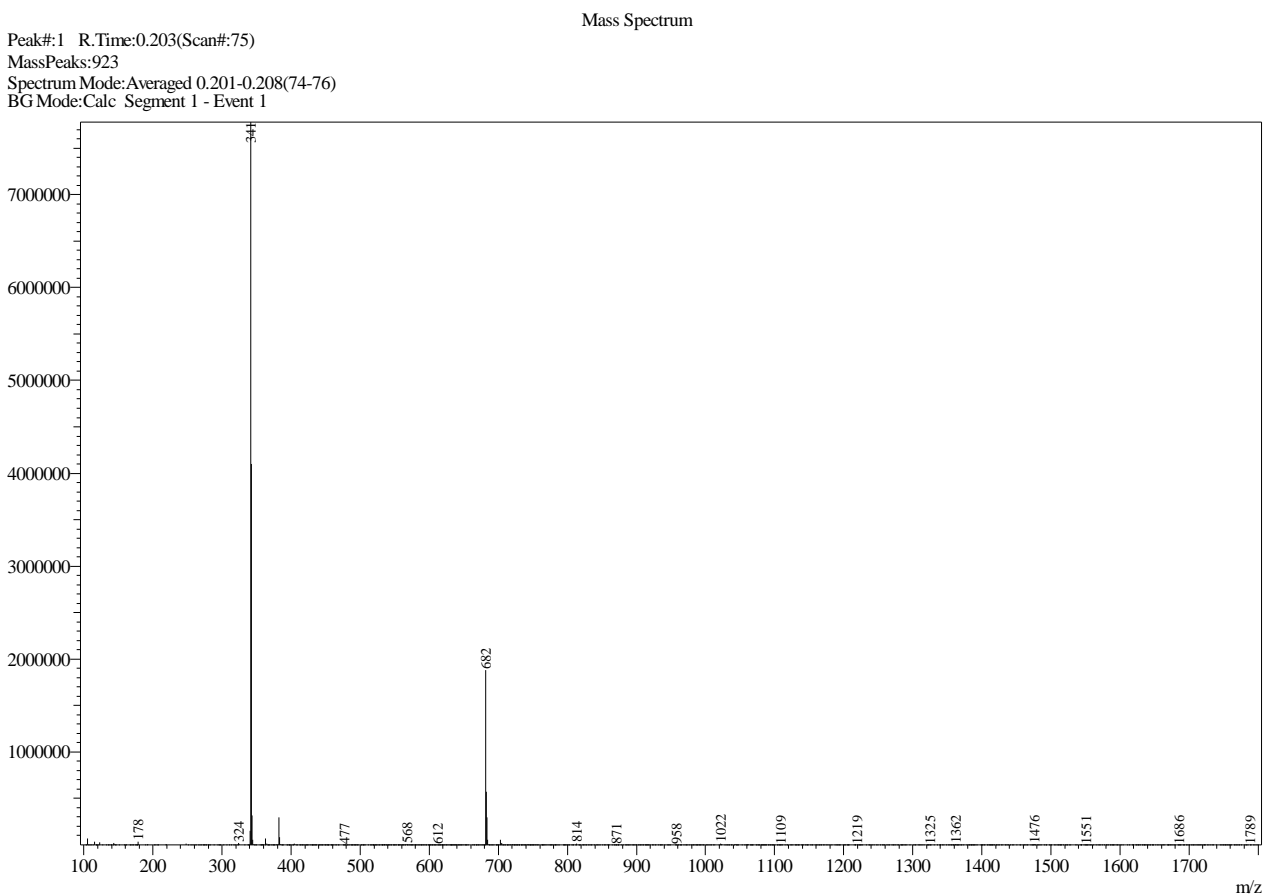
(x10,000,000)

TIC@1





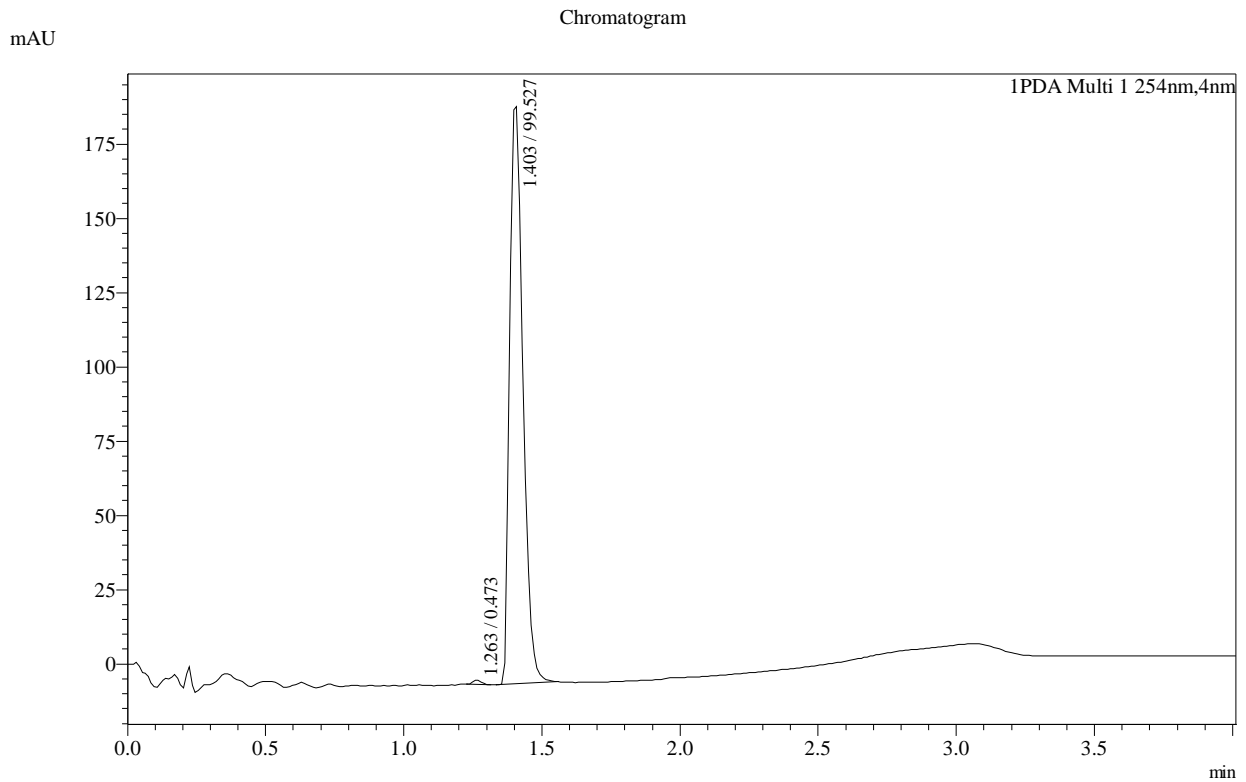
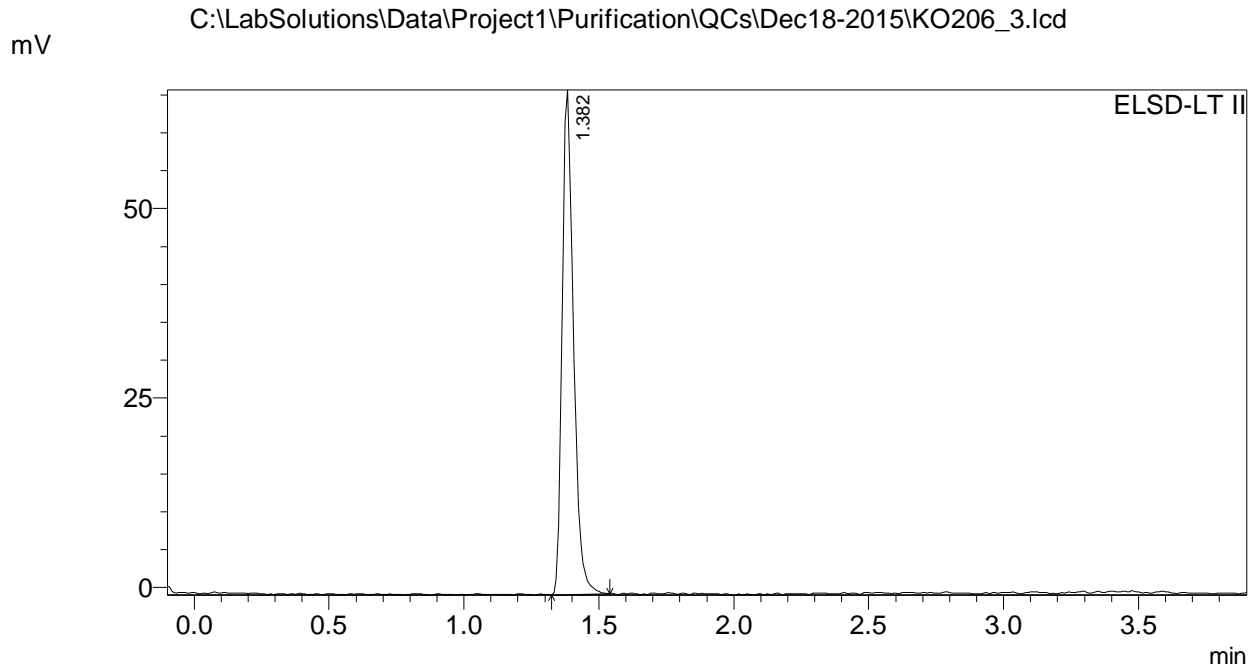
Peak#: 1 R.Time: 0.203(Scan#: 75)  
MassPeaks: 923  
Spectrum Mode: Averaged 0.201-0.208(74-76)  
BG Mode: Calc Segment 1 - Event 1



## ==== BIO5 Analytical Lab Report ====

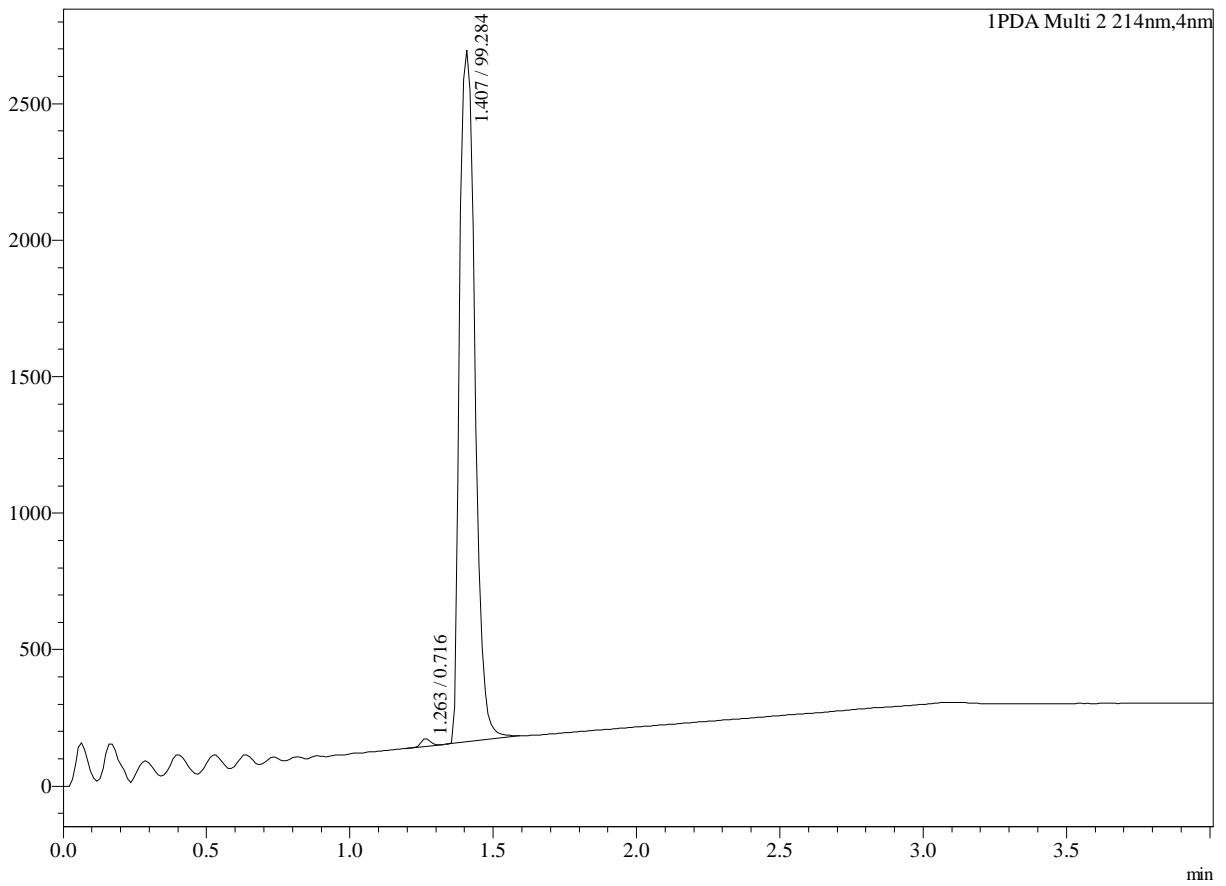
C:\LabSolutions\Data\Project1\Purification\QCs\Dec18-2015\KO206\_3.lcd

Sample Name : KO206\_3  
Vial# : 13  
Injection Volume : 10  
Data File : C:\LabSolutions\Data\Project1\Purification\QCs\Dec18-2015\KO206\_3.lcd  
Month-Day Acquired : 12/18/2015  
Original Method File : StandardRunPlates.lcm



mAU

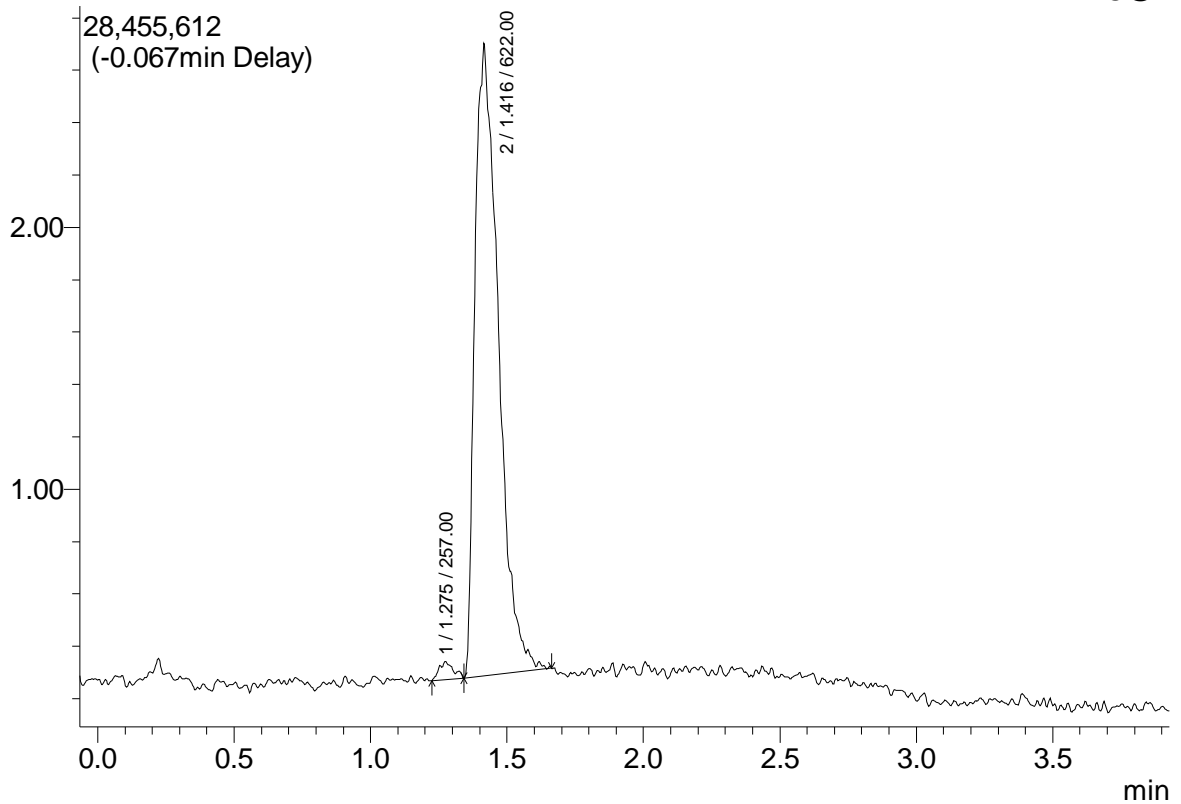
Chromatogram

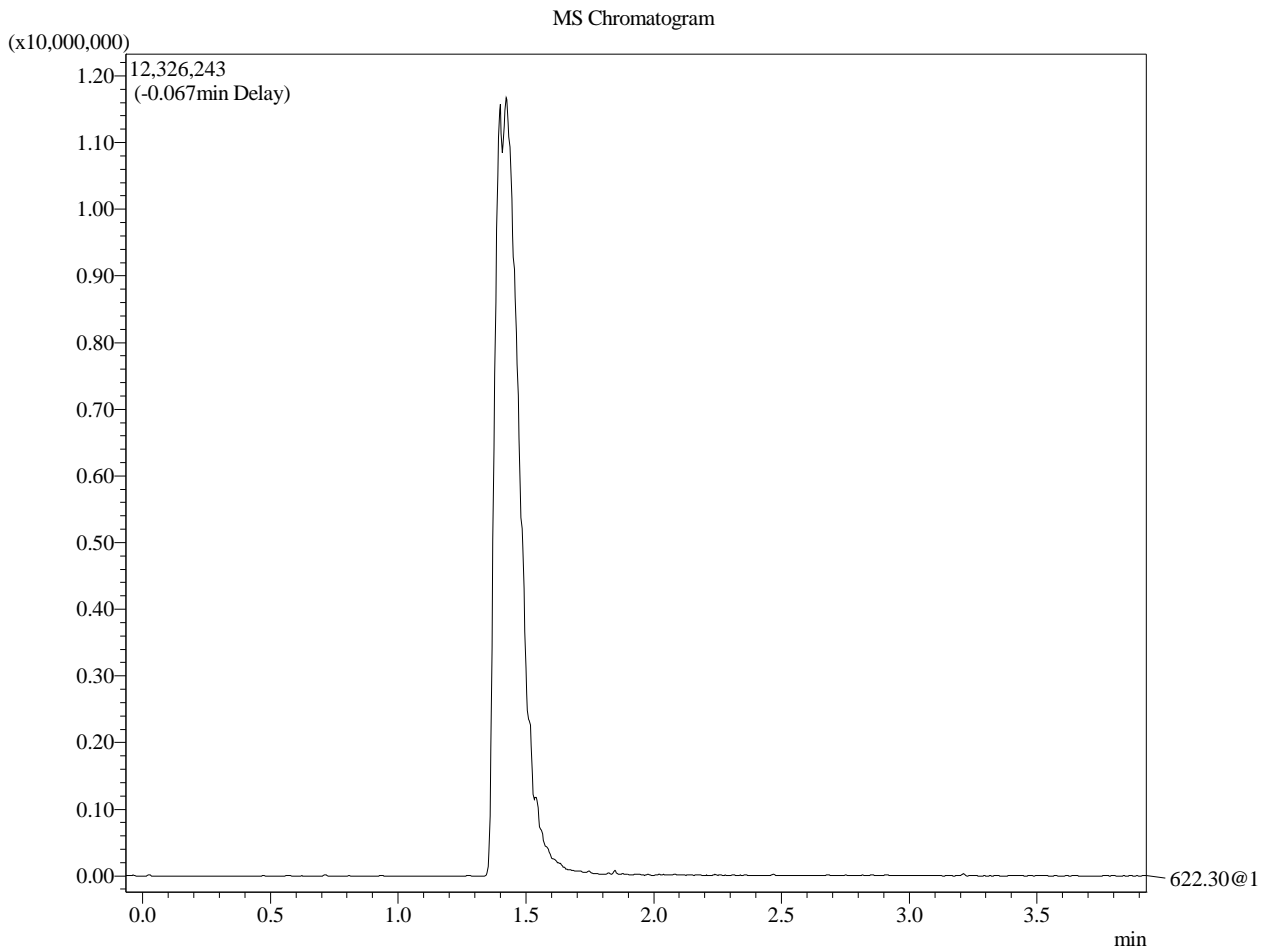


MS Chromatogram

(x10,000,000)

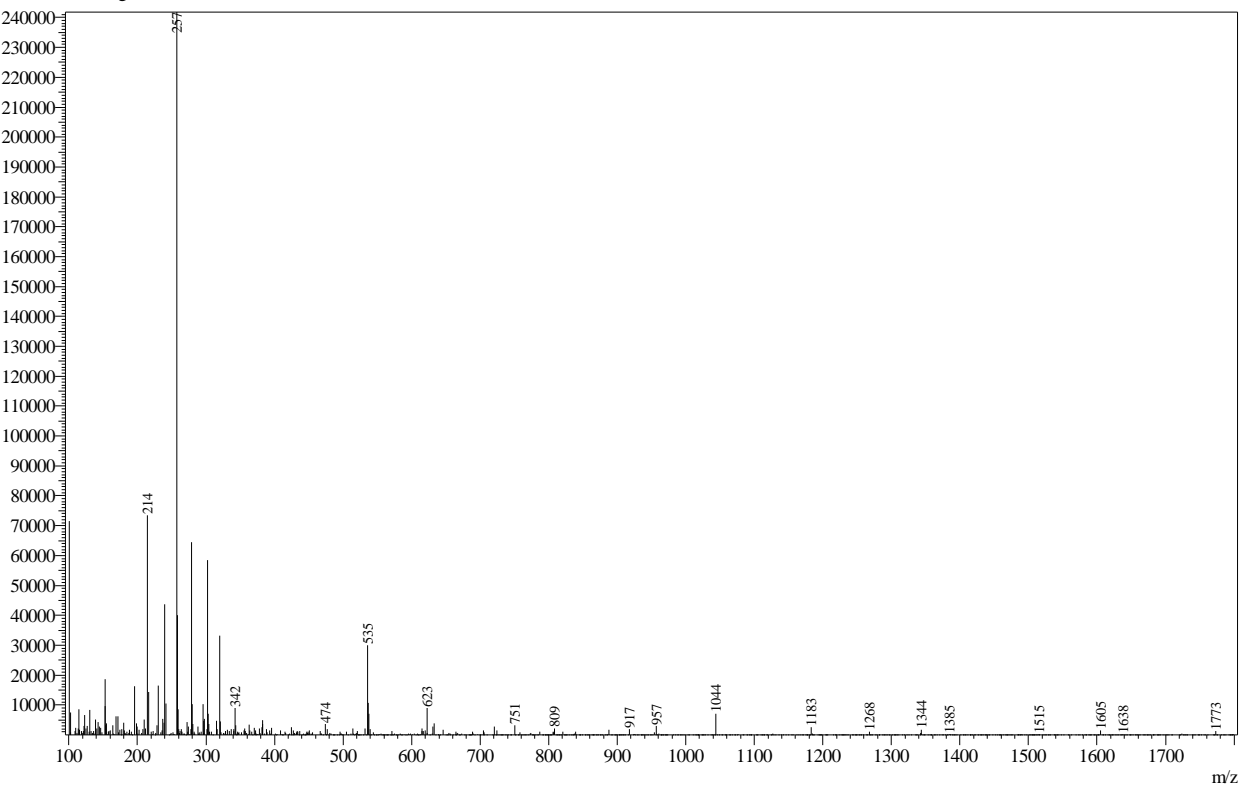
TIC@1



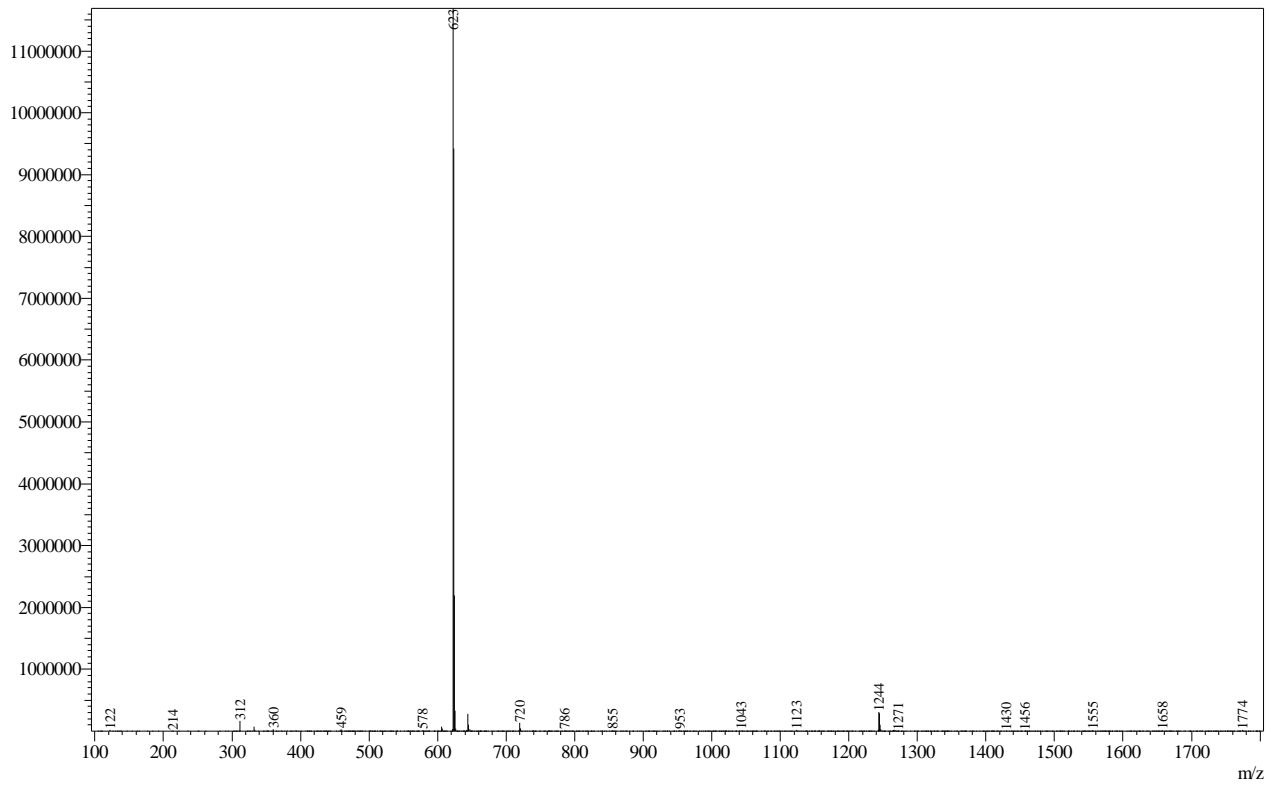


Peak#: 1 R.Time: 1.275(Scan#:367)  
MassPeaks: 864  
Spectrum Mode: Averaged 1.272-1.279(366-368)  
BG Mode: Calc Segment 1 - Event 1

Mass Spectrum



Peak#:2 R.Time:1.416(Scan#:405)  
MassPeaks:830  
Spectrum Mode:Averaged 1.411-1.418(404-406)  
BG Mode:Calc Segment 1 - Event 1



**==== BIO5 Analytical Lab Report ====**

C:\LabSolutions\Data\Project1\Purification\QCs\Jan29-2016\KO\DynA-1\_fracQC4.lcd

Sample Name : DynA-1\_fracQC4

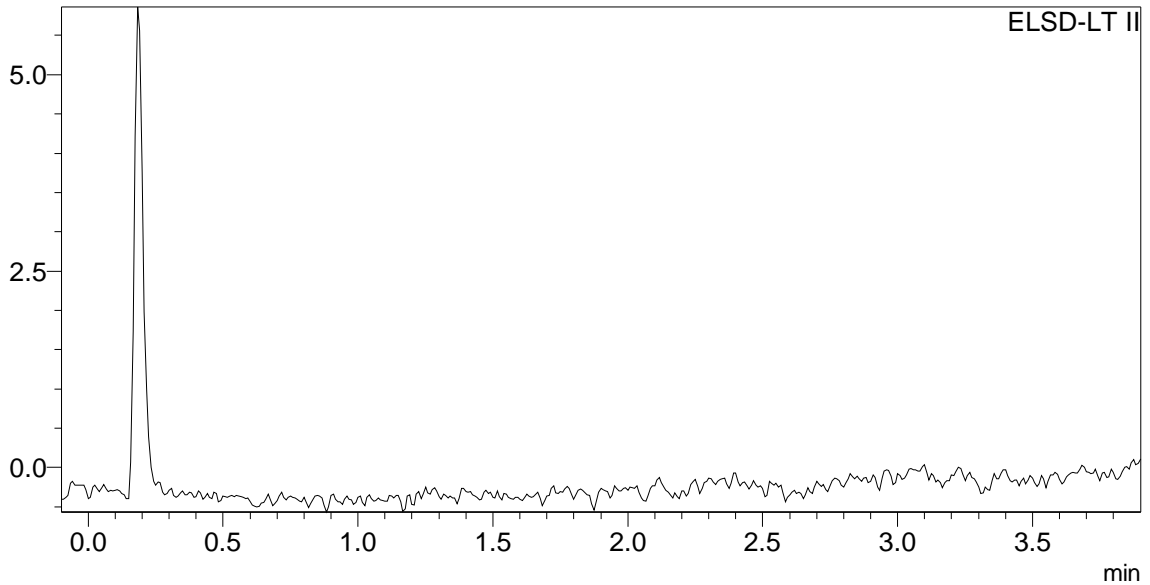
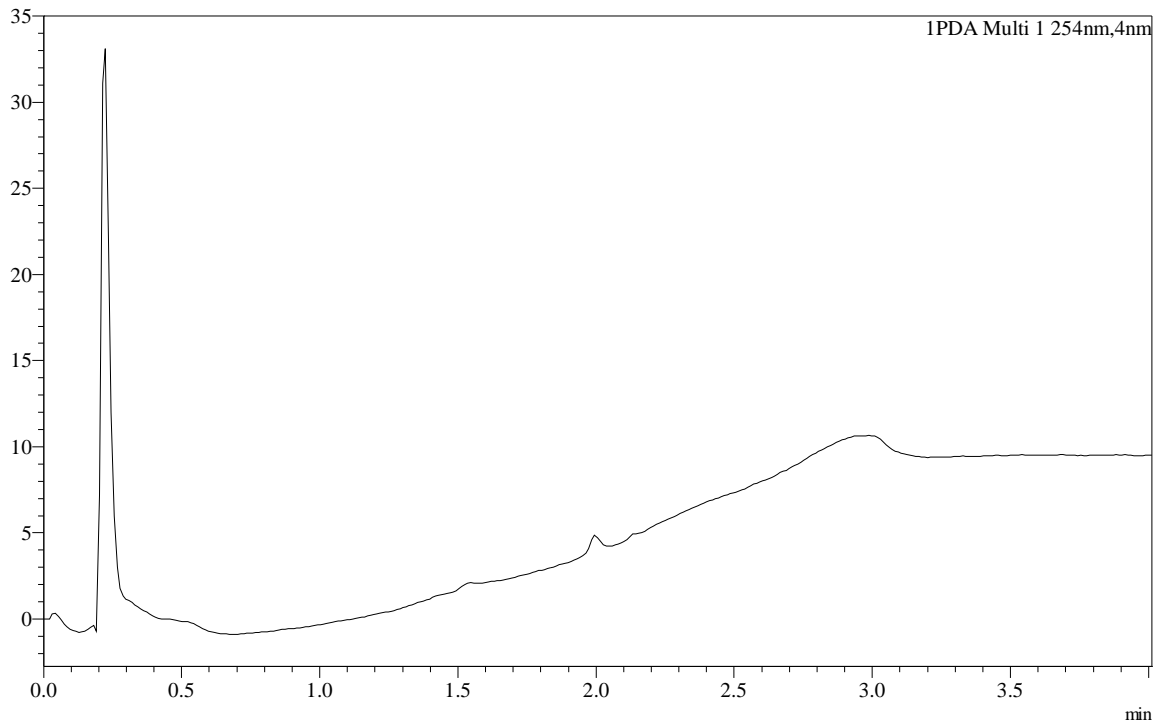
Vial# : 10

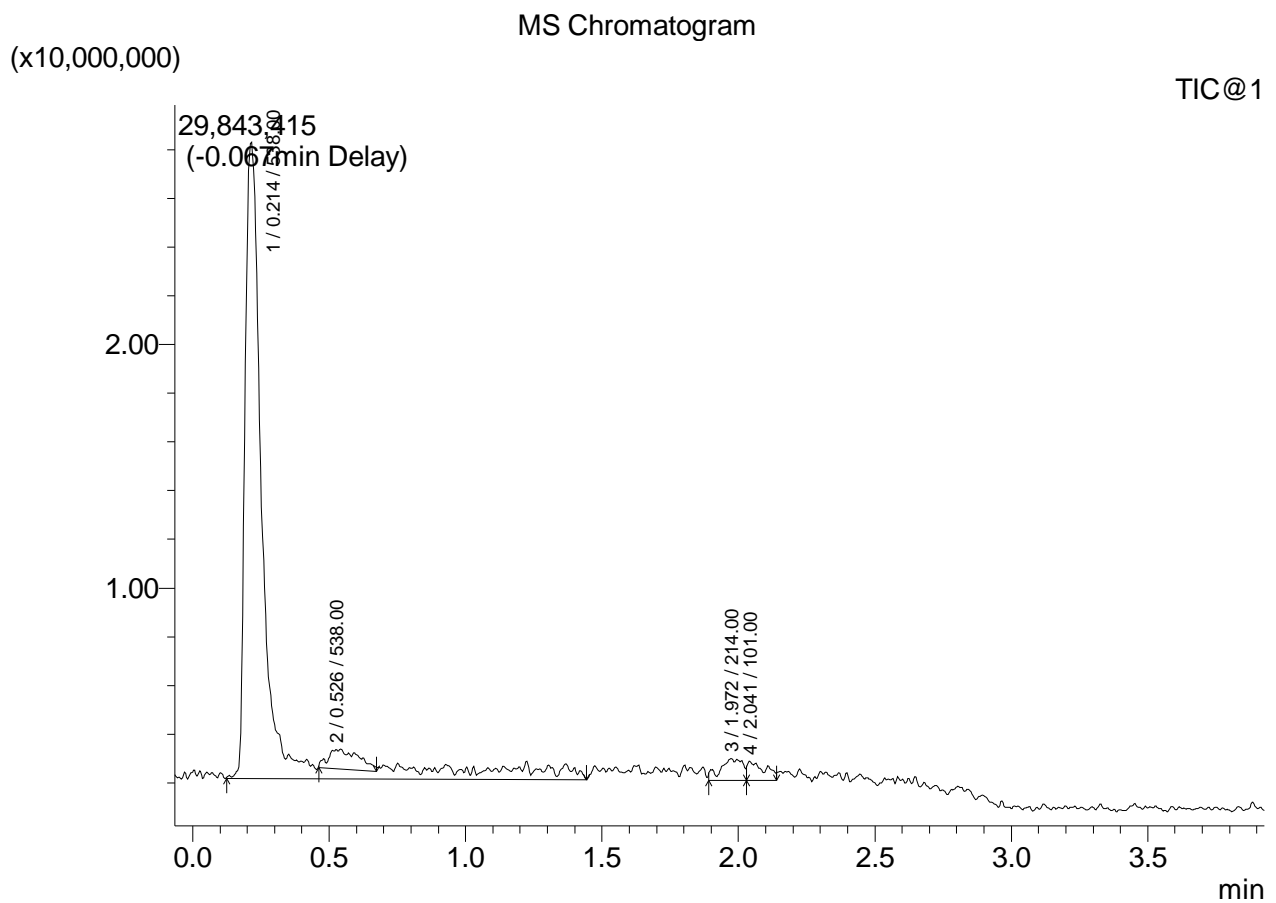
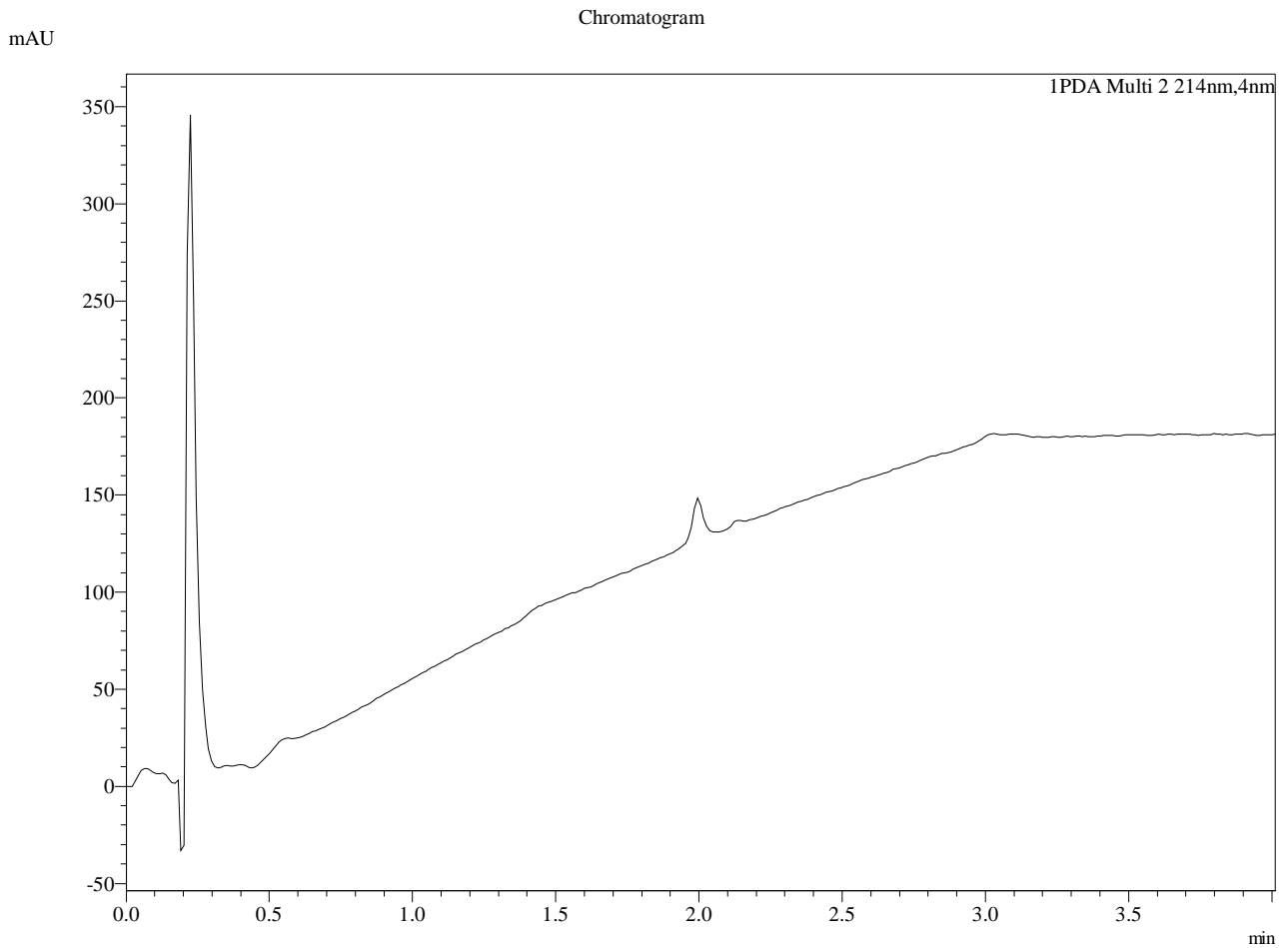
Injection Volume : 10

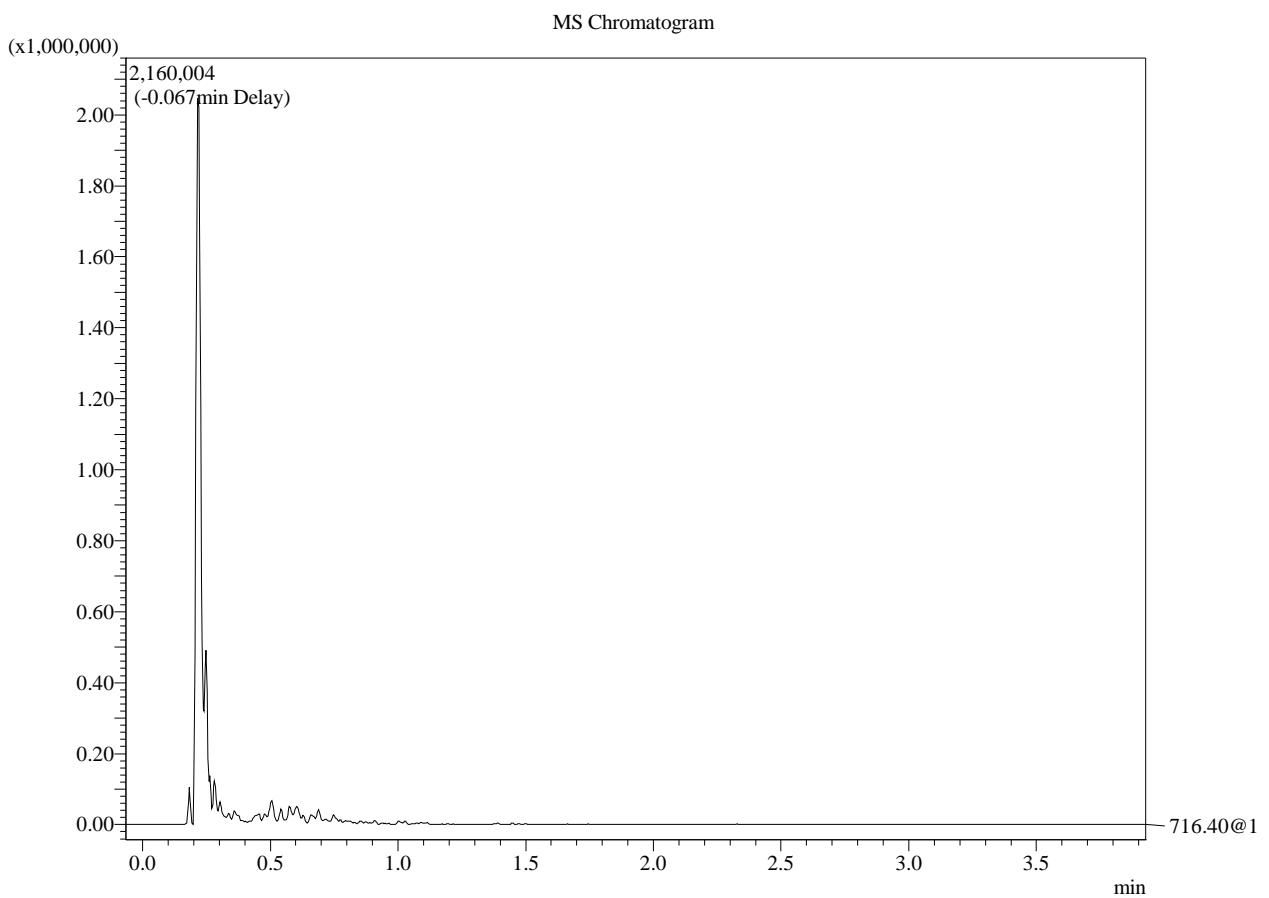
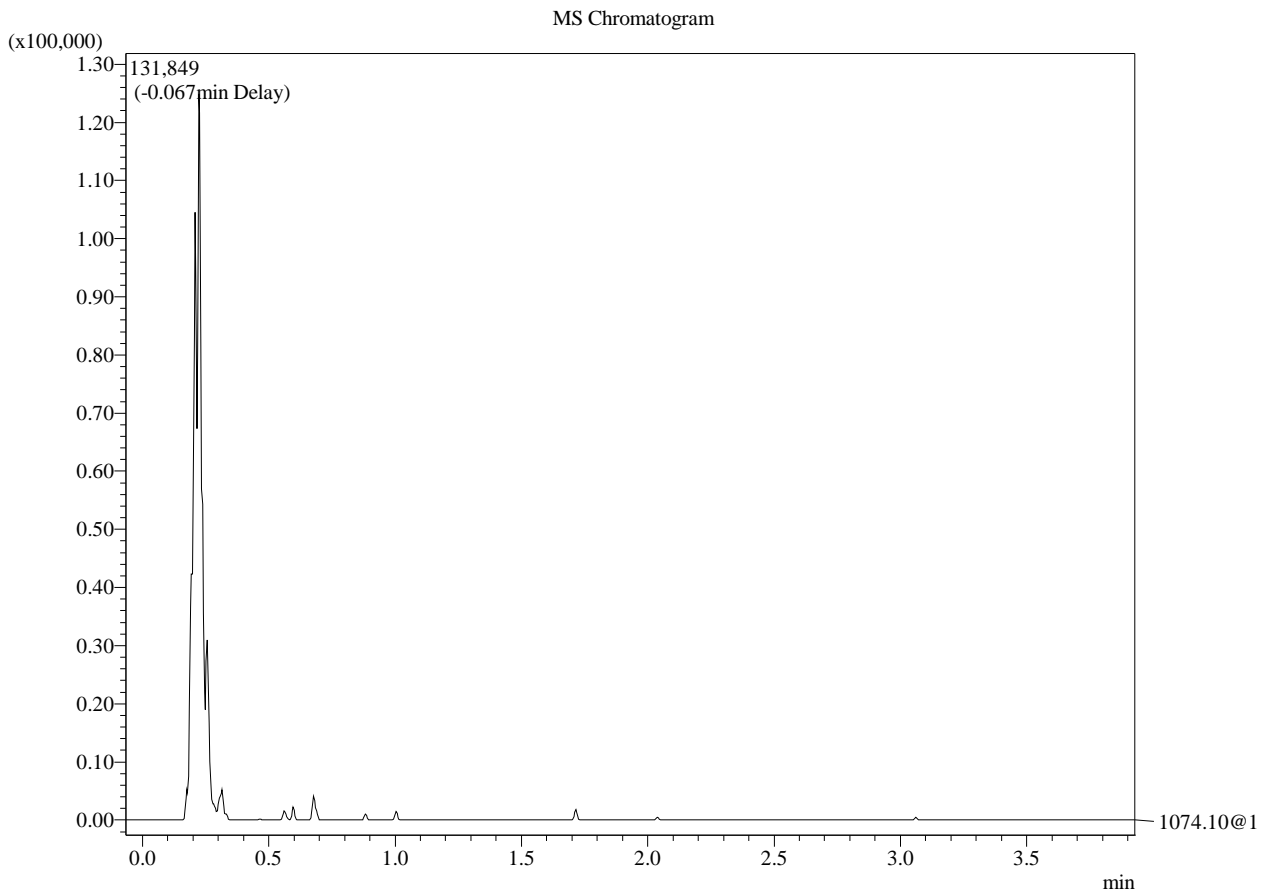
Data File : C:\LabSolutions\Data\Project1\Purification\QCs\Jan29-2016\KO\DynA-1\_fracQC4.lcd

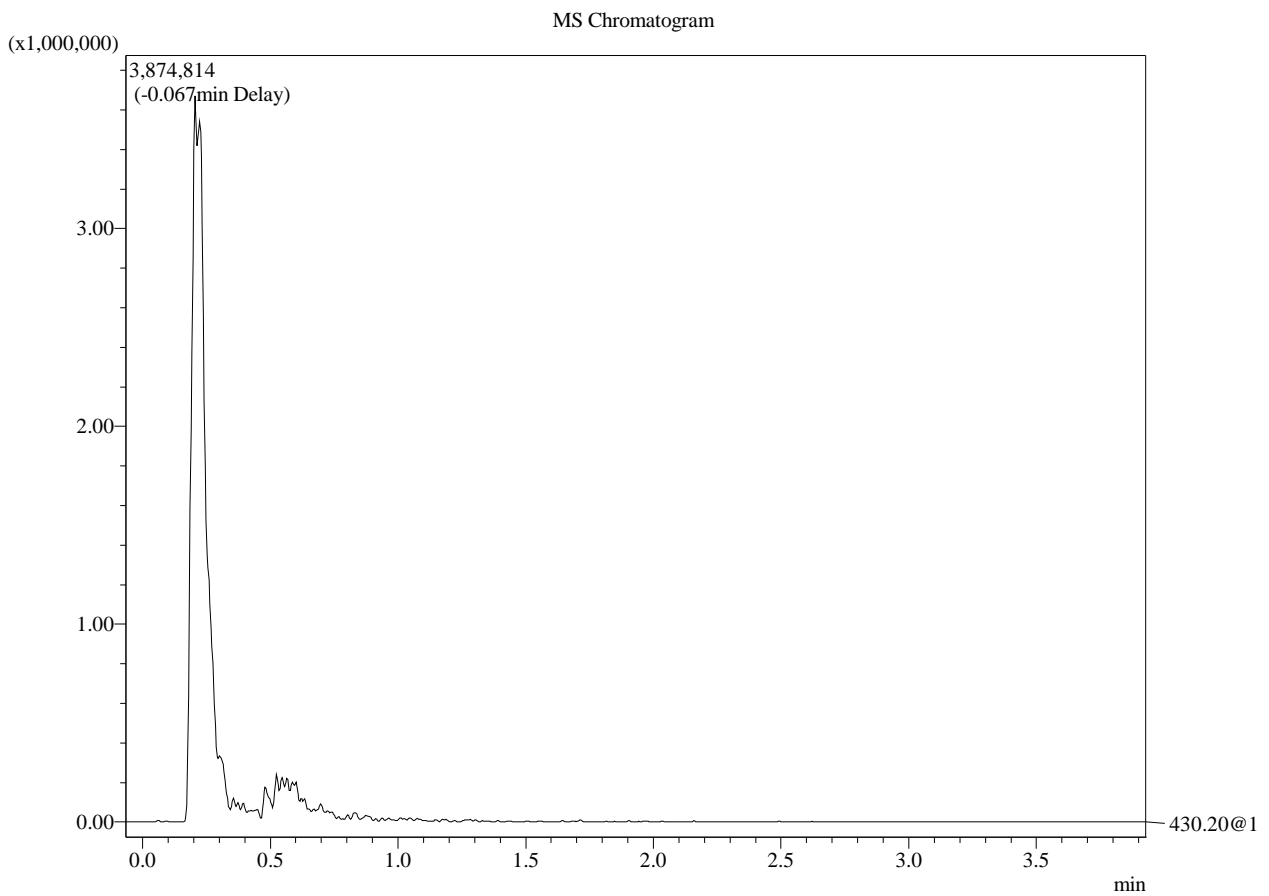
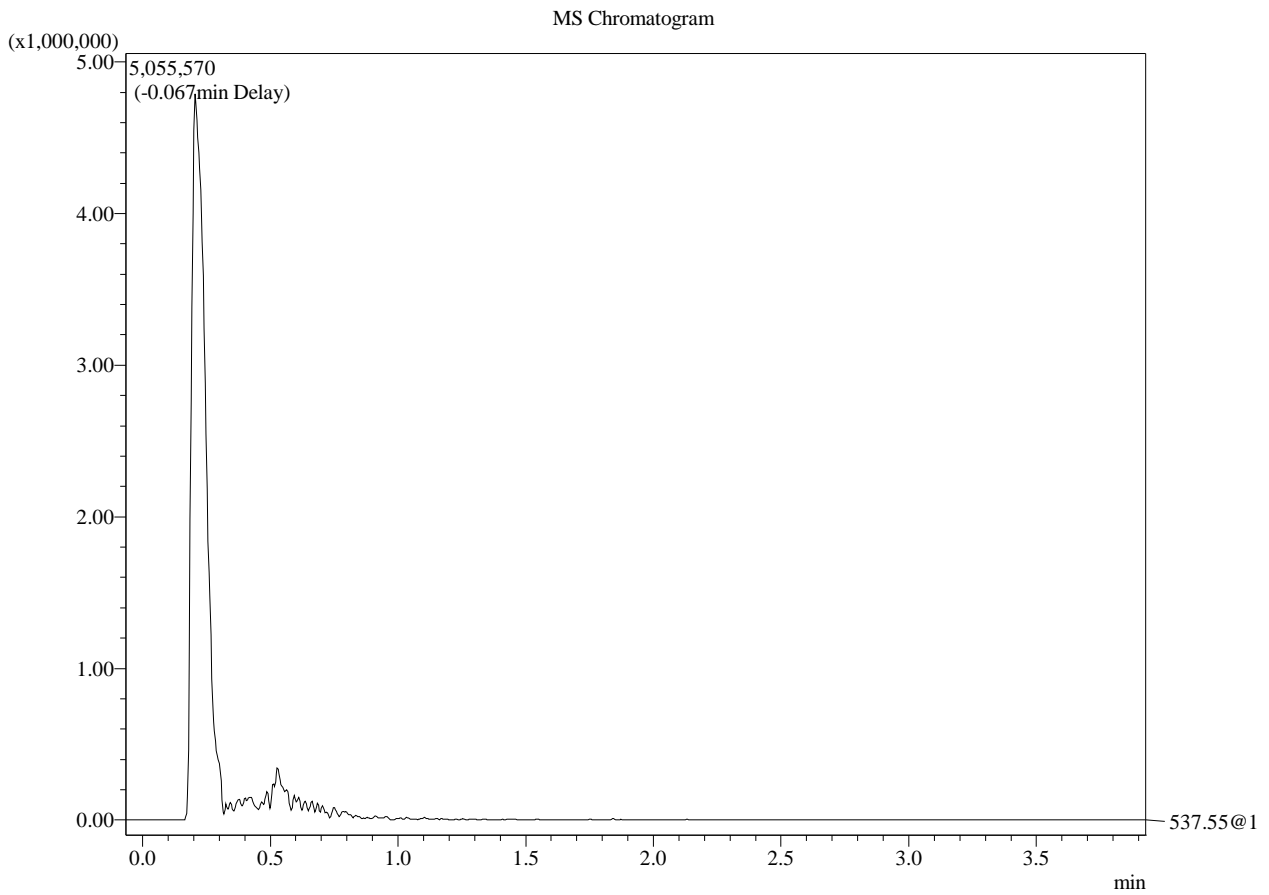
Month-Day Acquired : 1/28/2016

Original Method File : StandardRunPlates.lcm

C:\LabSolutions\Data\Project1\Purification\QCs\Jan29-2016\KO\DynA-1\_fracQC4.lcd  
mVmAU  
Chromatogram

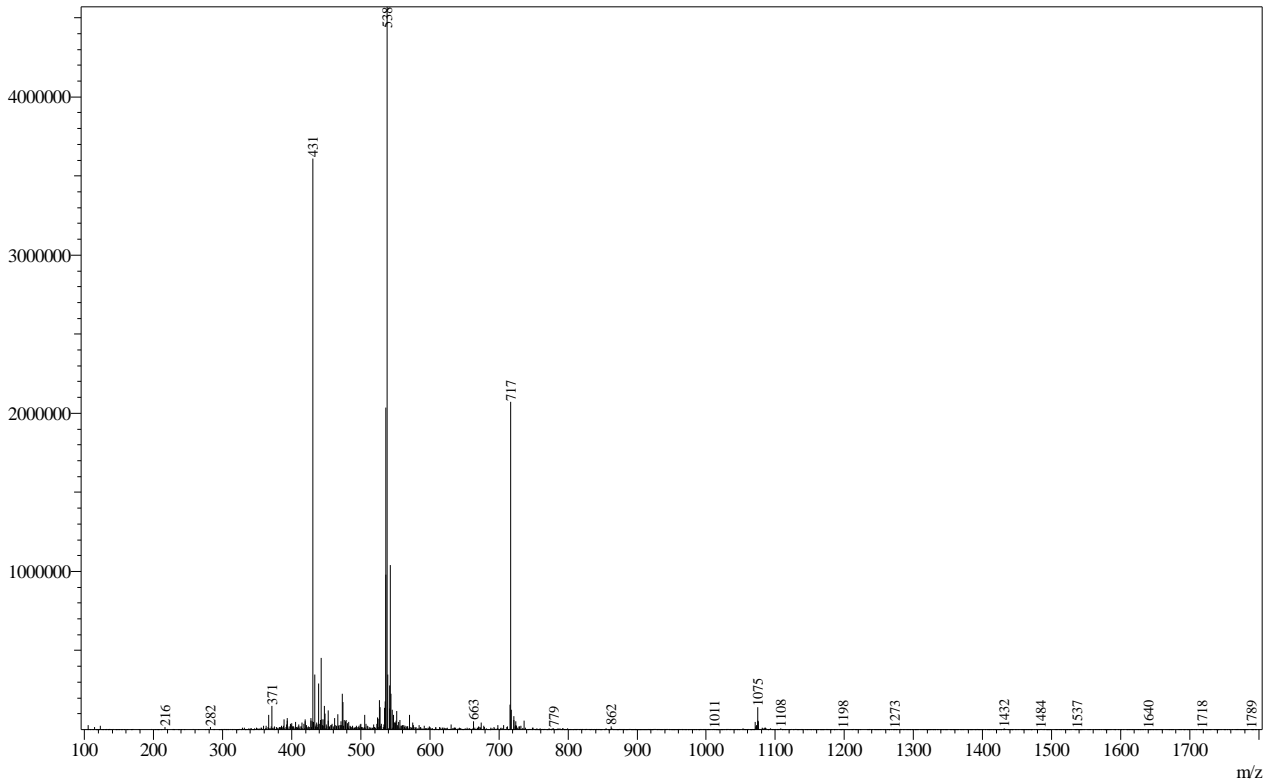




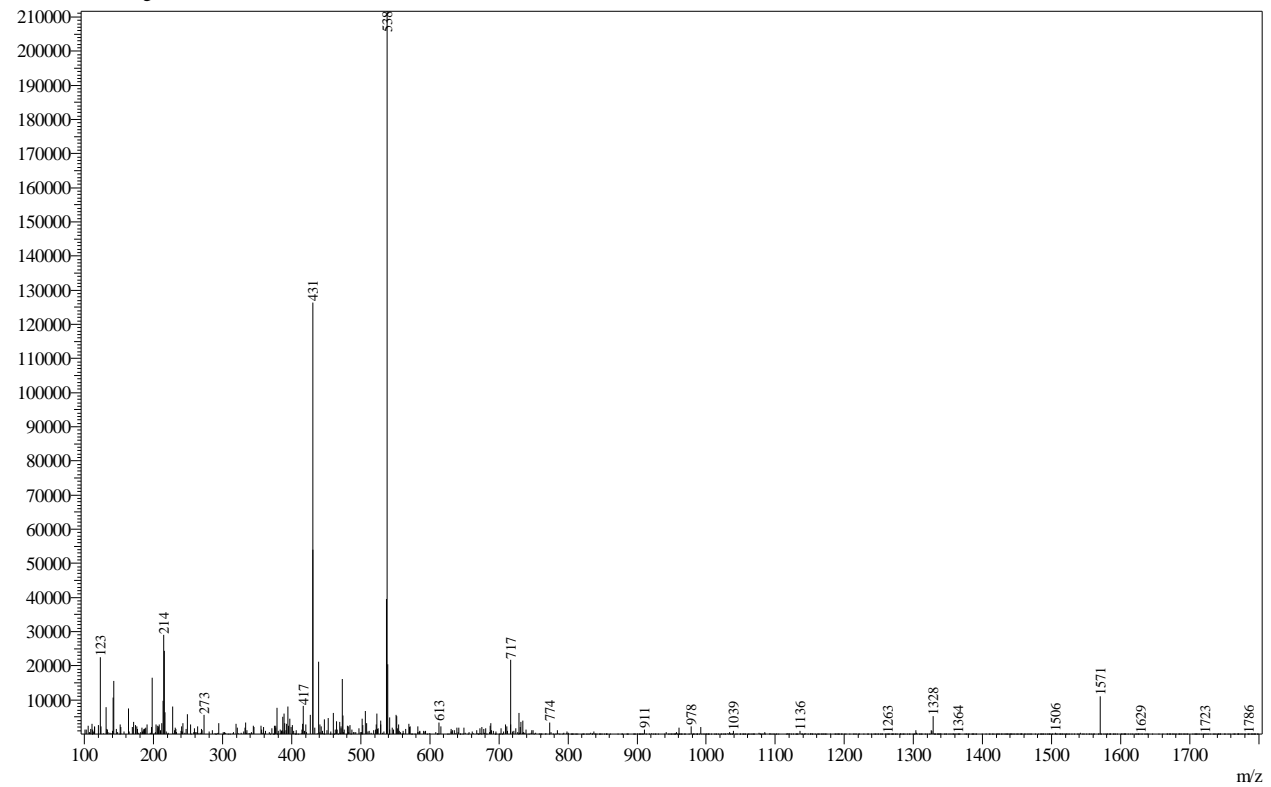


## Mass Spectrum

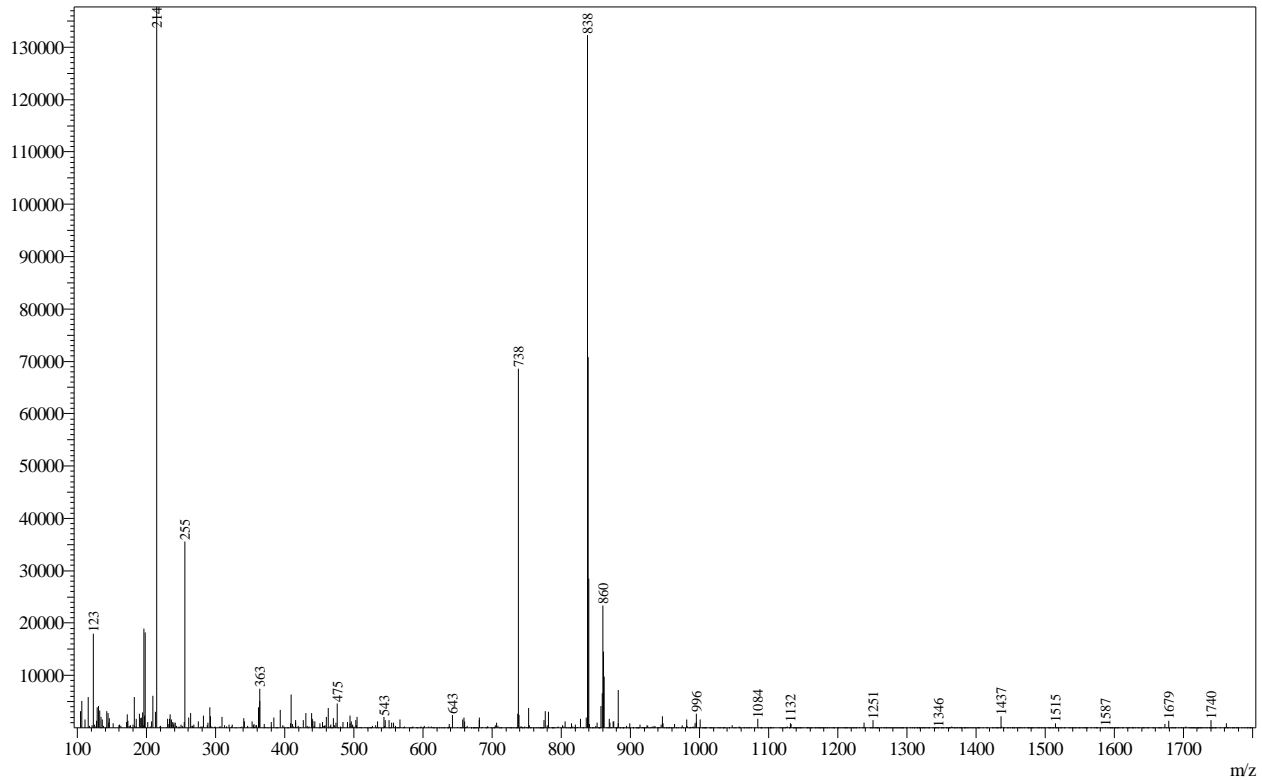
Peak#:1 R.Time:0.214(Scan#:78)  
MassPeaks:1232  
Spectrum Mode:Averaged 0.212-0.219(77-79)  
BG Mode:Calc Segment 1 - Event 1



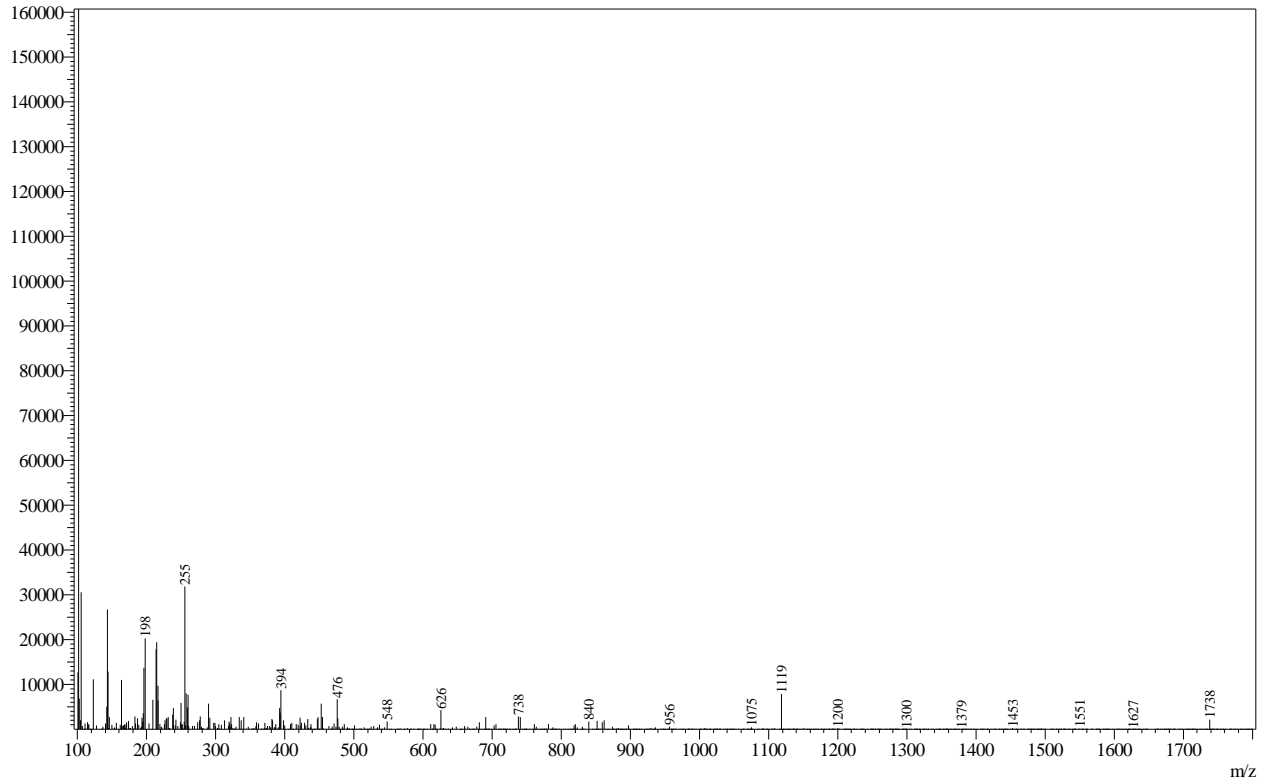
Peak#:2 R.Time:0.526(Scan#:163)  
MassPeaks:826  
Spectrum Mode:Averaged 0.524-0.531(162-164)  
BG Mode:Calc Segment 1 - Event 1



Peak#:3 R.Time:1.972(Scan#:557)  
MassPeaks:827  
Spectrum Mode:Averaged 1.968-1.976(556-558)  
BG Mode:Calc Segment 1 - Event 1



Peak#:4 R.Time:2.041(Scan#:576)  
MassPeaks:847  
Spectrum Mode:Averaged 2.038-2.045(575-577)  
BG Mode:Calc Segment 1 - Event 1



**==== BIO5 Analytical Lab Report ====**

C:\LabSolutions\Data\Project1\Purification\QCs\Jan12-2016\DynB\_fracQC-5.lcd

Sample Name : DynB\_fracQC-5

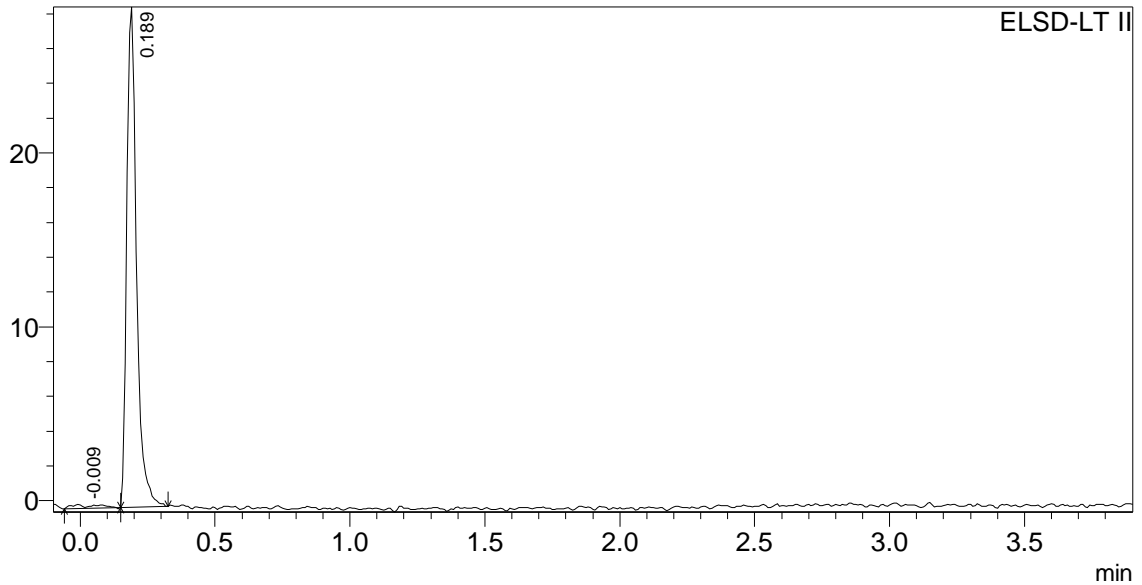
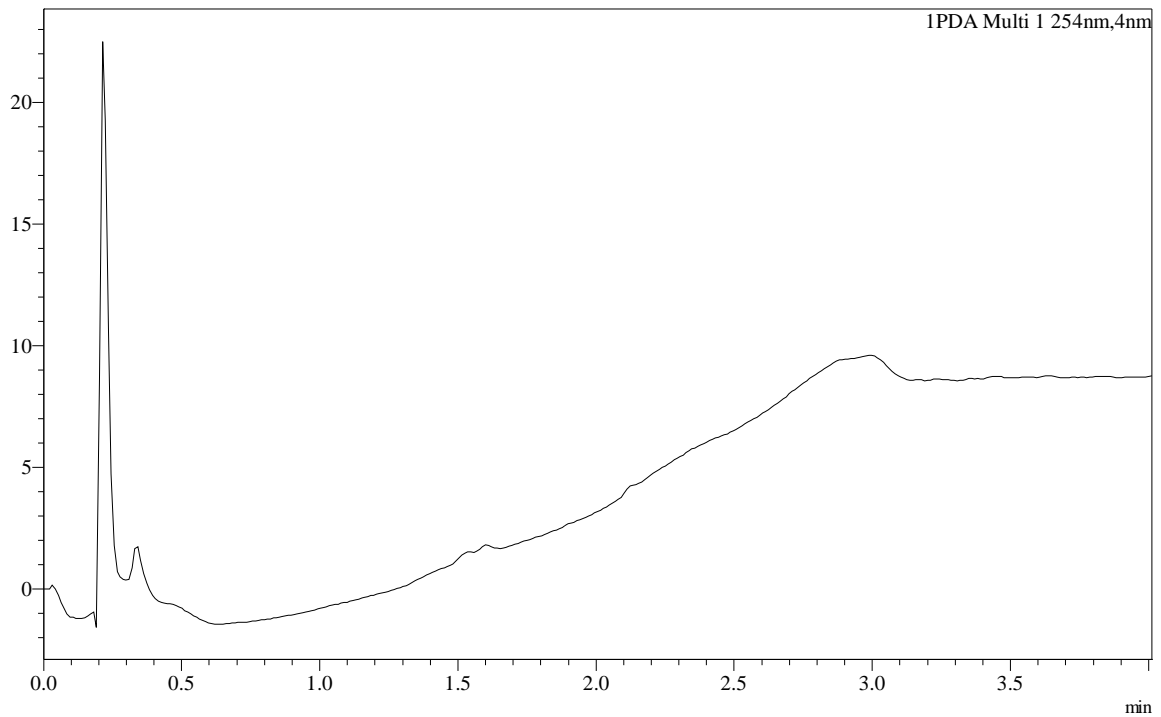
Vial# : 81

Injection Volume : 10

Data File : C:\LabSolutions\Data\Project1\Purification\QCs\Jan12-2016\DynB\_fracQC-5.lcd

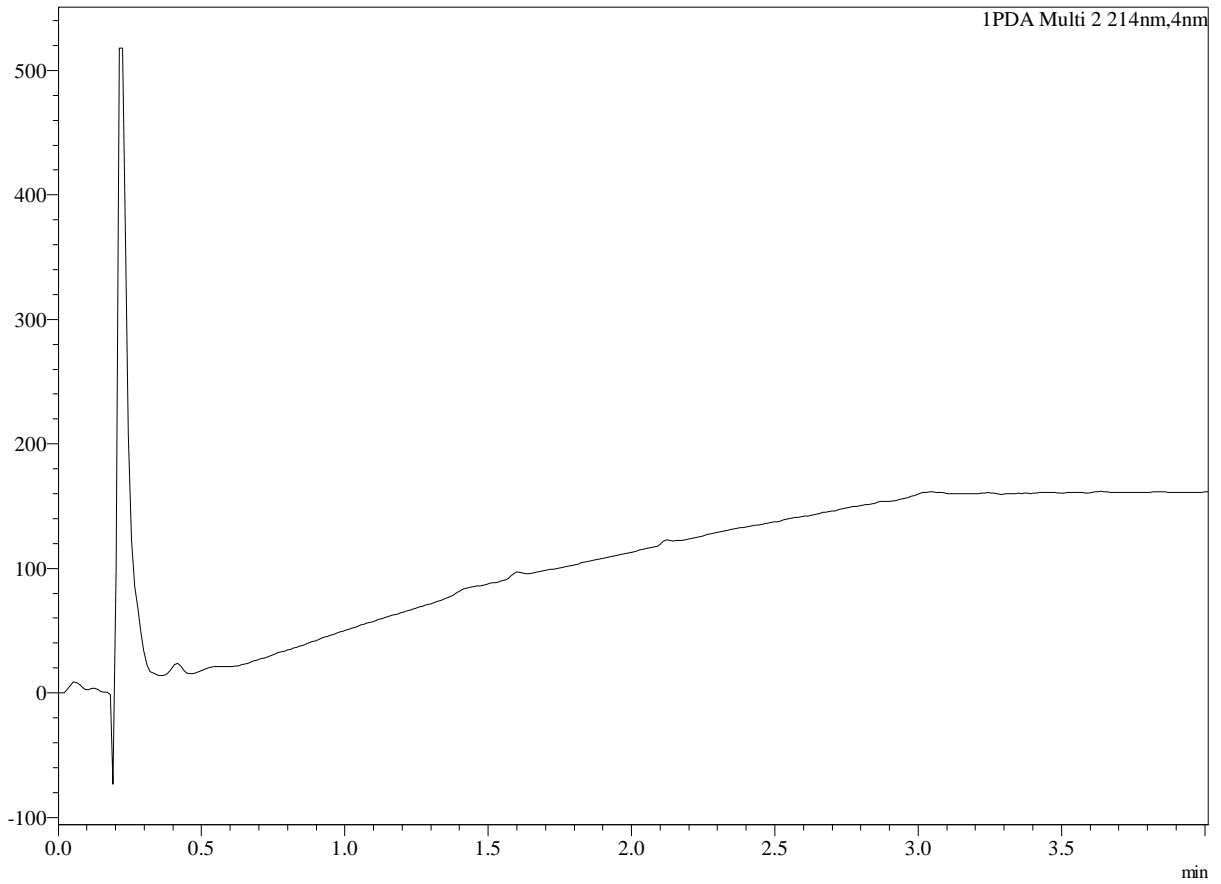
Month-Day Acquired : 1/12/2016

Original Method File : StandardRunPlates.lcm

C:\LabSolutions\Data\Project1\Purification\QCs\Jan12-2016\DynB\_fracQC-5.lcd  
mVmAU  
Chromatogram

mAU

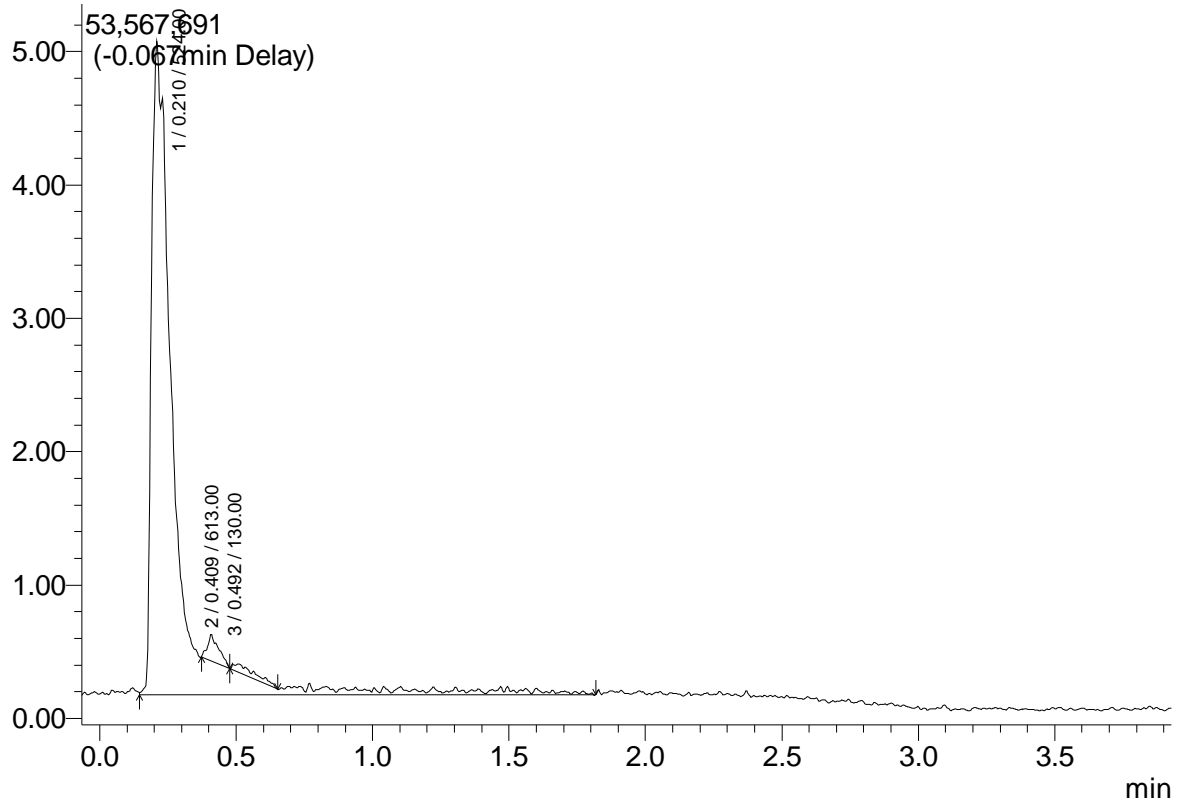
Chromatogram



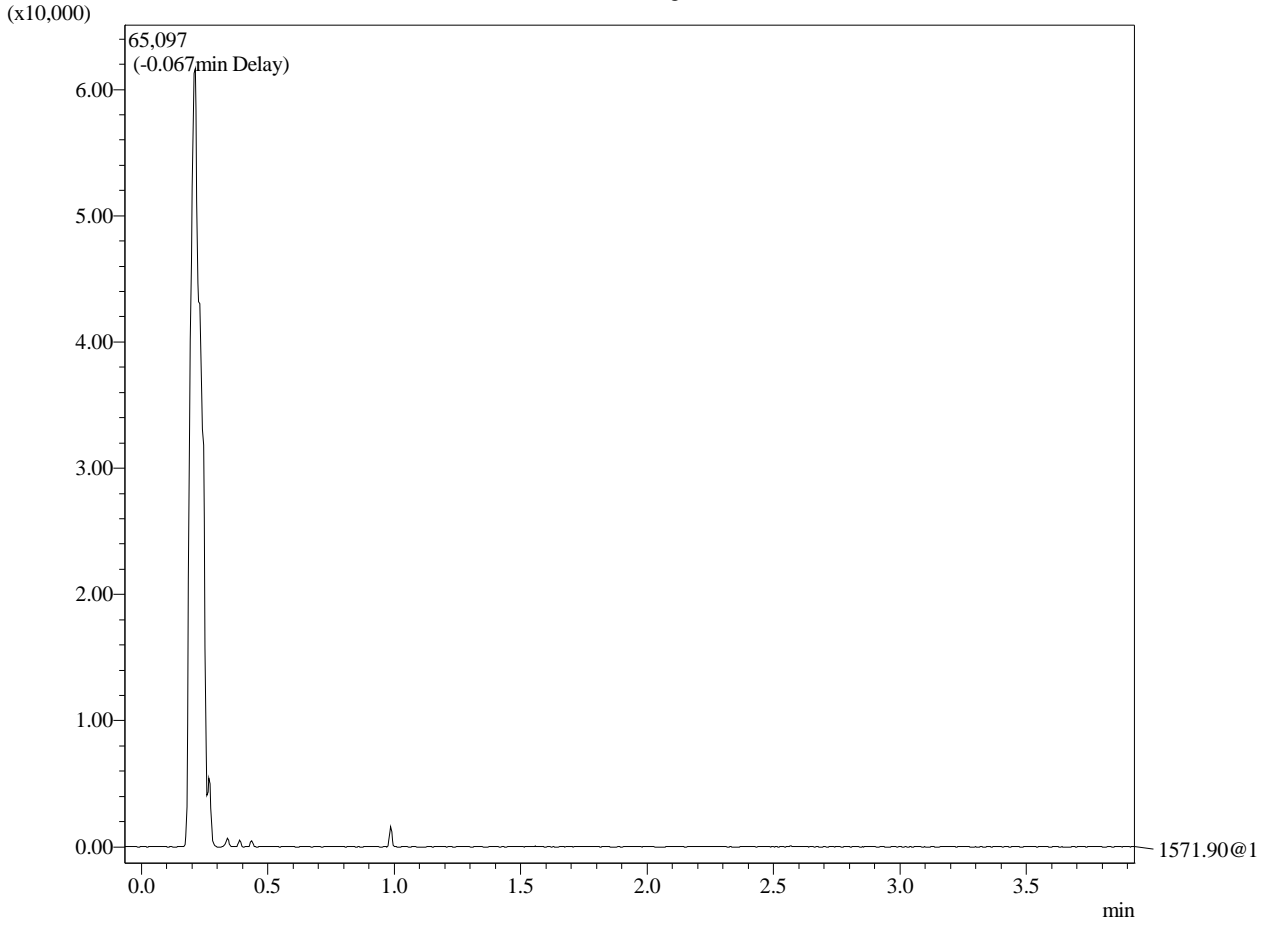
MS Chromatogram

(x10,000,000)

TIC@1

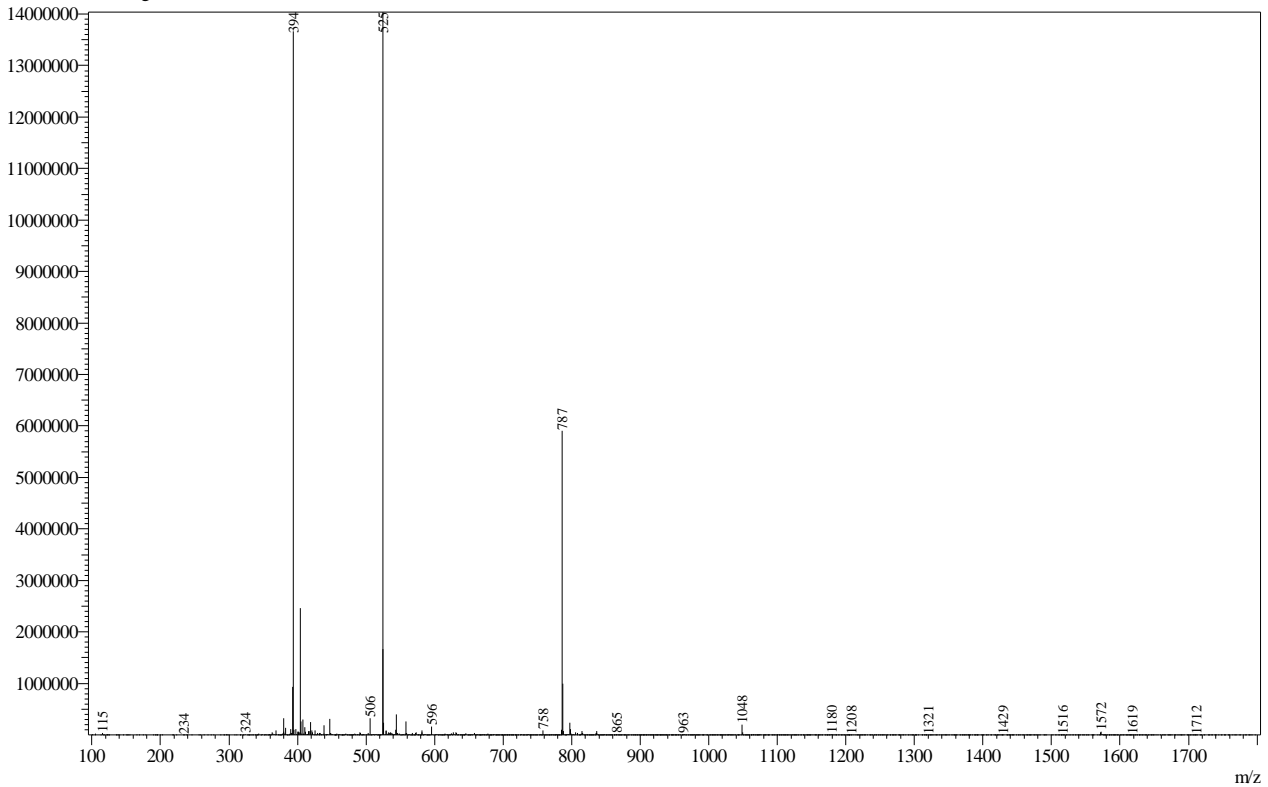


MS Chromatogram

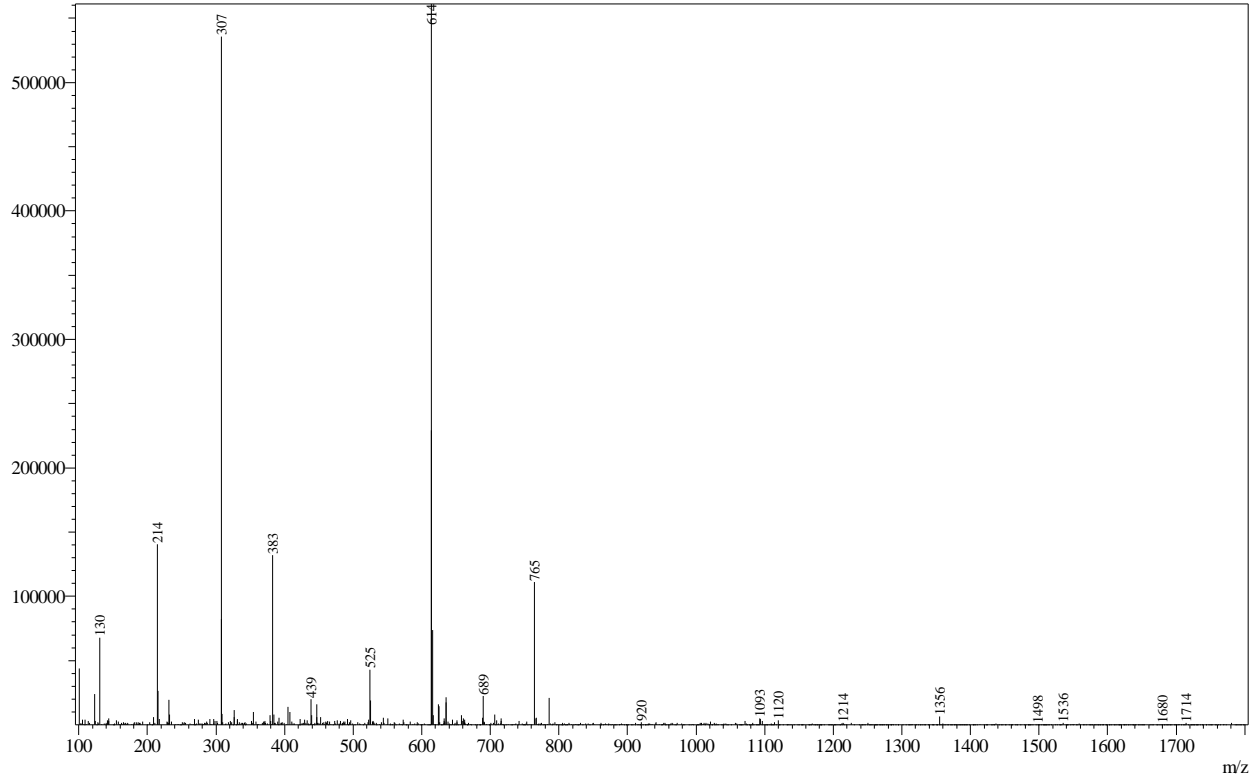


Mass Spectrum

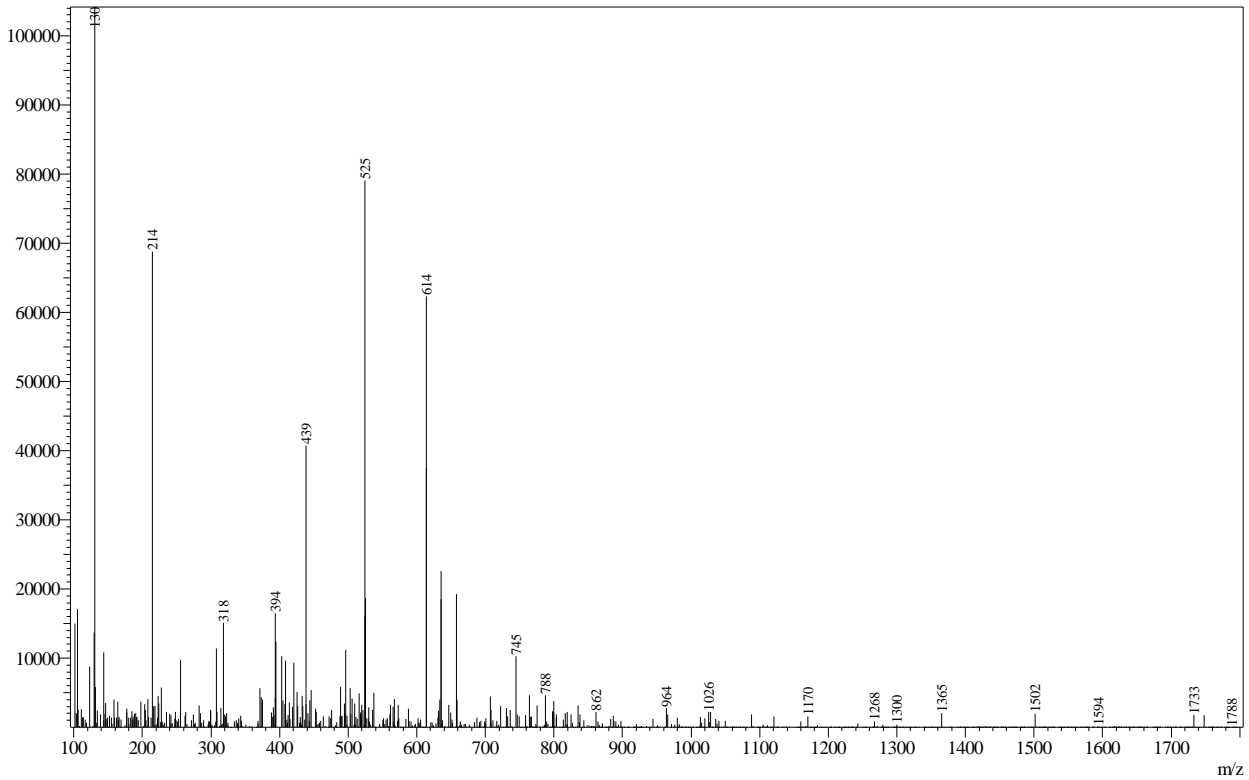
Peak#: 1 R.Time: 0.210 (Scan#: 76)  
 MassPeaks: 1199  
 Spectrum Mode: Averaged 0.205-0.212 (75-77)  
 BG Mode: Calc Segment 1 - Event 1



Peak#:2 R.Time:0.409(Scan#:131)  
MassPeaks:878  
Spectrum Mode:Averaged 0.406-0.414(130-132)  
BG Mode:Calc Segment 1 - Event 1



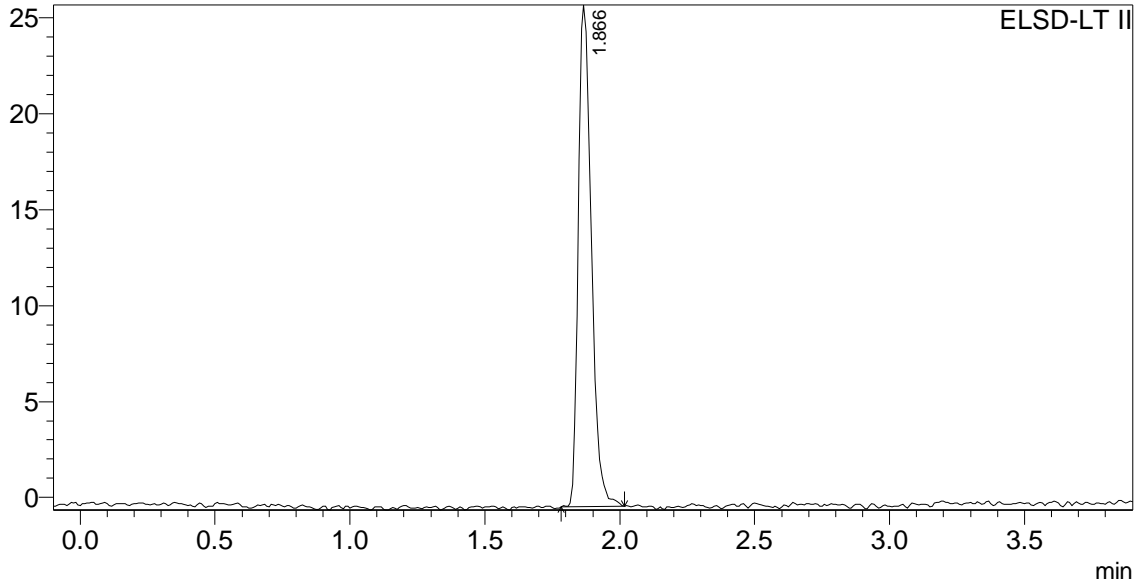
Peak#:3 R.Time:0.492(Scan#:153)  
MassPeaks:912  
Spectrum Mode:Averaged 0.487-0.494(152-154)  
BG Mode:Calc Segment 1 - Event 1



## ==== BIO5 Analytical Lab Report ====

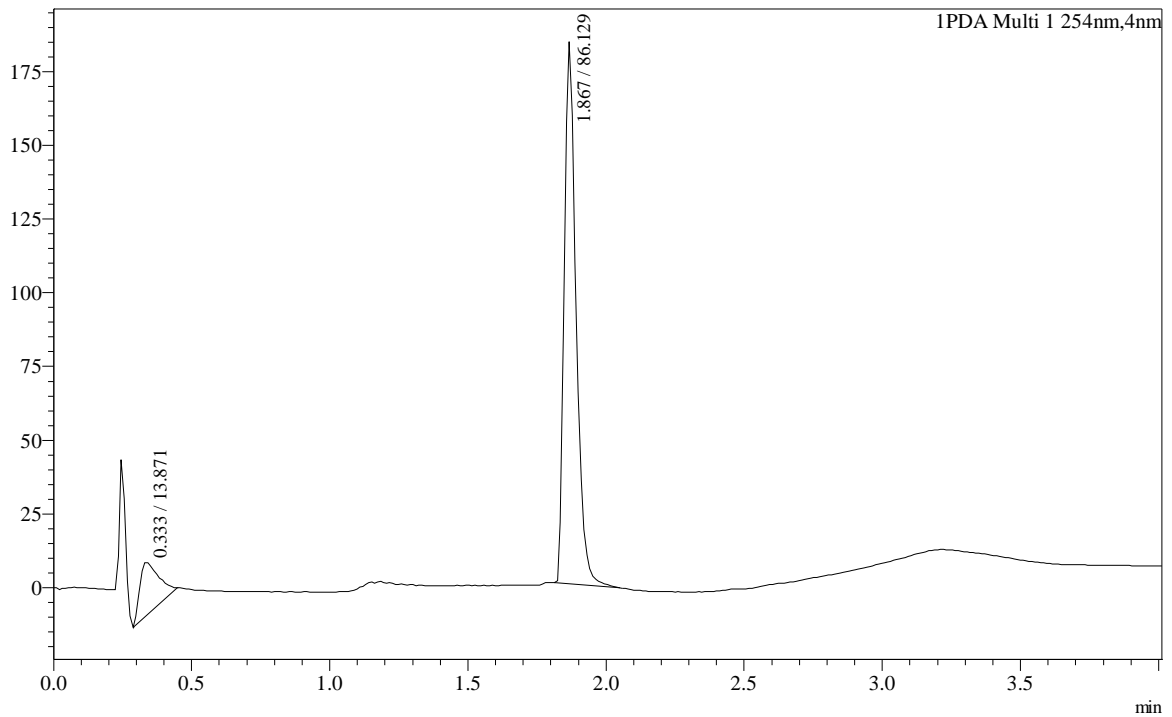
C:\LabSolutions\Data\Project1\Purification\QCs\Feb25-2016\Endomorphin-1\_4.lcd

Sample Name : Endomorphin-1\_4  
Vial# : 23  
Injection Volume : 10  
Data File : C:\LabSolutions\Data\Project1\Purification\QCs\Feb25-2016\Endomorphin-1\_4.lcd  
Month-Day Acquired : 2/25/2016  
Original Method File : StandardRunPlates.lcm

C:\LabSolutions\Data\Project1\Purification\QCs\Feb25-2016\Endomorphin-1\_4.lcd  
mV

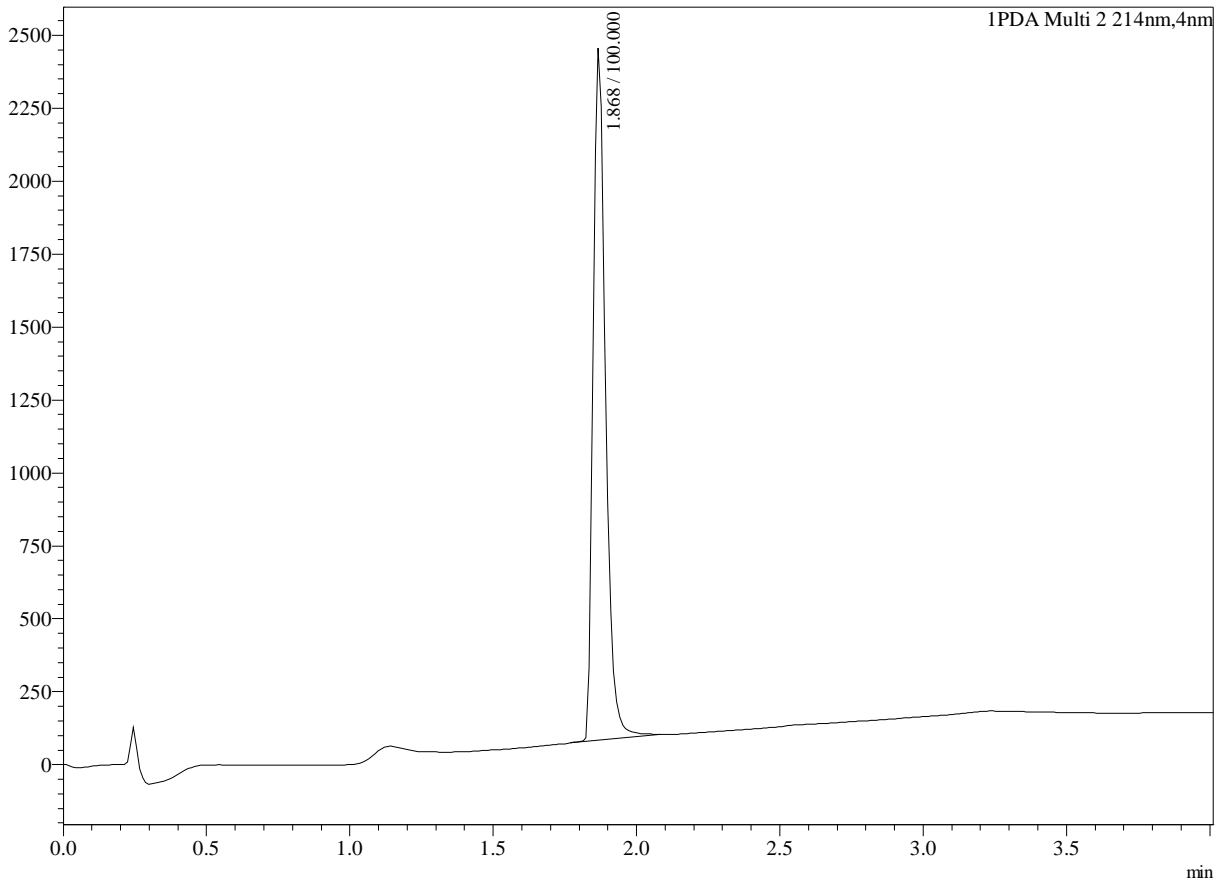
Chromatogram

mAU



mAU

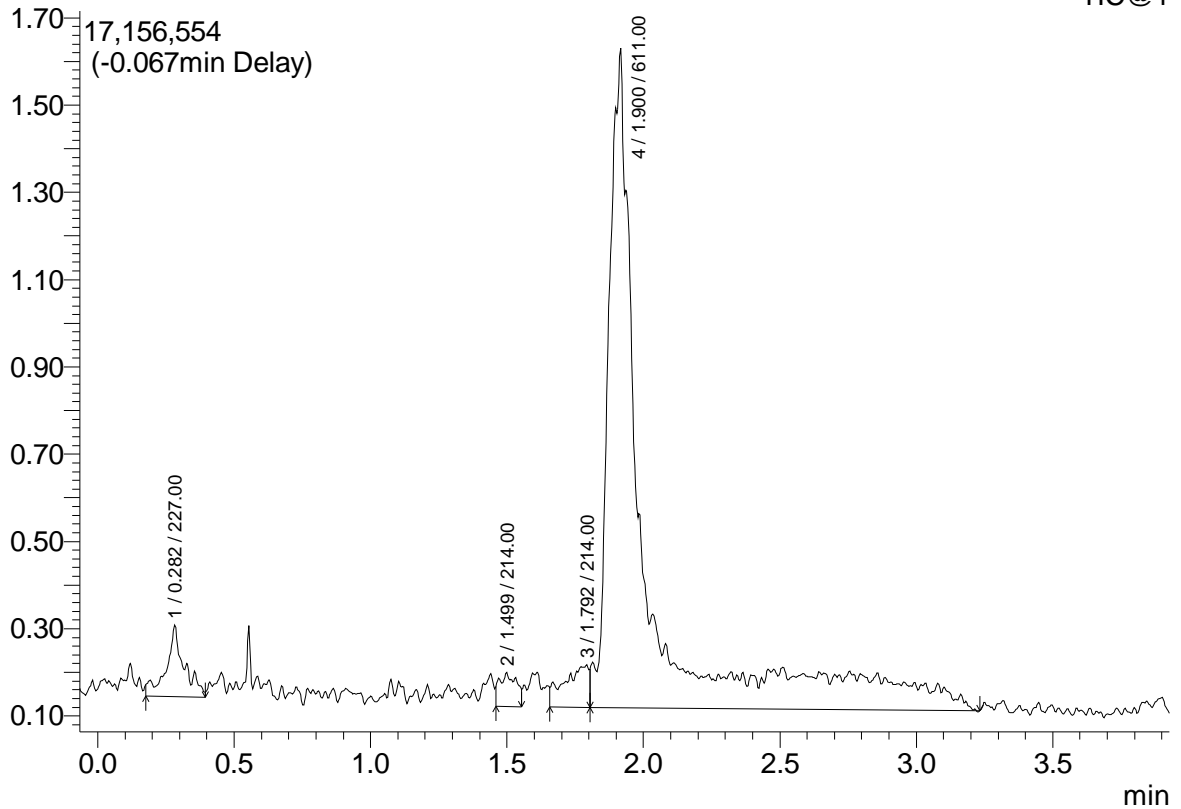
Chromatogram

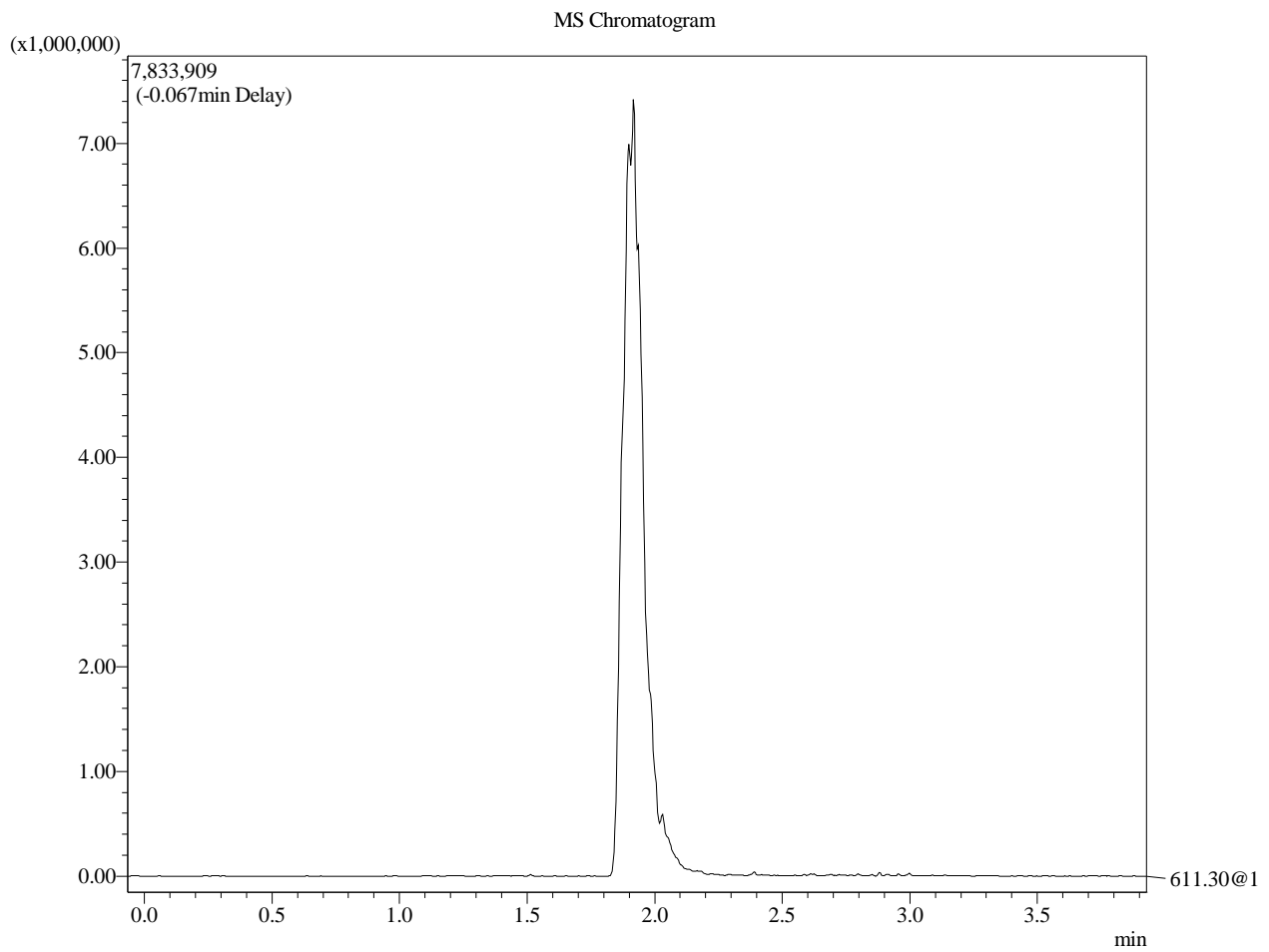


MS Chromatogram

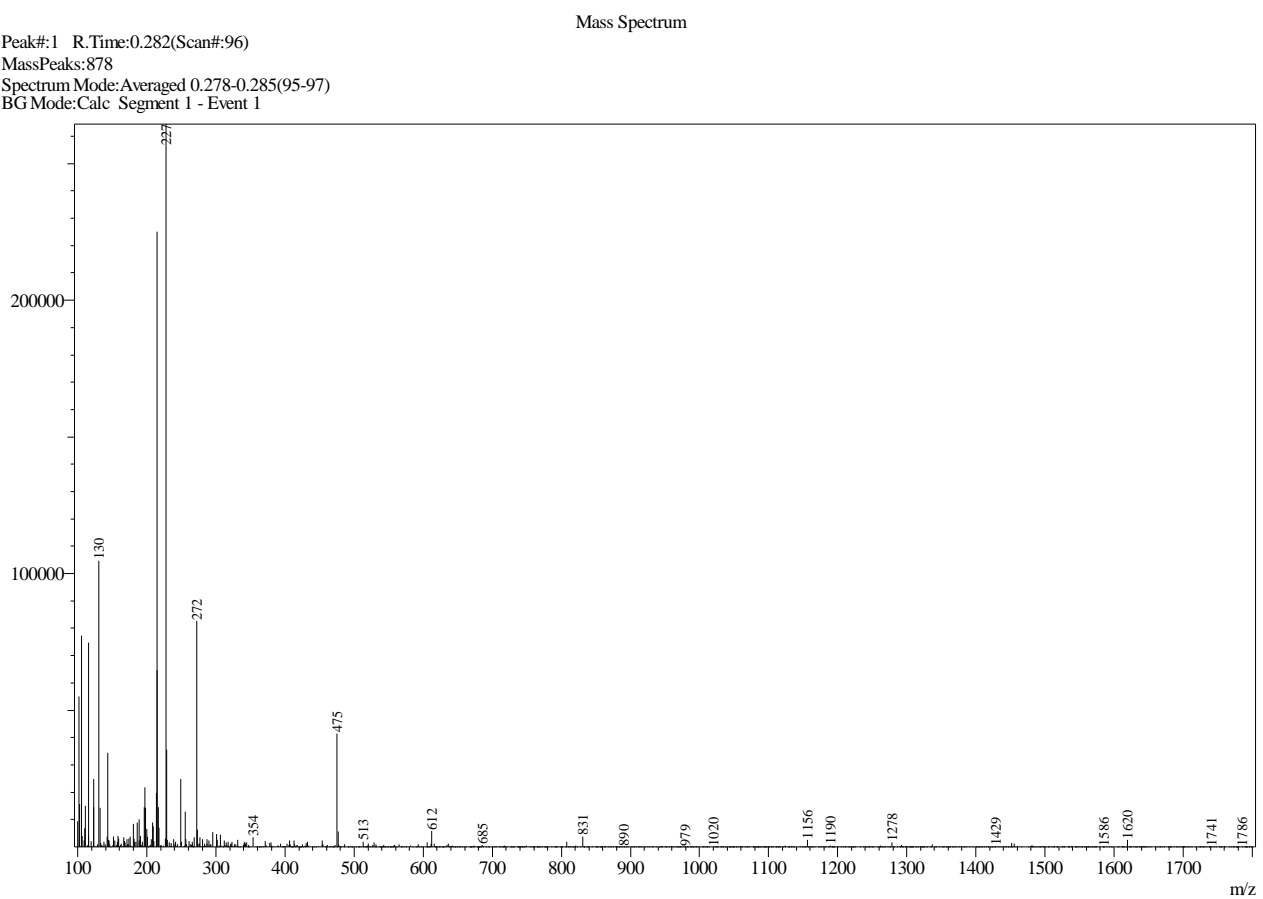
(x10,000,000)

TIC@1

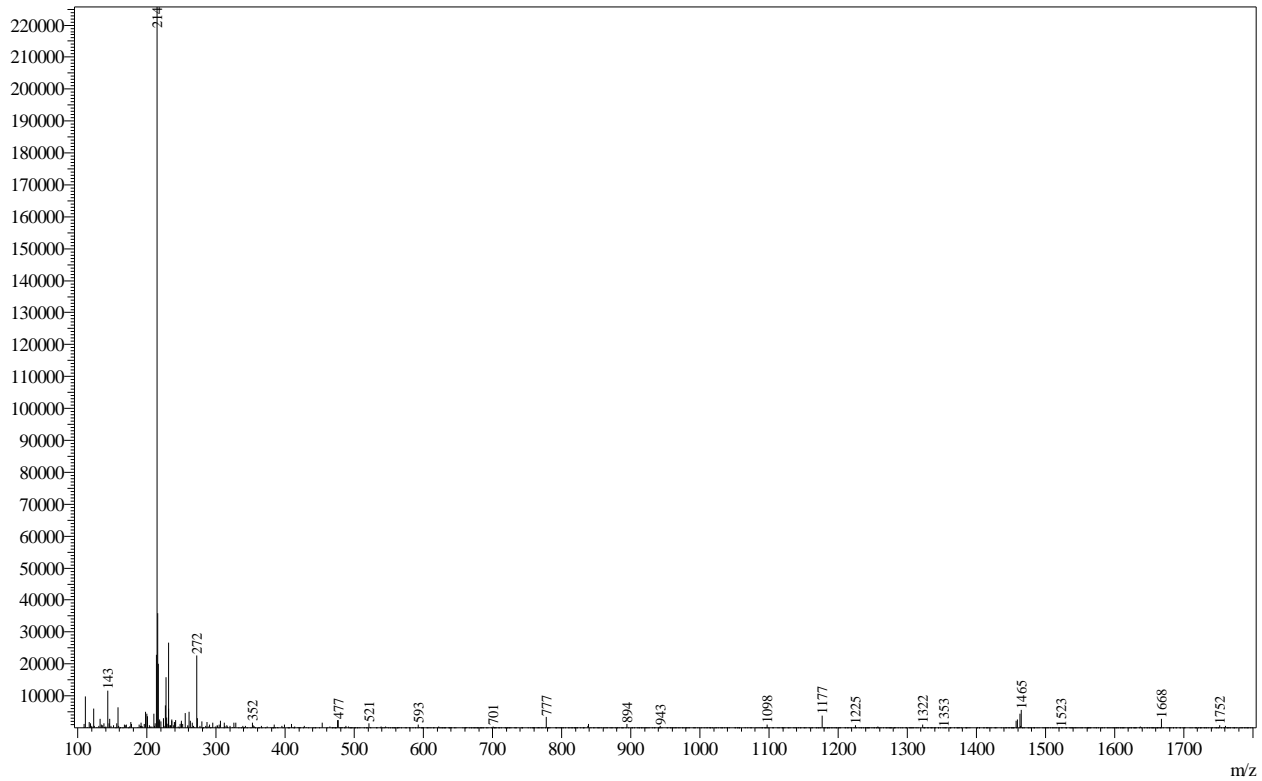




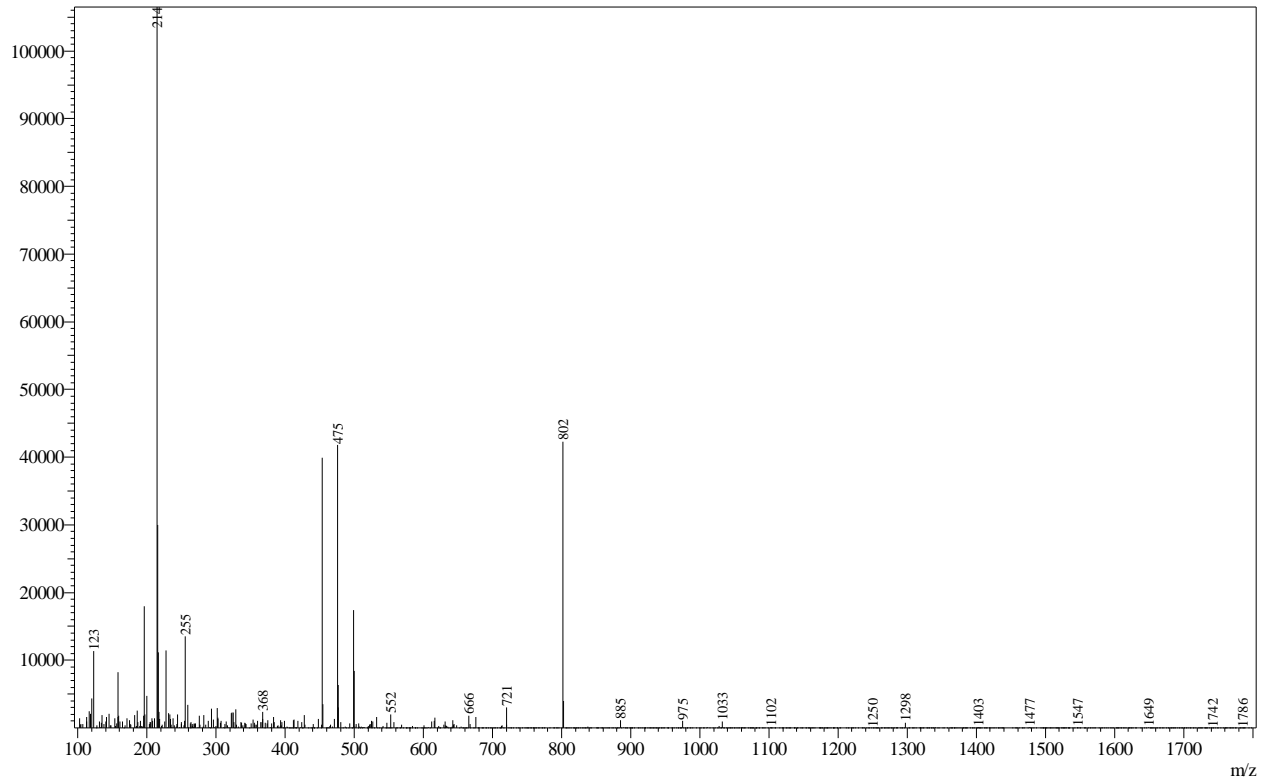
Peak#: 1 R.Time: 0.282(Scan#: 96)  
MassPeaks: 878  
Spectrum Mode: Averaged 0.278-0.285(95-97)  
BG Mode: Calc Segment 1 - Event 1



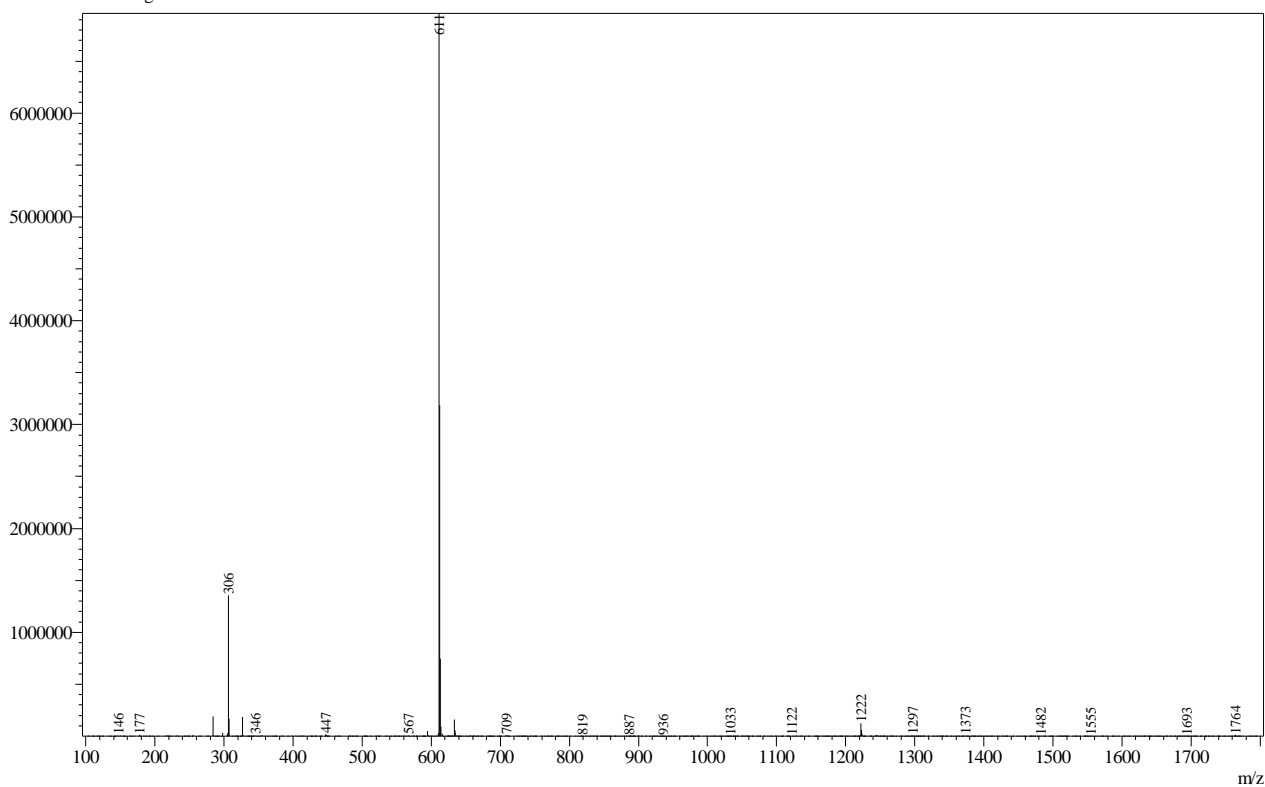
Peak#:2 R.Time:1.499(Scan#:428)  
MassPeaks:785  
Spectrum Mode:Averaged 1.495-1.503(427-429)  
BG Mode:Calc Segment 1 - Event 1



Peak#:3 R.Time:1.792(Scan#:508)  
MassPeaks:848  
Spectrum Mode:Averaged 1.789-1.796(507-509)  
BG Mode:Calc Segment 1 - Event 1



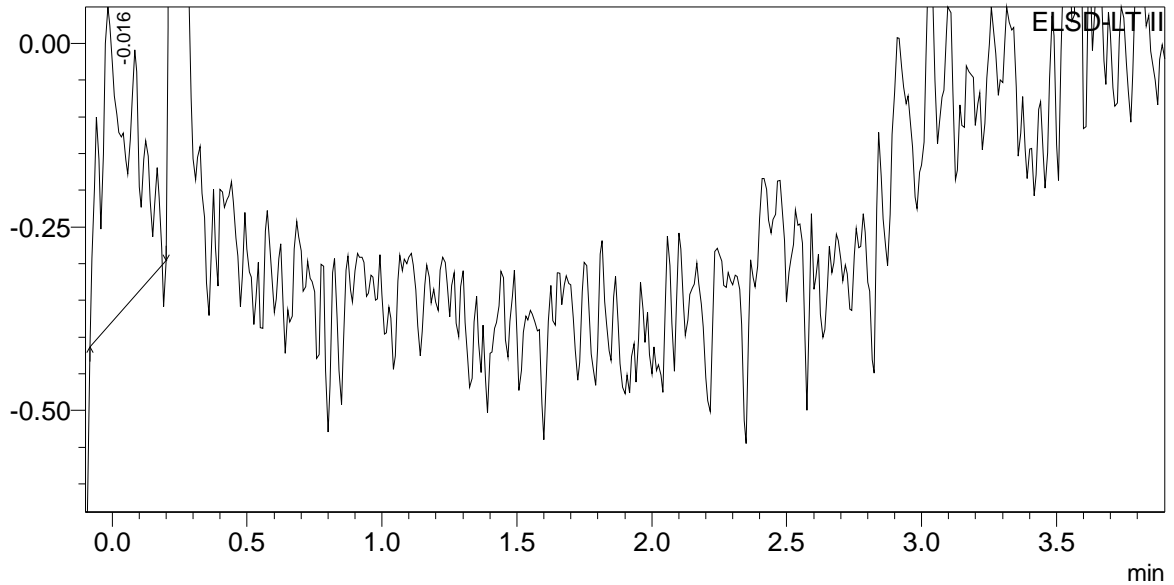
Peak#4 R.Time:1.900(Scan#:537)  
MassPeaks:904  
Spectrum Mode:Averaged 1.895-1.902(536-538)  
BG Mode:Calc Segment 1 - Event 1



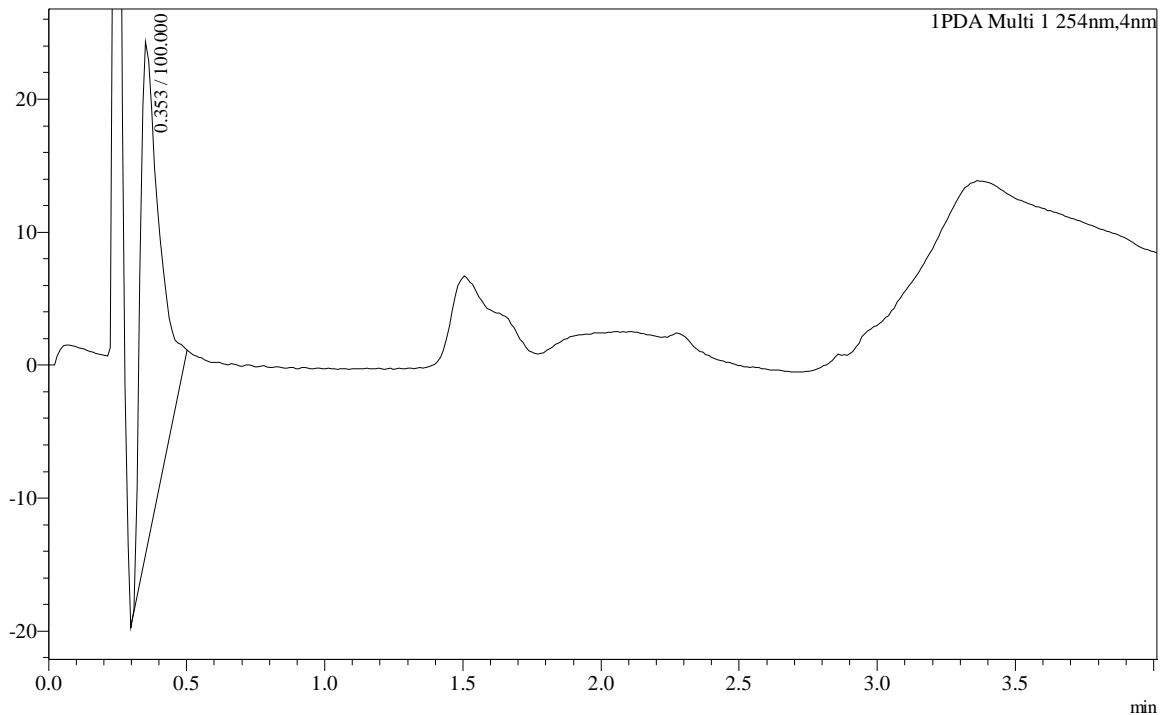
## ==== BIO5 Analytical Lab Report ====

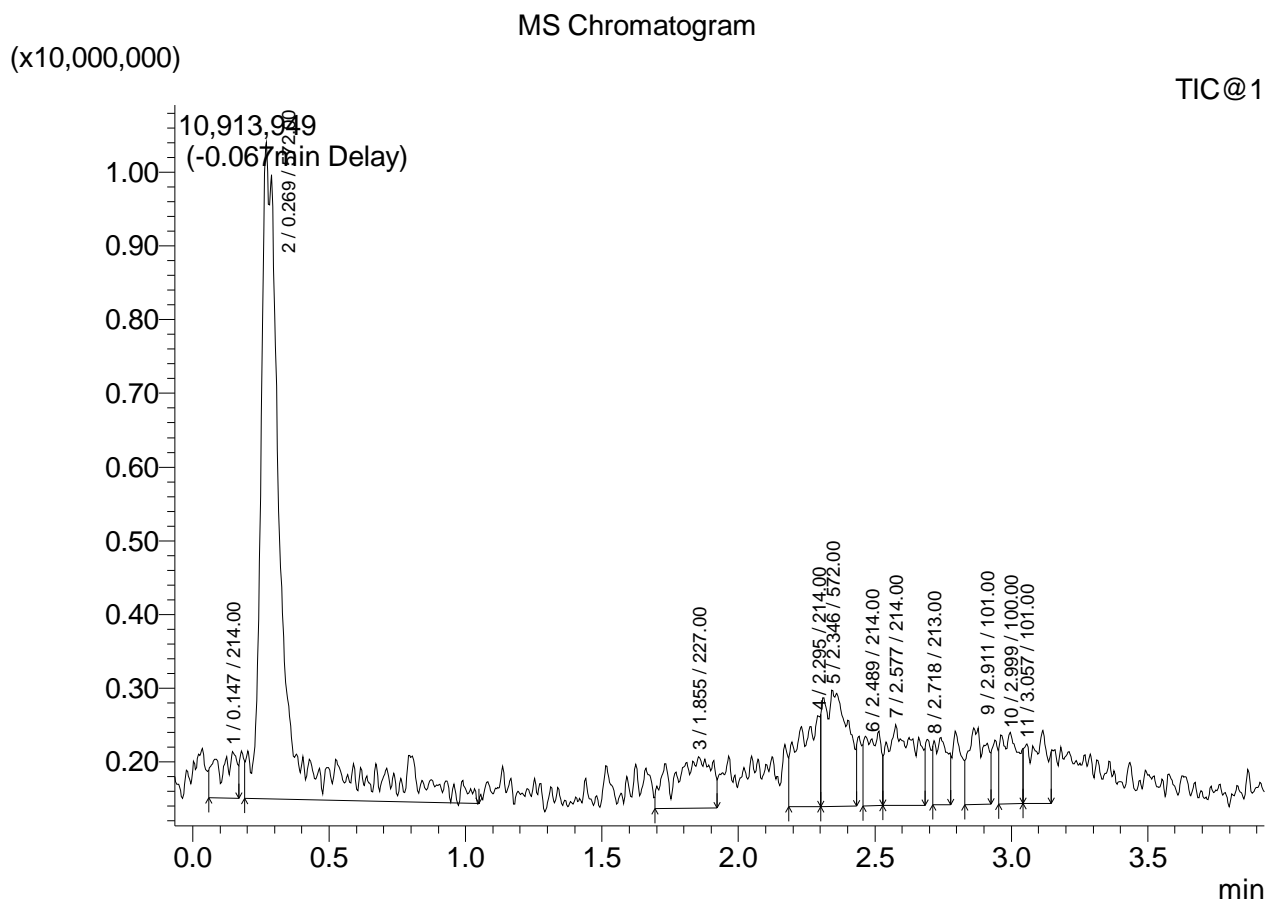
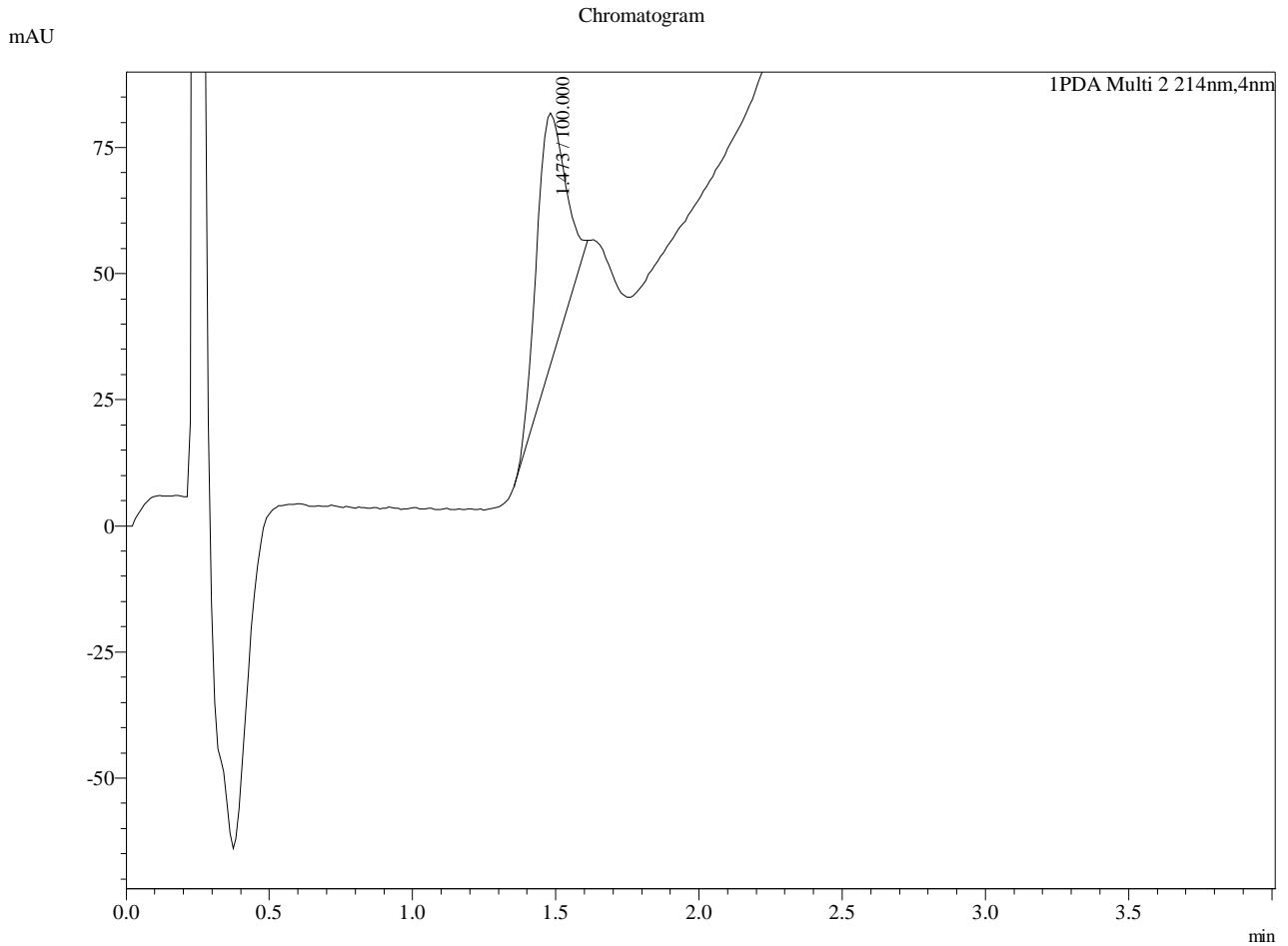
C:\LabSolutions\Data\Project1\Purification\QCs\Feb29-2016\Endomorphin-2c\_5.lcd  
Sample Name : Endomorphin-2c\_5  
Vial# : 46  
Injection Volume : 10  
Data File : C:\LabSolutions\Data\Project1\Purification\QCs\Feb29-2016\Endomorphin-2c\_5.lcd  
Month-Day Acquired : 2/29/2016  
Original Method File : StandardRunPlates.lcm

C:\LabSolutions\Data\Project1\Purification\QCs\Feb29-2016\Endomorphin-2c\_5.lcd  
mV

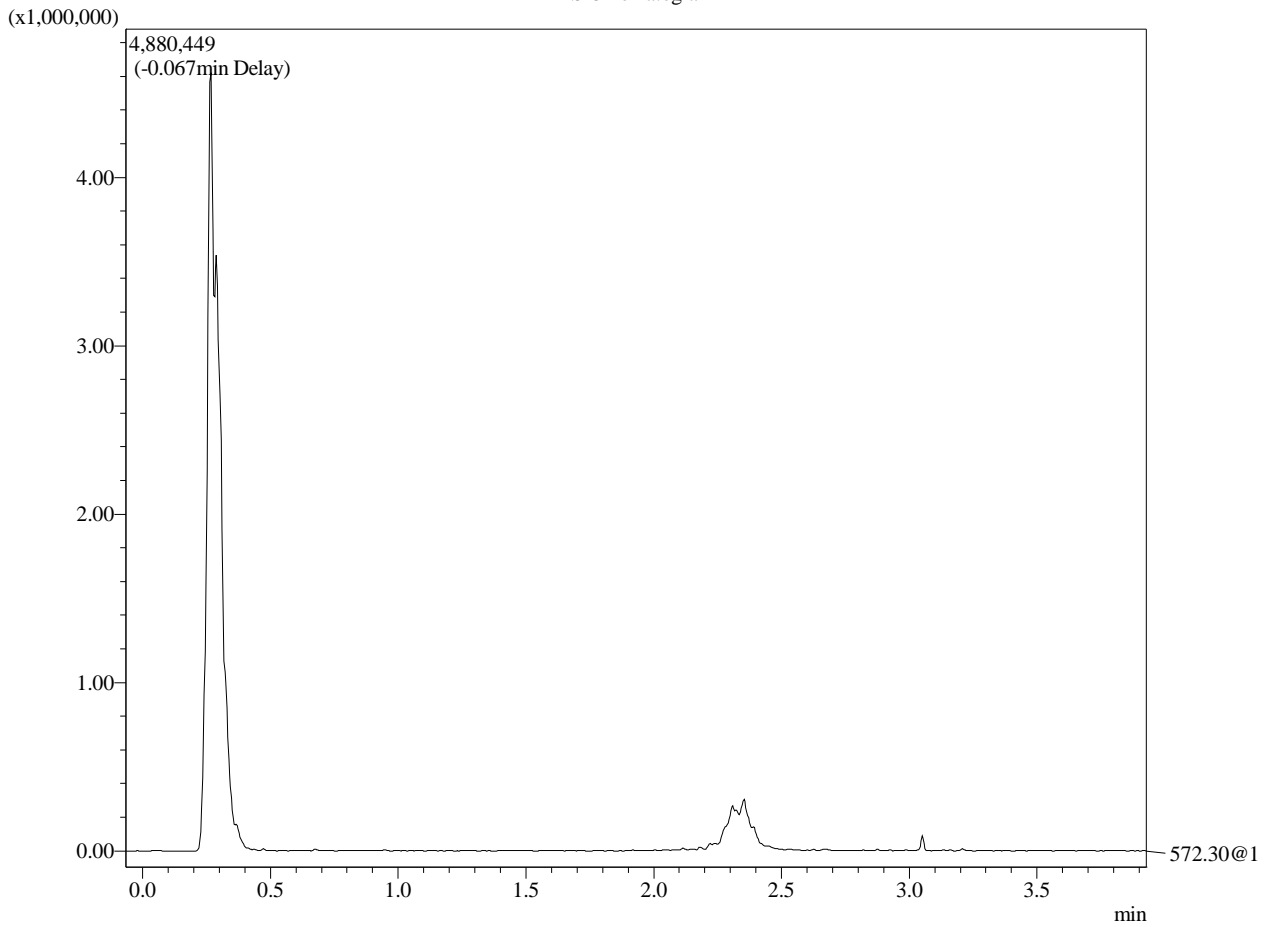


mAU  
Chromatogram





## MS Chromatogram



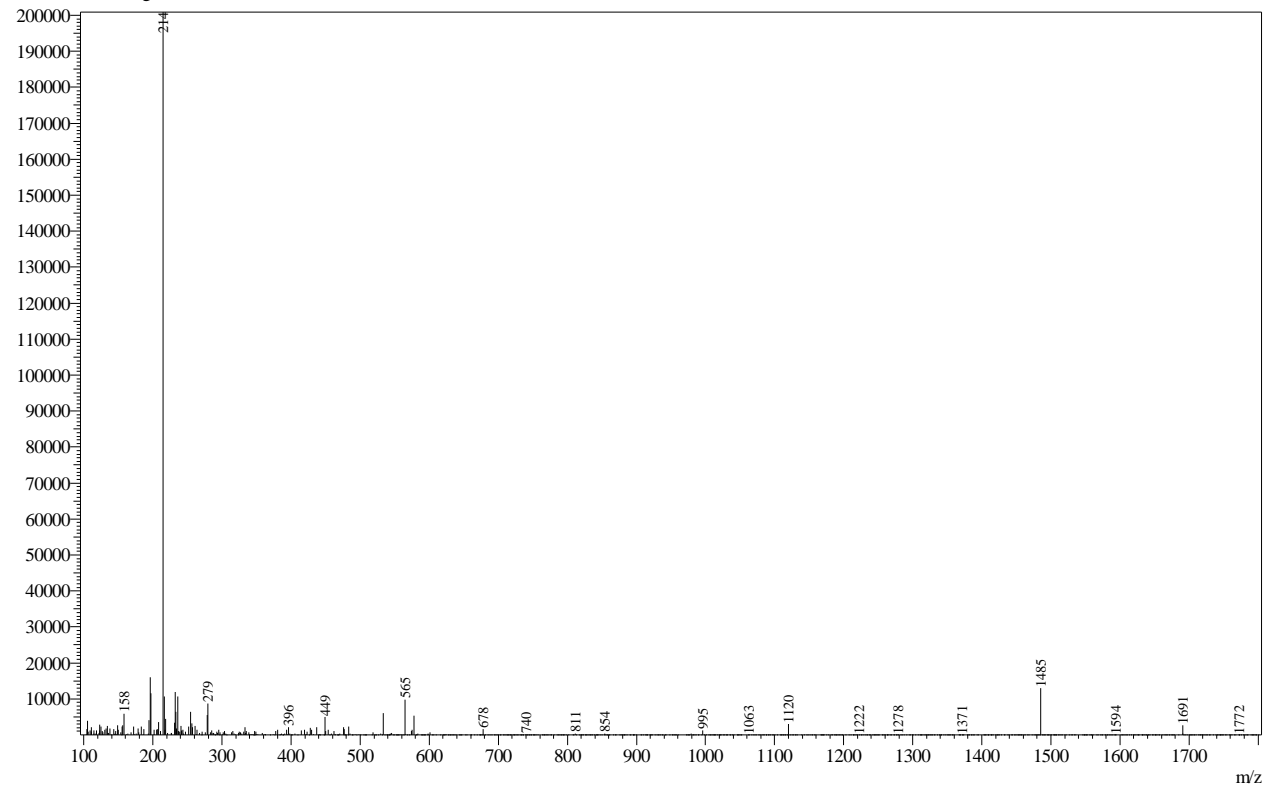
## Mass Spectrum

Peak#: 1 R.Time:0.147(Scan#:59)

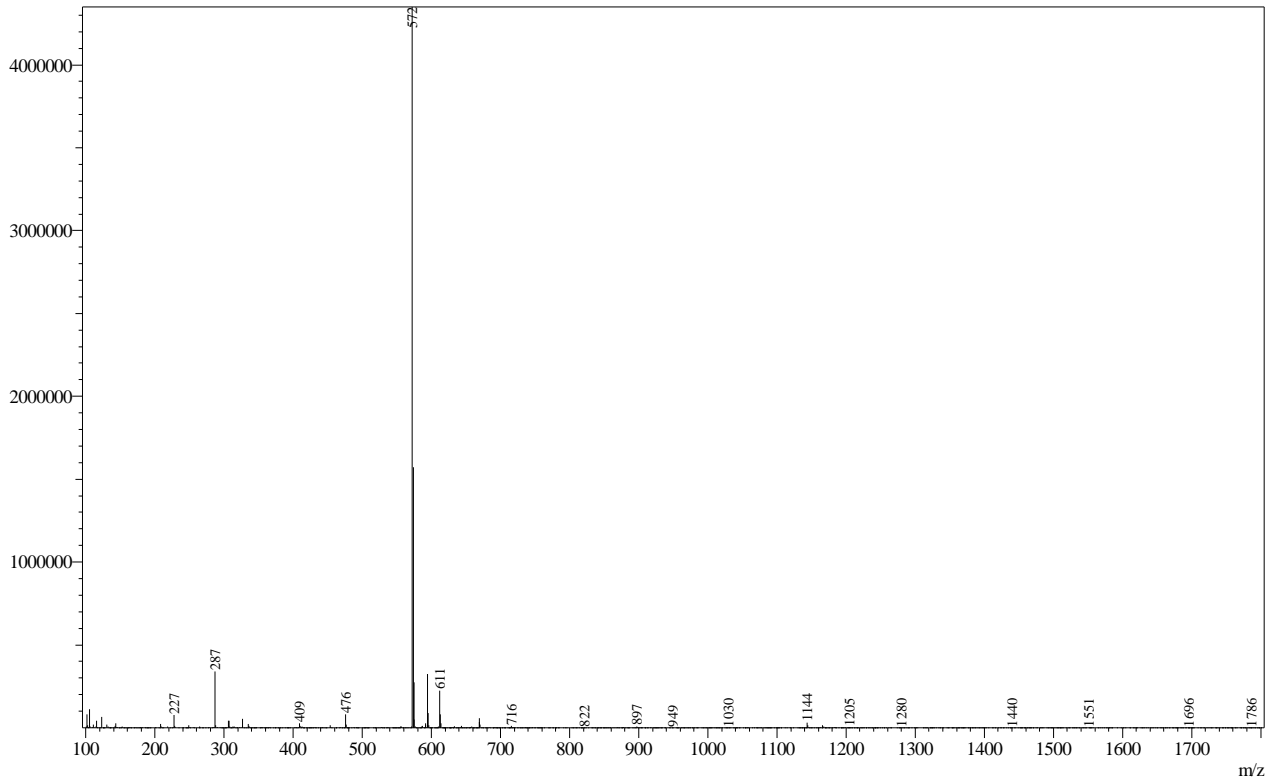
MassPeaks:819

Spectrum Mode:Averaged 0.142-0.150(58-60)

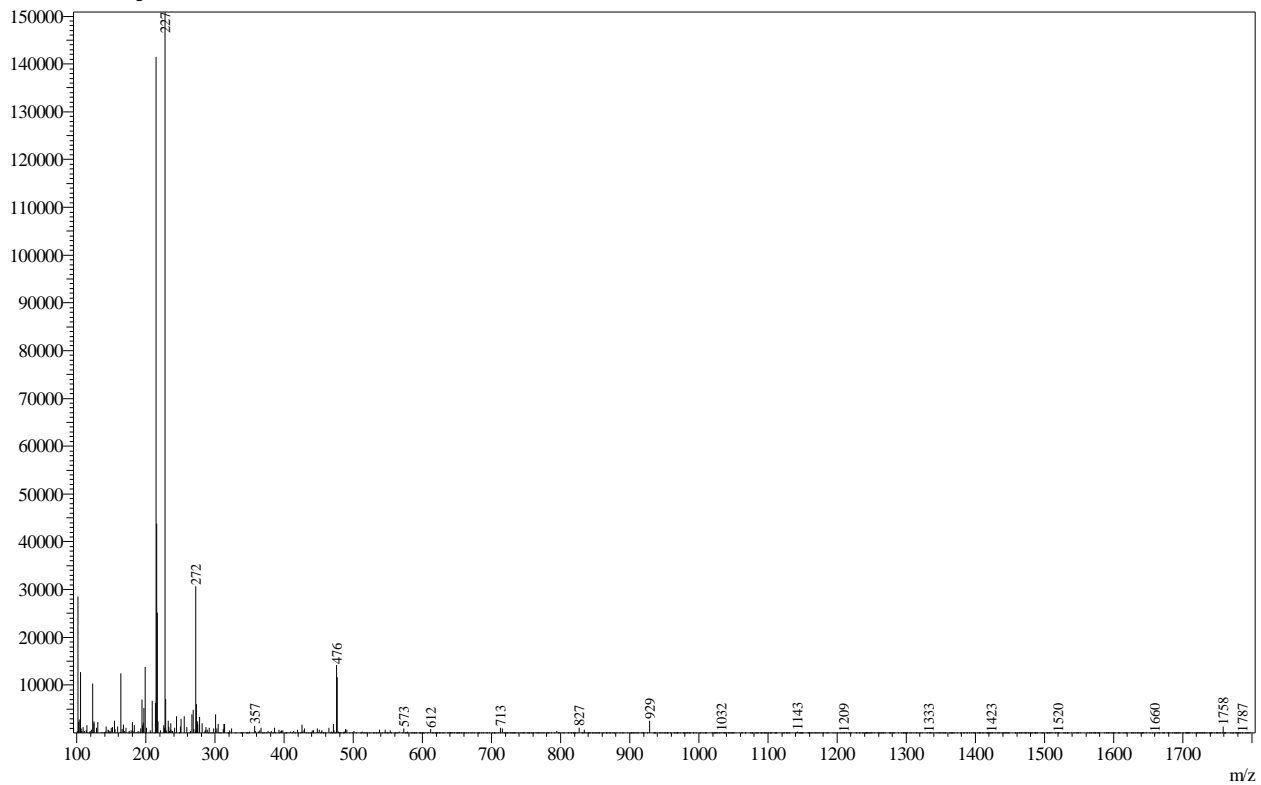
BG Mode:Calc Segment 1 - Event 1



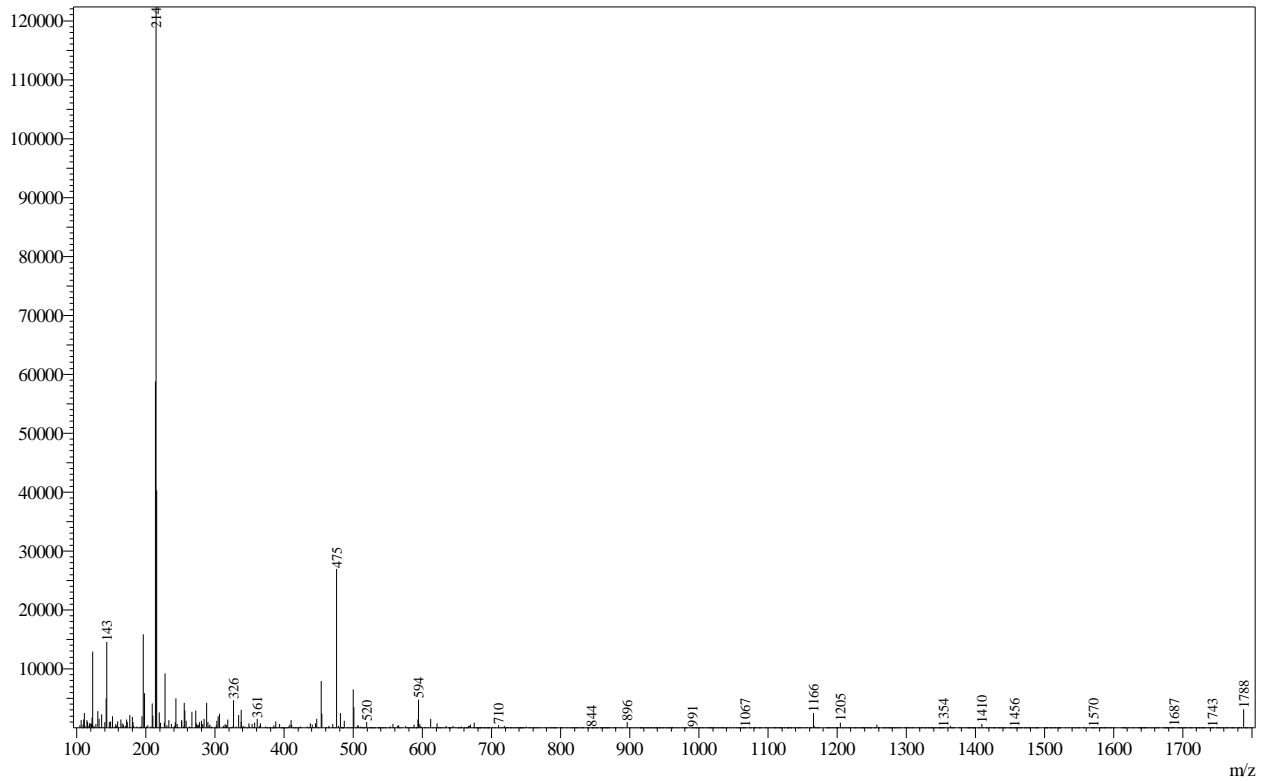
Peak#:2 R.Time:0.269(Scan#:93)  
MassPeaks:1023  
Spectrum Mode:Averaged 0.267-0.274(92-94)  
BG Mode:Calc Segment 1 - Event 1



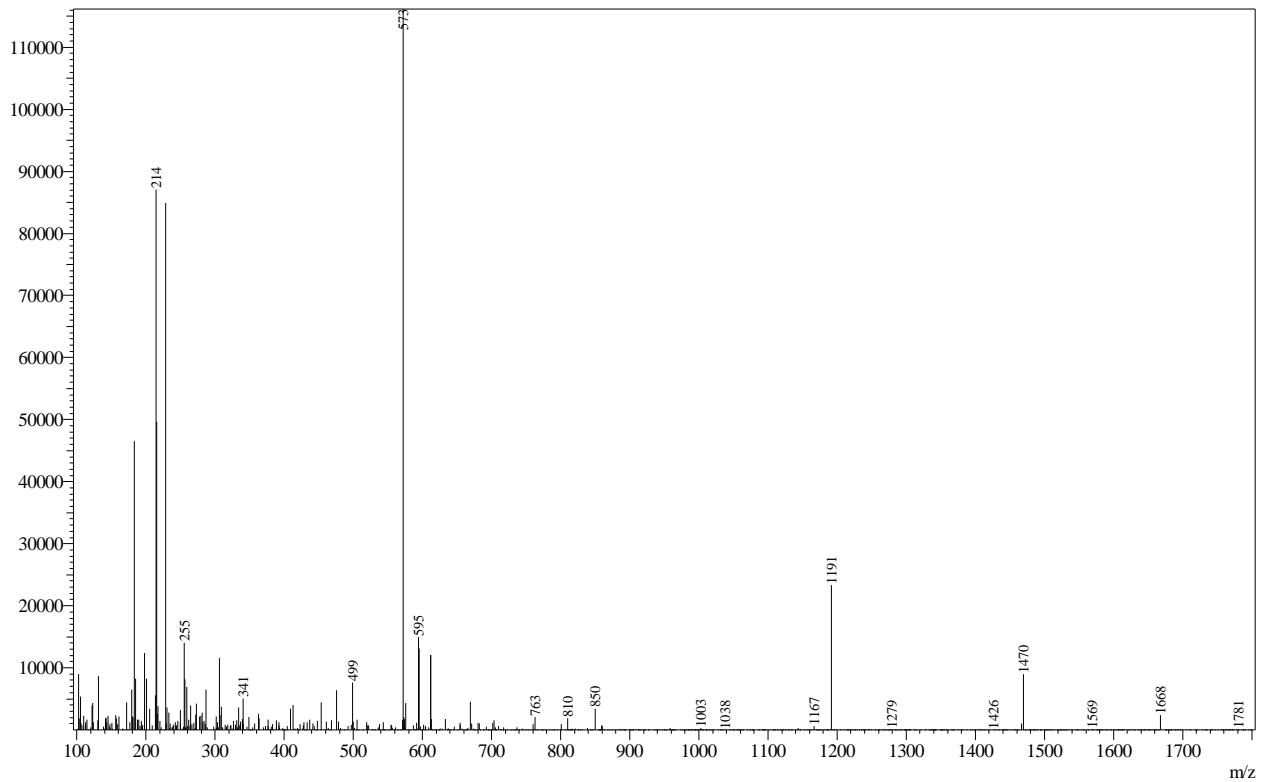
Peak#:3 R.Time:1.855(Scan#:525)  
MassPeaks:793  
Spectrum Mode:Averaged 1.851-1.858(524-526)  
BG Mode:Calc Segment 1 - Event 1



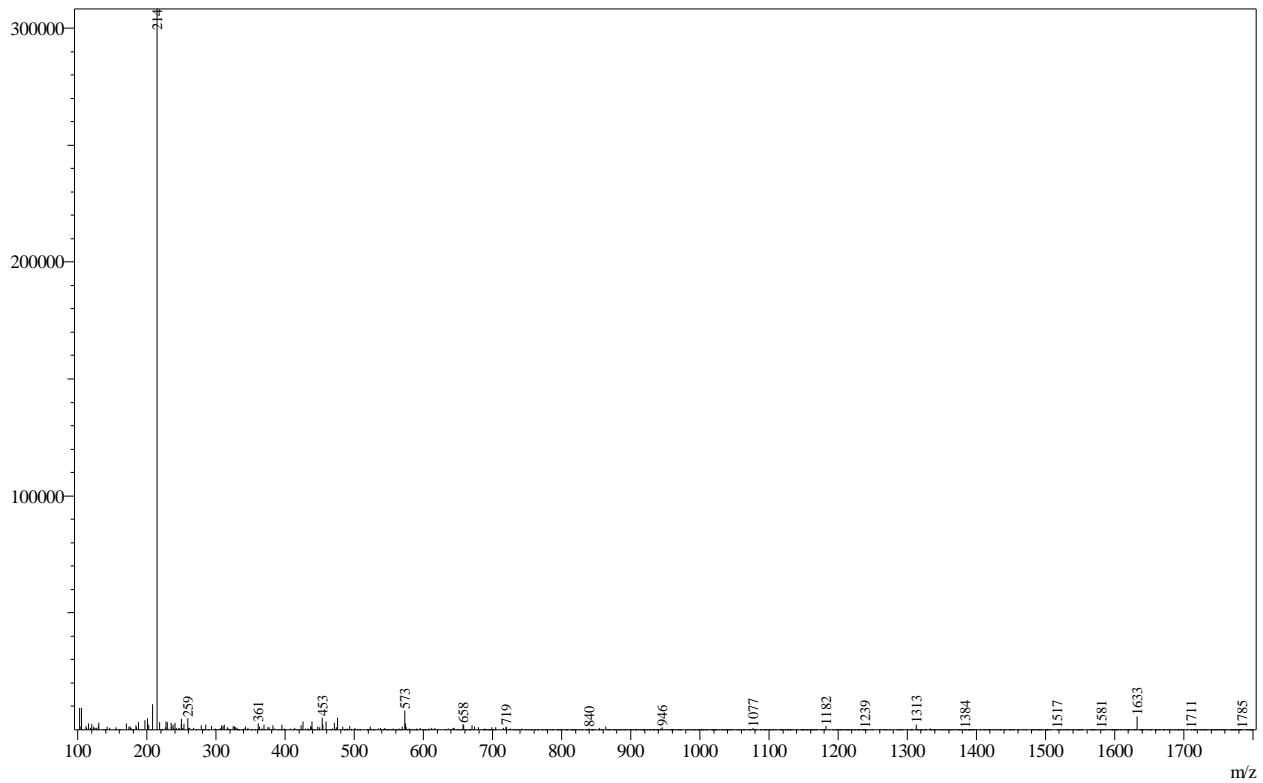
Peak#:4 R.Time:2.295(Scan#:645)  
MassPeaks:828  
Spectrum Mode:Averaged 2.291-2.298(644-646)  
BG Mode:Calc Segment 1 - Event 1



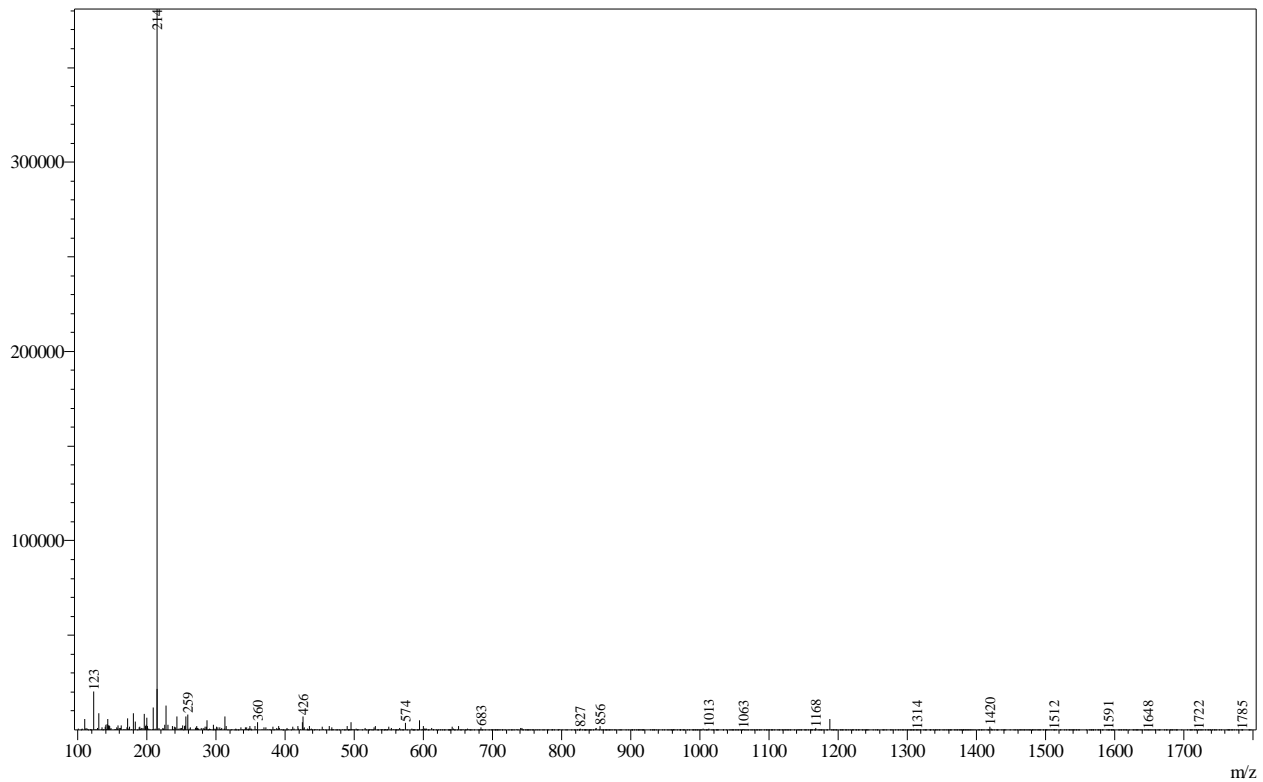
Peak#:5 R.Time:2.346(Scan#:659)  
MassPeaks:801  
Spectrum Mode:Averaged 2.342-2.350(658-660)  
BG Mode:Calc Segment 1 - Event 1



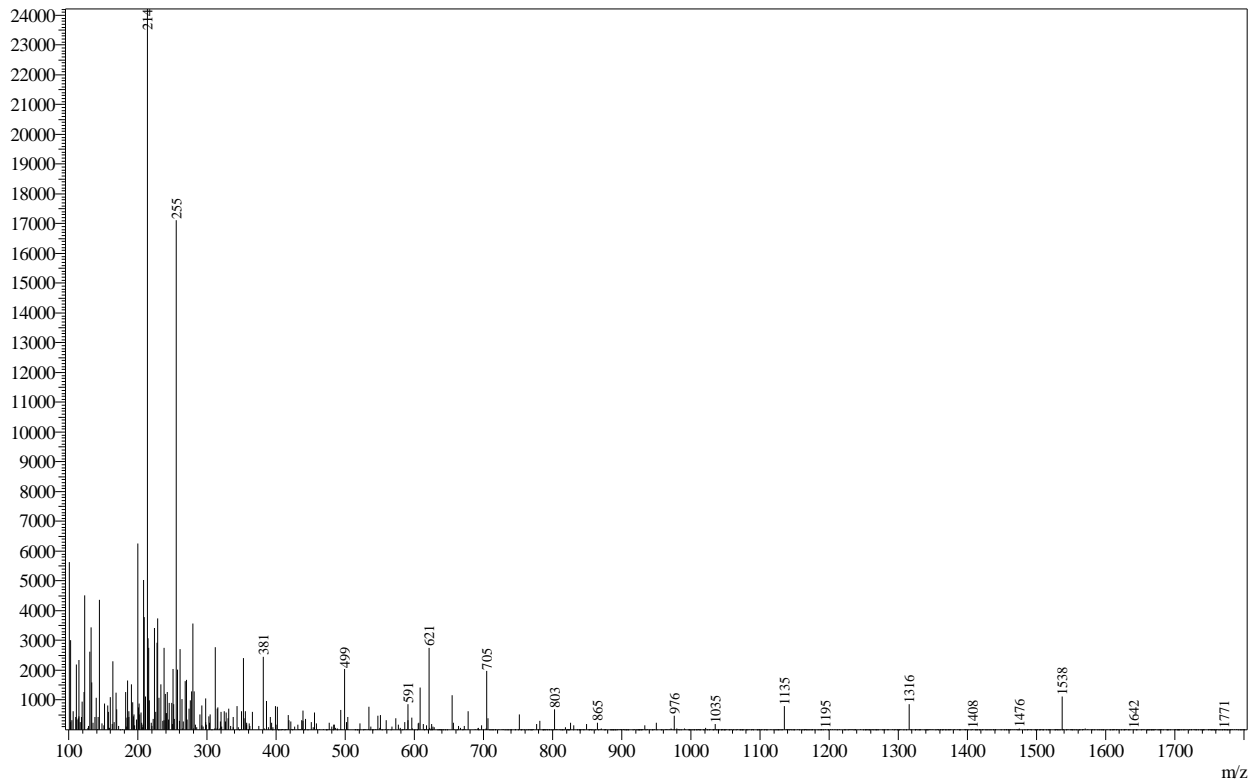
Peak#:6 R.Time:2.489(Scan#:698)  
MassPeaks:818  
Spectrum Mode:Averaged 2.485-2.493(697-699)  
BG Mode:Calc Segment 1 - Event 1



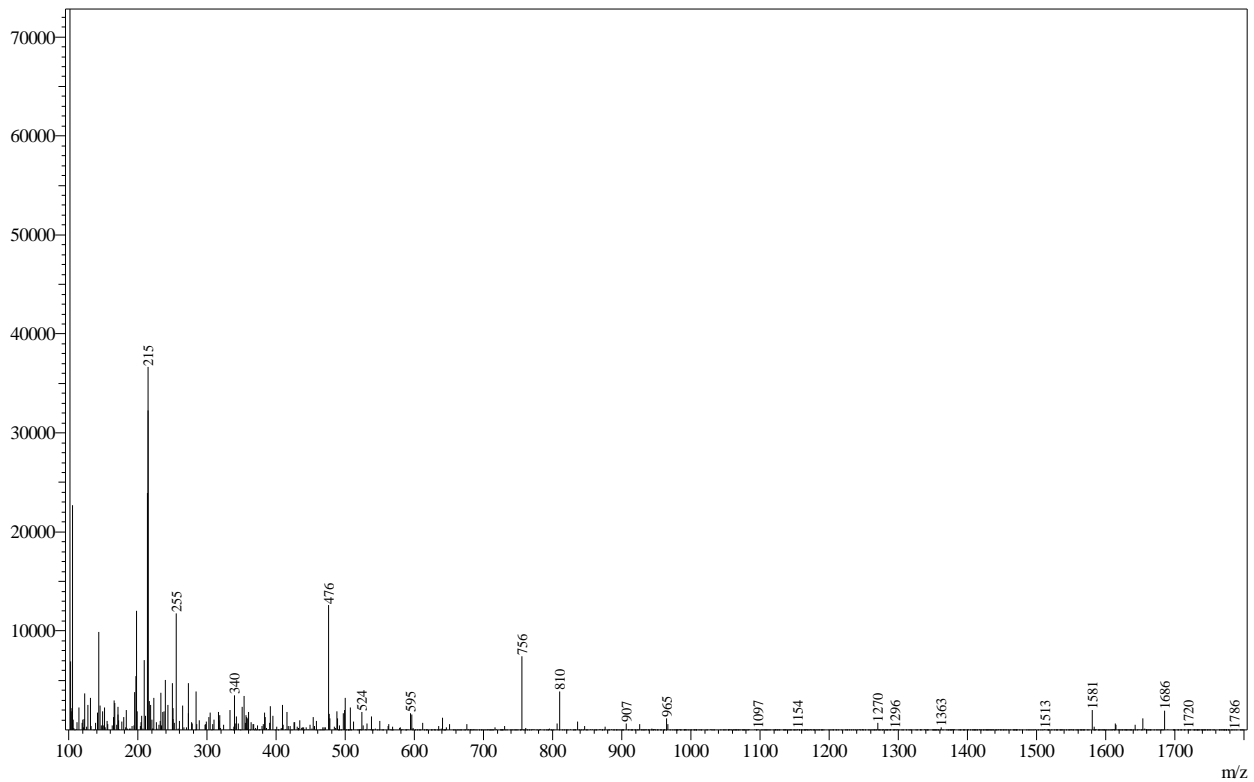
Peak#:7 R.Time:2.577(Scan#:722)  
MassPeaks:805  
Spectrum Mode:Averaged 2.573-2.581(721-723)  
BG Mode:Calc Segment 1 - Event 1



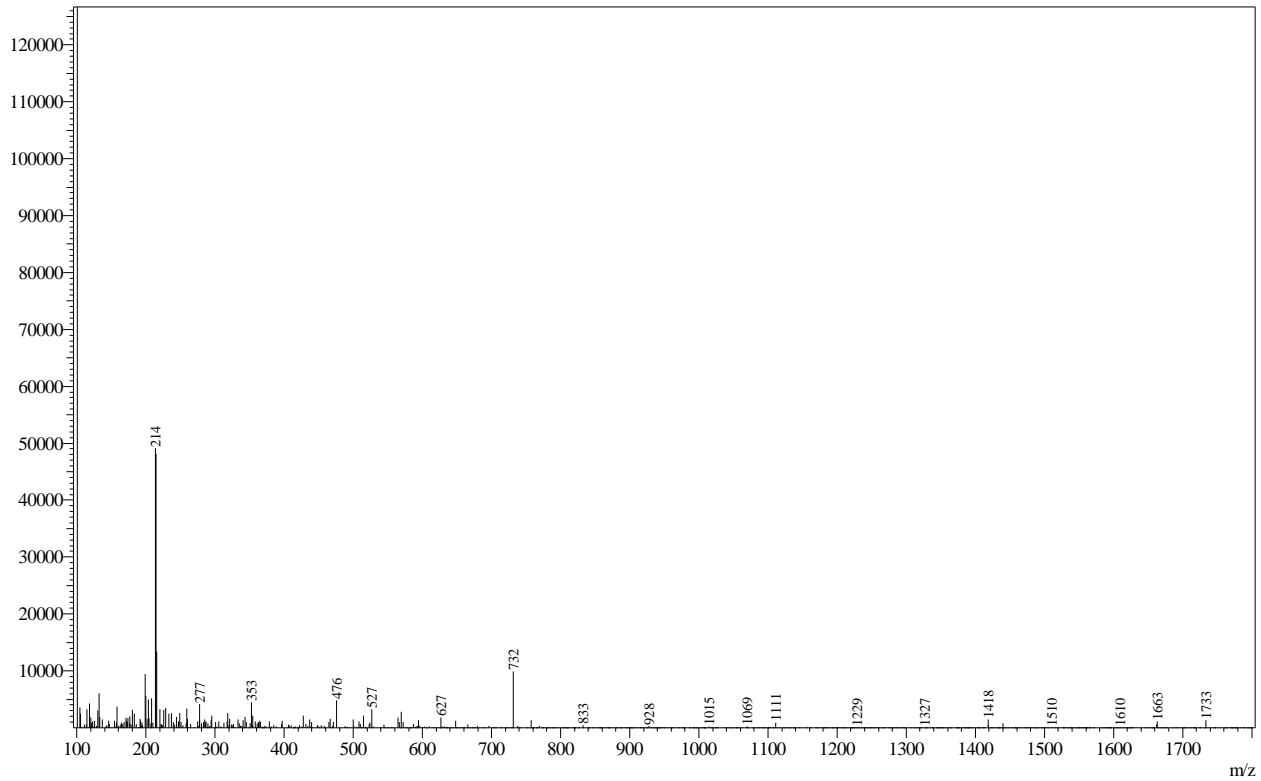
Peak#:8 R.Time:2.718(Scan#:760)  
MassPeaks:801  
Spectrum Mode:Averaged 2.713-2.720(759-761)  
BG Mode:Calc Segment 1 - Event 1



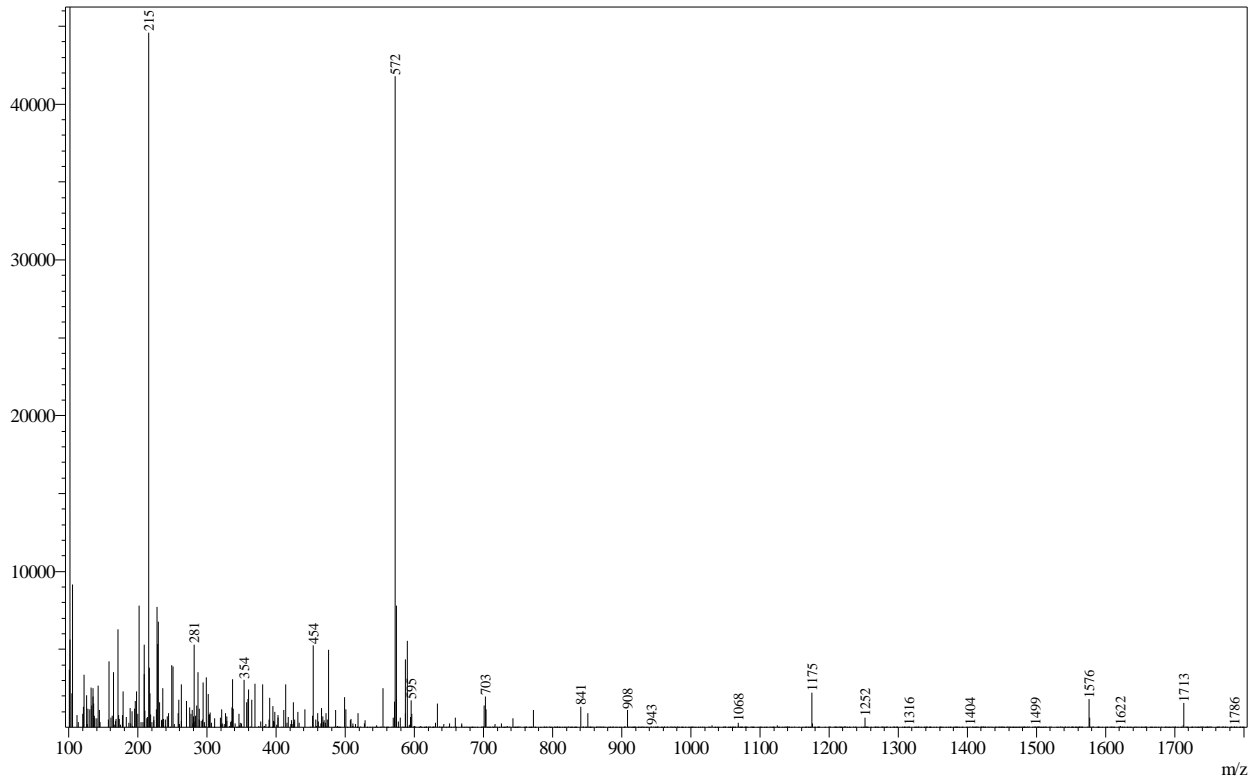
Peak#:9 R.Time:2.911(Scan#:813)  
MassPeaks:843  
Spectrum Mode:Averaged 2.907-2.914(812-814)  
BG Mode:Calc Segment 1 - Event 1



Peak#:10 R.Time:2.999(Scan#:837)  
MassPeaks:798  
Spectrum Mode:Averaged 2.995-3.002(836-838)  
BG Mode:Calc Segment 1 - Event 1



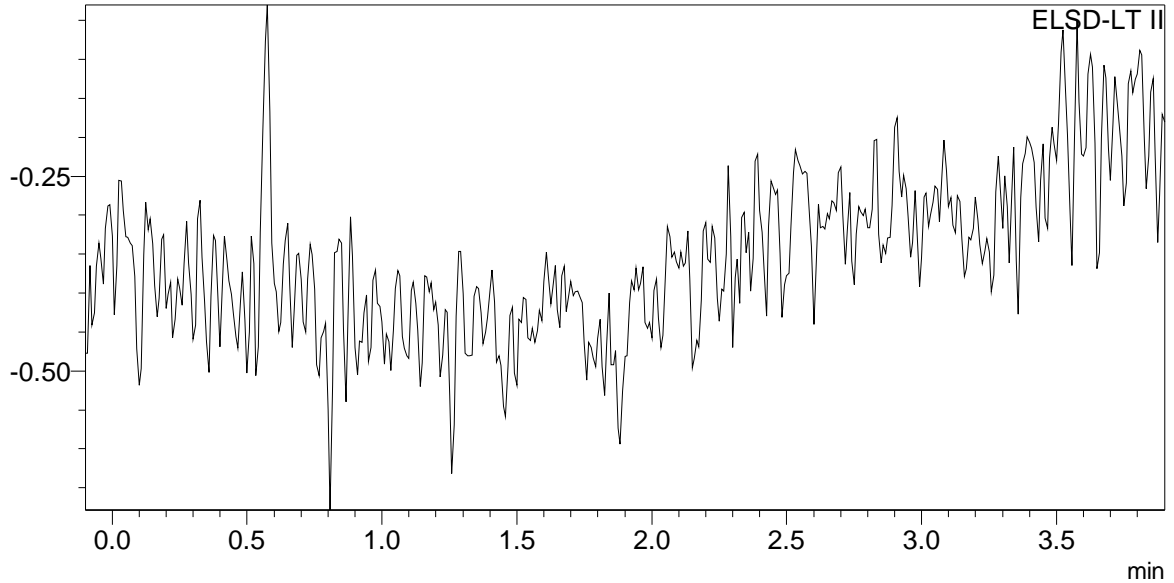
Peak#:11 R.Time:3.057(Scan#:853)  
MassPeaks:827  
Spectrum Mode:Averaged 3.054-3.061(852-854)  
BG Mode:Calc Segment 1 - Event 1



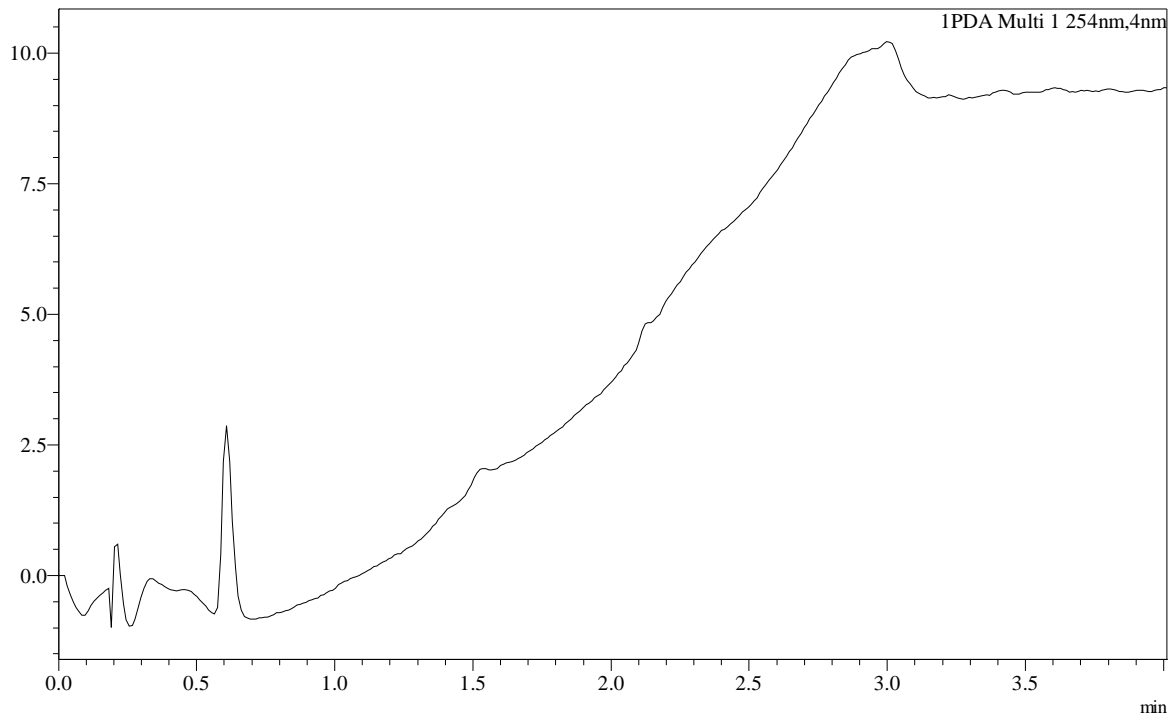
## ==== BIO5 Analytical Lab Report ====

C:\LabSolutions\Data\Project1\Purification\QCs\Jan12-2016\Leu-Enkephalin\_fracQC-2.lcd  
Sample Name : Leu-Enkephalin\_fracQC-2  
Vial# : 48  
Injection Volume : 10  
Data File : C:\LabSolutions\Data\Project1\Purification\QCs\Jan12-2016\Leu-Enkephalin\_fracQC-2  
Month-Day Acquired : 1/12/2016  
Original Method File : StandardRunPlates.lcm

C:\LabSolutions\Data\Project1\Purification\QCs\Jan12-2016\Leu-Enkephalin\_fracQC-2.lcd  
mV

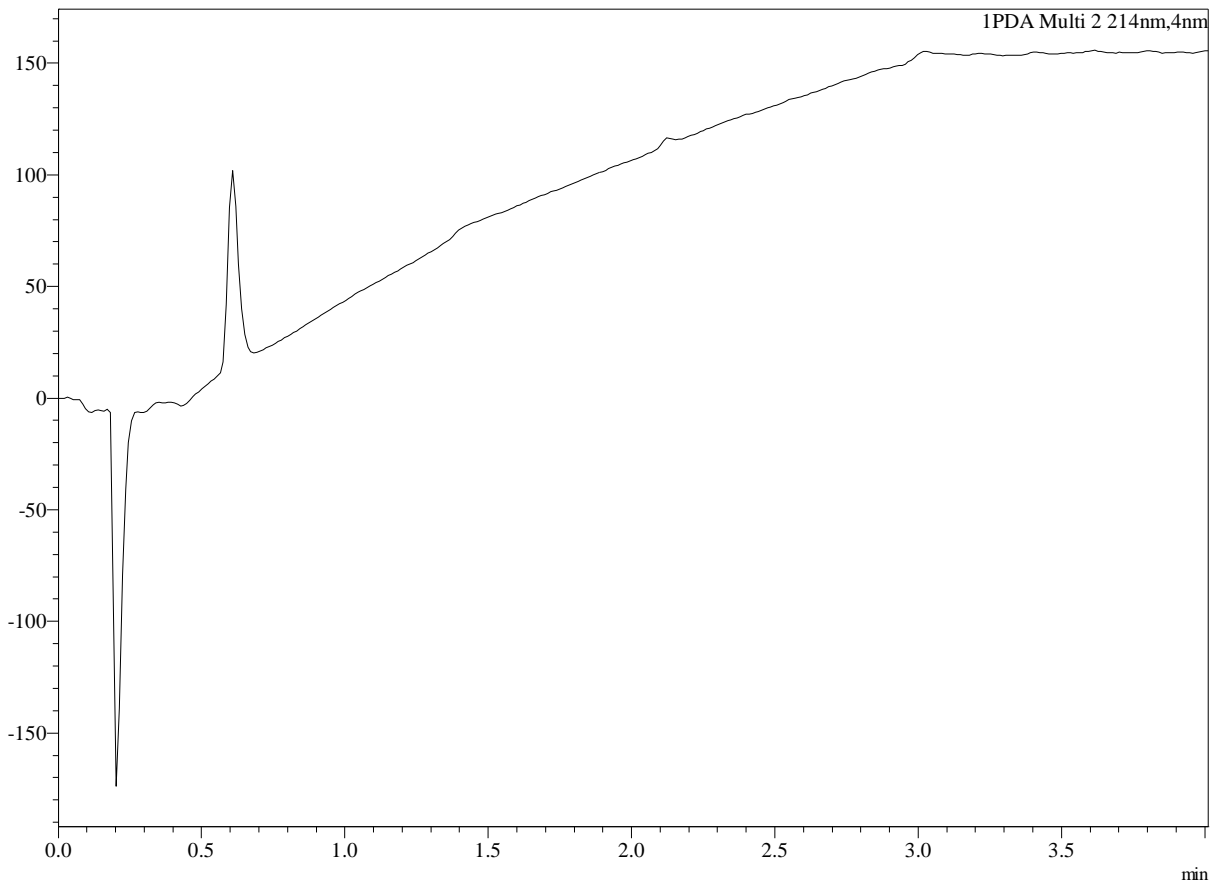


mAU



mAU

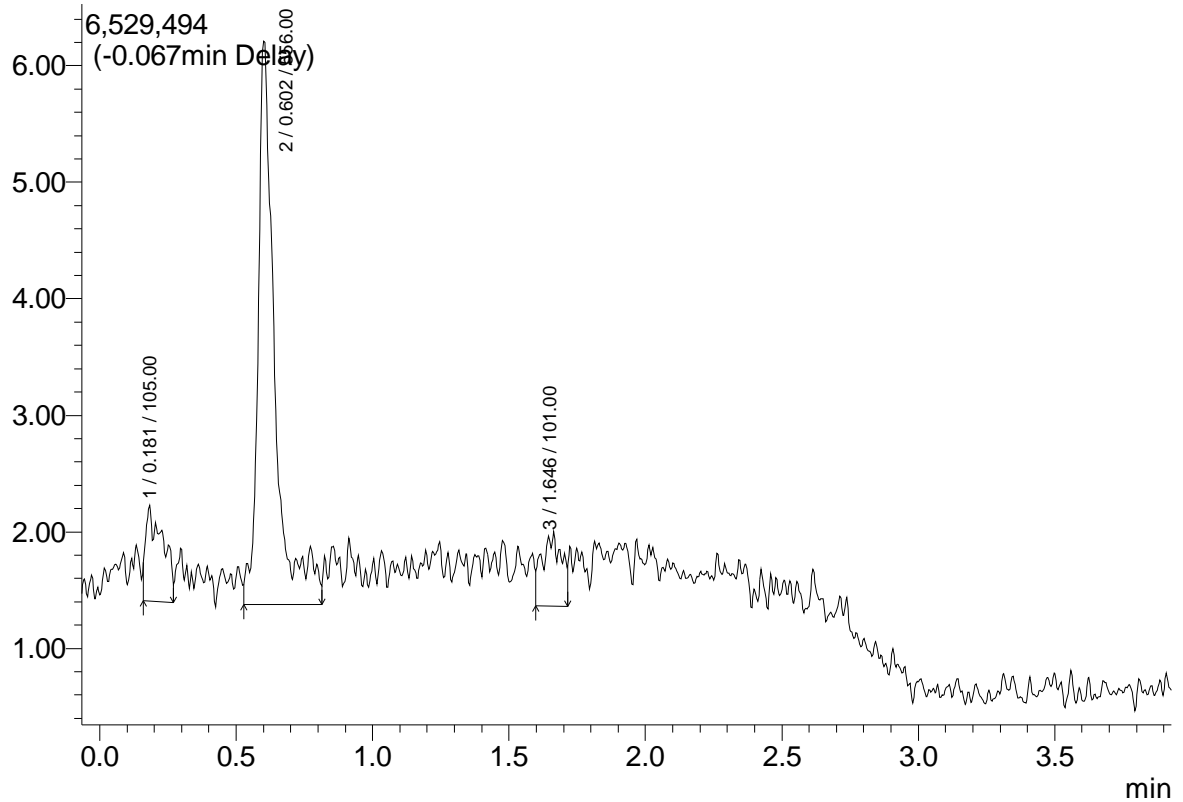
Chromatogram



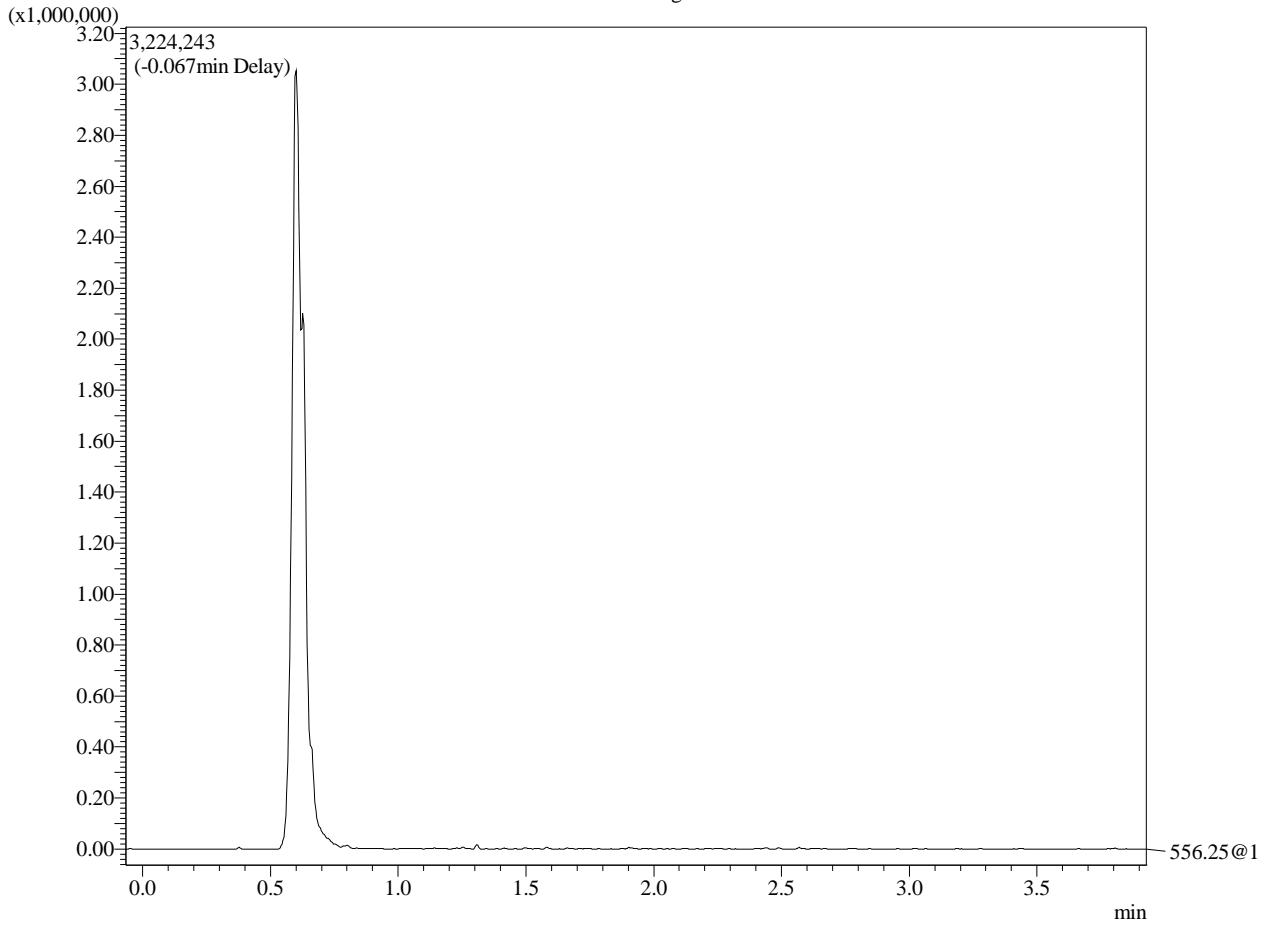
MS Chromatogram

(x1,000,000)

TIC@1

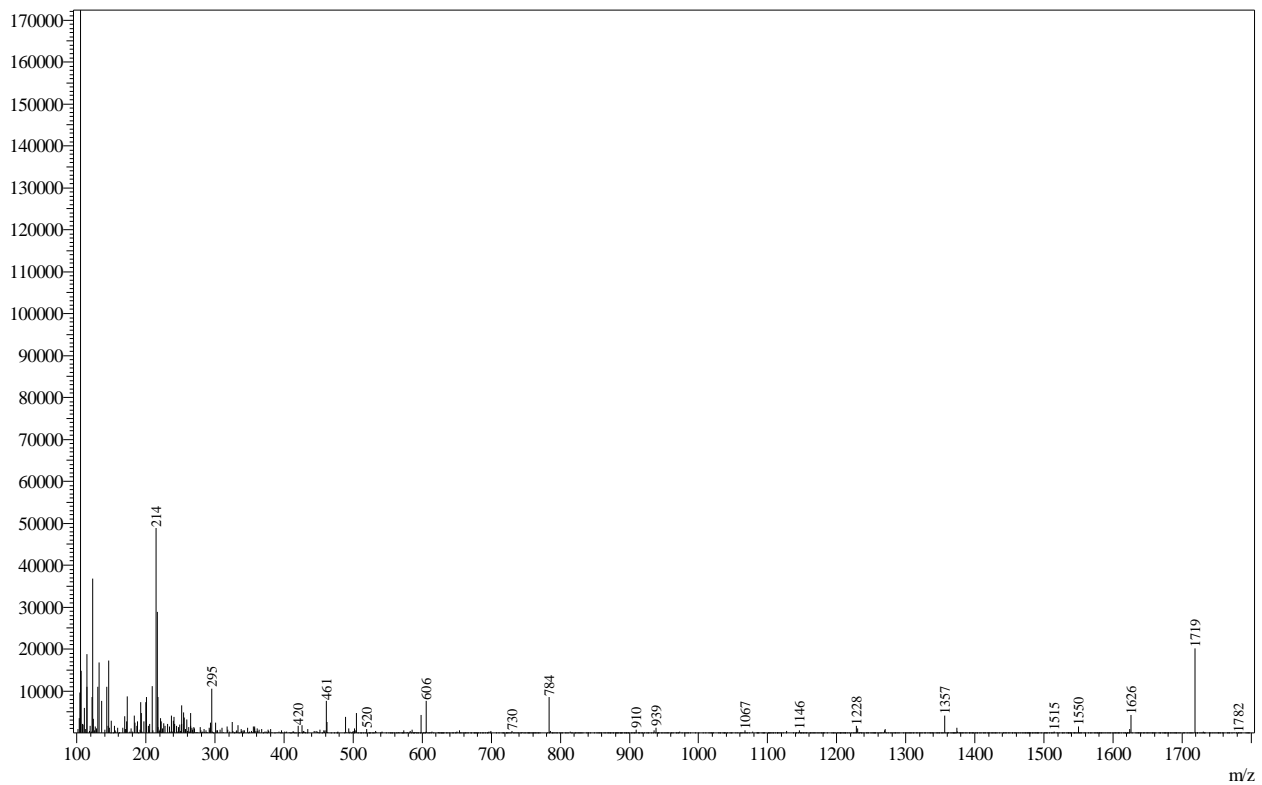


MS Chromatogram

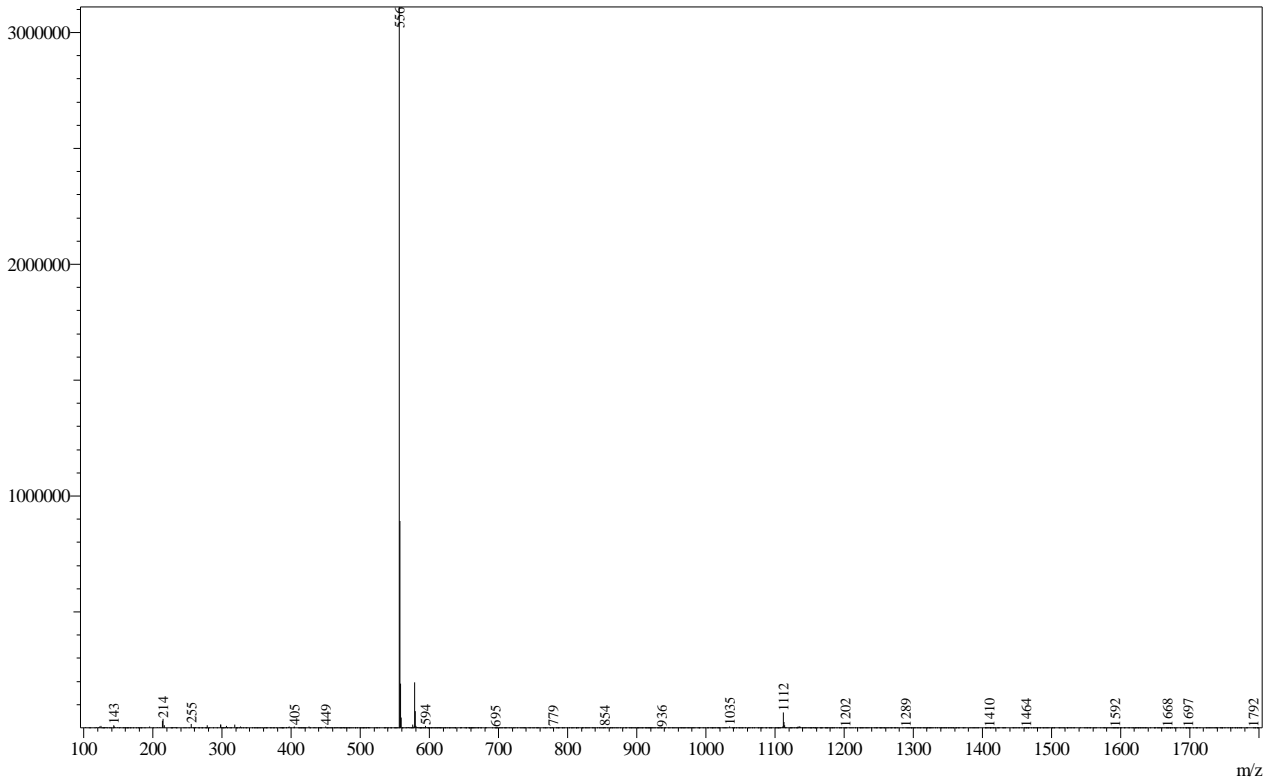


Mass Spectrum

Peak#: 1 R.Time: 0.181 (Scan#: 69)  
 MassPeaks: 860  
 Spectrum Mode: Averaged 0.179-0.186 (68-70)  
 BG Mode: Calc Segment 1 - Event 1



Peak#:2 R.Time:0.602(Scan#:183)  
MassPeaks:810  
Spectrum Mode:Averaged 0.597-0.604(182-184)  
BG Mode:Calc Segment 1 - Event 1



Peak#:3 R.Time:1.646(Scan#:468)  
MassPeaks:789  
Spectrum Mode:Averaged 1.642-1.649(467-469)  
BG Mode:Calc Segment 1 - Event 1

